

**Interior Penalty
Discontinuous Galerkin Methods
for Electromagnetic and Acoustic
Wave Equations**

Inauguraldissertation

zur

Erlangung der Würde eines Doktors der Philosophie
vorgelegt der
Philosophisch-Naturwissenschaftlichen Fakultät
der Universität Basel

von

Anna Schneebeli

aus Zürich (ZH)

Zürich, 2006

Genehmigt von der Philosophisch-Naturwissenschaftlichen Fakultät
auf Antrag von

Prof. Dr. M. J. Grote

Prof. Dr. I. Perugia (Università di Pavia)

Basel, den 4. Juli 2006

Prof. Dr. Hans-Jakob Wirz
Dekan

Contents

1	Introduction	4
1.1	Maxwell's equations	4
1.1.1	Variational formulation	6
1.2	Conforming FEM for Maxwell's equations	7
1.3	Conforming FEM for Maxwell's equations - numerical experiments and applications	8
1.3.1	Nodal elements vs. edge elements	8
1.3.2	An application: Near-field optical microscopy	8
I	Interior Penalty Methods for Time-Harmonic Maxwell's Equations	12
2	Interior Penalty Method for the Indefinite Maxwell's Equations	13
2.1	Introduction	13
2.1.1	Function spaces	15
2.1.2	Model problem	16
2.2	Discontinuous Galerkin discretization	16
2.3	A-priori error bounds	17
2.3.1	Gårding inequality	17
2.3.2	Energy error	18
2.3.3	Error in $\mathbf{L}^2(\Omega)^3$	18
2.4	Auxiliary results	19
2.4.1	Helmholtz decompositions	20
2.4.2	Standard approximation operators	20
2.4.3	Conforming approximation of discontinuous functions	21
2.4.4	Perturbed formulation	22
2.5	Proof of Theorem 2.3.2	24
2.5.1	A preliminary error bound	24
2.5.2	Estimate of $\mathcal{E}_h(\mathbf{u} - \mathbf{u}_h)$	25
2.5.3	The error bound in Theorem 2.3.2	27
2.6	Proof of Theorem 2.3.5 and Corollary 2.3.6	27
2.6.1	Proof of Theorem 2.3.5	27
2.6.2	Proof of Corollary 2.3.6	30
2.7	Numerical experiments	30
2.7.1	Example 1	31
2.7.2	Example 2	31

2.7.3	Example 3	37
2.8	Concluding remarks	37
3	Interior Penalty Method for the Indefinite Time-Harmonic Maxwell's Equation: Mixed Formulation	39
3.1	Introduction	40
3.2	Model problem	41
3.2.1	Indefinite time-harmonic Maxwell's equations	41
3.2.2	Mixed formulation	41
3.3	Discretization	42
3.3.1	Interior penalty method	42
3.3.2	Auxiliary forms and error equations	44
3.3.3	Continuity and stability properties	45
3.4	A-priori error estimates and well-posedness	47
3.5	Proof of Theorem 3.4.1 (energy norm error estimate)	49
3.5.1	Preliminary error bound	49
3.5.2	Estimate of $\mathcal{D}_h(\mathbf{u} - \mathbf{u}_h)$	52
3.5.3	Conclusion of the proof of Theorem 3.4.1	54
3.6	Proof of Theorem 3.4.4 (error estimate in the L^2 -norm)	55
3.6.1	The bound in Theorem 3.4.4	55
3.6.2	Proof of the auxiliary bound in (3.44)	55
3.7	Numerical experiments	60
3.7.1	Example 1	61
3.7.2	Example 2	62
3.8	Concluding remarks	64

II Interior Penalty Method for Transient Wave Propagation 67

4	Interior Penalty Method for the Acoustic Wave Equation	68
4.1	Introduction	68
4.2	Model problem	70
4.3	Discontinuous Galerkin discretization	71
4.3.1	Preliminaries	71
4.3.2	Discretization in space	72
4.4	A-priori error estimates	73
4.4.1	Main results	73
4.4.2	Preliminaries	75
4.4.3	Proof of Theorem 4.4.1	80
4.4.4	Proof of Theorem 4.4.2	82
4.5	Numerical results	86
4.5.1	Time discretization	86
4.5.2	Example 1: smooth solution	87
4.5.3	Example 2: singular solution	89
4.5.4	Example 3: inhomogeneous medium	90
4.6	Concluding remarks	91

5 Interior Penalty Method for Maxwell's Equations in Time Domain	93
5.1 Introduction	93
5.2 Model problem	95
5.3 Discontinuous Galerkin discretization	96
5.4 A-priori error bounds	98
5.5 Proofs of Theorems 5.4.1 and 5.4.2	100
5.5.1 Extension of the DG form and stability properties	100
5.5.2 Error equation	101
5.5.3 Approximation results	102
5.5.4 Proof of Theorem 5.4.1	104
5.5.5 Proof of Theorem 5.4.2	106
5.6 Proof of the L^2 -error bound	106
5.6.1 Auxiliary results	106
5.6.2 Proof of Theorem 5.4.3	112
5.7 Numerical results	115
5.7.1 Time discretization	115
5.7.2 Example 1: smooth solution	116
5.7.3 Example 2: singular solution	118
5.7.4 Example 3: inhomogeneous medium	119
5.8 Concluding remarks	120

Chapter 1

Introduction

In this thesis we present and analyze the numerical approximation of the second order electromagnetic and acoustic wave equation by the interior penalty (IP) discontinuous Galerkin (DG) finite element method (FEM). In Part I we focus on time-harmonic Maxwell source problems in the high-frequency regime. Part II is devoted to the study of the IP DG FEM for time-dependent acoustic and electromagnetic wave equations.

We begin by stating Maxwell's equations in time and frequency domain. We proceed by a variational formulation of Maxwell's equations, and describe the key challenges that are faced in the analysis of the Maxwell operator. Then, we review conforming finite element methods to discretize the second order Maxwell operator. We end this general introduction with some numerical results to highlight the performance and feasibility of conforming FEM for Maxwell's equations.

For an extensive discussion of Maxwell's equations and their conforming finite element discretization, we refer to [38, 55] and the references cited therein.

1.1 Maxwell's equations

A macroscopic electromagnetic field created by static electric charges with *charge density* ρ and a directed flow of electric charge with *current density* \mathcal{J} is described by the four Maxwell's equations,

$$\frac{\partial \mathcal{B}}{\partial t} + \nabla \times \mathcal{E} = 0, \quad (1.1)$$

$$\nabla \cdot \mathcal{D} = \rho, \quad (1.2)$$

$$\frac{\partial \mathcal{D}}{\partial t} - \nabla \times \mathcal{H} = -\mathcal{J}, \quad (1.3)$$

$$\nabla \cdot \mathcal{B} = 0. \quad (1.4)$$

The vector fields $\mathcal{E}, \mathcal{H}, \mathcal{D}, \mathcal{B}, \mathcal{J}$ and the scalar ρ are functions of position $\mathbf{x} \in \mathbb{R}^3$ and time t .

Equation (1.1), Faraday's law, describes the effect of a changing *magnetic induction* \mathcal{B} on the *electric field intensity* \mathcal{E} . Equation (1.2) is Gauss' law, and links the divergence of the *electric displacement* \mathcal{D} to the charge density ρ . Equation (1.3) is Ampère's law, and describes the effect of a changing electric

displacement \mathcal{D} and a flow of electric charges \mathcal{J} to the *magnetic field intensity* \mathcal{H} . The last equation is Gauss' law for magnetic charge, and reflects the fact that the *magnetic induction* \mathcal{B} is solenoidal.

It can be shown that from charge conservation

$$\nabla \cdot \mathcal{J} + \frac{\partial \rho}{\partial t} = 0 \quad (1.5)$$

and the fundamental field equations (1.1) and (1.3) follows

$$\frac{\partial}{\partial t} (\nabla \cdot \mathcal{B}) = \frac{\partial}{\partial t} (\nabla \cdot \mathcal{D} - \rho) = 0.$$

Hence, the divergence constraints (1.2) and (1.4) are not independent relations, and if they hold at one time, they hold for any time. In this sense, (1.2) and (1.4) can be viewed as consistency conditions on the initial data.

The set of six independent equations (1.1) and (1.3) for the twelve unknown field components is complemented by two constitutive laws that relate \mathcal{B} to \mathcal{H} and \mathcal{D} to \mathcal{E} respectively. For the case of *linear, isotropic, possibly inhomogeneous*, media we have

$$\mathcal{D} = \varepsilon \mathcal{E}, \quad (1.6)$$

$$\mathcal{B} = \mu \mathcal{H}, \quad (1.7)$$

with scalar, positive, bounded functions of position ε , μ . The *relative electric permittivity* ε and *relative magnetic permeability* μ are material properties. One further constitutive relation arises in conducting materials. Here, the electromagnetic field itself gives rise to currents. If the fields are not too strong, Ohm's law can be assumed.

$$\mathcal{J} = \sigma \mathcal{E} + \mathcal{J}_s. \quad (1.8)$$

The *conductivity* σ of the medium is a scalar function of position. σ is positive in a conductor and vanishes in an insulator. \mathcal{J}_s describes the applied current density.

By substituting (1.6)–(1.7) and (1.8) into (1.1) and (1.3), we obtain the fundamental equations for the electric and magnetic field

$$\varepsilon \frac{\partial \mathcal{E}}{\partial t} = \nabla \times \mathcal{H} - \sigma \mathcal{E} - \mathcal{J}_s, \quad (1.9)$$

$$\mu \frac{\partial \mathcal{H}}{\partial t} = -\nabla \times \mathcal{E}. \quad (1.10)$$

By formally taking the time derivative of equation (1.9) and the rotation of equation (1.10), we can eliminate the magnetic field \mathcal{H} , and the first order Maxwell system (1.9)–(1.10) reduces to a second order wave equation for the electric field \mathcal{E}

$$\varepsilon \frac{\partial^2 \mathcal{E}}{\partial t^2} + \sigma \frac{\partial \mathcal{E}}{\partial t} + \nabla \times (\mu^{-1} \nabla \times \mathcal{E}) = -\frac{\partial \mathcal{J}_s}{\partial t}. \quad (1.11)$$

Note that $(\varepsilon \mu)^{-\frac{1}{2}}$ is the wave speed in the medium. A similar equation can be derived for \mathcal{H} , if $\sigma = 0$, or if ε , $\sigma > 0$ are constant.

By taking the Fourier transform in time and analyzing a single frequency $\omega > 0$, or in the case where the source term \mathcal{J}_s and, for consistency, the charge

density ρ , vary sinusoidally time, the time-dependent Maxwell's equations can be reduced to stationary equations in frequency domain. We substitute *time-harmonic* fields

$$\mathcal{E}(\mathbf{x}, t) = \operatorname{Re}(\exp(i\omega t)\mathbf{E}(\mathbf{x})), \quad \mathcal{J}_s(\mathbf{x}, t) = \operatorname{Re}(\exp(i\omega t)\mathbf{J}_s(\mathbf{x})),$$

into (1.11), and obtain the second order time-harmonic Maxwell's equation for the complex-valued vector field $\mathbf{E}(\mathbf{x})$

$$\nabla \times (\mu^{-1} \nabla \times \mathbf{E}) - \omega^2 (\varepsilon - \frac{i\sigma}{\omega}) \mathbf{E} = \mathbf{j}, \quad (1.12)$$

with $\mathbf{j} = -i\omega\mathbf{J}_s$.

The *low-frequency* approximation of (1.12), or Eddy current problem, consists in neglecting $\omega\varepsilon$ in the case where $\sigma \gg \omega\varepsilon$. In turn, in the *high-frequency* regime ω is large and $\sigma \ll \omega\varepsilon$, and the expression $\frac{i\sigma}{\omega}$ is neglected.

By substituting the constitutive relation (1.6) in the divergence constraint (1.2) and combining it with the time-harmonic version of charge conservation (1.5) and Ohm's Law (1.8), we obtain the divergence constraint for \mathbf{E} , if $\omega > 0$,

$$\nabla \cdot \left(\omega^2 (\varepsilon - \frac{i\sigma}{\omega}) \mathbf{E} \right) = \frac{1}{\omega^2} \nabla \cdot \mathbf{j}.$$

Formally taking the divergence of equation (1.12) shows, that \mathbf{E} automatically satisfies this divergence condition.

We point out that although the divergence conditions (1.2) and (1.4) are consequences of the fundamental equations (1.1) and (1.3) for the continuous electromagnetic field, they should be taken into account when designing a numerical method to discretize Maxwell's equations. A numerical scheme should produce a numerical approximation that satisfies in some sense discrete analogs of the divergence conditions.

1.1.1 Variational formulation

In this section we describe the variational framework for Maxwell's equations. To do so, we consider the time-harmonic Maxwell's equation (1.12) with $\mu = 1$ in a Lipschitz domain $\Omega \in \mathbb{R}^3$ and augment (1.12) with a perfectly conducting boundary condition

$$\mathbf{n} \times \mathbf{E} = \mathbf{0} \quad \text{on } \Gamma,$$

where \mathbf{n} denotes the outward unit normal to $\Gamma = \partial\Omega$. In the Sobolev space

$$H_0(\operatorname{curl}; \Omega) := \{ \mathbf{v} \in L^2(\Omega)^3 : \nabla \times \mathbf{v} \in L^2(\Omega)^3, \mathbf{n} \times \mathbf{v} = \mathbf{0} \text{ on } \Gamma \},$$

endowed with the norm $\|\mathbf{v}\|_{\operatorname{curl}}^2 := \|\mathbf{v}\|_{L^2(\Omega)^3}^2 + \|\nabla \times \mathbf{v}\|_{L^2(\Omega)^3}^2$, the weak form reads: find $\mathbf{E} \in H_0(\operatorname{curl}; \Omega)$ such that

$$a(\mathbf{E}, \mathbf{v}) := \int_{\Omega} [\nabla \times \mathbf{E} \cdot \nabla \times \bar{\mathbf{v}} - \omega^2 (\varepsilon - \frac{i\sigma}{\omega}) \mathbf{E} \cdot \bar{\mathbf{v}}] dx = \int_{\Omega} \mathbf{j} \cdot \bar{\mathbf{v}} dx \quad (1.13)$$

for all $\mathbf{v} \in H_0(\operatorname{curl}; \Omega)$.

For the following discussion of existence and uniqueness of weak solutions of (1.12) we assume ε and $\sigma > 0$ to be constant.

For the *low-frequency* approximation of (1.12) the sesquilinear form a is coercive:

$$\begin{aligned} |a(\mathbf{v}, \mathbf{v})| &= \left| \int_{\Omega} [\nabla \times \mathbf{v} \cdot \nabla \times \bar{\mathbf{v}} + i\sigma\omega\mathbf{v} \cdot \bar{\mathbf{v}}] d\mathbf{x} \right| \\ &= \|\nabla \times \mathbf{v}\|_{L^2(\Omega)^3}^2 + \omega^2\sigma^2\|\mathbf{v}\|_{L^2(\Omega)^3}^2 > \gamma\|\mathbf{v}\|_{\text{curl}}^2 > 0. \end{aligned}$$

Hence, by the Lax-Milgram lemma, (1.13) is uniquely solvable in the low-frequency case.

In the *high-frequency* regime, equation (1.12) is of Helmholtz type, with indefinite sesquilinear form

$$\begin{aligned} |a(\mathbf{v}, \mathbf{v})| &= \left| \int_{\Omega} [\nabla \times \mathbf{v} \cdot \nabla \times \bar{\mathbf{v}} - \omega^2\varepsilon\mathbf{v} \cdot \bar{\mathbf{v}}] d\mathbf{x} \right| \\ &= \|\nabla \times \mathbf{v}\|_{L^2(\Omega)^3}^2 - \omega^2\varepsilon\|\mathbf{v}\|_{L^2(\Omega)^3}^2. \end{aligned}$$

However, in contrast to the Helmholtz equation, we do not straightforwardly obtain a compact perturbation of the form a and a Gårding inequality that implies existence and uniqueness of a high-frequency Maxwell solution. The reason lies in the fact that the Sobolev space $H(\text{curl}; \Omega)$ associated with the Maxwell operator is not compactly included in $L^2(\Omega)^3$. Indeed, since formally $\nabla \times (\nabla\phi) = 0$, the infinite dimensional space of gradients of $H_0^1(\Omega)$ functions lies in the null space of the curl operator. This characteristic of the Maxwell operator complicates the variational theory for the Maxwell problem substantially.

For a thorough analysis of the variational problem (1.13), we refer to, e. g., [55, Chapter 4]. In particular, if $\omega^2\varepsilon$ is not a Maxwell eigenvalue, the existence and uniqueness of a solution for the high-frequency approximation of (1.13) is shown.

1.2 Conforming FEM for Maxwell's equations

In the following, we discuss numerical approximations of the Maxwell operator by means of finite element methods.

The electromagnetic fields governed by Maxwell's equations typically have low regularity. In fact, even for smooth material parameters, the electromagnetic field components may have regularity below $H^1(\Omega)$ in non-convex polyhedra or polygons of engineering practice; see, e. g., [4]. It has been known for some time that nodal FEM (i. e., $H^1(\Omega)$ -conforming) discretizations of the Maxwell operator, albeit stable, could converge quasi-optimally to an electromagnetic field that misses certain singular solution components induced by reentrant vertices or edges (for more details, see, e. g., [25, 26] and the references cited therein). Consequently, in non-convex domains, setting the electromagnetic fields in $H^1(\Omega)$ leads to a well-posed problem where the fields lack certain singular (but physical) solution components.

The weighted regularization technique developed by Costabel and Dauge in [26], and extended by Hasler, Schneebeli and Schötzau to problems of incompressible magneto-hydrodynamics in [35], is a possible way to overcome these difficulties. However, in this approach appropriate weight functions have to be determined for every re-entrant corner or edge in the computational domain. This procedure may be inconvenient for complicated domains, especially in three dimensions.

The first family of $H(\text{curl}; \Omega)$ -conforming finite elements was proposed by Nédélec [58] in 1980. These elements are based on polynomial spaces \mathcal{R}^ℓ which are subspaces of the full polynomial spaces \mathcal{S}^ℓ of degree ℓ on the reference element. Nédélec proposed a second family of $H(\text{curl}; \Omega)$ -conforming edge elements based on the full polynomial spaces in [59]. Nédélec's $H(\text{curl}; \Omega)$ -conforming elements incorporate the minimal continuity of $H(\text{curl}; \Omega)$ -functions across boundaries of elements of a finite element triangulation of the domain Ω . In fact, vector fields in $H(\text{curl}; \Omega)$ have continuous *tangential* component, whereas the normal component is allowed to jump across element boundaries. In reference to the degrees of freedom, which include edge and face moments, $H(\text{curl}; \Omega)$ -conforming finite elements are also referred to as *edge elements*; for an overview on Nédélec's edge elements on tetrahedral and hexahedral finite element meshes see, e. g., [55, Chapters 5, 6].

Other families of $H(\text{curl}; \Omega)$ -conforming finite elements, which are better suited for *hp*-FEM than Nédélec's original elements, were proposed by Demkowicz and Vardapetyan in 1998 [28] and by Ainsworth and Coyle in 2001 [1].

1.3 Conforming FEM for Maxwell's equations - numerical experiments and applications

1.3.1 Nodal elements vs. edge elements

To illustrate the inaccuracy of nodal elements for Maxwell's equations, we approximate a singular solution to the low-frequency time-harmonic Maxwell model problem

$$\nabla \times \nabla \times \mathbf{E} + \mathbf{E} = \mathbf{j} \quad \text{in a 2d L-shaped domain } \Omega, \quad (1.14)$$

augmented with perfectly conducting boundary conditions. The data \mathbf{j} is chosen such, that $\mathbf{E} \in \nabla H_0^1(\Omega)$ is the gradient of the strongest corner singularity of the Dirichlet Laplacian in the L-shaped domain $\Omega = (-1, 1)^2 \setminus [0, 1]^2$. Thus \mathbf{E} has regularity below $H^1(\Omega)$. We employed the C^{++} classes of the finite element library `deal.II` [8, 7] to compute an approximate solution to (1.14). In Figure 1.1, we plot the field intensity $|\mathbf{E}|$ of an approximation using standard nodal elements (left plot) compared to an approximation with $H(\text{curl}; \Omega)$ -conforming lowest order Nédélec elements of first type (right plot). We clearly see that the corner singularity of \mathbf{E} is not resolved by the $H^1(\Omega)$ -conforming approximation.

1.3.2 An application: Near-field optical microscopy

In near-field optical microscopy, nanoscopic objects are observed in the spectrum of optical light. Thereby, the quality of the observations can highly be influenced by the geometry and materials of the microscope tip. However, methods for the practical construction of tips of a given design require an intensive development phase, and once established, a method is often limited to the production of one specific type of tips. As a consequence, the tuning and testing of the relevant parameters of the tip is usually not feasible by means of practical experiments.

¹URL: www.dealii.org.

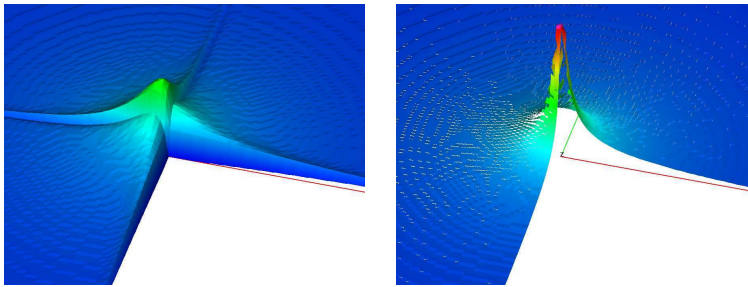


Figure 1.1: Approximation of a singular electric field by nodal elements (left) and edge elements (right). Plot of the field intensity around the re-entrant corner of the computational domain.

The restrictions imposed by practical limitations and economical aspects can however be overcome by the use of adequate mathematical models and simulations.

The electromagnetic fields around the light source of a scanning near-field optical microscope (SNOM) are described by the time-harmonic Maxwell's equations (1.12). In collaboration with Prof. Dr. D. Pohl and Prof. Dr. B. Hecht (Dept. of Physics, University of Basel) we formulated a two-dimensional model that describes the physical phenomena around the end of the tip (the light source) of a SNOM. Based on our implementation of Nédélec elements in `deal.II`, [69], we developed a computational tool, which allows us to recover, for a wide range of tips, the behavior of the electric and magnetic fields in the region around the end of the tip and around a possible sample. For the solution of the linear system resulting from the FEM discretization, we employed the sparse direct solver `PARDISO`² developed in the group of Scientific Computing at the University of Basel.

In Figure 1.2 we see the influence of the geometry of the tip on the electromagnetic fields in the presence of a nanoscopic sample.

In Figure 1.3, we can numerically observe so-called plasmon waves, which are excited by illumination at the surface of a thin metal film on top of an underlying glass plate.

²<http://www.computational.unibas.ch/cs/scicomp/software/pardiso>

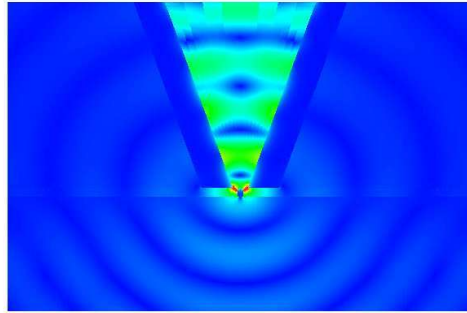


Figure 1.2: Two-dimensional model of the light source of a scanning near field optical microscope (SNOM): Intensity of the electric field around the microscope tip and a silver sample, computed by approximating the time-harmonic Maxwell's equations with Nédélec's edge elements of lowest order on a quadrilateral grid.

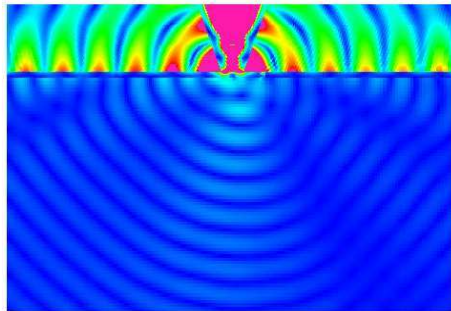


Figure 1.3: Two-dimensional model of the light source of a scanning near field optical microscope: The surface electrons of a thin metal film illuminated by a SNOM excite plasmon waves.

Acknowledgements

This thesis was written at the Mathematical Institute, University of Basel, Switzerland. It was supported by the Swiss National Science Foundation under the projects 21-068126.02 and 200020-105135.

My sincere thanks go to Prof. Dr. Marcus Grote for his excellent support and guidance through my doctoral studies and to Prof. Dr. Ilaria Perugia (Università di Pavia, Italy) for co-advising my thesis, and for her interest and helpful advice.

I am deeply grateful to Prof. Dr. Dominik Schötzau (University of British Columbia, Canada) who introduced me to discontinuous Galerkin methods. His expert knowledge and generous advice contributed significantly to the success of my thesis.

I thank Prof. Dr. Olaf Schenk and Michael Hagemann from the Computer Science Department, University of Basel, for consulting me in numerical solutions of large linear systems and for providing the sparse direct solver PARDISO.

I also thank Dr. Paul Ledger (Swansea University, UK), Prof. Dr. Ralf Hiptmair, Prof. Dr. Peter Arbenz, Prof. Dr. Martin Gutknecht, Dr. Oscar Chinelato (all ETH Zurich, Switzerland) and Prof. Dr. Andreas Prohl (University of Tübingen, Germany) for fruitful discussions on computational electromagnetics, Prof. Dr. Dieter Pohl and Prof. Dr. Bert Hecht (Physics Department, University of Basel) for their collaboration on numerical simulation of nano-optical phenomena, and Prof. Dr. Christoph Schwab for awakening my enthusiasm for numerical analysis during my undergraduate studies at ETH Zurich and for providing me a sound basis for my graduate studies.

Furthermore, my thanks go to my colleagues at the Mathematical Institute in Basel, in particular to Viviana Palumberi, for her friendship and for bringing touch of "Italianità" to our office.

My special thanks go to my parents for their interest, faith and loving support in and beyond my education, to my brother for sharing my company not only during my years in Basel, and, in particular, to Fabian Buchmann for patiently advising me in C++ programming and for wonderful years of love and laughter.

Part I

Interior Penalty Methods for Time-Harmonic Maxwell's Equations

Chapter 2

Interior Penalty Method for the Indefinite Maxwell's Equations

The content of this chapter has been published in Numer. Math. [40] (in collaboration with Paul Houston ¹, Ilaria Perugia ² and Dominik Schötzau ³).

Abstract

In this chapter, we introduce and analyze the interior penalty discontinuous Galerkin method for the numerical discretization of the *indefinite* time-harmonic Maxwell equations in high-frequency regime. Based on suitable duality arguments, we derive a-priori error bounds in the energy norm and the L^2 -norm. In particular, the error in the energy norm is shown to converge with the optimal order $\mathcal{O}(h^{\min\{s,\ell\}})$ with respect to the mesh size h , the polynomial degree ℓ , and the regularity exponent s of the analytical solution. Under additional regularity assumptions, the L^2 -error is shown to converge with the optimal order $\mathcal{O}(h^{\ell+1})$. The theoretical results are confirmed in a series of numerical experiments on triangular meshes.

The thesis' author's principal contributions are the proof of the L^2 -error bound in Section 2.6, and the proof of Lemma 2.4.1

2.1 Introduction

The main motivation for using a discontinuous Galerkin approach for the numerical approximation of the time-harmonic Maxwell's equation (1.12) is that

¹Prof. P. Houston, Department of Mathematics, University of Leicester, Leicester LE1 7RH, England, email: Paul.Houston@mcs.le.ac.uk

²Prof. I. Perugia, Dipartimento di Matematica, Università di Pavia, Via Ferrata 1, 27100 Pavia, Italy, email: perugia@dimat.unipv.it

³Prof. D. Schötzau, Mathematics Department, University of British Columbia, 121-1984 Mathematics Road, Vancouver V6T 1Z2, Canada, email: schoetzau@math.ubc.ca

DG methods, being based on discontinuous finite element spaces, can easily handle non-conforming meshes which contain hanging nodes and, in principle, local spaces of different polynomial orders; for the purposes of this chapter, we shall only consider the h -version of the DG method. Moreover, the implementation of discontinuous elements can be based on standard shape functions, without the need to employ curl-conforming elemental mappings - a convenience that is particularly advantageous for high-order elements and that is not straightforwardly shared by standard edge or face elements commonly used in computational electromagnetics (see [28, 73, 1] and the references therein for hp -adaptive edge element methods). A further benefit of DG methods is that the incorporation of inhomogeneous Dirichlet conditions in the DG context avoids explicit evaluations of edge- and face-element interpolation operators.

The theory presented in this chapter is a continuation of a series of papers that has been concerned with the development of DG finite element methods for the numerical approximation of the time-harmonic Maxwell equations. Indeed, in [62] an hp -local discontinuous Galerkin method was presented for the *low-frequency* approximation of these equations in heterogeneous media. The focus there was on the problem of how to discretize the curl-curl operator using discontinuous finite element spaces. The numerical experiments presented in [43] confirmed the expected hp -convergence rates, and indicate that DG methods can indeed be effective in a wide range of low-frequency applications with *coercive* bilinear forms. Then, in [63], [45], and [44], several *mixed* DG formulations were studied for the discretization of the time-harmonic Maxwell equations in mixed form. The mixed form was chosen to provide control on the divergence of the electric field and arises naturally in certain types of low-frequency models. In particular, it was shown that divergence constraints can be successfully incorporated within the DG framework by means of suitable Lagrange multipliers. Finally, we mention the recent work of [37] where extensive computational studies of DG discretizations applied to Maxwell eigenvalue problems can be found.

In this chapter we present the first numerical analysis of the interior penalty DG finite element method for the numerical discretization of the *indefinite* time-harmonic Maxwell equations (2.1).

We show that the error in the DG energy norm converges with the optimal order $\mathcal{O}(h^{\min\{s,\ell\}})$ with respect to the mesh size h , the polynomial degree ℓ , and the regularity exponent s of the analytical solution. Under additional regularity assumptions, we further prove that the error in the L^2 -norm converges with the full order $\mathcal{O}(h^{\ell+1})$. The derivation of these bounds relies on two crucial technical ingredients: the first one is that, as for conforming discretizations, the error between the analytical solution and its interior penalty approximation is *discretely divergence-free*. The second ingredient is an approximation property that ensures the existence of a conforming finite element function close to any discontinuous one and allows us to control the non-conformity of the method. This approximation property has been established in [40] using the techniques in [45, 44] for the analysis of mixed DG methods and in [49] for the study of a-posteriori error estimation for DG discretizations of diffusion problems. We report its original proof by Houston, Perugia and Schötzau in the Appendix 5.8.

Invoking these auxiliary results, the energy error bound is then derived by suitably modifying the argument in [56] and [55, Section 7.2], while the L^2 -error bound is obtained along the lines of the proof of [54, Theorem 3.2], adapted

to Nédélec's elements of second type. The theoretical error bounds and the performance of the proposed method are tested in a series of numerical examples in two dimensions, performed by Paul Houston.

We note that, being based on duality techniques, the analysis in this paper does not cover the case of non-smooth material coefficients. This is in contrast to the recent techniques developed for conforming methods that allow for non-smooth coefficients. We mention here [9], where the analysis relies on the uniform convergence of the Maxwell resolvent operator and on the abstract theory of [10] for the approximation of nonlinear problems, and [38, 11] (see also [12]), where the analysis is based on the theory of compactly perturbed linear operators and on uniformly stable discrete Helmholtz decompositions.

Recently, Buffa and Perugia [13] provided an alternative approach to show quasi-optimality of DG approximations of the indefinite Maxwell's equations (2.1). Their spectral theory for DG discretizations of the Maxwell Eigenproblem directly proves the well-posedness of the discrete Maxwell source problem (for a sufficiently small mesh size). The validity of a discrete inf-sup condition, together with consistency of the DG form, guarantees optimal order error estimates for the DG approximation of (2.1), also in the case of non-smooth coefficients.

The outline of this chapter is as follows. In Section 2.2, we introduce the interior penalty DG method for the discretization of (2.1). Our main results are the optimal a-priori error bounds stated and discussed in Section 2.3. These results are proved in Sections 2.4 through 2.6 and numerically confirmed in the tests presented in Section 2.7. We end this chapter with concluding remarks in Section 2.8.

2.1.1 Function spaces

For a bounded domain D in \mathbb{R}^3 , we denote by $H^s(D)$ the standard Sobolev space of order $s \geq 0$ and by $\|\cdot\|_{s,D}$ the usual Sobolev norm. When $D = \Omega$, we simply write $\|\cdot\|_s$. For $s = 0$, we write $L^2(D)$ in lieu of $H^0(D)$. We also use $\|\cdot\|_{s,D}$ to denote the norm for the space $H^s(D)^3$. $H_0^1(D)$ is the subspace of $H^1(D)$ of functions with zero trace on ∂D . If Λ is a subset of ∂D , we denote by $\|\cdot\|_{0,\Lambda}$ the L^2 -norm in $L^2(\Lambda)$ and $L^2(\Lambda)^3$. On the computational domain Ω , we introduce the spaces

$$\begin{aligned} H(\text{curl}; \Omega) &= \{ \mathbf{v} \in L^2(\Omega)^3 : \nabla \times \mathbf{v} \in L^2(\Omega)^3 \}, \\ H_0(\text{curl}; \Omega) &= \{ \mathbf{v} \in H(\text{curl}; \Omega) : \mathbf{n} \times \mathbf{v} = \mathbf{0} \text{ on } \Gamma \}, \end{aligned}$$

and endow them with the norm $\|\mathbf{v}\|_{\text{curl}}^2 := \|\mathbf{v}\|_0^2 + \|\nabla \times \mathbf{v}\|_0^2$. Similarly, we set

$$\begin{aligned} H(\text{div}; \Omega) &= \{ \mathbf{v} \in L^2(\Omega)^3 : \nabla \cdot \mathbf{v} \in L^2(\Omega) \}, \\ H_0(\text{div}; \Omega) &= \{ \mathbf{v} \in H(\text{div}; \Omega) : \mathbf{v} \cdot \mathbf{n} = 0 \text{ on } \Gamma \}, \\ H(\text{div}^0; \Omega) &= \{ \mathbf{v} \in H(\text{div}; \Omega) : \nabla \cdot \mathbf{v} = 0 \text{ in } \Omega \}, \end{aligned}$$

equipped with the norm $\|\mathbf{v}\|_{\text{div}}^2 := \|\mathbf{v}\|_0^2 + \|\nabla \cdot \mathbf{v}\|_0^2$. Finally, we denote by (\cdot, \cdot) the standard inner product in $L^2(\Omega)^3$ given by $(\mathbf{u}, \mathbf{v}) := \int_{\Omega} \mathbf{u} \cdot \mathbf{v} \, d\mathbf{x}$.

2.1.2 Model problem

We consider the indefinite time-harmonic Maxwell's equations in a lossless medium with a perfectly conducting boundary: find the (scaled) electric field $\mathbf{u} = \mathbf{u}(\mathbf{x})$ that satisfies

$$\begin{aligned} \nabla \times \nabla \times \mathbf{u} - k^2 \mathbf{u} &= \mathbf{j} && \text{in } \Omega, \\ \mathbf{n} \times \mathbf{u} &= \mathbf{0} && \text{on } \Gamma. \end{aligned} \quad (2.1)$$

Here, Ω is an open bounded Lipschitz polyhedron in \mathbb{R}^3 with boundary $\Gamma = \partial\Omega$ and outward normal unit vector \mathbf{n} . For simplicity, we assume Ω to be simply-connected and Γ to be connected. The right-hand side \mathbf{j} is a given external source field in $L^2(\Omega)^3$ and $k > 0$ is the wave number, i.e., $k = \omega \sqrt{\varepsilon_0 \mu_0}$, where $\omega > 0$ is a given temporal frequency, and ε_0 and μ_0 are the electric permittivity and the magnetic permeability, respectively, of the free space. We point out that we have assumed here that the relative material properties ε_r and μ_r are equal to 1.

The weak form of the equations (2.1) in the Sobolev space

$$H_0(\text{curl}; \Omega) := \{ \mathbf{v} \in L^2(\Omega)^3 : \nabla \times \mathbf{v} \in L^2(\Omega)^3, \mathbf{n} \times \mathbf{v} = \mathbf{0} \text{ on } \Gamma \},$$

reads: find $\mathbf{u} \in H_0(\text{curl}; \Omega)$ such that

$$a(\mathbf{u}, \mathbf{v}) := \int_{\Omega} [\nabla \times \mathbf{u} \cdot \nabla \times \mathbf{v} - k^2 \mathbf{u} \cdot \mathbf{v}] \, d\mathbf{x} = \int_{\Omega} \mathbf{j} \cdot \mathbf{v} \, d\mathbf{x} \quad (2.2)$$

for all $\mathbf{v} \in H_0(\text{curl}; \Omega)$. Under the assumption that k^2 is *not* a Maxwell eigenvalue, problem (2.2) is uniquely solvable; see, e.g., [55, Chapter 4] or [38, Section 5] for details.

2.2 Discontinuous Galerkin discretization

In this section, we introduce the interior penalty DG discretization of (2.1). To this end, we define the following notation.

We consider conforming, shape-regular partitions \mathcal{T}_h of Ω into tetrahedra $\{K\}$; here, h denotes the granularity of the mesh \mathcal{T}_h , i.e., $h = \max_{K \in \mathcal{T}_h} h_K$, where $h_K = \text{diam}(K)$ for all $K \in \mathcal{T}_h$. We denote by \mathcal{F}_h^I the set of all interior faces of \mathcal{T}_h , by \mathcal{F}_h^B the set of all boundary faces of \mathcal{T}_h , and set $\mathcal{F}_h = \mathcal{F}_h^I \cup \mathcal{F}_h^B$.

For piecewise smooth vector- and scalar-valued functions \mathbf{v} and q , respectively, we introduce the following trace operators. Let $F \in \mathcal{F}_h^I$ be an interior face shared by two elements K^+ and K^- with unit outward normal vectors \mathbf{n}^\pm , respectively. Denoting by \mathbf{v}^\pm and q^\pm the traces of \mathbf{v} and q on ∂K^\pm taken from within K^\pm , respectively, we define the *jumps* across F by

$$[[\mathbf{v}]]_T = \mathbf{n}^+ \times \mathbf{v}^+ + \mathbf{n}^- \times \mathbf{v}^-, \quad [[q]]_N = q^+ \mathbf{n}^+ + q^- \mathbf{n}^-,$$

and the *averages* by

$$\{\{\mathbf{v}\}\} = (\mathbf{v}^+ + \mathbf{v}^-)/2, \quad \{\{q\}\} = (q^+ + q^-)/2.$$

On a boundary face $F \in \mathcal{F}_h^B$, we set analogously $[[\mathbf{v}]]_T = \mathbf{n} \times \mathbf{v}$, $[[q]]_N = q \mathbf{n}$, $\{\{\mathbf{v}\}\} = \mathbf{v}$ and $\{\{q\}\} = q$.

For a given partition \mathcal{T}_h of Ω and an approximation order $\ell \geq 1$, we wish to approximate the time-harmonic Maxwell equations (2.1) in the finite element space

$$\mathbf{V}_h := \{\mathbf{v} \in L^2(\Omega)^3 : \mathbf{v}|_K \in \mathcal{P}^\ell(K)^3 \quad \forall K \in \mathcal{T}_h\}, \quad (2.3)$$

where $\mathcal{P}^\ell(K)$ denotes the space of polynomials of total degree at most ℓ on K .

Thereby, we consider the DG method: find $\mathbf{u}_h \in \mathbf{V}_h$ such that

$$a_h(\mathbf{u}_h, \mathbf{v}) = (\mathbf{j}, \mathbf{v}) \quad (2.4)$$

for all $\mathbf{v} \in \mathbf{V}_h$. The discrete form $a_h(\cdot, \cdot)$ is given by

$$\begin{aligned} a_h(\mathbf{u}, \mathbf{v}) := & (\nabla_h \times \mathbf{u}, \nabla_h \times \mathbf{v}) - k^2(\mathbf{u}, \mathbf{v}) - \int_{\mathcal{F}_h} [\![\mathbf{u}]\!]_T \cdot \{\!\{ \nabla_h \times \mathbf{v} \}\!\} ds \\ & - \int_{\mathcal{F}_h} [\![\mathbf{v}]\!]_T \cdot \{\!\{ \nabla_h \times \mathbf{u} \}\!\} ds + \int_{\mathcal{F}_h} \mathbf{a} [\![\mathbf{u}]\!]_T \cdot [\![\mathbf{v}]\!]_T ds. \end{aligned} \quad (2.5)$$

Here, we use ∇_h to denote the elementwise application of the operator ∇ . Further, we use the notation $\int_{\mathcal{F}_h} \varphi ds := \sum_{f \in \mathcal{F}_h} \int_f \varphi ds$. The function $\mathbf{a} \in L^\infty(\mathcal{F}_h)$ is the *interior penalty* stabilization function. To define it, we first introduce \mathbf{h} in $L^\infty(\mathcal{F}_h)$ as

$$\mathbf{h}(\mathbf{x}) := h_f, \quad \mathbf{x} \in f, \quad f \in \mathcal{F}_h,$$

with h_f denoting the diameter of face f . Then we set

$$\mathbf{a} := \alpha \mathbf{h}^{-1}, \quad (2.6)$$

where α is a positive parameter independent of the mesh size and the wave number.

2.3 A-priori error bounds

In this section, we state our main results, namely optimal a-priori error bounds for the DG method (2.4) with respect to a (broken) energy norm and the L^2 -norm.

2.3.1 Gårding inequality

Before stating the error bounds, we need to establish a Gårding-type stability result for the form $a_h(\cdot, \cdot)$. To this end, we set

$$\mathbf{V}(h) := H_0(\text{curl}; \Omega) + \mathbf{V}_h,$$

and define the following DG seminorm and norm on $\mathbf{V}(h)$, respectively:

$$|\mathbf{v}|_{DG}^2 := \|\nabla_h \times \mathbf{v}\|_0^2 + \|\mathbf{h}^{-\frac{1}{2}} [\![\mathbf{v}]\!]_T\|_{0, \mathcal{F}_h}^2, \quad \|\mathbf{v}\|_{DG}^2 := \|\mathbf{v}\|_0^2 + |\mathbf{v}|_{DG}^2.$$

Here, we write $\|\varphi\|_{0, \mathcal{F}_h}^2 := \sum_{f \in \mathcal{F}_h} \|\varphi\|_{0, f}^2$. The norm $\|\cdot\|_{DG}$ can be viewed as the *energy* norm for the discretization under consideration. With this notation, the following Gårding inequality holds.

LEMMA 2.3.1. *There exists a parameter $\alpha_{\min} > 0$, independent of the mesh size and the wave number, such that for $\alpha \geq \alpha_{\min}$ we have*

$$a_h(\mathbf{v}, \mathbf{v}) \geq \beta \|\mathbf{v}\|_{DG}^2 - (k^2 + \beta) \|\mathbf{v}\|_0^2 \quad \text{for all } \mathbf{v} \in \mathbf{V}_h,$$

with a constant $\beta > 0$ independent of the mesh size and the wave number.

Proof. Using standard inverse estimates, it can be readily seen that there is a parameter $\alpha_{\min} > 0$ such that for $\alpha \geq \alpha_{\min}$ we have

$$a_h(\mathbf{v}, \mathbf{v}) \geq \beta |\mathbf{v}|_{DG}^2 - k^2 \|\mathbf{v}\|_0^2 \quad \text{for all } \mathbf{v} \in \mathbf{V}_h,$$

for a constant $\beta > 0$ independent of the mesh size; we refer to [5, 43, 63] for details. The result of the lemma now follows immediately. \square

The condition $\alpha \geq \alpha_{\min} > 0$ is a restriction that is typical for interior penalty methods and may be omitted by using other DG discretizations of the curl-curl operator, such as the non-symmetric interior penalty or the LDG method; see, e.g., [5, 62] for details.

2.3.2 Energy error

We are now ready to state and discuss the following a-priori bound for the error in the energy norm $\|\cdot\|_{DG}$; the detailed proof will be carried out in Section 2.5.

THEOREM 2.3.2. *Assume that the analytical solution \mathbf{u} of (2.1) satisfies the regularity assumption*

$$\mathbf{u} \in H^s(\Omega)^3, \quad \nabla \times \mathbf{u} \in H^s(\Omega)^3, \quad (2.7)$$

for $s > \frac{1}{2}$. Furthermore, let \mathbf{u}_h denote the DG approximation defined by (2.4) with $\alpha \geq \alpha_{\min}$. Then there is a mesh size $h_0 > 0$ such that for $0 < h \leq h_0$, we have the optimal a priori error bound

$$\|\mathbf{u} - \mathbf{u}_h\|_{DG} \leq C h^{\min\{s, \ell\}} \left[\|\mathbf{u}\|_s + \|\nabla \times \mathbf{u}\|_s \right],$$

with a constant $C > 0$ independent of the mesh size.

REMARK 2.3.3. *For a source term $\mathbf{j} \in H(\text{div}; \Omega)$, the regularity assumption in (2.7) is ensured by the embedding results in [4, Proposition 3.7]; see also (2.8) below. In particular, assumption (2.7) is satisfied in the physically most relevant case of a solenoidal forcing term where $\nabla \cdot \mathbf{j} = 0$. In this sense, the smoothness requirement in (2.7) is minimal.*

Proceeding along the lines of [68], we conclude from the a-priori error bound in Theorem 2.3.2 the existence and uniqueness of discrete solutions.

COROLLARY 2.3.4. *For a stabilization parameter $\alpha \geq \alpha_{\min}$, the DG method (2.4) admits a unique solution $\mathbf{u}_h \in \mathbf{V}_h$, provided that $h \leq h_0$.*

Proof. We only need to establish that if $\mathbf{j} = \mathbf{0}$, then the only solution to (2.4) is $\mathbf{u}_h = \mathbf{0}$. In fact, if $\mathbf{j} = \mathbf{0}$, then $\mathbf{u} = \mathbf{0}$, and the estimate of Theorem 2.3.2 implies $\|\mathbf{u}_h\|_{DG} \leq 0$, thereby $\mathbf{u}_h = \mathbf{0}$, for $h \leq h_0$. \square

2.3.3 Error in $L^2(\Omega)^3$

Next, we state an a-priori bound for the error $\|\mathbf{u} - \mathbf{u}_h\|_0$ and show that the optimal order $\mathcal{O}(h^{\ell+1})$ is obtained for smooth solutions and convex domains. To this end, we will use the following embedding from [4, Proposition 3.7]: under the foregoing assumptions on the domain Ω , there exists a regularity exponent $\sigma \in (1/2, 1]$, depending only on Ω , such that

$$\begin{aligned} H_0(\text{curl}; \Omega) \cap H(\text{div}; \Omega) &\hookrightarrow H^\sigma(\Omega)^3, \\ H(\text{curl}; \Omega) \cap H_0(\text{div}; \Omega) &\hookrightarrow H^\sigma(\Omega)^3. \end{aligned} \quad (2.8)$$

The maximal value of σ for which the above embedding holds is closely related to the regularity properties of the Laplacian in polyhedra and only depends on the opening angles at the corners and edges of the domain, cf. [4]. In particular, for a convex domain, (2.8) holds with $\sigma = 1$.

Furthermore, let us denote by $\mathbf{\Pi}_N$ the curl-conforming Nédélec interpolation operator of the second kind into $\mathbf{V}_h \cap H_0(\text{curl}; \Omega)$; see [59] or [55, Section 8.2]. Then, we have the following result.

THEOREM 2.3.5. *Let \mathbf{u} denote the analytical solution of (2.1) and \mathbf{u}_h the DG approximation obtained by (2.4) with $\alpha \geq \alpha_{\min}$. Then there is a mesh size $h_1 > 0$ such that for $0 < h \leq h_1$ we have*

$$\|\mathbf{u} - \mathbf{u}_h\|_0 \leq Ch^\sigma \|\mathbf{u} - \mathbf{u}_h\|_{DG} + Ch^\sigma \|\mathbf{u} - \mathbf{\Pi}_N \mathbf{u}\|_{\text{curl}} + C \|\mathbf{u} - \mathbf{\Pi}_N \mathbf{u}\|_0,$$

with a constant $C > 0$ independent of the mesh size. The parameter $\sigma \in (1/2, 1]$ is the embedding exponent from (2.8).

Under additional smoothness assumptions on the analytical solution \mathbf{u} , the bound in Theorem 2.3.5 combined with the approximation properties for $\mathbf{\Pi}_N$ and the error estimate in Theorem 2.3.2 result in the following L^2 -error bound:

COROLLARY 2.3.6. *Assume that the analytical solution \mathbf{u} of (2.1) satisfies the regularity assumption*

$$\mathbf{u} \in H^{s+\sigma}(\Omega)^3, \quad \nabla \times \mathbf{u} \in H^s(\Omega)^3, \quad (2.9)$$

for $s > \frac{1}{2}$ and the parameter σ from (2.8). Let \mathbf{u}_h denote the DG approximation obtained by (2.4) with $\alpha \geq \alpha_{\min}$. Then there is a mesh size $h_2 > 0$ such that for $0 < h \leq h_2$ we have the a-priori error bound

$$\|\mathbf{u} - \mathbf{u}_h\|_0 \leq Ch^{\min\{s, \ell\} + \sigma} \left[\|\mathbf{u}\|_{s+\sigma} + \|\nabla \times \mathbf{u}\|_s \right],$$

with a constant $C > 0$ independent of the mesh size h .

REMARK 2.3.7. *In particular, for a convex domain where $\sigma = 1$ and an analytical solution $\mathbf{u} \in H^{\ell+1}(\Omega)^3$, Corollary 2.3.6 ensures the optimal error bound*

$$\|\mathbf{u} - \mathbf{u}_h\|_0 \leq Ch^{\ell+1} \|\mathbf{u}\|_{\ell+1},$$

holds, with a constant $C > 0$ independent of the mesh size.

The detailed proofs of Theorem 2.3.5 and Corollary 2.3.6 can be found in Section 2.6.

2.4 Auxiliary results

This section is devoted to the collection of some auxiliary results which will be required throughout the rest of this article. In Section 2.4.1 and Section 2.4.2, we start by recalling some well-known facts from the finite element theory of Maxwell's equations; see, e.g., [38, 55] and the references cited therein. Then, in Section 2.4.3, we present novel approximation results that allow us to control the non-conformity of the interior penalty method. Note that similar approximation techniques have been used in [45, 44] for the analysis of mixed DG methods and in [49] for the derivation of a-posteriori error bounds for DG discretizations of diffusion problems. In Section 2.4.4, we rewrite the interior penalty method (2.4) in a perturbed form and establish crucial properties of this auxiliary formulation. In particular, we show that the error $\mathbf{u} - \mathbf{u}_h$ is discretely divergence-free.

2.4.1 Helmholtz decompositions

We begin by recalling the subsequent continuous Helmholtz decomposition: under the foregoing assumptions on the domain, we have

$$L^2(\Omega)^3 = H(\operatorname{div}^0; \Omega) \oplus \nabla H_0^1(\Omega); \quad (2.10)$$

the decomposition being orthogonal in $L^2(\Omega)^3$; see, e.g., [31, Section 4].

A similar decomposition holds on the discrete level. To this end, we define \mathbf{V}_h^c to be the largest conforming space underlying \mathbf{V}_h , that is,

$$\mathbf{V}_h^c := \mathbf{V}_h \cap H_0(\operatorname{curl}; \Omega). \quad (2.11)$$

In fact, \mathbf{V}_h^c is Nédélec's space of the second kind; see [59] or [55, Section 8.2]. The space \mathbf{V}_h^c can then be decomposed into

$$\mathbf{V}_h^c = \mathbf{X}_h \oplus \nabla S_h, \quad (2.12)$$

with the spaces S_h and \mathbf{X}_h given by

$$S_h := \{q \in H_0^1(\Omega) : q|_K \in \mathcal{P}^{\ell+1}(K), K \in \mathcal{T}_h\}, \quad (2.13)$$

$$\mathbf{X}_h := \{\mathbf{v} \in \mathbf{V}_h^c : (\mathbf{v}, \nabla q) = 0 \ \forall q \in S_h\}, \quad (2.14)$$

respectively. The space \mathbf{X}_h is referred to as the space of *discretely divergence-free* functions. By construction, the decomposition (2.12) is orthogonal in $L^2(\Omega)^3$; cf. [55, Section 8.2].

2.4.2 Standard approximation operators

Next, we introduce standard approximation operators and state their properties. We start by recalling the properties of the curl-conforming Nédélec interpolant $\mathbf{\Pi}_N$ of the second kind.

LEMMA 2.4.1. *There exists a positive constant C , independent of the mesh size, such that, for any $\mathbf{v} \in H_0(\operatorname{curl}; \Omega) \cap H^t(\Omega)^3$ with $\nabla \times \mathbf{v} \in H^t(\Omega)^3$, $t > \frac{1}{2}$,*

$$\|\mathbf{v} - \mathbf{\Pi}_N \mathbf{v}\|_{\operatorname{curl}} \leq C h^{\min\{t, \ell\}} [\|\mathbf{v}\|_t + \|\nabla \times \mathbf{v}\|_t], \quad (2.15)$$

$$\|\nabla \times (\mathbf{v} - \mathbf{\Pi}_N \mathbf{v})\|_0 \leq C h^{\min\{t, \ell\}} \|\nabla \times \mathbf{v}\|_t. \quad (2.16)$$

Moreover, there exists a positive constant C , independent of the mesh size, such that, for any $\mathbf{v} \in H_0(\operatorname{curl}; \Omega) \cap H^{1+t}(\Omega)^3$ with $t > 0$,

$$\|\mathbf{v} - \mathbf{\Pi}_N \mathbf{v}\|_0 \leq C h^{\min\{t, \ell\}+1} \|\mathbf{v}\|_{1+t}. \quad (2.17)$$

Proof. A proof of the first two results can be found in [55, Theorem 5.41, Remark 5.42 and Theorem 8.15].

To prove (2.17), we first consider the case $t \in (0, 1)$ and establish the corresponding estimate on the reference tetrahedron \widehat{K} . From the stability of the Nédélec interpolation operator $\widehat{\mathbf{\Pi}}_N$ in $W^{1,p}(\widehat{K})^3$ for any $p > 2$ (see [55, Lemma 5.38], [54], and references therein) and the embedding $H^{1+t}(\widehat{K})^3 \hookrightarrow W^{1,p}(\widehat{K})^3$ for $p = \frac{6}{3-2t}$ (see, e.g., [55, Theorem 3.7]), we conclude that

$$\begin{aligned} \|\widehat{\mathbf{v}} - \widehat{\mathbf{\Pi}}_N \widehat{\mathbf{v}}\|_{0, \widehat{K}} &\leq \inf_{\widehat{\mathbf{q}} \in \mathcal{P}^\ell(\widehat{K})^3} \left\{ \|\widehat{\mathbf{v}} - \widehat{\mathbf{q}}\|_{0, \widehat{K}} + \|\widehat{\mathbf{\Pi}}_N (\widehat{\mathbf{v}} - \widehat{\mathbf{q}})\|_{0, \widehat{K}} \right\} \\ &\leq C \inf_{\widehat{\mathbf{q}} \in \mathcal{P}^\ell(\widehat{K})^3} \|\widehat{\mathbf{v}} - \widehat{\mathbf{q}}\|_{W^{1,p}(\widehat{K})} \leq C \inf_{\widehat{\mathbf{q}} \in \mathcal{P}^\ell(\widehat{K})^3} \|\widehat{\mathbf{v}} - \widehat{\mathbf{q}}\|_{1+t, \widehat{K}}. \end{aligned}$$

By a Bramble-Hilbert argument for fractional order Sobolev spaces, we therefore obtain

$$\|\widehat{\mathbf{v}} - \widehat{\mathbf{\Pi}}_{\mathbf{N}}\widehat{\mathbf{v}}\|_{0,\widehat{K}} \leq C |\widehat{\mathbf{v}}|_{t+1,\widehat{K}}. \quad (2.18)$$

The bound in (2.17) follows then from (2.18) by a scaling argument. The proof for $t \geq 1$ is carried out similarly, using the H^2 -stability of $\mathbf{\Pi}_{\mathbf{N}}$; see [59]. \square

Furthermore, for any $\mathbf{v} \in H_0(\text{curl}; \Omega)$, we define the projection $\mathbf{\Pi}^c \mathbf{v} \in \mathbf{V}_h^c$ by

$$(\nabla \times (\mathbf{v} - \mathbf{\Pi}^c \mathbf{v}), \nabla \times \mathbf{w}) + (\mathbf{v} - \mathbf{\Pi}^c \mathbf{v}, \mathbf{w}) = 0 \quad \forall \mathbf{w} \in \mathbf{V}_h^c. \quad (2.19)$$

An immediate consequence of this definition is that

$$\|\mathbf{v} - \mathbf{\Pi}^c \mathbf{v}\|_{\text{curl}} = \inf_{\mathbf{w} \in \mathbf{V}_h^c} \|\mathbf{v} - \mathbf{w}\|_{\text{curl}}.$$

Thus, from property (2.15) in Lemma 2.4.1 we obtain the following approximation result.

LEMMA 2.4.2. *There exists a positive constant C , independent of the mesh size, such that, for any $\mathbf{v} \in H_0(\text{curl}; \Omega) \cap H^t(\Omega)^3$ with $\nabla \times \mathbf{v} \in H^t(\Omega)^3$, $t > \frac{1}{2}$,*

$$\|\mathbf{v} - \mathbf{\Pi}^c \mathbf{v}\|_{\text{curl}} \leq C h^{\min\{t,\ell\}} [\|\mathbf{v}\|_t + \|\nabla \times \mathbf{v}\|_t].$$

Next, let us denote by $\mathbf{\Pi}_h$ the L^2 -projection onto \mathbf{V}_h . The following approximation result is well-known.

LEMMA 2.4.3. *There exists a positive constant C , independent of the local mesh sizes h_K , such that, for any $\mathbf{v} \in H^t(K)^3$, $K \in \mathcal{T}_h$, $t > \frac{1}{2}$,*

$$\|\mathbf{v} - \mathbf{\Pi}_h \mathbf{v}\|_{0,K}^2 + h_K \|\mathbf{v} - \mathbf{\Pi}_h \mathbf{v}\|_{0,\partial K}^2 \leq C h_K^{2t} \|\mathbf{v}\|_{t,K}^2.$$

Finally, we recall the following result that allows us to approximate discretely divergence-free functions by exactly divergence-free ones.

LEMMA 2.4.4. *For any discretely divergence-free function $\mathbf{v} \in \mathbf{X}_h$, define $\mathbf{H}\mathbf{v} \in H_0(\text{curl}; \Omega) \cap H(\text{div}^0; \Omega)$ by $\nabla \times \mathbf{H}\mathbf{v} = \nabla \times \mathbf{v}$. Then, there exists a constant $C > 0$ such that*

$$\|\mathbf{v} - \mathbf{H}\mathbf{v}\|_0 \leq C h^\sigma \|\nabla \times \mathbf{v}\|_0,$$

with the parameter σ from (2.8). Moreover, there holds $\|\mathbf{H}\mathbf{v}\|_0 \leq \|\mathbf{v}\|_0$.

The result in Lemma 2.4.4 is obtained by proceeding as in [38, Lemma 4.5] and [55, Lemma 7.6] using Nédélec's second family of elements. The L^2 -stability of \mathbf{H} is a consequence of the L^2 -orthogonality of the continuous Helmholtz decomposition.

2.4.3 Conforming approximation of discontinuous functions

The following approximation result is instrumental in our analysis; it allows us to find a conforming finite element function close to any discontinuous one. This result is obtained by using the same techniques as those in [49, Section 2.1] and

[44, Appendix]. The proof is due to Houston, Perugia and Schötzau. For sake of completeness, we report the original proof in the Appendix of this Thesis.

PROPOSITION 2.4.5. *Let $\mathbf{v} \in \mathbf{V}_h$. Then there is a function $\mathbf{v}^c \in \mathbf{V}_h^c$ such that*

$$\begin{aligned}\|\mathbf{v} - \mathbf{v}^c\|_0^2 &\leq C \int_{\mathcal{F}_h} \mathbf{h} |[\![\mathbf{v}]\!]_T|^2 ds, \\ \|\mathbf{v} - \mathbf{v}^c\|_{DG}^2 &\leq C \int_{\mathcal{F}_h} \mathbf{h}^{-1} |[\![\mathbf{v}]\!]_T|^2 ds,\end{aligned}$$

with a constant $C > 0$ independent of the mesh size.

Proposition 2.4.5 and the definition of the norm $\|\cdot\|_{DG}$ immediately imply the following result.

PROPOSITION 2.4.6. *Let $\mathbf{v} \in \mathbf{V}_h$. Then the conforming approximation $\mathbf{v}^c \in \mathbf{V}_h^c$ from Proposition 2.4.5 satisfies*

$$\begin{aligned}\|\mathbf{v} - \mathbf{v}^c\|_{DG} + \|\mathbf{v}^c\|_{DG} &\leq C \|\mathbf{v}\|_{DG}, \\ \|\mathbf{v} - \mathbf{v}^c\|_0 &\leq Ch \|\mathbf{v}\|_{DG},\end{aligned}$$

with a constant $C > 0$ independent of the mesh size.

We will further need the following consequence of Proposition 2.4.5, which follows from the fact that $[\![\mathbf{w}]\!]_T = \mathbf{0}$ on \mathcal{F}_h , for any $\mathbf{w} \in H_0(\text{curl}; \Omega)$, and the definition of the norm $\|\cdot\|_{DG}$.

PROPOSITION 2.4.7. *Let $\mathbf{v} \in \mathbf{V}_h$ and $\mathbf{w} \in H_0(\text{curl}; \Omega)$. Let $\mathbf{v}^c \in \mathbf{V}_h^c$ be the conforming approximation of \mathbf{v} from Proposition 2.4.5. Then we have*

$$\begin{aligned}\|\mathbf{v} - \mathbf{v}^c\|_{DG} &\leq C \|\mathbf{v} - \mathbf{w}\|_{DG}, \\ \|\mathbf{v} - \mathbf{v}^c\|_0 &\leq Ch \|\mathbf{v} - \mathbf{w}\|_{DG},\end{aligned}$$

with a constant $C > 0$ independent of the mesh size.

2.4.4 Perturbed formulation

Following [5], we rewrite the method (2.4) in a slightly perturbed form. To this end, we define for $\mathbf{v} \in \mathbf{V}(h)$ the lifting $\mathcal{L}(\mathbf{v}) \in \mathbf{V}_h$ by

$$(\mathcal{L}(\mathbf{v}), \mathbf{w}) = \int_{\mathcal{F}_h} [\![\mathbf{v}]\!]_T \cdot \{\!\!\{ \mathbf{w} \}\!\!\} ds \quad \forall \mathbf{w} \in \mathbf{V}_h. \quad (2.20)$$

Then we introduce the form

$$\begin{aligned}\tilde{a}_h(\mathbf{u}, \mathbf{v}) &:= (\nabla_h \times \mathbf{u}, \nabla_h \times \mathbf{v}) - k^2(\mathbf{u}, \mathbf{v}) - (\mathcal{L}(\mathbf{u}), \nabla_h \times \mathbf{v}) \\ &\quad - (\mathcal{L}(\mathbf{v}), \nabla_h \times \mathbf{u}) + \int_{\mathcal{F}_h} \mathbf{a} [\![\mathbf{u}]\!]_T \cdot [\![\mathbf{v}]\!]_T ds.\end{aligned}$$

Note that $a_h = \tilde{a}_h$ in $\mathbf{V}_h \times \mathbf{V}_h$ although this is no longer true in $\mathbf{V}(h) \times \mathbf{V}(h)$. The discrete problem (2.4) can equivalently be formulated as: find $\mathbf{u}_h \in \mathbf{V}_h$ such that

$$\tilde{a}_h(\mathbf{u}_h, \mathbf{v}) = (\mathbf{j}, \mathbf{v}) \quad \forall \mathbf{v} \in \mathbf{V}_h. \quad (2.21)$$

Next, let us establish some useful properties of the form $\tilde{a}_h(\cdot, \cdot)$.

LEMMA 2.4.8. *There holds:*

(i) For $\mathbf{u}, \mathbf{v} \in H_0(\text{curl}; \Omega)$, we have

$$\tilde{a}_h(\mathbf{u}, \mathbf{v}) = a(\mathbf{u}, \mathbf{v}),$$

with the form $a(\cdot, \cdot)$ defined in (2.2).

(ii) There is a constant $\gamma > 0$, independent of the mesh size and the wave number, such that

$$|\tilde{a}_h(\mathbf{u}, \mathbf{v})| \leq (k^2 + \gamma) \|\mathbf{u}\|_{DG} \|\mathbf{v}\|_{DG}$$

for all $\mathbf{u}, \mathbf{v} \in \mathbf{V}(h)$.

Proof. The first property follows from the fact that for $\mathbf{w} \in H_0(\text{curl}; \Omega)$ we have $\mathcal{L}(\mathbf{w}) = \mathbf{0}$ and $[\![\mathbf{w}]\!]_T = \mathbf{0}$ on \mathcal{F}_h . To see the second property, we note that, by the definition of the interior penalty function \mathbf{a} in (2.6), there is a continuity constant $\gamma > 0$ such that

$$|\tilde{a}_h(\mathbf{u}, \mathbf{v})| \leq \gamma \|\mathbf{u}\|_{DG} \|\mathbf{v}\|_{DG} + k^2 \|\mathbf{u}\|_0 \|\mathbf{v}\|_0;$$

see [62, Section 4] or [43, Proposition 1]. The claim now follows from the definition of the DG norm. \square

For the analytical solution \mathbf{u} of (2.1), we define the residual

$$r_h(\mathbf{u}; \mathbf{v}) := \tilde{a}_h(\mathbf{u}, \mathbf{v}) - (\mathbf{j}, \mathbf{v}), \quad \mathbf{v} \in \mathbf{V}_h. \quad (2.22)$$

Thus, if \mathbf{u}_h is the DG approximation in (2.4), we have the error equation

$$\tilde{a}_h(\mathbf{u} - \mathbf{u}_h, \mathbf{v}) = r_h(\mathbf{u}; \mathbf{v}) \quad (2.23)$$

for all $\mathbf{v} \in \mathbf{V}_h$.

LEMMA 2.4.9. *Let \mathbf{u} be the analytical solution of (2.1). Then:*

(i) For $\mathbf{v} \in \mathbf{V}_h \cap H_0(\text{curl}; \Omega)$, we have

$$r_h(\mathbf{u}; \mathbf{v}) = 0.$$

(ii) Additionally, let $\nabla \times \mathbf{u} \in H^s(\Omega)^3$ for $s > \frac{1}{2}$. Then

$$r_h(\mathbf{u}; \mathbf{v}) = \int_{\mathcal{F}_h} [\![\mathbf{v}]\!]_T \cdot \{\!\{ \nabla \times \mathbf{u} - \mathbf{\Pi}_h(\nabla \times \mathbf{u}) \}\!\} ds, \quad \mathbf{v} \in \mathbf{V}_h.$$

Moreover, there holds

$$|r_h(\mathbf{u}; \mathbf{v})| \leq Ch^{\min\{s, \ell\}} \|\mathbf{v}\|_{DG} \|\nabla \times \mathbf{u}\|_s,$$

where C is a positive constant, independent of the mesh size.

Proof. The first claim follows readily from property (i) in Lemma 2.4.8, equation (2.2) and the definition of $r_h(\cdot; \cdot)$. The residual expression in (ii) is obtained as in [62, Lemma 4.10] or [43, Proposition 2] using integration by parts, the definition of $\tilde{a}_h(\cdot, \cdot)$ and $r_h(\cdot; \cdot)$, the defining properties of the L^2 -projection $\mathbf{\Pi}_h$, and the differential equation (2.1). The desired bound for $|r_h(\mathbf{u}; \mathbf{v})|$ follows with the weighted Cauchy-Schwarz inequality, the definition of $\|\cdot\|_{DG}$ and \mathbf{a} in (2.6), and the approximation property in Lemma 2.4.3 for $\mathbf{\Pi}_h$. \square

Finally, let us show that the error $\mathbf{u} - \mathbf{u}_h$ is discretely divergence-free in the following sense.

PROPOSITION 2.4.10. *Let \mathbf{u} be the analytical solution of (2.1) and \mathbf{u}_h the discontinuous Galerkin approximation obtained in (2.4). Then there holds*

$$(\mathbf{u} - \mathbf{u}_h, \nabla q) = 0 \quad \forall q \in S_h,$$

with the space S_h defined in (2.13).

Proof. Note that, for $q \in S_h$, we have $\nabla q \in \mathbf{V}_h \cap H_0(\text{curl}; \Omega)$. Using the error equation (2.23) and property (i) of Lemma 2.4.9 gives

$$\tilde{a}_h(\mathbf{u} - \mathbf{u}_h, \nabla q) = 0 \quad \forall q \in S_h.$$

The definition of $\tilde{a}_h(\cdot, \cdot)$, property (i) of Lemma 2.4.8, and the fact that $\nabla_h \times \nabla q = \mathbf{0}$ and $[\nabla q]_T = \mathbf{0}$ on \mathcal{F}_h result in

$$\tilde{a}_h(\mathbf{u}_h, \nabla q) = -k^2(\mathbf{u}_h, \nabla q) \quad \text{and} \quad \tilde{a}_h(\mathbf{u}, \nabla q) = a(\mathbf{u}, \nabla q) = -k^2(\mathbf{u}, \nabla q).$$

Thereby, the statement of the proposition follows directly. \square

2.5 Proof of Theorem 2.3.2

The proof of Theorem 2.3.2 essentially follows the approach given in [55, Section 7.2] and [56] for conforming finite elements, in combination with the crucial approximation results in Proposition 2.4.5.

2.5.1 A preliminary error bound

In this section, we prove a preliminary error bound along the lines of [55, Lemma 7.5].

PROPOSITION 2.5.1. *Let \mathbf{u} be the analytical solution of (2.1) and \mathbf{u}_h the approximation obtained in (2.4) with $\alpha \geq \alpha_{\min}$. Then there holds*

$$\|\mathbf{u} - \mathbf{u}_h\|_{DG} \leq C \left[\inf_{\mathbf{v} \in \mathbf{V}_h} \|\mathbf{u} - \mathbf{v}\|_{DG} + \mathcal{R}_h(\mathbf{u}) + \mathcal{E}_h(\mathbf{u} - \mathbf{u}_h) \right],$$

with a constant $C > 0$ independent of the mesh size. Here, we set

$$\mathcal{R}_h(\mathbf{u}) := \sup_{\mathbf{0} \neq \mathbf{v} \in \mathbf{V}_h} \frac{r_h(\mathbf{u}; \mathbf{v})}{\|\mathbf{v}\|_{DG}}, \quad \mathcal{E}_h(\mathbf{u} - \mathbf{u}_h) := \sup_{\mathbf{0} \neq \mathbf{v} \in \mathbf{V}_h} \frac{|(\mathbf{u} - \mathbf{u}_h, \mathbf{v})|}{\|\mathbf{v}\|_{DG}}.$$

Proof. Let $\mathbf{v} \in \mathbf{V}_h$ be arbitrary. We first bound $\|\mathbf{v} - \mathbf{u}_h\|_{DG}$. Using the Gårding inequality in Lemma 2.3.1, the definition of $\tilde{a}_h(\cdot, \cdot)$ and the error equation (2.23), we obtain

$$\begin{aligned} \beta \|\mathbf{v} - \mathbf{u}_h\|_{DG}^2 &\leq a_h(\mathbf{v} - \mathbf{u}_h, \mathbf{v} - \mathbf{u}_h) + (k^2 + \beta)(\mathbf{v} - \mathbf{u}_h, \mathbf{v} - \mathbf{u}_h) \\ &= \tilde{a}_h(\mathbf{v} - \mathbf{u}_h, \mathbf{v} - \mathbf{u}_h) + (k^2 + \beta)(\mathbf{v} - \mathbf{u}_h, \mathbf{v} - \mathbf{u}_h) \\ &= \tilde{a}_h(\mathbf{v} - \mathbf{u}, \mathbf{v} - \mathbf{u}_h) + r_h(\mathbf{u}; \mathbf{v} - \mathbf{u}_h) \\ &\quad + (k^2 + \beta)(\mathbf{v} - \mathbf{u}, \mathbf{v} - \mathbf{u}_h) + (k^2 + \beta)(\mathbf{u} - \mathbf{u}_h, \mathbf{v} - \mathbf{u}_h). \end{aligned}$$

From the continuity of $\tilde{a}_h(\cdot, \cdot)$ in (ii) of Lemma 2.4.8 and the definition of \mathcal{R}_h and \mathcal{E}_h , we conclude that

$$\begin{aligned} \|\mathbf{v} - \mathbf{u}_h\|_{DG} &\leq \beta^{-1} \left[(k^2 + \gamma) \|\mathbf{u} - \mathbf{v}\|_{DG} + \mathcal{R}_h(\mathbf{u}) \right. \\ &\quad \left. + (k^2 + \beta) \|\mathbf{u} - \mathbf{v}\|_{DG} + (k^2 + \beta) \mathcal{E}_h(\mathbf{u} - \mathbf{u}_h) \right] \\ &\leq C \left[\|\mathbf{u} - \mathbf{v}\|_{DG} + \mathcal{R}_h(\mathbf{u}) + \mathcal{E}_h(\mathbf{u} - \mathbf{u}_h) \right]. \end{aligned}$$

Applying the triangle inequality gives

$$\begin{aligned} \|\mathbf{u} - \mathbf{u}_h\|_{DG} &\leq \|\mathbf{u} - \mathbf{v}\|_{DG} + \|\mathbf{v} - \mathbf{u}_h\|_{DG} \\ &\leq C \left[\|\mathbf{u} - \mathbf{v}\|_{DG} + \mathcal{R}_h(\mathbf{u}) + \mathcal{E}_h(\mathbf{u} - \mathbf{u}_h) \right]. \end{aligned}$$

Taking the infimum over $\mathbf{v} \in \mathbf{V}_h$ gives the assertion. \square

2.5.2 Estimate of $\mathcal{E}_h(\mathbf{u} - \mathbf{u}_h)$

Next, we estimate the error term $\mathcal{E}_h(\mathbf{u} - \mathbf{u}_h)$ defined in Proposition 2.5.1.

PROPOSITION 2.5.2. *There exists a positive constant C , independent of the mesh size, such that*

$$\mathcal{E}_h(\mathbf{u} - \mathbf{u}_h) \leq Ch^\sigma \|\mathbf{u} - \mathbf{u}_h\|_{DG},$$

with the parameter $\sigma \in (1/2, 1]$ from (2.8).

Proof. Fix $\mathbf{v} \in \mathbf{V}_h$, and let $\mathbf{v}^c \in \mathbf{V}_h^c$ be the conforming approximation of \mathbf{v} from Proposition 2.4.5. We bound $(\mathbf{u} - \mathbf{u}_h, \mathbf{v})$ in the following steps.

Step 1. Representation result: using the Helmholtz decomposition (2.12), we decompose \mathbf{v}^c as

$$\mathbf{v}^c = \mathbf{v}_0^c \oplus \nabla r, \quad (2.24)$$

with $\mathbf{v}_0^c \in \mathbf{X}_h$ and $r \in S_h$. Employing (2.24), we obtain

$$\begin{aligned} (\mathbf{u} - \mathbf{u}_h, \mathbf{v}) &= (\mathbf{u} - \mathbf{u}_h, \mathbf{v} - \mathbf{v}^c) + (\mathbf{u} - \mathbf{u}_h, \mathbf{v}^c) = (\mathbf{u} - \mathbf{u}_h, \mathbf{v} - \mathbf{v}^c) + (\mathbf{u} - \mathbf{u}_h, \mathbf{v}_0^c) \\ &= (\mathbf{u} - \mathbf{u}_h, \mathbf{v} - \mathbf{v}^c) + (\mathbf{u} - \mathbf{u}_h, \mathbf{v}_0^c - \mathbf{H}\mathbf{v}_0^c) + (\mathbf{u} - \mathbf{u}_h, \mathbf{H}\mathbf{v}_0^c) \\ &\equiv T_1 + T_2 + T_3, \end{aligned}$$

with $\mathbf{H}\mathbf{v}_0^c$ from Lemma 2.4.4. Here, we have used the orthogonality property of the error $\mathbf{u} - \mathbf{u}_h$ in Proposition 2.4.10. It remains to bound the terms T_1 , T_2 and T_3 .

Step 2. Bound for T_1 : the Cauchy-Schwarz inequality and the approximation result in Proposition 2.4.6 yields

$$|T_1| \leq \|\mathbf{u} - \mathbf{u}_h\|_0 \|\mathbf{v} - \mathbf{v}^c\|_0 \leq Ch \|\mathbf{u} - \mathbf{u}_h\|_0 \|\mathbf{v}\|_{DG}. \quad (2.25)$$

Step 3. Bound for T_2 : using the Cauchy-Schwarz inequality and the approximation results in Lemma 2.4.4 and Proposition 2.4.6, we have

$$\begin{aligned} |T_2| &\leq \|\mathbf{u} - \mathbf{u}_h\|_0 \|\mathbf{v}_0^c - \mathbf{H}\mathbf{v}_0^c\|_0 \leq Ch^\sigma \|\mathbf{u} - \mathbf{u}_h\|_0 \|\nabla \times \mathbf{v}_0^c\|_0 \\ &= Ch^\sigma \|\mathbf{u} - \mathbf{u}_h\|_0 \|\nabla \times \mathbf{v}^c\|_0 \leq Ch^\sigma \|\mathbf{u} - \mathbf{u}_h\|_0 \|\mathbf{v}^c\|_{DG} \\ &\leq Ch^\sigma \|\mathbf{u} - \mathbf{u}_h\|_0 \|\mathbf{v}\|_{DG}. \end{aligned} \quad (2.26)$$

Step 4. Bound for T_3 : to bound T_3 , we use a duality approach. To this end, we set $\mathbf{w} := \mathbf{H}\mathbf{v}_0^c$ and let \mathbf{z} denote the solution of the following problem:

$$\begin{aligned} \nabla \times \nabla \times \mathbf{z} - k^2 \mathbf{z} &= \mathbf{w} && \text{in } \Omega, \\ \mathbf{n} \times \mathbf{z} &= \mathbf{0} && \text{on } \Gamma. \end{aligned} \quad (2.27)$$

Since $\mathbf{w} \in H(\operatorname{div}^0; \Omega)$, the solution \mathbf{z} belongs to $H(\operatorname{div}^0; \Omega)$. As in [55, Lemma 7.7], we obtain from the embeddings in (2.8) that $\mathbf{z} \in H^\sigma(\Omega)^3$, $\nabla \times \mathbf{z} \in H^\sigma(\Omega)^3$ and

$$\|\mathbf{z}\|_\sigma + \|\nabla \times \mathbf{z}\|_\sigma \leq C \|\mathbf{w}\|_0, \quad (2.28)$$

for a stability constant $C > 0$ and the parameter $\sigma \in (1/2, 1]$ in (2.8).

Hence, multiplying the dual problem with $\mathbf{e}_h := \mathbf{u} - \mathbf{u}_h$ and integrating by parts, since $\nabla \times \mathbf{z} \in H(\operatorname{curl}; \Omega)$, we obtain

$$\begin{aligned} (\mathbf{e}_h, \mathbf{w}) &= (\nabla \times \mathbf{z}, \nabla_h \times \mathbf{e}_h) - k^2(\mathbf{z}, \mathbf{e}_h) - \sum_{K \in \mathcal{T}_h} \int_{\partial K} \mathbf{n}_K \times \mathbf{e}_h \cdot \nabla \times \mathbf{z} \, ds \\ &= (\nabla \times \mathbf{z}, \nabla_h \times \mathbf{e}_h) - k^2(\mathbf{z}, \mathbf{e}_h) - \int_{\mathcal{F}_h} \llbracket \mathbf{e}_h \rrbracket_T \cdot \llbracket \nabla \times \mathbf{z} \rrbracket \, ds. \end{aligned}$$

Let $\mathbf{z}_h = \mathbf{\Pi}_N \mathbf{z} \in \mathbf{V}_h^c$ be the Nédélec interpolant of the second kind of \mathbf{z} in (2.15) of Lemma 2.4.1, and $\mathbf{\Pi}_h$ the L^2 -projection onto \mathbf{V}_h . Using the definition of $\tilde{a}_h(\cdot, \cdot)$, the fact that $\mathbf{z} \in H_0(\operatorname{curl}; \Omega)$, the error equation (2.23), property (i) of Lemma 2.4.9, and the definition of $\mathbf{\Pi}_h$ and \mathcal{L} , we obtain

$$\begin{aligned} (\mathbf{e}_h, \mathbf{w}) &= \tilde{a}_h(\mathbf{e}_h, \mathbf{z}) + (\mathcal{L}(\mathbf{e}_h), \nabla \times \mathbf{z}) - \int_{\mathcal{F}_h} \llbracket \mathbf{e}_h \rrbracket_T \cdot \llbracket \nabla \times \mathbf{z} \rrbracket \, ds \\ &= \tilde{a}_h(\mathbf{e}_h, \mathbf{z} - \mathbf{z}_h) + (\mathcal{L}(\mathbf{e}_h), \mathbf{\Pi}_h(\nabla \times \mathbf{z})) - \int_{\mathcal{F}_h} \llbracket \mathbf{e}_h \rrbracket_T \cdot \llbracket \nabla \times \mathbf{z} \rrbracket \, ds \\ &= \tilde{a}_h(\mathbf{e}_h, \mathbf{z} - \mathbf{z}_h) - \int_{\mathcal{F}_h} \llbracket \mathbf{e}_h \rrbracket_T \cdot \llbracket \nabla \times \mathbf{z} - \mathbf{\Pi}_h(\nabla \times \mathbf{z}) \rrbracket \, ds. \end{aligned}$$

First, we note that, employing the weighted Cauchy-Schwarz inequality, the approximation properties in Lemma 2.4.3 and the stability bound (2.28), we get

$$\begin{aligned} &\left| \int_{\mathcal{F}_h} \llbracket \mathbf{e}_h \rrbracket_T \cdot \llbracket \nabla \times \mathbf{z} - \mathbf{\Pi}_h(\nabla \times \mathbf{z}) \rrbracket \, ds \right| \\ &\leq C \left(\int_{\mathcal{F}_h} \mathbf{h}^{-1} |\llbracket \mathbf{e}_h \rrbracket_T|^2 \, ds \right)^{\frac{1}{2}} \left(\sum_{K \in \mathcal{T}_h} h_K \|\nabla \times \mathbf{z} - \mathbf{\Pi}_h(\nabla \times \mathbf{z})\|_{0, \partial K}^2 \right)^{\frac{1}{2}} \\ &\leq Ch^\sigma \|\mathbf{e}_h\|_{DG} \|\nabla \times \mathbf{z}\|_\sigma \leq Ch^\sigma \|\mathbf{e}_h\|_{DG} \|\mathbf{w}\|_0. \end{aligned}$$

Furthermore, the continuity of $\tilde{a}_h(\cdot, \cdot)$ in Lemma 2.4.8, the approximation property (2.15) in Lemma 2.4.1 and the stability estimate (2.28) yield

$$\tilde{a}_h(\mathbf{e}_h, \mathbf{z} - \mathbf{z}_h) \leq Ch^\sigma \|\mathbf{e}_h\|_{DG} \|\mathbf{w}\|_0.$$

Combining the above bounds gives

$$(\mathbf{e}_h, \mathbf{w}) \leq Ch^\sigma \|\mathbf{e}_h\|_{DG} \|\mathbf{w}\|_0.$$

Since $\|\mathbf{w}\|_0 \leq \|\mathbf{v}_0^c\|_0 \leq \|\mathbf{v}^c\|_0 \leq C\|\mathbf{v}\|_{DG}$, in view of Lemma 2.4.4 and Proposition 2.4.6, we conclude that

$$|T_3| \leq Ch^\sigma \|\mathbf{u} - \mathbf{u}_h\|_{DG} \|\mathbf{v}\|_{DG}. \quad (2.29)$$

Step 5. Conclusion: referring to (2.25), (2.26) and (2.29) yields

$$|(\mathbf{u} - \mathbf{u}_h, \mathbf{v})| \leq Ch^\sigma \|\mathbf{u} - \mathbf{u}_h\|_{DG} \|\mathbf{v}\|_{DG},$$

from where the assertion follows. \square

2.5.3 The error bound in Theorem 2.3.2

We are now ready to complete the proof of Theorem 2.3.2. From Proposition 2.5.1 and Proposition 2.5.2, we obtain

$$\begin{aligned} \|\mathbf{u} - \mathbf{u}_h\|_{DG} &\leq C \left[\inf_{\mathbf{v} \in \mathbf{V}_h} \|\mathbf{u} - \mathbf{v}\|_{DG} + \mathcal{R}_h(\mathbf{u}) + \mathcal{E}_h(\mathbf{u} - \mathbf{u}_h) \right] \\ &\leq C \left[\inf_{\mathbf{v} \in \mathbf{V}_h} \|\mathbf{u} - \mathbf{v}\|_{DG} + \mathcal{R}_h(\mathbf{u}) + h^\sigma \|\mathbf{u} - \mathbf{u}_h\|_{DG} \right]. \end{aligned} \quad (2.30)$$

Hence, if the mesh size is sufficiently small we can absorb the third term on the right-hand of (2.30) into the left-hand side; thereby,

$$\|\mathbf{u} - \mathbf{u}_h\|_{DG} \leq C \left[\inf_{\mathbf{v} \in \mathbf{V}_h} \|\mathbf{u} - \mathbf{v}\|_{DG} + \mathcal{R}_h(\mathbf{u}) \right].$$

Choosing $\mathbf{v} = \mathbf{\Pi}_N \mathbf{u}$, the Nédélec interpolant of \mathbf{u} , from the interpolation estimate (2.15) in Lemma 2.4.1 and the estimate of the residual in (ii) of Lemma 2.4.9 give the result in Theorem 2.3.2.

2.6 Proof of Theorem 2.3.5 and Corollary 2.3.6

In this section, we complete the proof of Theorem 2.3.5 and Corollary 2.3.6. Our analysis proceeds along the lines of [54, Section 4].

2.6.1 Proof of Theorem 2.3.5

In order to prove Theorem 2.3.5, let $\mathbf{u}_h^c \in \mathbf{V}_h^c$ be the conforming approximation of \mathbf{u}_h from Proposition 2.4.5. We can write

$$\|\mathbf{u} - \mathbf{u}_h\|_0^2 = (\mathbf{u} - \mathbf{u}_h, \mathbf{u} - \mathbf{\Pi}_N \mathbf{u}) + (\mathbf{u} - \mathbf{u}_h, \mathbf{\Pi}_N \mathbf{u} - \mathbf{u}_h^c) + (\mathbf{u} - \mathbf{u}_h, \mathbf{u}_h^c - \mathbf{u}_h).$$

By using the Cauchy-Schwarz inequality and Proposition 2.4.7, we have

$$\|\mathbf{u} - \mathbf{u}_h\|_0 \leq \|\mathbf{u} - \mathbf{\Pi}_N \mathbf{u}\|_0 + Ch \|\mathbf{u} - \mathbf{u}_h\|_{DG} + \frac{|(\mathbf{u} - \mathbf{u}_h, \mathbf{\Pi}_N \mathbf{u} - \mathbf{u}_h^c)|}{\|\mathbf{u} - \mathbf{u}_h\|_0}, \quad (2.31)$$

with $C > 0$ independent of the mesh size. For the last term on the right-hand side of (2.31), we claim that, for a sufficiently small mesh size, there holds:

$$\frac{|(\mathbf{u} - \mathbf{u}_h, \mathbf{\Pi}_N \mathbf{u} - \mathbf{u}_h^c)|}{\|\mathbf{u} - \mathbf{u}_h\|_0} \leq C \|\mathbf{u} - \mathbf{\Pi}_N \mathbf{u}\|_0 + Ch^\sigma [\|\mathbf{u} - \mathbf{\Pi}_N \mathbf{u}\|_{\text{curl}} + \|\mathbf{u} - \mathbf{u}_h\|_{DG}], \quad (2.32)$$

with $C > 0$ independent of the mesh size, and σ denoting the parameter in (2.8). Inserting (2.32) into (2.31) then proves Theorem 2.3.5.

In order to prove (2.32), we proceed in several steps.

Step 1. Preliminaries: we start by invoking the Helmholtz decomposition in (2.12) and write

$$\mathbf{\Pi}_N \mathbf{u} - \mathbf{u}_h^c =: \mathbf{w}_0^c \oplus \nabla r, \quad (2.33)$$

with $\mathbf{w}_0^c \in \mathbf{X}_h$ and $r \in S_h$, \mathbf{X}_h and S_h being the spaces in (2.13). By using (2.33) and the orthogonality property of the error $\mathbf{u} - \mathbf{u}_h$ in Proposition 2.4.10, we have

$$(\mathbf{u} - \mathbf{u}_h, \mathbf{\Pi}_N \mathbf{u} - \mathbf{u}_h^c) = (\mathbf{u} - \mathbf{u}_h, \mathbf{w}_0^c) = (\mathbf{u} - \mathbf{u}_h, \mathbf{w}_0^c - \mathbf{w}) + (\mathbf{u} - \mathbf{u}_h, \mathbf{w}),$$

where we have defined $\mathbf{w} := \mathbf{H}\mathbf{w}_0^c$, the exactly divergence-free approximation of \mathbf{w}_0^c from Lemma 2.4.4. Therefore,

$$\frac{|(\mathbf{u} - \mathbf{u}_h, \mathbf{\Pi}_N \mathbf{u} - \mathbf{u}_h^c)|}{\|\mathbf{u} - \mathbf{u}_h\|_0} \leq \|\mathbf{w}_0^c - \mathbf{w}\|_0 + \|\mathbf{w}\|_0, \quad (2.34)$$

so that it remains to estimate $\|\mathbf{w}_0^c - \mathbf{w}\|_0$ and $\|\mathbf{w}\|_0$.

Step 2: Estimate of $\|\mathbf{w}_0^c - \mathbf{w}\|_0$: we claim that

$$\|\mathbf{w}_0^c - \mathbf{w}\|_0 \leq Ch^\sigma [\|\mathbf{u} - \mathbf{\Pi}_N \mathbf{u}\|_{\text{curl}} + \|\mathbf{u} - \mathbf{u}_h\|_{DG}], \quad (2.35)$$

with a constant $C > 0$ independent of the mesh size.

To prove (2.35), note that, in view of the definition of \mathbf{H} and (2.33), there holds

$$\nabla \times \mathbf{w} = \nabla \times \mathbf{w}_0^c = \nabla \times (\mathbf{\Pi}_N \mathbf{u} - \mathbf{u}_h^c). \quad (2.36)$$

Thus, the result in Lemma 2.4.4, the triangle inequality and Proposition 2.4.7 yield

$$\begin{aligned} \|\mathbf{w}_0^c - \mathbf{w}\|_0 &\leq Ch^\sigma \|\nabla \times (\mathbf{\Pi}_N \mathbf{u} - \mathbf{u}_h^c)\|_0 \\ &\leq Ch^\sigma [\|\nabla \times (\mathbf{\Pi}_N \mathbf{u} - \mathbf{u})\|_0 + \|\nabla_h \times (\mathbf{u} - \mathbf{u}_h)\|_0 + \|\nabla_h \times (\mathbf{u}_h - \mathbf{u}_h^c)\|_0] \\ &\leq Ch^\sigma [\|\mathbf{u} - \mathbf{\Pi}_N \mathbf{u}\|_{\text{curl}} + \|\mathbf{u} - \mathbf{u}_h\|_{DG}]. \end{aligned}$$

This completes the proof of (2.35).

Step 3: Estimate of $\|\mathbf{w}\|_0$: we bound $\|\mathbf{w}\|_0$ in (2.34) employing a duality approach and claim that, for a sufficiently small mesh size, there holds

$$\|\mathbf{w}\|_0 \leq C\|\mathbf{u} - \mathbf{\Pi}_N \mathbf{u}\|_0 + Ch^\sigma [\|\mathbf{u} - \mathbf{\Pi}_N \mathbf{u}\|_{\text{curl}} + \|\mathbf{u} - \mathbf{u}_h\|_{DG}], \quad (2.37)$$

with a constant $C > 0$ independent of the mesh size.

Let \mathbf{z} be the solution of the dual problem (2.27) with right-hand side $\mathbf{w} = \mathbf{H}\mathbf{w}_0^c$. Again, $\mathbf{w} \in H(\text{div}^0; \Omega)$, so that \mathbf{z} has the same smoothness as in the proof of Proposition 2.5.2 and (2.28) still holds. Moreover, let $\mathbf{z}_h \in \mathbf{V}_h$ solve the discontinuous Galerkin approximation of the dual problem (2.27):

$$\tilde{a}_h(\mathbf{z}_h, \mathbf{v}) = (\mathbf{w}, \mathbf{v}) \quad \forall \mathbf{v} \in \mathbf{V}_h. \quad (2.38)$$

For a sufficiently small mesh size, Theorem 2.3.2 and Corollary 2.3.4 apply to (2.38) and ensure existence and uniqueness of \mathbf{z}_h , as well as the a-priori bound

$$\|\mathbf{z} - \mathbf{z}_h\|_{DG} \leq Ch^\sigma [\|\mathbf{z}\|_\sigma + \|\nabla \times \mathbf{z}\|_\sigma] \leq Ch^\sigma \|\mathbf{w}\|_0, \quad (2.39)$$

where we have taken into account the stability bound (2.28).

After these preliminary considerations, we multiply equation (2.27) by \mathbf{w} and integrate by parts to obtain

$$\|\mathbf{w}\|_0^2 = a(\mathbf{z}, \mathbf{w}) = a(\mathbf{z} - \mathbf{\Pi}^c \mathbf{z}, \mathbf{w}) + a(\mathbf{\Pi}^c \mathbf{z}, \mathbf{w}), \quad (2.40)$$

with the projection $\mathbf{\Pi}^c$ from (2.19). By the definition of the projection $\mathbf{\Pi}^c$ and since $\nabla \times \mathbf{w} = \nabla \times \mathbf{w}_0^c$, we conclude that

$$\begin{aligned} a(\mathbf{z} - \mathbf{\Pi}^c \mathbf{z}, \mathbf{w}) &= -(\mathbf{z} - \mathbf{\Pi}^c \mathbf{z}, \mathbf{w}_0^c) - k^2(\mathbf{z} - \mathbf{\Pi}^c \mathbf{z}, \mathbf{w}) \\ &= -(\mathbf{z} - \mathbf{\Pi}^c \mathbf{z}, \mathbf{w}_0^c - \mathbf{w}) - (1 + k^2)(\mathbf{z} - \mathbf{\Pi}^c \mathbf{z}, \mathbf{w}). \end{aligned}$$

The approximation result for $\mathbf{\Pi}^c$ in Lemma 2.4.2 and the bound in (2.28) yield

$$\|\mathbf{z} - \mathbf{\Pi}^c \mathbf{z}\|_0 \leq \|\mathbf{z} - \mathbf{\Pi}^c \mathbf{z}\|_{\text{curl}} \leq Ch^\sigma \|\mathbf{w}\|_0. \quad (2.41)$$

For later use, we also point out that the stability of $\mathbf{\Pi}^c$ and (2.28) give

$$\|\mathbf{\Pi}^c \mathbf{z}\|_0 \leq C \|\mathbf{w}\|_0. \quad (2.42)$$

Hence, the Cauchy-Schwarz inequality and the estimates (2.35) and (2.41) yield

$$\begin{aligned} |a(\mathbf{z} - \mathbf{\Pi}^c \mathbf{z}, \mathbf{w})| &\leq \|\mathbf{z} - \mathbf{\Pi}^c \mathbf{z}\|_0 \|\mathbf{w} - \mathbf{w}_0^c\|_0 + C \|\mathbf{z} - \mathbf{\Pi}^c \mathbf{z}\|_0 \|\mathbf{w}\|_0 \\ &\leq Ch^{2\sigma} \|\mathbf{w}\|_0 [\|\mathbf{u} - \mathbf{\Pi}_N \mathbf{u}\|_{\text{curl}} + \|\mathbf{u} - \mathbf{u}_h\|_{DG}] + Ch^\sigma \|\mathbf{w}\|_0^2. \end{aligned} \quad (2.43)$$

It remains to bound the term $a(\mathbf{\Pi}^c \mathbf{z}, \mathbf{w})$ in (2.40). To this end, in view of (2.36) and (2.33), we first note that

$$\begin{aligned} a(\mathbf{\Pi}^c \mathbf{z}, \mathbf{w}) &= (\nabla \times \mathbf{\Pi}^c \mathbf{z}, \nabla \times \mathbf{w}) - k^2(\mathbf{\Pi}^c \mathbf{z}, \mathbf{w}) \\ &= (\nabla \times \mathbf{\Pi}^c \mathbf{z}, \nabla \times (\mathbf{\Pi}_N \mathbf{u} - \mathbf{u}_h^c)) - k^2(\mathbf{\Pi}^c \mathbf{z}, \mathbf{w} - \mathbf{w}_0^c) - k^2(\mathbf{\Pi}^c \mathbf{z}, \mathbf{w}_0^c) \\ &= (\nabla \times \mathbf{\Pi}^c \mathbf{z}, \nabla \times (\mathbf{\Pi}_N \mathbf{u} - \mathbf{u}_h^c)) - k^2(\mathbf{\Pi}^c \mathbf{z}, \mathbf{w} - \mathbf{w}_0^c) - k^2(\mathbf{\Pi}^c \mathbf{z}, \mathbf{\Pi}_N \mathbf{u} - \mathbf{u}_h^c) \\ &= a(\mathbf{\Pi}^c \mathbf{z}, \mathbf{\Pi}_N \mathbf{u} - \mathbf{u}_h^c) - k^2(\mathbf{\Pi}^c \mathbf{z}, \mathbf{w} - \mathbf{w}_0^c). \end{aligned}$$

Here, we have used that

$$(\mathbf{\Pi}^c \mathbf{z}, \nabla r) = (\mathbf{z}, \nabla r) = 0,$$

which follows readily from the definition of $\mathbf{\Pi}^c$ and the fact that \mathbf{z} is divergence-free. From the identity (i) in Lemma 2.4.8, we further have

$$a(\mathbf{\Pi}^c \mathbf{z}, \mathbf{\Pi}_N \mathbf{u} - \mathbf{u}_h^c) = a(\mathbf{\Pi}^c \mathbf{z}, \mathbf{\Pi}_N \mathbf{u} - \mathbf{u}) + \tilde{a}_h(\mathbf{\Pi}^c \mathbf{z}, \mathbf{u} - \mathbf{u}_h) + \tilde{a}_h(\mathbf{\Pi}^c \mathbf{z}, \mathbf{u}_h - \mathbf{u}_h^c).$$

Using the symmetry of $\tilde{a}_h(\cdot, \cdot)$, the error equation (2.23), and part (i) of Lemma 2.4.9, we note that $\tilde{a}_h(\mathbf{\Pi}^c \mathbf{z}, \mathbf{u} - \mathbf{u}_h) = 0$. Thus, by further decompositions, we can write

$$\begin{aligned} a(\mathbf{\Pi}^c \mathbf{z}, \mathbf{w}) &= a(\mathbf{\Pi}^c \mathbf{z} - \mathbf{z}, \mathbf{\Pi}_N \mathbf{u} - \mathbf{u}) + a(\mathbf{z}, \mathbf{\Pi}_N \mathbf{u} - \mathbf{u}) \\ &\quad + \tilde{a}_h(\mathbf{\Pi}^c \mathbf{z} - \mathbf{z}, \mathbf{u}_h - \mathbf{u}_h^c) + \tilde{a}_h(\mathbf{z} - \mathbf{z}_h, \mathbf{u}_h - \mathbf{u}_h^c) \\ &\quad + \tilde{a}_h(\mathbf{z}_h, \mathbf{u}_h - \mathbf{u}_h^c) - k^2(\mathbf{\Pi}^c \mathbf{z}, \mathbf{w} - \mathbf{w}_0^c), \end{aligned} \quad (2.44)$$

with \mathbf{z}_h denoting the approximation (2.38) of the dual problem (2.27).

Using the dual problem (2.27) and the discrete formulation (2.38), we have

$$a(\mathbf{z}, \mathbf{\Pi}_N \mathbf{u} - \mathbf{u}) = (\mathbf{w}, \mathbf{\Pi}_N \mathbf{u} - \mathbf{u}), \quad \tilde{a}_h(\mathbf{z}_h, \mathbf{u}_h - \mathbf{u}_h^c) = (\mathbf{w}, \mathbf{u}_h - \mathbf{u}_h^c).$$

These identities, together with the continuity property (ii) in Lemma 2.4.8 and the Cauchy-Schwarz inequality, give

$$\begin{aligned} |a(\mathbf{\Pi}^c \mathbf{z}, \mathbf{w})| &\leq C \|\mathbf{z} - \mathbf{\Pi}^c \mathbf{z}\|_{\text{curl}} \|\mathbf{u} - \mathbf{\Pi}_N \mathbf{u}\|_{\text{curl}} + \|\mathbf{w}\|_0 \|\mathbf{u} - \mathbf{\Pi}_N \mathbf{u}\|_0 \\ &\quad + C \|\mathbf{u}_h - \mathbf{u}_h^c\|_{DG} \left[\|\mathbf{z} - \mathbf{\Pi}^c \mathbf{z}\|_{\text{curl}} + \|\mathbf{z} - \mathbf{z}_h\|_{DG} \right] \\ &\quad + \|\mathbf{w}\|_0 \|\mathbf{u}_h - \mathbf{u}_h^c\|_0 + C \|\mathbf{\Pi}^c \mathbf{z}\|_0 \|\mathbf{w} - \mathbf{w}_0^c\|_0. \end{aligned}$$

From Proposition 2.4.7, we have

$$\|\mathbf{u}_h - \mathbf{u}_h^c\|_{DG} \leq C \|\mathbf{u} - \mathbf{u}_h\|_{DG}, \quad \|\mathbf{u}_h - \mathbf{u}_h^c\|_0 \leq Ch \|\mathbf{u} - \mathbf{u}_h\|_{DG}.$$

Thus, using (2.41), (2.39), (2.42) and (2.35), we conclude that

$$a(\mathbf{\Pi}^c \mathbf{z}, \mathbf{w}) \leq \|\mathbf{w}\|_0 \left[Ch^\sigma \|\mathbf{u} - \mathbf{\Pi}_N \mathbf{u}\|_{\text{curl}} + Ch^\sigma \|\mathbf{u} - \mathbf{u}_h\|_{DG} + \|\mathbf{u} - \mathbf{\Pi}_N \mathbf{u}\|_0 \right]. \quad (2.45)$$

Inserting (2.43) and (2.45) into (2.40) results in

$$\|\mathbf{w}\|_0 \leq \|\mathbf{u} - \mathbf{\Pi}_N \mathbf{u}\|_0 + Ch^\sigma \left[\|\mathbf{u} - \mathbf{\Pi}_N \mathbf{u}\|_{\text{curl}} + \|\mathbf{u} - \mathbf{u}_h\|_{DG} \right] + Ch^\sigma \|\mathbf{w}\|_0. \quad (2.46)$$

Hence, for a sufficiently small mesh size, we obtain the result in (2.37).

Step 4. Conclusion: the proof of the bound (2.32) follows now from (2.34), (2.35) and (2.46).

2.6.2 Proof of Corollary 2.3.6

To complete the proof of Corollary 2.3.6, we note that Theorem 2.3.5, Theorem 2.3.2 and the approximation property (2.17) in Lemma 2.4.1 for $\mathbf{\Pi}_N$ result in

$$\|\mathbf{u} - \mathbf{u}_h\|_0 \leq Ch^{\min\{s, \ell\} + \sigma} \left[\|\mathbf{u}\|_s + \|\nabla \times \mathbf{u}\|_s \right] + Ch^{\min\{s + \sigma, \ell + 1\}} \|\mathbf{u}\|_{s + \sigma}.$$

Since $\|\mathbf{u}\|_s \leq \|\mathbf{u}\|_{s + \sigma}$ and $\min\{s + \sigma, \ell + 1\} \geq \min\{s, \ell\} + \sigma$, the assertion of Corollary 2.3.6 follows.

2.7 Numerical experiments

In this section we present a series of numerical experiments to highlight the practical performance of the DG method introduced and analyzed in this article for the numerical approximation of the indefinite time-harmonic Maxwell equations in (2.1). For simplicity, we restrict ourselves to two-dimensional model problems; additionally, we note that throughout this section we select the interior penalty parameter α in (2.6) as follows:

$$\alpha = 10 \ell^2.$$

The dependence of α on the polynomial degree ℓ has been chosen in order to guarantee the stability property in Lemma 2.3.1 independently of ℓ , cf. [43], for example.

	$\ell = 1$		$\ell = 2$		$\ell = 3$	
Elements	$\ \mathbf{u} - \mathbf{u}_h\ _{DG}$	r	$\ \mathbf{u} - \mathbf{u}_h\ _{DG}$	r	$\ \mathbf{u} - \mathbf{u}_h\ _{DG}$	r
26	1.853e-1	-	2.009e-2	-	5.044e-4	-
104	9.122e-2	1.02	5.004e-3	2.01	6.471e-5	2.96
416	4.455e-2	1.03	1.250e-3	2.00	8.131e-6	2.99
1664	2.194e-2	1.02	3.123e-4	2.00	1.017e-6	3.00
6656	1.088e-2	1.01	7.808e-5	2.00	1.271e-7	3.00

Table 2.1: Example 1. Convergence of $\|\mathbf{u} - \mathbf{u}_h\|_{DG}$ with $k = 1$.

2.7.1 Example 1

In this first example we select $\Omega \subset \mathbb{R}^2$ to be the square domain $(-1, 1)^2$. Furthermore, we set $\mathbf{j} = \mathbf{0}$ and select suitable non-homogeneous boundary conditions for \mathbf{u} so that the analytical solution to the two-dimensional analogue of (2.1) is given by the smooth field

$$\mathbf{u}(x, y) = (\sin(ky), \sin(kx))^T.$$

Here, the boundary conditions are enforced in the usual DG manner by adding boundary terms in the formulation (2.4); see [43, 45] for details. We investigate the asymptotic convergence of the DG method on a sequence of successively finer (quasi-uniform) unstructured triangular meshes for $\ell = 1, 2, 3$ as the wave number k increases. To this end, in Tables 2.1, 2.2, 2.3 and 2.4 we present numerical experiments for $k = 1, 2, 4, 8$, respectively. In each case we show the number of elements in the computational mesh, the corresponding DG-norm of the error and the numerical rate of convergence r . Here, we observe that (asymptotically) $\|\mathbf{u} - \mathbf{u}_h\|_{DG}$ converges to zero at the optimal rate $\mathcal{O}(h^\ell)$, for each fixed ℓ and each k , as h tends to zero, as predicted by Theorem 2.3.2. In particular, we make two key observations: firstly, we note that for a given fixed mesh and fixed polynomial degree, an increase in the wave number k leads to an increase in the DG-norm of the error in the approximation to \mathbf{u} . In particular, as pointed out in [1], where curl-conforming finite element methods were employed for the numerical approximation of (2.1), the pre-asymptotic region increases as k increases. This is particularly evident when $k = 8$, cf. Table 2.4. Secondly, we observe that the DG-norm of the error decreases when either the mesh is refined, or the polynomial degree is increased as we would expect for this smooth problem.

Finally, in Figure 2.1 we present a comparison of the $L^2(\Omega)^2$ -norm of the error in the approximation to \mathbf{u} , with the square root of the number of degrees of freedom in the finite element space \mathbf{V}_h . Here, we observe that (asymptotically) $\|\mathbf{u} - \mathbf{u}_h\|_0$ converges to zero at the rate $\mathcal{O}(h^{\ell+1})$, for each fixed ℓ and each k , as h tends to zero. This is in full agreement with the optimal rate predicted by Corollary 2.3.6 and Remark 2.3.7.

2.7.2 Example 2

In this second example, we investigate the performance of the DG method (2.4) for a problem with a non-smooth solution. To this end, let Ω be the L-shaped do-

	$\ell = 1$		$\ell = 2$		$\ell = 3$	
Elements	$\ \mathbf{u} - \mathbf{u}_h\ _{DG}$	r	$\ \mathbf{u} - \mathbf{u}_h\ _{DG}$	r	$\ \mathbf{u} - \mathbf{u}_h\ _{DG}$	r
26	1.113	-	1.265e-1	-	1.242e-2	-
104	5.397e-1	1.04	3.217e-2	1.98	1.582e-3	2.97
416	2.635e-1	1.03	8.078e-3	1.99	1.985e-4	2.99
1664	1.302e-1	1.02	2.022e-3	2.00	2.483e-5	3.00
6656	6.477e-2	1.01	5.055e-4	2.00	3.103e-6	3.00

Table 2.2: Example 1. Convergence of $\|\mathbf{u} - \mathbf{u}_h\|_{DG}$ with $k = 2$.

	$\ell = 1$		$\ell = 2$		$\ell = 3$	
Elements	$\ \mathbf{u} - \mathbf{u}_h\ _{DG}$	r	$\ \mathbf{u} - \mathbf{u}_h\ _{DG}$	r	$\ \mathbf{u} - \mathbf{u}_h\ _{DG}$	r
26	3.868	-	1.275	-	1.429e-1	-
104	2.016	0.94	2.971e-1	2.10	2.289e-2	2.64
416	9.871e-1	1.03	7.401e-2	2.01	2.952e-3	2.96
1664	4.865e-1	1.02	1.849e-2	2.00	3.715e-4	2.99
6656	2.415e-1	1.01	4.623e-3	2.00	4.650e-5	3.00

Table 2.3: Example 1. Convergence of $\|\mathbf{u} - \mathbf{u}_h\|_{DG}$ with $k = 4$.

main $(-1, 1)^2 \setminus [0, 1) \times (-1, 0]$ and select \mathbf{j} (and suitable non-homogeneous boundary conditions for \mathbf{u}) so that the analytical solution \mathbf{u} to the two-dimensional analogue of (2.1) is given, in terms of the polar coordinates (r, ϑ) , by

$$\mathbf{u}(x, y) = \nabla S(r, \vartheta), \quad \text{where} \quad S(r, \vartheta) = J_\alpha(kr) \sin(\alpha\vartheta), \quad (2.47)$$

where J_α denotes the Bessel function of the first kind and α is a real number. We set $\alpha = 2n/3$, where n is a positive integer; the analytical solution given by (2.47) then contains a singularity at the re-entrant corner located at the origin of Ω . In particular, we note that \mathbf{u} lies in the Sobolev space $H^{2n/3-\varepsilon}(\Omega)^2$, $\varepsilon > 0$. This example represents a slight modification of the numerical experiment presented in [1].

In this example we again consider the convergence of the DG method (2.4) on a sequence of successively finer (quasi-uniform) unstructured triangular meshes for $\ell = 1, 2, 3$ as the wave number k increases. We first consider the case of the strongest singularity when $n = 1$; to this end, in Tables 2.5, 2.6, 2.7 and 2.8 we present numerical experiments for $k = 1, 2, 4, 6$, respectively. Here, we observe that (asymptotically) $\|\mathbf{u} - \mathbf{u}_h\|_{DG}$ converges to zero at the optimal rate $\mathcal{O}(h^{\min\{2/3-\varepsilon, \ell\}})$, for each fixed ℓ and each k , as h tends to zero, as predicted by Theorem 2.3.2. As in the previous example, we see that the DG-norm of the error in the approximation to \mathbf{u} increases as the wave number k increases for a fixed mesh size and polynomial degree; and again, that the pre-asymptotic region increases as k increases. Moreover, even for this non-smooth example, for a fixed mesh and wave number, an increase in the polynomial degree leads to a decrease in $\|\mathbf{u} - \mathbf{u}_h\|_{DG}$; this is also the case, when the DG-norm of the error is compared with the total number of degrees of freedom employed in the underlying finite element space, for each fixed k ; for brevity these results have been omitted.

	$\ell = 1$		$\ell = 2$		$\ell = 3$	
Elements	$\ \mathbf{u} - \mathbf{u}_h\ _{DG}$	r	$\ \mathbf{u} - \mathbf{u}_h\ _{DG}$	r	$\ \mathbf{u} - \mathbf{u}_h\ _{DG}$	r
26	30.73	-	9.018	-	2.451	-
104	9.434	1.70	2.118	2.09	4.051e-1	2.60
416	4.777	0.98	5.396e-1	1.97	5.245e-2	2.95
1664	2.196	1.12	1.363e-1	1.98	6.625e-3	2.99
6656	1.071	1.04	3.420e-2	1.99	8.301e-4	3.00

Table 2.4: Example 1. Convergence of $\|\mathbf{u} - \mathbf{u}_h\|_{DG}$ with $k = 8$.

	$\ell = 1$		$\ell = 2$		$\ell = 3$	
Elements	$\ \mathbf{u} - \mathbf{u}_h\ _{DG}$	r	$\ \mathbf{u} - \mathbf{u}_h\ _{DG}$	r	$\ \mathbf{u} - \mathbf{u}_h\ _{DG}$	r
24	1.052e-1	-	6.185e-2	-	4.239e-2	-
96	6.175e-2	0.77	3.749e-2	0.72	2.612e-2	0.70
384	3.761e-2	0.72	2.324e-2	0.69	1.631e-2	0.68
1536	2.336e-2	0.69	1.455e-2	0.68	1.024e-2	0.67
6144	1.463e-2	0.68	9.140e-3	0.67	6.439e-3	0.67

Table 2.5: Example 2. Convergence of $\|\mathbf{u} - \mathbf{u}_h\|_{DG}$ with $n = 1$ and $k = 1$.

Analogous behavior is also observed when $n = 2$ and $n = 4$; for brevity, in Tables 2.9 and 2.10, we present results for $n = 2$ and $n = 4$, respectively, only for the case when $k = 1$. As before larger wave numbers lead to an increase in the magnitude of the error as well as an increase in the pre-asymptotic region. Here, we again observe that (asymptotically) $\|\mathbf{u} - \mathbf{u}_h\|_{DG}$ converges to zero at (at least) the optimal rate $\mathcal{O}(h^{\min\{2n/3-\varepsilon, \ell\}})$, for each fixed ℓ , as h tends to zero, as predicted by Theorem 2.3.2. We remark that, when linear elements are employed, in both cases with $n = 2$ and $n = 4$, we observe that a slightly superior rate of convergence is attained in practice; analogous behaviour is also observed when quadratic elements are employed in the case when $n = 4$.

Finally, we end this section by considering the rate of convergence of the error in the approximation to \mathbf{u} measured in terms of the $L^2(\Omega)^2$ -norm. To this end, in Figure 2.2 we plot the $L^2(\Omega)^2$ -norm of the error in the approximation to \mathbf{u} , with the square root of the number of degrees of freedom in the finite element space \mathbf{V}_h , for $n = 1, 2, 4$, in the case when $k = 1$. Here, we observe that (asymptotically) $\|\mathbf{u} - \mathbf{u}_h\|_0$ converges to zero at the rate $\mathcal{O}(h^{\min\{2n/3, \ell+1\}})$, for each fixed ℓ , as h tends to zero. In the case of the strongest singularity when $n = 1$, the regularity assumptions required in the statement of Corollary 2.3.6 do not hold. However, this rate is in agreement with Corollary 2.3.6 when $n = 2$; in this case the embedding parameter (which only depends on Ω) is $\sigma = 2/3$, cf. [42] and $s = 2/3$. For the case when $n = 4$, we have $s = 2$; thereby, while for $\ell = 2, 3$, the order of convergence of the $L^2(\Omega)^2$ -norm of the error is in agreement with Corollary 2.3.6, the theoretically predicted rate of $\mathcal{O}(h^{5/3})$ for $\ell = 1$ is slightly pessimistic in comparison to the full order $\mathcal{O}(h^2)$ that we observe numerically. Analogous results are attained with higher wave numbers; for brevity, these numerics have been omitted.

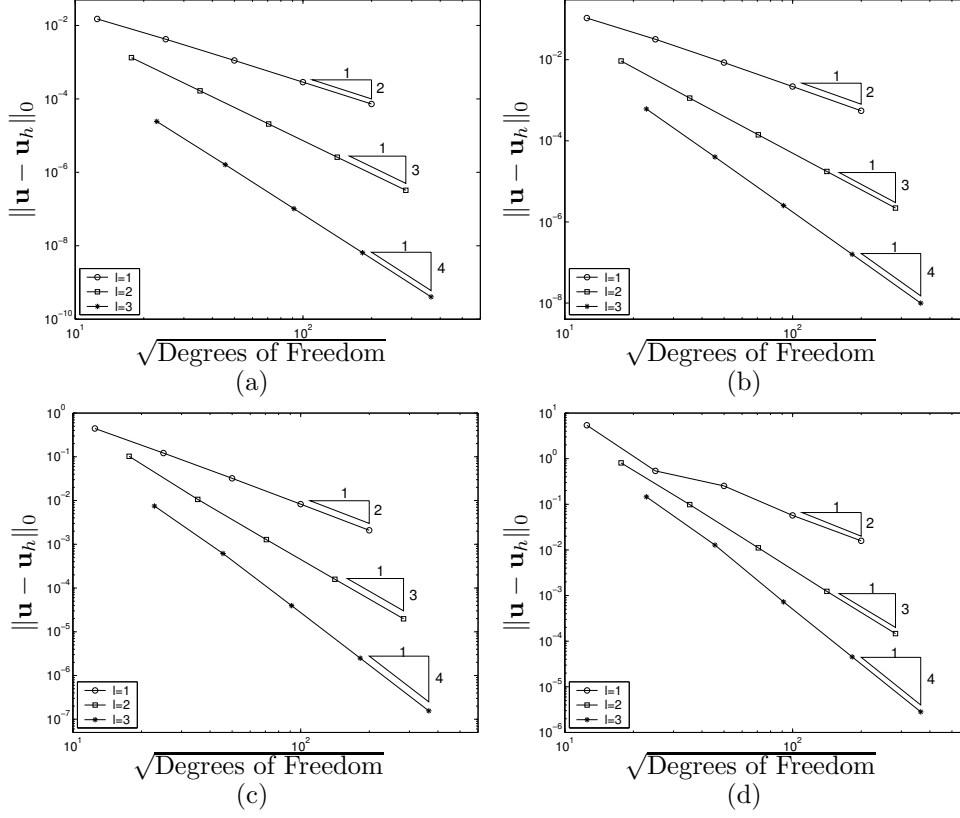


Figure 2.1: Example 1. Convergence of $\|\mathbf{u} - \mathbf{u}_h\|_0$ for: (a) $k = 1$; (b) $k = 2$; (c) $k = 4$; (d) $k = 8$.

Elements	$\ell = 1$		$\ell = 2$		$\ell = 3$	
	$\ \mathbf{u} - \mathbf{u}_h\ _{DG}$	r	$\ \mathbf{u} - \mathbf{u}_h\ _{DG}$	r	$\ \mathbf{u} - \mathbf{u}_h\ _{DG}$	r
24	1.556e-1	-	9.423e-2	-	6.613e-2	-
96	9.493e-2	0.71	5.869e-2	0.68	4.118e-2	0.68
384	5.897e-2	0.69	3.671e-2	0.68	2.582e-2	0.67
1536	3.690e-2	0.68	2.305e-2	0.67	1.623e-2	0.67
6144	2.318e-2	0.67	1.450e-2	0.67	1.022e-2	0.67

Table 2.6: Example 2. Convergence of $\|\mathbf{u} - \mathbf{u}_h\|_{DG}$ with $n = 1$ and $k = 2$.

	$\ell = 1$		$\ell = 2$		$\ell = 3$	
Elements	$\ \mathbf{u} - \mathbf{u}_h\ _{DG}$	r	$\ \mathbf{u} - \mathbf{u}_h\ _{DG}$	r	$\ \mathbf{u} - \mathbf{u}_h\ _{DG}$	r
24	7.467e-1	-	2.511e-1	-	1.579e-1	-
96	2.561e-1	1.54	1.278e-1	0.97	8.058e-2	0.97
384	1.251e-1	1.03	6.815e-2	0.91	4.507e-2	0.84
1536	6.747e-2	0.89	3.921e-2	0.80	2.683e-2	0.75
6144	3.916e-2	0.79	2.369e-2	0.73	1.649e-2	0.70

Table 2.7: Example 2. Convergence of $\|\mathbf{u} - \mathbf{u}_h\|_{DG}$ with $n = 1$ and $k = 4$.

	$\ell = 1$		$\ell = 2$		$\ell = 3$	
Elements	$\ \mathbf{u} - \mathbf{u}_h\ _{DG}$	r	$\ \mathbf{u} - \mathbf{u}_h\ _{DG}$	r	$\ \mathbf{u} - \mathbf{u}_h\ _{DG}$	r
24	6.351	-	5.228e-1	-	4.033e-1	-
96	5.394e-1	3.56	3.613e-1	0.53	1.426e-1	1.50
384	2.260e-1	1.26	1.139e-1	1.67	6.983e-2	1.03
1536	1.289e-1	0.81	5.844e-2	0.96	3.810e-2	0.87
6144	5.777e-2	1.16	3.295e-2	0.83	2.238e-2	0.77

Table 2.8: Example 2. Convergence of $\|\mathbf{u} - \mathbf{u}_h\|_{DG}$ with $n = 1$ and $k = 6$.

	$\ell = 1$		$\ell = 2$		$\ell = 3$	
Elements	$\ \mathbf{u} - \mathbf{u}_h\ _{DG}$	r	$\ \mathbf{u} - \mathbf{u}_h\ _{DG}$	r	$\ \mathbf{u} - \mathbf{u}_h\ _{DG}$	r
24	1.676e-2	-	5.049e-3	-	2.512e-3	-
96	6.138e-3	1.45	2.007e-3	1.33	9.982e-4	1.33
384	2.347e-3	1.39	7.975e-4	1.33	3.962e-4	1.33
1536	9.140e-4	1.36	3.166e-4	1.33	1.573e-4	1.33
6144	3.590e-4	1.35	1.257e-4	1.33	6.242e-5	1.33

Table 2.9: Example 2. Convergence of $\|\mathbf{u} - \mathbf{u}_h\|_{DG}$ with $n = 2$ and $k = 1$.

	$\ell = 1$		$\ell = 2$		$\ell = 3$	
Elements	$\ \mathbf{u} - \mathbf{u}_h\ _{DG}$	r	$\ \mathbf{u} - \mathbf{u}_h\ _{DG}$	r	$\ \mathbf{u} - \mathbf{u}_h\ _{DG}$	r
24	4.811e-3	-	3.059e-4	-	3.214e-5	-
96	1.386e-3	1.80	4.556e-5	2.75	5.108e-6	2.65
384	4.195e-4	1.72	7.041e-6	2.69	8.078e-7	2.66
1536	1.338e-4	1.65	1.119e-6	2.65	1.274e-7	2.66
6144	4.448e-5	1.59	1.817e-7	2.62	2.008e-8	2.67

Table 2.10: Example 2. Convergence of $\|\mathbf{u} - \mathbf{u}_h\|_{DG}$ with $n = 4$ and $k = 1$.

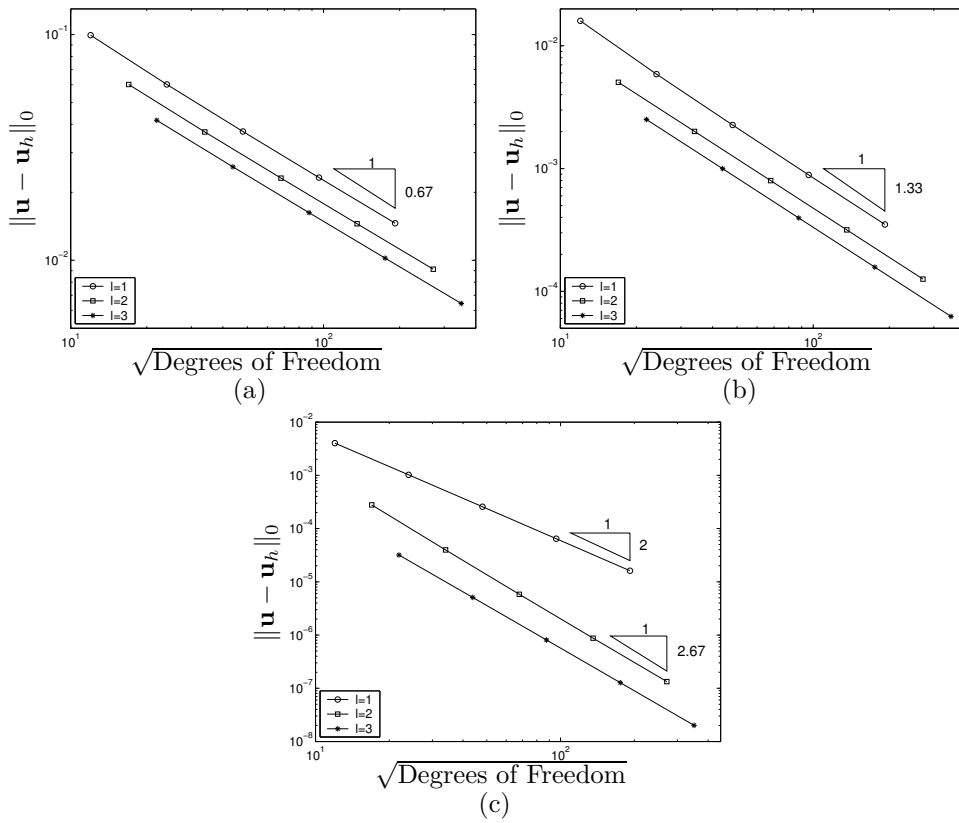


Figure 2.2: Example 2. Convergence of $\|\mathbf{u} - \mathbf{u}_h\|_0$ when $k = 1$ for: (a) $n = 1$; (b) $n = 2$; (c) $n = 4$.

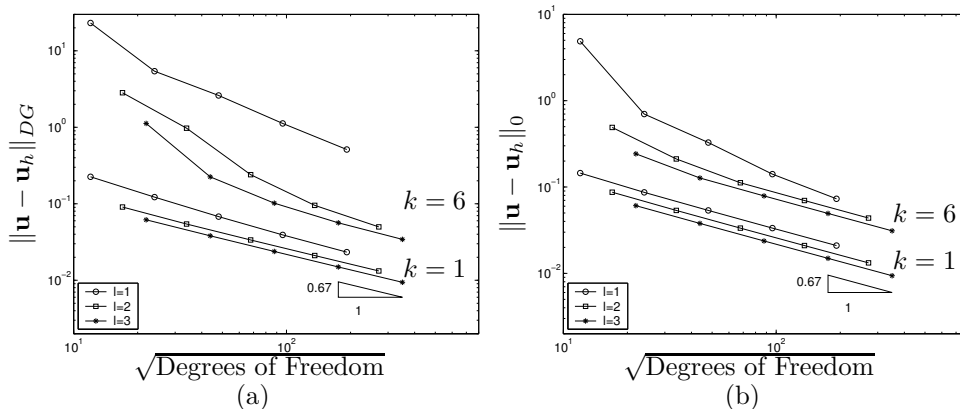


Figure 2.3: Example 3. Convergence of: (a) $\|\mathbf{u} - \mathbf{u}_h\|_{DG}$; (b) $\|\mathbf{u} - \mathbf{u}_h\|_0$.

2.7.3 Example 3

In this final example, we consider the performance of the DG method (2.4) in the general setting of a non-curl free analytical solution which is non-smooth. To this end, let Ω be the L-shaped domain employed in Example 2 above, and select \mathbf{j} (and suitable non-homogeneous boundary conditions for \mathbf{u}) so that the analytical solution \mathbf{u} to the two-dimensional analogue of (2.1) is given, in terms of the polar coordinates (r, ϑ) , by

$$\mathbf{u}(x, y) = \nabla S'(r, \vartheta) + (\sin(ky), \sin(kx))^T, \quad \text{where } S'(r, \vartheta) = (kr)^{2/3} \sin(2\vartheta/3);$$

here, \mathbf{u} lies in the Sobolev space $H^{2/3-\varepsilon}(\Omega)^2$, $\varepsilon > 0$.

In Figure 2.3 we show the convergence of both the DG- and $L^2(\Omega)^2$ -norm of the error in the DG method (2.4) on a sequence of successively finer (quasi-uniform) unstructured triangular meshes for $\ell = 1, 2, 3$ and $k = 1, 6$. As in the previous example, we clearly observe that (asymptotically) both $\|\mathbf{u} - \mathbf{u}_h\|_{DG}$ and $\|\mathbf{u} - \mathbf{u}_h\|_0$ converge to zero at the optimal rate $\mathcal{O}(h^{\min\{2/3-\varepsilon, \ell\}})$, for each fixed ℓ and each k , as h tends to zero. The observed convergence rate for the error measured in terms of the DG-norm is in agreement with the rate predicted by Theorem 2.3.2; though as in Section 2.7.2, the regularity assumptions required for the $L^2(\Omega)^2$ error bound in the statement of Corollary 2.3.6 do not hold. Finally, we point out that as in the previous two examples, an increase in the wave number k leads to an increase in the size of the error (measured in terms of both the DG- and $L^2(\Omega)^2$ -norm), as well as an increase in the size of the pre-asymptotic region.

2.8 Concluding remarks

In this paper, we have presented the *first* a-priori error analysis of the interior penalty discontinuous Galerkin method applied to the *indefinite* time-harmonic Maxwell equations in non-mixed form. In particular, by employing a technique in the spirit of [55, Section 7.2] and [56], combined with a crucial approximation result for discontinuous finite element functions, we have shown that the error in

the DG energy norm converges optimally with respect to the mesh size. Under additional regularity assumptions, we have further shown that the error in the L^2 -norm converges with the optimal order $\mathcal{O}(h^{\ell+1})$.

Ongoing research includes an implementation of the method for the discretization of $3D$ problems of engineering practice, in particular for the simulation of time-harmonic fields in the context of $3D$ models of optical nano-antennas in scanning-near field optical microscopy. The hope is, that employing a high-order (DG) discretization on a rather coarse FE mesh leads to a better resolution and is more feasible for sparse direct linear solvers than a discretization by low-order edge elements (see, e. g., Section 1.3.2).

For future investigation, an hp -analysis of DG methods for the indefinite Maxwell's equations would be interesting. As a preliminary, optimal order p -interpolation estimates for the underlying $H(\text{curl}; \Omega)$ -conforming FE spaces have to be available. In [27], Demkowicz and Babuska prove such estimates in $2D$. The extension of this result to $3D$ is still open.

Chapter 3

Interior Penalty Method for the Indefinite Time-Harmonic Maxwell's Equation: Mixed Formulation

The content of this chapter has been published in Math. Model. Numer. Anal. [41] (in collaboration with Paul Houston¹, Ilaria Perugia² and Dominik Schötzau³).

Abstract

We present and analyze an interior penalty method for the numerical discretization of the indefinite time-harmonic Maxwell equations in mixed form. The method is based on the mixed discretization of the curl-curl operator developed in [44] and can be understood as a non-stabilized variant of the approach proposed in [63]. We show the well-posedness of this approach and derive optimal a-priori error estimates in the energy-norm as well as the L^2 -norm. The theoretical results are confirmed in a series of numerical experiments.

The thesis' author's principal contribution is the proof of the L^2 -error bound in Section 3.6.

¹Prof. P. Houston, Department of Mathematics, University of Leicester, Leicester LE1 7RH, England, email: Paul.Houston@mcs.le.ac.uk

²Prof. I. Perugia, Dipartimento di Matematica, Università di Pavia, Via Ferrata 1, 27100 Pavia, Italy, email: perugia@dimat.unipv.it

³Prof. D. Schötzau, Mathematics Department, University of British Columbia, 121-1984 Mathematics Road, Vancouver V6T 1Z2, Canada, email: schoetzau@math.ubc.ca

3.1 Introduction

The series of articles [43, 44, 45, 62, 63], and Chapter 2 have been concerned with the design and analysis of interior penalty discontinuous Galerkin methods for Maxwell's equations in the frequency-domain; indeed, both the *low-frequency* and *high-frequency* regimes have been considered. In the low-frequency case, we first mention the work [62, 43] where Houston, Perugia and Schötzau introduced and analyzed several *hp*-version discontinuous Galerkin methods for low-frequency models where the resulting bilinear forms are coercive. Such models typically arise in conducting materials or after time discretization of the full time-domain Maxwell equations. In order to incorporate the divergence-free constraint on the electric field within insulating materials, Houston, Perugia and Schötzau then proposed a Lagrange multiplier approach and analyzed two families of mixed interior penalty methods; see [45, 44]. The scheme in [45] is based on elements of the same order for the approximation of the electric field and the Lagrange multiplier, and on the introduction of a normal jump stabilization term for the electric field. However, this stabilization term is unphysical and has been observed to lead to spurious oscillations in the vicinity of strong singularities in the underlying analytical solution. Fortunately, this stabilization can be avoided altogether by increasing the approximation degree for the Lagrange multiplier by one. The resulting mixed interior penalty method has been studied in [44]; it can be viewed as a discontinuous version of the natural pairing that is obtained when Nédélec's second family of elements of degree ℓ and standard nodal elements of degree $\ell + 1$ are employed; cf. [59, 55].

While the above interior penalty methods can be immediately extended to the time-harmonic Maxwell equations in the high-frequency regime, their numerical analysis becomes much more involved in this case, due to the indefiniteness of the underlying problem; a discrepancy that also arises for conforming finite element methods. In [63], a first error analysis of a stabilized mixed interior penalty method was carried out for the indefinite Maxwell system. The analysis there heavily relies on the introduction of certain volume stabilization terms, which have been numerically observed to be unnecessary. In fact, much of the efforts in [45] and [44] were directed towards reducing the stabilization of [63], though in the context of low-frequency models.

In this chapter, we revisit the stabilized mixed interior penalty method in [63] and devise and analyze a non-stabilized variant thereof, by using the mixed approach of [44] for the discretization of the curl-curl operator. Thus, we propose a new mixed interior penalty method for the indefinite time-harmonic Maxwell equations where the stabilization terms of [63] can be avoided altogether (except for the interior penalty terms, of course). Using the techniques introduced in Chapter 2, we carry out the error analysis of this approach and derive optimal a-priori error estimates in the energy-norm, as well as in the L^2 -norm. As in Chapter 2, our analysis employs duality techniques (see [55, Section 7.2]), and does not cover the case of non-smooth material coefficients. With respect to the direct formulation in Chapter 2, the mixed formulation studied here is equally applicable to both the low-frequency and high-frequency regimes, since control of the divergence of the electric field is achieved by the introduction of an appropriate Lagrange multiplier variable. Indeed, the numerical analysis of the corresponding mixed interior penalty method for the principal operator of the time-harmonic Maxwell equations in a heterogeneous insulating medium

has already been undertaken in the article [44].

The outline of the chapter is as follows: In Section 3.2 we introduce the mixed form of the indefinite time-harmonic Maxwell equations and, in Section 3.3, we present their mixed interior penalty discretization and review some basic properties of the discrete scheme. The a-priori error bounds are stated in Section 3.4; the proofs of these estimates are carried out in Sections 3.5 and 3.6. The numerical performance of the proposed method is demonstrated in Section 3.7.

The main contributor of the section on numerical experiments is Paul Houston.

Finally, in Section 3.8 we summarize the work presented in this paper and draw some conclusions.

3.2 Model problem

In this section, we introduce the model problem we shall consider in this paper. We will use the notation introduced in Section 2.1.1 of Chapter 2.

3.2.1 Indefinite time-harmonic Maxwell's equations

Let $\Omega \subset \mathbb{R}^3$ be a lossless isotropic medium with constant magnetic permeability μ , constant electric permittivity ε and a perfectly conducting boundary $\Gamma = \partial\Omega$. For a given temporal frequency $\omega > 0$, we seek to determine the time-harmonic electric field $\mathcal{E}(t, \mathbf{x}) = \Re(\exp(i\omega t)\mathbf{E}(\mathbf{x}))$ whose spatial component \mathbf{E} satisfies the indefinite equations

$$\nabla \times \nabla \times \mathbf{E} - k^2 \mathbf{E} = \mathbf{j} \quad \text{in } \Omega, \quad (3.1)$$

$$\mathbf{n} \times \mathbf{E} = \mathbf{0} \quad \text{on } \Gamma. \quad (3.2)$$

Here, we take Ω to be an open bounded Lipschitz polyhedron with unit outward normal vector \mathbf{n} on Γ . In order to avoid topological complications, we assume that Ω is simply-connected and that Γ is connected. The parameter $k > 0$ is the wave number given by $k = \omega\sqrt{\varepsilon\mu}$. Throughout, we assume that k^2 is *not* an interior Maxwell eigenvalue, i.e., for any $\mathbf{E} \neq \mathbf{0}$, the pair $(\lambda = k^2, \mathbf{E})$ is *not* an eigensolution of $\nabla \times \nabla \times \mathbf{E} = \lambda \mathbf{E}$ in Ω , $\mathbf{n} \times \mathbf{E} = \mathbf{0}$ on Γ . Finally, the right-hand side \mathbf{j} is a given generic source field in $L^2(\Omega)^3$ corresponding to a time-harmonic excitation.

3.2.2 Mixed formulation

The interior penalty method proposed in this article is based on a mixed formulation of (3.1)–(3.2) already used in the *hp*-approaches of [28] and [1], as well as in the mortar approach [16]. To this end, we decompose the field \mathbf{E} as

$$\mathbf{E} = \mathbf{u} + \nabla\varphi, \quad (3.3)$$

where φ is scalar function in $H_0^1(\Omega)$ and \mathbf{u} belongs to $H_0(\text{curl}; \Omega) \cap H(\text{div}^0; \Omega)$. The decomposition (3.3) is orthogonal in $L^2(\Omega)^3$, which implies that

$$(\mathbf{u}, \nabla q) = 0 \quad \forall q \in H_0^1(\Omega); \quad (3.4)$$

see [31] for details. Thus, upon setting

$$p = k^2 \varphi, \quad (3.5)$$

we are led to consider the following system: find (\mathbf{u}, p) such that

$$\nabla \times \nabla \times \mathbf{u} - k^2 \mathbf{u} - \nabla p = \mathbf{j} \quad \text{in } \Omega, \quad (3.6)$$

$$\nabla \cdot \mathbf{u} = 0 \quad \text{in } \Omega, \quad (3.7)$$

$$\mathbf{n} \times \mathbf{u} = \mathbf{0} \quad \text{on } \Gamma, \quad (3.8)$$

$$p = 0 \quad \text{on } \Gamma. \quad (3.9)$$

Introducing the spaces $\mathbf{V} = H_0(\text{curl}; \Omega)$ and $Q = H_0^1(\Omega)$, the weak formulation of problem (3.6)–(3.9) consists in finding $(\mathbf{u}, p) \in \mathbf{V} \times Q$ such that

$$\begin{aligned} a(\mathbf{u}, \mathbf{v}) - k^2(\mathbf{u}, \mathbf{v}) + b(\mathbf{v}, p) &= (\mathbf{j}, \mathbf{v}), \\ b(\mathbf{u}, q) &= 0 \end{aligned} \quad (3.10)$$

for all $(\mathbf{v}, q) \in \mathbf{V} \times Q$, where the forms a and b are defined, respectively, by

$$a(\mathbf{u}, \mathbf{v}) = (\nabla \times \mathbf{u}, \nabla \times \mathbf{v}), \quad b(\mathbf{v}, p) = -(\mathbf{v}, \nabla p).$$

We notice that the form a is bilinear, continuous and coercive on the kernel of b , and b is bilinear, continuous, and satisfies the inf-sup condition; see, e.g., [28, 55, 73]. Hence, problem (3.6)–(3.9) is well-posed (provided that k^2 is not an interior Maxwell eigenvalue) and there is a constant depending on Ω and k^2 such that

$$\|\mathbf{u}\|_{\text{curl}} + \|p\|_1 \leq C \|\mathbf{j}\|_0; \quad (3.11)$$

cf. [63, Proposition 1]. Moreover, under the foregoing assumptions on Ω , there exists a regularity exponent $\sigma = \sigma(\Omega) > 1/2$, only depending on Ω , such that

$$\mathbf{u} \in H^\sigma(\Omega)^3, \quad \nabla \times \mathbf{u} \in H^\sigma(\Omega)^3, \quad \text{and} \quad \|\mathbf{u}\|_\sigma + \|\nabla \times \mathbf{u}\|_\sigma \leq C \|\mathbf{j}\|_0, \quad (3.12)$$

for a constant C depending on Ω and k^2 ; see [63, Proposition 2].

We recall that the regularity exponent $\sigma = \sigma(\Omega) > 1/2$ stems from the embeddings (2.8), and that in particular, for a convex domain, the embeddings in (2.8) hold with $\sigma = 1$.

3.3 Discretization

In this section, we introduce an interior penalty discretization for the system (3.6)–(3.9) and discuss its stability and consistency properties. We employ the notation introduced in Section 2.2 of Chapter 2.

3.3.1 Interior penalty method

For a given partition \mathcal{T}_h of Ω and an approximation order $\ell \geq 1$, we wish to approximate (\mathbf{u}, p) by (\mathbf{u}_h, p_h) in the finite element space $\mathbf{V}_h \times Q_h$, where

$$\begin{aligned} \mathbf{V}_h &:= \{\mathbf{v} \in L^2(\Omega)^3 : \mathbf{v}|_K \in \mathcal{P}^\ell(K)^3 \quad \forall K \in \mathcal{T}_h\}, \\ Q_h &:= \{q \in L^2(\Omega) : q|_K \in \mathcal{P}^{\ell+1}(K) \quad \forall K \in \mathcal{T}_h\}, \end{aligned}$$

and $\mathcal{P}^m(K)$ denotes the space of polynomials of total degree at most m on K . To this end, we consider the discontinuous Galerkin method: find $\mathbf{u}_h \in \mathbf{V}_h$ and $p_h \in Q_h$ such that

$$\begin{aligned} a_h(\mathbf{u}_h, \mathbf{v}) - k^2(\mathbf{u}_h, \mathbf{v}) + b_h(\mathbf{v}, p_h) &= (\mathbf{j}, \mathbf{v}), \\ b_h(\mathbf{u}_h, q) - c_h(p_h, q) &= 0 \end{aligned} \quad (3.13)$$

for all $(\mathbf{v}, q) \in \mathbf{V}_h \times Q_h$, with discrete forms $a_h(\cdot, \cdot)$, $b_h(\cdot, \cdot)$ and $c_h(\cdot, \cdot)$ defined by

$$\begin{aligned} a_h(\mathbf{u}, \mathbf{v}) &= (\nabla_h \times \mathbf{u}, \nabla_h \times \mathbf{v}) - \int_{\mathcal{F}_h} \llbracket \mathbf{u} \rrbracket_T \cdot \{\{\nabla_h \times \mathbf{v}\}\} ds \\ &\quad - \int_{\mathcal{F}_h} \llbracket \mathbf{v} \rrbracket_T \cdot \{\{\nabla_h \times \mathbf{u}\}\} ds + \int_{\mathcal{F}_h} \mathbf{a} \llbracket \mathbf{u} \rrbracket_T \cdot \llbracket \mathbf{v} \rrbracket_T ds, \\ b_h(\mathbf{v}, p) &= -(\mathbf{v}, \nabla_h p) + \int_{\mathcal{F}_h} \{\{\mathbf{v}\}\} \cdot \llbracket p \rrbracket_N ds, \\ c_h(p, q) &= \int_{\mathcal{F}_h} \mathbf{c} \llbracket p \rrbracket_N \cdot \llbracket q \rrbracket_N ds, \end{aligned}$$

respectively. Here, ∇_h is the discrete ‘*nabla*’ operator defined elementwise (i.e., $\nabla_h \times \mathbf{v} = \sum_{K \in \mathcal{T}_h} \nabla \times \mathbf{v}|_K$ and $\nabla_h q = \sum_{K \in \mathcal{T}_h} \nabla q|_K$) and use the convention that

$$\int_{\mathcal{F}_h} \psi ds = \sum_{F \in \mathcal{F}_h} \int_F \psi ds.$$

The functions \mathbf{a} and \mathbf{c} are the so-called interior penalty stabilization functions that are taken as follows:

$$\mathbf{a} = \alpha \mathbf{h}^{-1}, \quad \mathbf{c} = \gamma \mathbf{h}^{-1}. \quad (3.14)$$

Here, \mathbf{h} is the mesh size function given by $\mathbf{h}|_F \equiv h_F = \text{diam}(F)$ for all $F \in \mathcal{F}_h$. Furthermore, α and γ are positive parameters independent of the mesh size.

We observe that the jumps $\llbracket \mathbf{v} \rrbracket_T$ and $\llbracket q \rrbracket_N$ are well-defined for elements of \mathbf{V}_h and Q_h , respectively, since the elements of \mathbf{V}_h and Q_h are elementwise polynomials, and therefore elementwise arbitrarily smooth.

The well-posedness of the method (3.13) will be established in Corollary 3.4.3 below.

REMARK 3.3.1. *We note that the formulation (3.13) is a non-stabilized variant of the one proposed in [63]. Furthermore, we point out that the formulation (3.13) can be easily modified in order to include non-constant material coefficients, see [62, 63, 44]. However, while the subsequent analysis, based on employing duality arguments, can be immediately extended to the case of smooth material coefficients, problems with non-smooth coefficients cannot be dealt with using this approach. Indeed, in this latter case, the error analysis of the proposed interior penalty method remains an open issue.*

REMARK 3.3.2. *Instead of the interior penalty approach presented here, many other discontinuous Galerkin methods could be employed for the discretization of the curl-curl operator; see [5] for a presentation of different discontinuous Galerkin discretizations of second order operators, and [62] for details on the LDG discretization of the curl-curl operator.*

3.3.2 Auxiliary forms and error equations

In order to study the discretization in (3.13), we first define how a_h and b_h should be understood on the continuous level. To this end, we introduce the spaces $\mathbf{V}(h)$ and $Q(h)$ given by

$$\mathbf{V}(h) = \mathbf{V} + \mathbf{V}_h, \quad Q(h) = Q + Q_h,$$

and endow them with the following DG-norms:

$$\begin{aligned} \|\mathbf{v}\|_{\mathbf{V}(h)}^2 &= \|\mathbf{v}\|_0^2 + \|\nabla_h \times \mathbf{v}\|_0^2 + \|\mathbf{h}^{-\frac{1}{2}}[\![\mathbf{v}]\!]_T\|_{0,\mathcal{F}_h}^2, \\ \|q\|_{Q(h)}^2 &= \|\nabla_h q\|_0^2 + \|\mathbf{h}^{-\frac{1}{2}}[\![q]\!]_N\|_{0,\mathcal{F}_h}^2, \end{aligned}$$

respectively. Here, we use the notation

$$\|\psi\|_{0,\mathcal{F}_h}^2 = \sum_{F \in \mathcal{F}_h} \|\psi\|_{0,F}^2.$$

Then, for $\mathbf{v} \in \mathbf{V}(h)$, we define the lifted element $\mathcal{L}(\mathbf{v}) \in \mathbf{V}_h$ by

$$(\mathcal{L}(\mathbf{v}), \mathbf{w}) = \int_{\mathcal{F}_h} [\![\mathbf{v}]\!]_T \cdot \{\!\!\{ \mathbf{w} \}\!\!\} ds \quad \forall \mathbf{w} \in \mathbf{V}_h.$$

Similarly, for q in $Q(h)$, we define $\mathcal{M}(q) \in \mathbf{V}_h$ by

$$(\mathcal{M}(q), \mathbf{w}) = \int_{\mathcal{F}_h} \{\!\!\{ \mathbf{w} \}\!\!\} \cdot [\![q]\!]_N ds \quad \forall \mathbf{w} \in \mathbf{V}_h.$$

The lifting operators \mathcal{L} and \mathcal{M} are well-defined; see [63, Proposition 12].

Next, we introduce the auxiliary forms

$$\begin{aligned} \tilde{a}_h(\mathbf{u}, \mathbf{v}) &= (\nabla_h \times \mathbf{u}, \nabla_h \times \mathbf{v}) - (\mathcal{L}(\mathbf{u}), \nabla_h \times \mathbf{v}) \\ &\quad - (\mathcal{L}(\mathbf{v}), \nabla_h \times \mathbf{u}) + \int_{\mathcal{F}_h} \mathbf{a} [\![\mathbf{u}]\!]_T \cdot [\![\mathbf{v}]\!]_T ds, \\ \tilde{b}_h(\mathbf{v}, p) &= -(\mathbf{v}, \nabla_h p - \mathcal{M}(p)). \end{aligned}$$

Then, we have

$$\tilde{a}_h = a_h \quad \text{on } \mathbf{V}_h \times \mathbf{V}_h, \quad \tilde{a}_h = a \quad \text{on } \mathbf{V} \times \mathbf{V},$$

as well as

$$\tilde{b}_h = b_h \quad \text{on } \mathbf{V}_h \times Q_h, \quad \tilde{b}_h = b \quad \text{on } \mathbf{V} \times Q.$$

Hence, \tilde{a}_h and \tilde{b}_h can be viewed as extensions of a_h and b_h , as well as a and b , to the spaces $\mathbf{V}(h) \times \mathbf{V}(h)$ and $\mathbf{V}(h) \times Q(h)$, respectively. With this notation, we may reformulate the discrete problem (3.13) in the following equivalent way: find (\mathbf{u}_h, p_h) in $\mathbf{V}_h \times Q_h$ such that

$$\begin{aligned} \tilde{a}_h(\mathbf{u}_h, \mathbf{v}) - k^2(\mathbf{u}_h, \mathbf{v}) + \tilde{b}_h(\mathbf{v}, p_h) &= (\mathbf{j}, \mathbf{v}), \\ \tilde{b}_h(\mathbf{u}_h, q) - c_h(p_h, q) &= 0 \end{aligned} \tag{3.15}$$

for all $(\mathbf{v}, q) \in \mathbf{V}_h \times Q_h$.

Let (\mathbf{u}, p) be the analytical solution of (3.6)–(3.9) and $(\mathbf{v}, q) \in \mathbf{V}_h \times Q_h$. We define

$$\begin{aligned} R_1(\mathbf{u}, p; \mathbf{v}) &:= \tilde{a}_h(\mathbf{u}, \mathbf{v}) - k^2(\mathbf{u}, \mathbf{v}) + \tilde{b}_h(\mathbf{v}, p) - (\mathbf{j}, \mathbf{v}), \\ R_2(\mathbf{u}; q) &:= \tilde{b}_h(\mathbf{u}, q) = \tilde{b}_h(\mathbf{u}, q) - c_h(p, q), \end{aligned}$$

where we have used that $c_h(p, q) = 0$ for any $q \in Q_h$. The functionals R_1 and R_2 measure how well the analytical solution (\mathbf{u}, p) satisfies the formulation in (3.15). Owing to the regularity properties in (3.12), it is possible to show that

$$\begin{aligned} R_1(\mathbf{u}, p; \mathbf{v}) &= \int_{\mathcal{F}_h} \llbracket \mathbf{v} \rrbracket_T \cdot \{ \nabla \times \mathbf{u} - \mathbf{\Pi}_h(\nabla \times \mathbf{u}) \} ds, \\ R_2(\mathbf{u}; q) &= \int_{\mathcal{F}_h} \llbracket q \rrbracket_N \cdot \{ \mathbf{u} - \mathbf{\Pi}_h \mathbf{u} \} ds, \end{aligned} \quad (3.16)$$

with $\mathbf{\Pi}_h$ denoting the L^2 -projection onto \mathbf{V}_h ; see [63, Lemma 24] for details. In particular, we have that R_1 is independent of p , and that $R_1(\mathbf{u}, p; \mathbf{v}) = 0$ for all $\mathbf{v} \in \mathbf{V}_h \cap \mathbf{V}$, as well as $R_2(\mathbf{u}; q) = 0$ for all $q \in Q_h \cap Q$.

With these definitions, it is obvious that the error $(\mathbf{u} - \mathbf{u}_h, p - p_h)$ between the analytical solution (\mathbf{u}, p) and the mixed DG approximation (\mathbf{u}_h, p_h) satisfies

$$\tilde{a}_h(\mathbf{u} - \mathbf{u}_h, \mathbf{v}) - k^2(\mathbf{u} - \mathbf{u}_h, \mathbf{v}) + \tilde{b}_h(\mathbf{v}, p - p_h) = R_1(\mathbf{u}, p; \mathbf{v}) \quad \forall \mathbf{v} \in \mathbf{V}_h, \quad (3.17)$$

as well as

$$\tilde{b}_h(\mathbf{u} - \mathbf{u}_h, q) - c_h(p - p_h, q) = R_2(\mathbf{u}; q) \quad \forall q \in Q_h. \quad (3.18)$$

Here, (3.17) and (3.18) are referred to as the error equations.

3.3.3 Continuity and stability properties

Next, let us review the main stability results for the forms \tilde{a}_h and \tilde{b}_h , as well as some crucial properties of the discrete solution (\mathbf{u}_h, p_h) . To this end, we first note that the following continuity properties hold.

PROPOSITION 3.3.3. *There are continuity constants C_A and C_B , independent of the mesh size, such that*

$$\begin{aligned} |\tilde{a}_h(\mathbf{u}, \mathbf{v})| &\leq C_A \|\mathbf{u}\|_{\mathbf{V}(h)} \|\mathbf{v}\|_{\mathbf{V}(h)} \quad \forall \mathbf{u}, \mathbf{v} \in \mathbf{V}(h), \\ |\tilde{b}_h(\mathbf{v}, q)| &\leq C_B \|\mathbf{v}\|_{\mathbf{V}(h)} \|q\|_{Q(h)} \quad \forall (\mathbf{v}, q) \in \mathbf{V}(h) \times Q(h). \end{aligned}$$

The linear functional on the right-hand side of the first equation in (3.15) satisfies

$$|(\mathbf{j}, \mathbf{v})| \leq \|\mathbf{j}\|_0 \|\mathbf{v}\|_{\mathbf{V}(h)} \quad \forall \mathbf{v} \in \mathbf{V}_h.$$

Furthermore, there is a constant C_R , independent of the mesh size, such that

$$\begin{aligned} |R_1(\mathbf{u}, p; \mathbf{v})| &\leq C_R \|\mathbf{v}\|_{\mathbf{V}(h)} \mathcal{E}_{1,h}(\mathbf{u}) \quad \forall \mathbf{v} \in \mathbf{V}_h, \\ |R_2(\mathbf{u}; q)| &\leq C_R \|q\|_{Q(h)} \mathcal{E}_{2,h}(\mathbf{u}) \quad \forall q \in Q_h. \end{aligned}$$

Here, we have set

$$\begin{aligned}\mathcal{E}_{1,h}(\mathbf{u})^2 &:= \sum_K h_K \|\nabla \times \mathbf{u} - \mathbf{\Pi}_h(\nabla \times \mathbf{u})\|_{0,\partial K}^2, \\ \mathcal{E}_{2,h}(\mathbf{u})^2 &:= \sum_K h_K \|\mathbf{u} - \mathbf{\Pi}_h \mathbf{u}\|_{0,\partial K}^2,\end{aligned}\tag{3.19}$$

where we recall that $\mathbf{\Pi}_h$ denotes the L^2 -projection onto \mathbf{V}_h .

Proof. For the proof of the first three assertions, we refer the reader to [45, Proposition 5.1]. The stability bounds for R_1 and R_2 in (3.19) follow immediately from weighted Cauchy-Schwarz inequalities and the definitions of the norms $\|\cdot\|_{\mathbf{V}(h)}$, $\|\cdot\|_{Q(h)}$ and the parameters \mathbf{a} , \mathbf{c} in (3.14). \square

The form \tilde{a}_h satisfies the following Gårding-type inequality.

PROPOSITION 3.3.4. *There exists a parameter $\alpha_{\min} > 0$, independent of the mesh size, such that for $\alpha \geq \alpha_{\min}$ we have*

$$\tilde{a}_h(\mathbf{v}, \mathbf{v}) \geq C_G \|\mathbf{v}\|_{\mathbf{V}(h)}^2 - \|\mathbf{v}\|_0^2 \quad \forall \mathbf{v} \in \mathbf{V}_h,$$

with a constant $C_G > 0$ independent of the mesh size.

Proof. The Gårding-type inequality readily follows from the fact that there is an $\alpha_{\min} > 0$, independent of the mesh size, such that for $\alpha \geq \alpha_{\min}$

$$\tilde{a}_h(\mathbf{v}, \mathbf{v}) \geq C \left[\|\nabla_h \times \mathbf{v}\|_0^2 + \|\mathbf{h}^{-\frac{1}{2}}[\![\mathbf{v}]\!]_T\|_{0,\mathcal{F}_h}^2 \right];$$

see [43, 45] for details. \square

Next, let us recall a stability property of the form \tilde{b}_h on the conforming subspaces underlying \mathbf{V}_h and Q_h . To this end, we set

$$\mathbf{V}_h^c = \mathbf{V}_h \cap \mathbf{V}, \quad Q_h^c = Q_h \cap Q.\tag{3.20}$$

Notice that \mathbf{V}_h^c is the Nédélec finite element space of second type (see [59] or [55, Section 8.2]), with zero tangential trace prescribed on Γ , and Q_h^c is the space of continuous polynomials of degree $\ell + 1$, with zero trace prescribed on Γ .

The following inf-sup condition holds on $\mathbf{V}_h^c \times Q_h^c$; see [44, Lemma 1] for details.

LEMMA 3.3.5. *There is a stability constant C_S , independent of the mesh size, such that*

$$\inf_{q \in Q_h^c \setminus \{0\}} \sup_{\mathbf{v} \in \mathbf{V}_h^c \setminus \{0\}} \frac{\tilde{b}_h(\mathbf{v}, q)}{\|\mathbf{v}\|_{\mathbf{V}(h)} \|q\|_{Q(h)}} \geq C_S > 0.\tag{3.21}$$

Note that, since $\mathbf{V}_h^c \subset \mathbf{V}_h$, the inf-sup condition (3.21) in Lemma 3.3.5 remains valid when \mathbf{V}_h^c is replaced by \mathbf{V}_h , with the same inf-sup constant.

Now, define the discrete kernel

$$\mathbf{Z}_h = \{\mathbf{v} \in \mathbf{V}_h : \tilde{b}_h(\mathbf{v}, q) = 0 \ \forall q \in Q_h^c\}.\tag{3.22}$$

LEMMA 3.3.6. *Let \mathbf{u} be the vector-valued component of the analytical solution of (3.6)–(3.9) and \mathbf{u}_h its discontinuous Galerkin approximation obtained in (3.13). Then,*

(i) $\mathbf{u}_h \in \mathbf{Z}_h$;

(ii) $(\mathbf{u} - \mathbf{u}_h, \nabla q) = 0$ for all $q \in Q_h^c$.

Proof. Since $c_h(p_h, q) = 0$ for all $q \in Q_h^c$, the first claim follows immediately. Furthermore, in view of (3.4), $(\mathbf{u} - \mathbf{u}_h, \nabla q) = -(\mathbf{u}_h, \nabla q)$ for all $q \in Q_h^c$. Since $-(\mathbf{u}_h, \nabla q) = \tilde{b}(\mathbf{u}_h, q)$, the second claim follows from the first one. \square

Finally, we will make use of a discrete Helmholtz decomposition: the space \mathbf{V}_h^c can be written as

$$\mathbf{V}_h^c = \mathbf{X}_h \oplus \nabla Q_h^c, \quad (3.23)$$

with \mathbf{X}_h given by

$$\mathbf{X}_h := \{\mathbf{v} \in \mathbf{V}_h^c : (\mathbf{v}, \nabla q) = 0 \ \forall q \in Q_h^c\}. \quad (3.24)$$

By construction, the decomposition (3.23) is orthogonal in $L^2(\Omega)^3$; cf. [55, Section 8.2].

3.4 A-priori error estimates and well-posedness

In this section, we state optimal a-priori error estimates in the DG energy-norm and the L^2 -norm. We further show that the energy error estimates imply the well-posedness of the interior penalty formulation (3.13); see [68].

The following result addresses the error in the energy-norm.

THEOREM 3.4.1. *Suppose that the analytical solution (\mathbf{u}, p) of (3.6)–(3.9) satisfies*

$$\mathbf{u} \in H^s(\Omega)^3, \quad \nabla \times \mathbf{u} \in H^s(\Omega)^3, \quad p \in H^{s+1}(\Omega), \quad (3.25)$$

for a parameter $s > 1/2$. Let (\mathbf{u}_h, p_h) be the mixed DG approximation obtained by (3.13) with $\alpha \geq \alpha_{\min}$ and $\gamma > 0$. Then, there exists a mesh size $h_0 > 0$ such that

$$\|\mathbf{u} - \mathbf{u}_h\|_{\mathbf{V}(h)} + \|p - p_h\|_{Q(h)} \leq C h^{\min\{s, \ell\}} [\|\mathbf{u}\|_s + \|\nabla \times \mathbf{u}\|_s + \|p\|_{s+1}]$$

for all meshes \mathcal{T}_h of mesh size $h < h_0$. The constant $C > 0$ is independent of the mesh size.

REMARK 3.4.2. *We observe that the regularity assumption on p in Theorem 3.4.1 is automatically fulfilled, with $s = \sigma$, as soon as $\nabla \cdot \mathbf{j} \in L^2(\Omega)$.*

By proceeding along the lines of [68], well-posedness of the formulation (3.13) can be established from the a-priori estimate in Theorem 3.4.1.

COROLLARY 3.4.3. *For stabilization parameters $\alpha \geq \alpha_{\min} > 0$ and $\gamma > 0$, and mesh sizes $h < h_0$, the method (3.13) has a unique solution.*

Proof. If $\mathbf{j} = \mathbf{0}$, then $(\mathbf{u}, p) = (\mathbf{0}, 0)$ and the estimate in Theorem 3.4.1 implies that $\|\mathbf{u}_h\|_{\mathbf{V}(h)} + \|p_h\|_{Q(h)} \leq 0$ for $h < h_0$. Hence, $(\mathbf{u}_h, p_h) = (\mathbf{0}, 0)$ for $h < h_0$. \square

Next, we state an a-priori bound for the error $\|\mathbf{u} - \mathbf{u}_h\|_0$ and show that the optimal order $\mathcal{O}(h^{\ell+1})$ is obtained for smooth solutions and convex domains.

THEOREM 3.4.4. *Suppose the vector-valued component \mathbf{u} of the analytical solution (\mathbf{u}, p) of (3.6)–(3.9) satisfies*

$$\mathbf{u} \in H^{s+\sigma}(\Omega)^3, \quad \nabla \times \mathbf{u} \in H^s(\Omega)^3,$$

for a parameter $s > 1/2$ and the embedding exponent $\sigma \in (1/2, 1]$ from (2.8). Let \mathbf{u}_h be the DG approximation obtained by (3.13) with $\alpha \geq \alpha_{\min} > 0$ and $\gamma > 0$. Then there is a mesh size $0 < h_1 < 1$ such that for all meshes \mathcal{T}_h of mesh size $0h < h_1$ we have

$$\|\mathbf{u} - \mathbf{u}_h\|_0 \leq C h^{\min\{s, \ell\} + \sigma} [\|\mathbf{u}\|_{s+\sigma} + \|\nabla \times \mathbf{u}\|_s] + C h^\sigma [\|\mathbf{u} - \mathbf{u}_h\|_{\mathbf{V}(h)} + \|p - p_h\|_{Q(h)}],$$

where the constant $C > 0$ is independent of the mesh size.

We note that the minimal mesh sizes h_0 in Theorem 3.4.1 and h_1 in Theorem 3.4.4 depend on the wave number k and the regularity exponent σ in the embedding (2.8).

Theorem 3.4.4 and Theorem 3.4.1 ensure optimal L^2 -error estimates for smooth solutions and convex domains.

COROLLARY 3.4.5. *For a convex domain where $\sigma = 1$ and an analytical solution $(\mathbf{u}, p) \in H^{\ell+1}(\Omega)^3 \times H^{\ell+1}(\Omega)$, we obtain for $h < \min\{h_0, h_1\}$ the optimal error bound*

$$\|\mathbf{u} - \mathbf{u}_h\|_0 \leq C h^{\ell+1} [\|\mathbf{u}\|_{\ell+1} + \|p\|_{\ell+1}],$$

with a constant $C > 0$ independent of the mesh size.

The proofs of Theorem 3.4.1 and Theorem 3.4.4 are given in Section 3.5 and Section 3.6, respectively. Before we start, we recall the result that allows us to find a conforming function close to any discontinuous one. This result is essential to the error analysis of the method in (3.13).

THEOREM 3.4.6. *There exist approximants $\mathbf{A} : \mathbf{V}_h \rightarrow \mathbf{V}_h^c$ and $A : Q_h \rightarrow Q_h^c$ such that*

$$\begin{aligned} \|\mathbf{v} - \mathbf{A}\mathbf{v}\|_0^2 &\leq C \int_{\mathcal{F}_h} \mathfrak{h} |[\![\mathbf{v}]\!]_T|^2 ds, \\ \|\mathbf{v} - \mathbf{A}\mathbf{v}\|_{\mathbf{V}(h)}^2 &\leq C \int_{\mathcal{F}_h} \mathfrak{h}^{-1} |[\![\mathbf{v}]\!]_T|^2 ds, \\ \|q - Aq\|_{Q(h)}^2 &\leq C \int_{\mathcal{F}_h} \mathfrak{h}^{-1} |[\![q]\!]_N|^2 ds \end{aligned}$$

for all $\mathbf{v} \in \mathbf{V}_h$ and $q \in Q_h$. The constant $C > 0$ solely depends on the shape-regularity of the mesh and the polynomial degree ℓ .

For the space \mathbf{V}_h , this result corresponds to the result in Proposition 2.4.5. It has been proved in [40, Appendix A] which is also reported in Appendix 5.8. The result for Q_h can be found in [49, Section 2.1]. Theorem 3.4.6 and the definition of the DG-norms $\|\cdot\|_{\mathbf{V}(h)}$ and $\|\cdot\|_{Q(h)}$ immediately imply the following result.

COROLLARY 3.4.7. *There is a constant $C > 0$ independent of the mesh size such that*

$$\begin{aligned} \|\mathbf{v} - \mathbf{A}\mathbf{v}\|_{\mathbf{V}(h)} + \|\mathbf{A}\mathbf{v}\|_{\mathbf{V}(h)} + h^{-1} \|\mathbf{v} - \mathbf{A}\mathbf{v}\|_0 &\leq C \|\mathbf{v}\|_{\mathbf{V}(h)}, \\ \|q - Aq\|_{Q(h)} + \|Aq\|_{Q(h)} &\leq C \|q\|_{Q(h)} \end{aligned}$$

for all $\mathbf{v} \in \mathbf{V}_h$ and $q \in Q_h$.

We will further need the following consequence of Theorem 3.4.6, which follows from the fact that $[\![\mathbf{w}]\!]_T = \mathbf{0}$ on \mathcal{F}_h , for any $\mathbf{w} \in \mathbf{V}$, and the definition of the DG-norm $\|\cdot\|_{\mathbf{V}(h)}$.

COROLLARY 3.4.8. *Let $\mathbf{v} \in \mathbf{V}_h$ and $\mathbf{w} \in \mathbf{V}$. Let \mathbf{A} be the conforming approximant from Theorem 3.4.6. Then we have*

$$\begin{aligned}\|\mathbf{v} - \mathbf{A}\mathbf{v}\|_{\mathbf{V}(h)} &\leq C\|\mathbf{v} - \mathbf{w}\|_{\mathbf{V}(h)}, \\ \|\mathbf{v} - \mathbf{A}\mathbf{v}\|_0 &\leq Ch\|\mathbf{v} - \mathbf{w}\|_{\mathbf{V}(h)},\end{aligned}$$

with a constant $C > 0$ that is independent of the mesh size.

In the analysis for (3.13) we shall further need the results on standart approximation operators stated in Section 2.4.2 of Chapter 2.

3.5 Proof of Theorem 3.4.1 (energy norm error estimate)

In this section, we prove the result of Theorem 3.4.1 by proceeding along the lines of Section 2.5, [56] and [55, Section 7.2].

To this end, we define

$$\mathcal{D}_h(\mathbf{u} - \mathbf{u}_h) := \sup_{\mathbf{0} \neq \mathbf{v} \in \mathbf{V}_h} \frac{(\mathbf{u} - \mathbf{u}_h, \mathbf{v})}{\|\mathbf{v}\|_{\mathbf{V}(h)}}. \quad (3.26)$$

We start by proving a preliminary energy norm error bound in terms of $\mathcal{E}_{1,h}(\mathbf{u})$, $\mathcal{E}_{2,h}(\mathbf{u})$ and $\mathcal{D}_h(\mathbf{u} - \mathbf{u}_h)$. Then, we estimate these quantities separately; in particular, a duality argument will be used for bounding $\mathcal{D}_h(\mathbf{u} - \mathbf{u}_h)$.

3.5.1 Preliminary error bound

We first prove the following error bound.

PROPOSITION 3.5.1. *Let (\mathbf{u}, p) be the analytical solution of (3.6)–(3.9), and let (\mathbf{u}_h, p_h) be the solution of (3.13) obtained with $\alpha \geq \alpha_{\min} > 0$ and $\gamma > 0$. Then we have that*

$$\begin{aligned}\|\mathbf{u} - \mathbf{u}_h\|_{\mathbf{V}(h)} + \|p - p_h\|_{Q(h)} &\leq C[\|\mathbf{u} - \mathbf{v}\|_{\mathbf{V}(h)} + \|p - q\|_{Q(h)} \\ &\quad + \mathcal{E}_{1,h}(\mathbf{u}) + \mathcal{E}_{2,h}(\mathbf{u}) + \mathcal{D}_h(\mathbf{u} - \mathbf{u}_h)]\end{aligned}$$

for all $\mathbf{v} \in \mathbf{V}_h^c$ and all $q \in Q_h^c$, with $\mathcal{E}_{1,h}$, $\mathcal{E}_{2,h}$ and \mathcal{D}_h defined in (3.19) and (3.26), respectively. Here, the constant $C > 0$ is independent of the mesh size.

Proof. We decompose \mathbf{u}_h and p_h into a conforming part and a remainder by setting

$$\mathbf{u}_h = \mathbf{u}_h^c + \mathbf{u}_h^\perp, \quad p_h = p_h^c + p_h^\perp, \quad (3.27)$$

where $\mathbf{u}_h^c = \mathbf{A}\mathbf{u}_h$, $\mathbf{u}_h^\perp = \mathbf{u}_h - \mathbf{A}\mathbf{u}_h$, $p_h^c = Ap_h$, $p_h^\perp = p_h - Ap_h$, \mathbf{A} and A being the approximants from Theorem 3.4.6. We now proceed in three steps.

Step 1: Estimate of $\|p_h^\perp\|_{Q(h)}$ and $\|\mathbf{u} - \mathbf{u}_h\|_{\mathbf{V}(h)}$. We claim that

$$\begin{aligned}\|\mathbf{u} - \mathbf{u}_h\|_{\mathbf{V}(h)} + \|p_h^\perp\|_{Q(h)} &\leq C[\|\mathbf{u} - \mathbf{v}\|_{\mathbf{V}(h)} + \|p - q\|_{Q(h)} \\ &\quad + \mathcal{E}_{1,h}(\mathbf{u}) + \mathcal{E}_{2,h}(\mathbf{u}) + \mathcal{D}_h(\mathbf{u} - \mathbf{u}_h)]\end{aligned} \quad (3.28)$$

for all $\mathbf{v} \in \mathbf{V}_h^c$ and $q \in Q_h^c$, with a positive constant C independent of the mesh size.

We start by showing that (3.28) holds for any $\mathbf{v} \in \mathbf{V}_h^c \cap \mathbf{Z}_h$ and $q \in Q_h^c$. To this end, fix $\mathbf{v} \in \mathbf{V}_h^c \cap \mathbf{Z}_h$ and $q \in Q_h^c$; Theorem 3.4.6 then yields

$$C \|p_h^\perp\|_{Q(h)}^2 \leq c_h(p_h^\perp, p_h^\perp) = c_h(p_h - q, p_h - q).$$

This, together with the Gårding-type inequality in Proposition 3.3.4, gives the bound

$$\begin{aligned} & \min\{C_G, C\} [\|\mathbf{u}_h - \mathbf{v}\|_{\mathbf{V}(h)}^2 + \|p_h^\perp\|_{Q(h)}^2] \\ & \leq C_G \|\mathbf{u}_h - \mathbf{v}\|_{\mathbf{V}(h)}^2 + C \|p_h^\perp\|_{Q(h)}^2 \\ & \leq \tilde{a}_h(\mathbf{u}_h - \mathbf{v}, \mathbf{u}_h - \mathbf{v}) + c_h(p_h - q, p_h - q) + (\mathbf{u}_h - \mathbf{v}, \mathbf{u}_h - \mathbf{v}) \\ & \equiv T_1 + T_2 + T_3, \end{aligned} \quad (3.29)$$

where

$$\begin{aligned} T_1 &= \tilde{a}_h(\mathbf{u}_h - \mathbf{v}, \mathbf{u}_h - \mathbf{v}) - k^2(\mathbf{u}_h - \mathbf{v}, \mathbf{u}_h - \mathbf{v}) + \tilde{b}_h(\mathbf{u}_h - \mathbf{v}, p_h - q), \\ T_2 &= -\tilde{b}_h(\mathbf{u}_h - \mathbf{v}, p_h - q) + c_h(p_h - q, p_h - q), \\ T_3 &= (k^2 + 1)(\mathbf{u}_h - \mathbf{v}, \mathbf{u}_h - \mathbf{v}). \end{aligned}$$

We now proceed to bound the three terms T_1 , T_2 , and T_3 .

For T_1 , the error equation (3.17) and the continuity properties in Proposition 3.3.3 yield

$$\begin{aligned} T_1 &= -R_1(\mathbf{u}, p; \mathbf{u}_h - \mathbf{v}) + \tilde{a}_h(\mathbf{u} - \mathbf{v}, \mathbf{u}_h - \mathbf{v}) \\ & \quad - k^2(\mathbf{u} - \mathbf{v}, \mathbf{u}_h - \mathbf{v}) + \tilde{b}_h(\mathbf{u}_h - \mathbf{v}, p - q) \\ & \leq \|\mathbf{u}_h - \mathbf{v}\|_{\mathbf{V}(h)} [C_R \mathcal{E}_{1,h}(\mathbf{u}) + (C_A + k^2) \|\mathbf{u} - \mathbf{v}\|_{\mathbf{V}(h)} + C_B \|p - q\|_{Q(h)}] \end{aligned} \quad (3.30)$$

Similarly, using the error equation in (3.18), the term T_2 can be written as

$$\begin{aligned} T_2 &= R_2(\mathbf{u}; p_h - q) - \tilde{b}_h(\mathbf{u} - \mathbf{v}, p_h - q) + c_h(p - q, p_h - q) \\ &= R_2(\mathbf{u}; p_h - q) - \tilde{b}_h(\mathbf{u} - \mathbf{v}, p_h - q), \end{aligned}$$

where we also have used the fact that $c_h(p - q, p_h - q) = 0$ (since $p - q \in Q$). Then, we observe that

$$\tilde{b}_h(\mathbf{u} - \mathbf{v}, p_h - q) = \tilde{b}_h(\mathbf{u} - \mathbf{v}, p_h^c - q) + \tilde{b}_h(\mathbf{u} - \mathbf{v}, p_h^\perp) = \tilde{b}_h(\mathbf{u} - \mathbf{v}, p_h^\perp),$$

since \mathbf{u} is divergence-free, see (3.4), and \mathbf{v} belongs to the kernel \mathbf{Z}_h . Furthermore, we conclude from (3.16) that $R_2(\mathbf{u}; p_h - q) = R_2(\mathbf{u}; p_h^\perp)$. Hence, we obtain

$$T_2 = R_2(\mathbf{u}; p_h^\perp) - \tilde{b}_h(\mathbf{u} - \mathbf{v}, p_h^\perp),$$

and the continuity properties in Proposition 3.3.3 yield

$$T_2 \leq \|p_h^\perp\|_{Q(h)} [C_R \mathcal{E}_{2,h}(\mathbf{u}) + C_B \|\mathbf{u} - \mathbf{v}\|_{\mathbf{V}(h)}]. \quad (3.31)$$

The term T_3 can be estimated in a similar fashion:

$$\begin{aligned} T_3 &= (k^2 + 1)(\mathbf{u}_h - \mathbf{u}, \mathbf{u}_h - \mathbf{v}) + (k^2 + 1)(\mathbf{u} - \mathbf{v}, \mathbf{u}_h - \mathbf{v}) \\ & \leq (k^2 + 1) \|\mathbf{u}_h - \mathbf{v}\|_{\mathbf{V}(h)} [\mathcal{D}_h(\mathbf{u} - \mathbf{u}_h) + \|\mathbf{u} - \mathbf{v}\|_{\mathbf{V}(h)}]. \end{aligned} \quad (3.32)$$

By combining (3.29) with the estimates in (3.30)–(3.32), and by dividing the resulting inequality by $(\|\mathbf{u}_h - \mathbf{v}\|_{\mathbf{V}(h)}^2 + \|p_h^\perp\|_{Q(h)}^2)^{\frac{1}{2}}$, we obtain that

$$\begin{aligned} \|\mathbf{u}_h - \mathbf{v}\|_{\mathbf{V}(h)} + \|p_h^\perp\|_{Q(h)} &\leq C[(2k^2 + 1 + C_A + C_B)\|\mathbf{u} - \mathbf{v}\|_{\mathbf{V}(h)} + C_B\|p - q\|_{Q(h)} \\ &\quad + C_R\mathcal{E}_{1,h}(\mathbf{u}) + C_R\mathcal{E}_{2,h}(\mathbf{u}) + (k^2 + 1)\mathcal{D}_h(\mathbf{u} - \mathbf{u}_h)]. \end{aligned}$$

This bound and the triangle inequality

$$\|\mathbf{u} - \mathbf{u}_h\|_{\mathbf{V}(h)} \leq \|\mathbf{u} - \mathbf{v}\|_{\mathbf{V}(h)} + \|\mathbf{u}_h - \mathbf{v}\|_{\mathbf{V}(h)}$$

result in

$$\begin{aligned} \|\mathbf{u} - \mathbf{u}_h\|_{\mathbf{V}(h)} + \|p_h^\perp\|_{Q(h)} &\leq C[\|\mathbf{u} - \mathbf{v}\|_{\mathbf{V}(h)} + \|p - q\|_{Q(h)} \\ &\quad + \mathcal{E}_{1,h}(\mathbf{u}) + \mathcal{E}_{2,h}(\mathbf{u}) + \mathcal{D}_h(\mathbf{u} - \mathbf{u}_h)]. \end{aligned}$$

This shows (3.28) for all $\mathbf{v} \in \mathbf{V}_h^c \cap \mathbf{Z}_h$ and all $q \in Q_h^c$.

In order to complete the proof of (3.28), it remains to show that the estimate (3.28) is also valid for any $\mathbf{v} \in \mathbf{V}_h^c$. To this end, fix $\mathbf{v} \in \mathbf{V}_h^c$ and choose $\mathbf{r} \in \mathbf{V}_h^c$ such that

$$\begin{aligned} \tilde{b}_h(\mathbf{r}, s) &= \tilde{b}_h(\mathbf{u} - \mathbf{v}, s) \quad \forall s \in Q_h^c, \\ \|\mathbf{r}\|_{\mathbf{V}(h)} &\leq C_S^{-1}C_B\|\mathbf{u} - \mathbf{v}\|_{\mathbf{V}(h)}; \end{aligned}$$

the existence of such a \mathbf{r} is guaranteed by the inf-sup condition in Lemma 3.3.5. We set $\mathbf{w} := \mathbf{r} + \mathbf{v}$; by construction, $\mathbf{w} \in \mathbf{V}_h^c \cap \mathbf{Z}_h$. Thereby,

$$\|\mathbf{u} - \mathbf{w}\|_{\mathbf{V}(h)} \leq \|\mathbf{u} - \mathbf{v}\|_{\mathbf{V}(h)} + \|\mathbf{r}\|_{\mathbf{V}(h)} \leq (1 + C_S^{-1}C_B)\|\mathbf{u} - \mathbf{v}\|_{\mathbf{V}(h)},$$

from which (3.28) follows.

Step 2: Estimate of $\|p - p_h\|_{Q(h)}$. Next, we address the error in the multiplier p and show that, for any $q \in Q_h^c$,

$$\|p - p_h\|_{Q(h)} \leq C[\|\mathbf{u} - \mathbf{u}_h\|_{\mathbf{V}(h)} + \|p - q\|_{Q(h)} + \|p_h^\perp\|_{Q(h)} + k^2\mathcal{D}_h(\mathbf{u} - \mathbf{u}_h)]. \quad (3.33)$$

To prove (3.33), fix $q \in Q_h^c$. From the triangle inequality and the decomposition $p_h = p_h^c + p_h^\perp$, we have

$$\|p - p_h\|_{Q(h)} \leq \|p - q\|_{Q(h)} + \|q - p_h^c\|_{Q(h)} + \|p_h^\perp\|_{Q(h)}. \quad (3.34)$$

The inf-sup condition (3.21) in Lemma 3.3.5 implies that

$$\begin{aligned} C_S\|q - p_h^c\|_{Q(h)} &\leq \sup_{\mathbf{0} \neq \mathbf{v} \in \mathbf{V}_h^c} \frac{\tilde{b}_h(\mathbf{v}, q - p_h^c)}{\|\mathbf{v}\|_{\mathbf{V}(h)}} \\ &= \sup_{\mathbf{0} \neq \mathbf{v} \in \mathbf{V}_h^c} \frac{\tilde{b}_h(\mathbf{v}, q - p) + \tilde{b}_h(\mathbf{v}, p - p_h) + \tilde{b}_h(\mathbf{v}, p_h^\perp)}{\|\mathbf{v}\|_{\mathbf{V}(h)}}. \end{aligned}$$

Notice that the error equation (3.17) yields, for $\mathbf{v} \in \mathbf{V}_h^c$,

$$\tilde{b}_h(\mathbf{v}, p - p_h) = -\tilde{a}_h(\mathbf{u} - \mathbf{u}_h, \mathbf{v}) + k^2(\mathbf{u} - \mathbf{u}_h, \mathbf{v}),$$

where we have used the fact that $R_1(\mathbf{u}, p; \mathbf{v}) = 0$ for $\mathbf{v} \in \mathbf{V}_h^c$. Hence,

$$C_S \|q - p_h^c\|_{Q(h)} \leq \sup_{\mathbf{0} \neq \mathbf{v} \in \mathbf{V}_h^c} \frac{\tilde{b}_h(\mathbf{v}, q - p) - \tilde{a}_h(\mathbf{u} - \mathbf{u}_h, \mathbf{v}) + k^2(\mathbf{u} - \mathbf{u}_h, \mathbf{v}) + \tilde{b}_h(\mathbf{v}, p_h^\perp)}{\|\mathbf{v}\|_{\mathbf{V}(h)}}.$$

Then, the continuity properties of \tilde{a}_h and \tilde{b}_h in Proposition 3.3.3 and (3.26) yield the bound

$$C_S \|q - p_h^c\|_{Q(h)} \leq C_B \|p - q\|_{Q(h)} + C_A \|\mathbf{u} - \mathbf{u}_h\|_{\mathbf{V}(h)} + C_B \|p_h^\perp\|_{Q(h)} + k^2 \mathcal{D}_h(\mathbf{u} - \mathbf{u}_h);$$

substituting this estimate into (3.34), we deduce (3.33).

Step 3: Conclusion. The statement of the proposition readily follows from (3.28) and (3.33) in Step 1 and Step 2, respectively. \square

3.5.2 Estimate of $\mathcal{D}_h(\mathbf{u} - \mathbf{u}_h)$

To estimate \mathcal{D}_h , we proceed along the same lines as in the proof of [63, Proposition 4.2] and in Proposition 2.5.2 of Chapter 2; to this end, the following result holds.

PROPOSITION 3.5.2. *There exists $C > 0$, independent of the mesh size, such that*

$$\mathcal{D}_h(\mathbf{u} - \mathbf{u}_h) \leq C h^\sigma [\|\mathbf{u} - \mathbf{u}_h\|_{\mathbf{V}(h)} + \|p - p_h\|_{Q(h)}],$$

with the parameter $\sigma \in (1/2, 1]$ from (3.12).

Proof. Fix $\mathbf{v} \in \mathbf{V}_h$, and let $\mathbf{v}^c = \mathbf{A}\mathbf{v} \in \mathbf{V}_h^c$ be the conforming approximation of \mathbf{v} from Theorem 3.4.6. Employing the Helmholtz decomposition (3.23), we decompose \mathbf{v}^c as

$$\mathbf{v}^c = \mathbf{v}_0^c + \nabla r, \quad (3.35)$$

with $\mathbf{v}_0^c \in \mathbf{X}_h$ and $r \in Q_h^c$. Employing (3.35), we obtain

$$\begin{aligned} (\mathbf{u} - \mathbf{u}_h, \mathbf{v}) &= (\mathbf{u} - \mathbf{u}_h, \mathbf{v} - \mathbf{v}^c) + (\mathbf{u} - \mathbf{u}_h, \mathbf{v}^c) \\ &= (\mathbf{u} - \mathbf{u}_h, \mathbf{v} - \mathbf{v}^c) + (\mathbf{u} - \mathbf{u}_h, \mathbf{v}_0^c) \\ &= (\mathbf{u} - \mathbf{u}_h, \mathbf{v} - \mathbf{v}^c) + (\mathbf{u} - \mathbf{u}_h, \mathbf{v}_0^c - \mathbf{H}\mathbf{v}_0^c) + (\mathbf{u} - \mathbf{u}_h, \mathbf{H}\mathbf{v}_0^c) \\ &\equiv T_1 + T_2 + T_3, \end{aligned}$$

with $\mathbf{H}\mathbf{v}_0^c$ from Lemma 2.4.4. Here, we have used the orthogonality property of the error $\mathbf{u} - \mathbf{u}_h$ in Lemma 3.3.6. We now proceed to estimate each of the terms T_1 , T_2 and T_3 below.

Exploiting the Cauchy-Schwarz inequality and the approximation result in Corollary 3.4.7 yields

$$|T_1| \leq \|\mathbf{u} - \mathbf{u}_h\|_0 \|\mathbf{v} - \mathbf{v}^c\|_0 \leq Ch \|\mathbf{u} - \mathbf{u}_h\|_0 \|\mathbf{v}\|_{\mathbf{V}(h)}. \quad (3.36)$$

Similarly, using the Cauchy-Schwarz inequality and the approximation results stated in Lemma 2.4.4 and Corollary 3.4.7, we obtain

$$\begin{aligned} |T_2| &\leq \|\mathbf{u} - \mathbf{u}_h\|_0 \|\mathbf{v}_0^c - \mathbf{H}\mathbf{v}_0^c\|_0 \leq Ch^\sigma \|\mathbf{u} - \mathbf{u}_h\|_0 \|\nabla \times \mathbf{v}_0^c\|_0 \\ &= Ch^\sigma \|\mathbf{u} - \mathbf{u}_h\|_0 \|\nabla \times \mathbf{v}^c\|_0 \leq Ch^\sigma \|\mathbf{u} - \mathbf{u}_h\|_0 \|\mathbf{v}^c\|_{\mathbf{V}(h)} \\ &\leq Ch^\sigma \|\mathbf{u} - \mathbf{u}_h\|_0 \|\mathbf{v}\|_{\mathbf{V}(h)}. \end{aligned} \quad (3.37)$$

Next, we prove the bound

$$|T_3| \leq Ch^\sigma \|\mathbf{v}\|_{\mathbf{V}(h)} \left[\|\mathbf{u} - \mathbf{u}_h\|_{\mathbf{V}(h)} + \|p - p_h\|_{Q(h)} \right], \quad (3.38)$$

by employing a duality approach.

To this end, we set $\mathbf{w} = \mathbf{H}\mathbf{v}_0^c$ and let \mathbf{z} denote the solution of the following problem:

$$\begin{aligned} \nabla \times \nabla \times \mathbf{z} - k^2 \mathbf{z} &= \mathbf{w} && \text{in } \Omega, \\ \mathbf{n} \times \mathbf{z} &= \mathbf{0} && \text{on } \Gamma. \end{aligned} \quad (3.39)$$

Since $\mathbf{w} \in H(\operatorname{div}^0; \Omega)$, the solution \mathbf{z} belongs to $H_0(\operatorname{curl}; \Omega) \cap H(\operatorname{div}^0; \Omega)$. As in [55, Lemma 7.7], we obtain from the embeddings in (2.8) that $\mathbf{z} \in H^\sigma(\Omega)^3$, $\nabla \times \mathbf{z} \in H^\sigma(\Omega)^3$ and

$$\|\mathbf{z}\|_\sigma + \|\nabla \times \mathbf{z}\|_\sigma \leq C \|\mathbf{w}\|_0, \quad (3.40)$$

for a stability constant $C > 0$ and the parameter $\sigma \in (1/2, 1]$ in (2.8).

Hence, multiplying the dual problem (3.39) with $\mathbf{e}_h := \mathbf{u} - \mathbf{u}_h$ and integrating by parts, since $\nabla \times \mathbf{z} \in H(\operatorname{curl}; \Omega)$, we obtain

$$(\mathbf{e}_h, \mathbf{w}) = (\nabla_h \times \mathbf{e}_h, \nabla \times \mathbf{z}) - k^2(\mathbf{e}_h, \mathbf{z}) - \int_{\mathcal{F}_h} \llbracket \mathbf{e}_h \rrbracket_T \cdot \llbracket \nabla \times \mathbf{z} \rrbracket ds.$$

Then, using the definitions of \tilde{a}_h , \tilde{b}_h , \mathcal{L} , \mathcal{M} , the properties of the L^2 -projection $\mathbf{\Pi}_h$, integration by parts and the fact that $\mathbf{z} \in H_0(\operatorname{curl}; \Omega) \cap H(\operatorname{div}^0; \Omega)$, we obtain

$$\begin{aligned} (\mathbf{e}_h, \mathbf{w}) &= \tilde{a}_h(\mathbf{e}_h, \mathbf{z}) - k^2(\mathbf{e}_h, \mathbf{z}) + \tilde{b}_h(\mathbf{z}, p - p_h) + (\mathbf{z}, \nabla_h(p - p_h) - \mathcal{M}(p - p_h)) \\ &\quad + (\mathcal{L}(\mathbf{e}_h), \nabla \times \mathbf{z}) - \int_{\mathcal{F}_h} \llbracket \mathbf{e}_h \rrbracket_T \cdot \llbracket \nabla \times \mathbf{z} \rrbracket ds \\ &= \tilde{a}_h(\mathbf{e}_h, \mathbf{z}) - k^2(\mathbf{e}_h, \mathbf{z}) + \tilde{b}_h(\mathbf{z}, p - p_h) \\ &\quad + \int_{\mathcal{F}_h} \llbracket p - p_h \rrbracket_N \cdot \llbracket \mathbf{z} - \mathbf{\Pi}_h \mathbf{z} \rrbracket ds \\ &\quad - \int_{\mathcal{F}_h} \llbracket \mathbf{e}_h \rrbracket_T \cdot \llbracket \nabla \times \mathbf{z} - \mathbf{\Pi}_h(\nabla \times \mathbf{z}) \rrbracket ds. \end{aligned}$$

Let now $\mathbf{z}_h = \mathbf{\Pi}_N \mathbf{z} \in \mathbf{V}_h^c$ be the Nédélec interpolant of the second kind of \mathbf{z} , according to Lemma 2.4.1. Owing to the error equation (3.17) and the fact that $R_1(\mathbf{u}, p; \mathbf{z}_h) = 0$ (since $\mathbf{z}_h \in \mathbf{V}_h^c$), we have

$$\begin{aligned} (\mathbf{e}_h, \mathbf{w}) &= \tilde{a}_h(\mathbf{e}_h, \mathbf{z} - \mathbf{z}_h) - k^2(\mathbf{e}_h, \mathbf{z} - \mathbf{z}_h) + \tilde{b}_h(\mathbf{z} - \mathbf{z}_h, p - p_h) \\ &\quad + \int_{\mathcal{F}_h} \llbracket p - p_h \rrbracket_N \cdot \llbracket \mathbf{z} - \mathbf{\Pi}_h \mathbf{z} \rrbracket ds - \int_{\mathcal{F}_h} \llbracket \mathbf{e}_h \rrbracket_T \cdot \llbracket \nabla \times \mathbf{z} - \mathbf{\Pi}_h(\nabla \times \mathbf{z}) \rrbracket ds. \end{aligned}$$

Employing the weighted Cauchy-Schwarz inequality, the approximation properties in Lemma 2.4.3 and the stability bound (3.40), we get

$$\begin{aligned} &\left| \int_{\mathcal{F}_h} \llbracket p - p_h \rrbracket_N \cdot \llbracket \mathbf{z} - \mathbf{\Pi}_h \mathbf{z} \rrbracket ds \right| \\ &\leq C \left(\int_{\mathcal{F}_h} \mathbf{h}^{-1} |\llbracket p - p_h \rrbracket_N|^2 ds \right)^{\frac{1}{2}} \left(\sum_{K \in \mathcal{T}_h} h_K \|\mathbf{z} - \mathbf{\Pi}_h \mathbf{z}\|_{0, \partial K}^2 \right)^{\frac{1}{2}} \\ &\leq Ch^\sigma \|p - p_h\|_{Q(h)} \|\mathbf{z}\|_\sigma \leq Ch^\sigma \|p - p_h\|_{Q(h)} \|\mathbf{w}\|_0. \end{aligned}$$

Similarly,

$$\begin{aligned} & \left| \int_{\mathcal{F}_h} [\mathbf{e}_h]_T \cdot \{\{\nabla \times \mathbf{z} - \mathbf{\Pi}_h(\nabla \times \mathbf{z})\}\} ds \right| \\ & \leq C \left(\int_{\mathcal{F}_h} \mathbf{h}^{-1} |[\mathbf{e}_h]_T|^2 ds \right)^{\frac{1}{2}} \left(\sum_{K \in \mathcal{T}_h} h_K \|\nabla \times \mathbf{z} - \mathbf{\Pi}_h(\nabla \times \mathbf{z})\|_{0,\partial K}^2 \right)^{\frac{1}{2}} \\ & \leq Ch^\sigma \|\mathbf{e}_h\|_{\mathbf{V}(h)} \|\nabla \times \mathbf{z}\|_\sigma \leq Ch^\sigma \|\mathbf{e}_h\|_{\mathbf{V}(h)} \|\mathbf{w}\|_0. \end{aligned}$$

Furthermore, the continuity of \tilde{a}_h and \tilde{b}_h in Proposition 3.3.3, the approximation property (2.15) in Lemma 2.4.1 and the stability estimate (3.40) give

$$\begin{aligned} \tilde{a}_h(\mathbf{e}_h, \mathbf{z} - \mathbf{z}_h) - k^2(\mathbf{e}_h, \mathbf{z} - \mathbf{z}_h) + \tilde{b}_h(\mathbf{z} - \mathbf{z}_h, p - p_h) \leq \\ Ch^\sigma \|\mathbf{w}\|_0 [\|\mathbf{e}_h\|_{\mathbf{V}(h)} + \|p - p_h\|_{Q(h)}]. \end{aligned}$$

Hence, the above bounds yield

$$(\mathbf{u} - \mathbf{u}_h, \mathbf{w}) \leq Ch^\sigma \|\mathbf{w}\|_0 [\|\mathbf{u} - \mathbf{u}_h\|_{\mathbf{V}(h)} + \|p - p_h\|_{Q(h)}].$$

Since $\|\mathbf{w}\|_0 \leq \|\mathbf{v}_0^c\|_0 \leq \|\mathbf{v}^c\|_0 \leq C\|\mathbf{v}\|_{\mathbf{V}(h)}$, in view of Lemma 2.4.4, the $L^2(\Omega)^3$ -orthogonality of the Helmholtz decomposition (3.35), and Corollary 3.4.7, we conclude that (3.38) holds.

By combining (3.36), (3.37) and (3.38), we obtain

$$|(\mathbf{u} - \mathbf{u}_h, \mathbf{v})| \leq Ch^\sigma \|\mathbf{v}\|_{\mathbf{V}(h)} [\|\mathbf{u} - \mathbf{u}_h\|_{\mathbf{V}(h)} + \|p - p_h\|_{Q(h)}]$$

for all $\mathbf{v} \in \mathbf{V}_h$, which immediately implies the desired bound for $\mathcal{D}_h(\mathbf{u} - \mathbf{u}_h)$. \square

3.5.3 Conclusion of the proof of Theorem 3.4.1

From the abstract estimate in Proposition 3.5.1 and the bound on $\mathcal{D}_h(\mathbf{u} - \mathbf{u}_h)$ in Proposition 3.5.2, we have that there exists $h_0 > 0$ such that, for any $h < h_0$,

$$\|\mathbf{u} - \mathbf{u}_h\|_{\mathbf{V}(h)} + \|p - p_h\|_{Q(h)} \leq C [\|\mathbf{u} - \mathbf{v}\|_{\mathbf{V}(h)} + \|p - q\|_{Q(h)} + \mathcal{E}_{1,h}(\mathbf{u}) + \mathcal{E}_{2,h}(\mathbf{u})] \quad (3.41)$$

for all $\mathbf{v} \in \mathbf{V}_h^c$ and all $q \in Q_h^c$, with a constant $C > 0$ independent of the mesh size. Notice that h_0 also depends on the wave number and on the regularity exponent σ .

Let us now suppose that the analytical solution (\mathbf{u}, p) satisfies (3.25). First, we use the Nédélec interpolant of the second kind in Lemma 2.4.1 to obtain

$$\inf_{\mathbf{v} \in \mathbf{V}_h^c} \|\mathbf{u} - \mathbf{v}\|_{\mathbf{V}(h)} \leq \|\mathbf{u} - \mathbf{\Pi}_N \mathbf{u}\|_{\mathbf{V}(h)} \leq Ch^{\min\{s,\ell\}} [\|\mathbf{u}\|_s + \|\nabla \times \mathbf{u}\|_s].$$

Then, standard approximation properties for Q_h^c give

$$\inf_{q \in Q_h^c} \|p - q\|_{Q(h)} \leq Ch^{\min\{s,\ell\}} \|p\|_{s+1}.$$

Finally, using Lemma 2.4.3, we conclude that

$$\begin{aligned} \mathcal{E}_{1,h}(\mathbf{u}) & \leq C h^{\min\{s,\ell+1\}} \|\nabla \times \mathbf{u}\|_s, \\ \mathcal{E}_{2,h}(\mathbf{u}) & \leq C h^{\min\{s,\ell+1\}} \|\mathbf{u}\|_s. \end{aligned} \quad (3.42)$$

Inserting these bounds into (3.41) completes the proof of Theorem 3.4.1.

3.6 Proof of Theorem 3.4.4 (error estimate in the L^2 -norm)

In this section, we present the proof of Theorem 3.4.4. Our analysis proceeds along the lines of the proof of Theorem 2.3.5 in Chapter 2 which, in turn, relies on the ideas of [54, Section 4] where an L^2 -error estimate is derived for conforming discretizations of the indefinite time-harmonic Maxwell's equations.

3.6.1 The bound in Theorem 3.4.4

To derive the bound in Theorem 3.4.4, we start by splitting \mathbf{u}_h into $\mathbf{u}_h = \mathbf{u}_h^c + \mathbf{u}_h^\perp$, where $\mathbf{u}_h^c := \mathbf{A}\mathbf{u}_h \in \mathbf{V}_h^c$ is the conforming approximation from Theorem 3.4.6 and $\mathbf{u}_h^\perp = \mathbf{u}_h - \mathbf{A}\mathbf{u}_h$. We further recall that $\mathbf{\Pi}_N\mathbf{u}$ denotes the curl-conforming Nédélec interpolant of the second kind, and write

$$\|\mathbf{u} - \mathbf{u}_h\|_0^2 = (\mathbf{u} - \mathbf{u}_h, \mathbf{u} - \mathbf{\Pi}_N\mathbf{u}) + (\mathbf{u} - \mathbf{u}_h, \mathbf{\Pi}_N\mathbf{u} - \mathbf{u}_h^c) - (\mathbf{u} - \mathbf{u}_h, \mathbf{u}_h^\perp).$$

By using the triangle inequality, the Cauchy-Schwarz inequality and the result in Corollary 3.4.8, we have

$$\|\mathbf{u} - \mathbf{u}_h\|_0 \leq \|\mathbf{u} - \mathbf{\Pi}_N\mathbf{u}\|_0 + Ch\|\mathbf{u} - \mathbf{u}_h\|_{\mathbf{V}(h)} + \frac{|(\mathbf{u} - \mathbf{u}_h, \mathbf{\Pi}_N\mathbf{u} - \mathbf{u}_h^c)|}{\|\mathbf{u} - \mathbf{u}_h\|_0}, \quad (3.43)$$

with $C > 0$ independent of the mesh size.

Defining

$$T := \frac{|(\mathbf{u} - \mathbf{u}_h, \mathbf{\Pi}_N\mathbf{u} - \mathbf{u}_h^c)|}{\|\mathbf{u} - \mathbf{u}_h\|_0},$$

we claim that, for a sufficiently small mesh size,

$$T \leq C\|\mathbf{u} - \mathbf{\Pi}_N\mathbf{u}\|_0 + Ch^\sigma [\|\mathbf{u} - \mathbf{\Pi}_N\mathbf{u}\|_{\text{curl}} + \|\mathbf{u} - \mathbf{u}_h\|_{\mathbf{V}(h)} + \|p - p_h\|_{Q(h)}], \quad (3.44)$$

with $C > 0$ independent of the mesh size, and $\sigma \in (1/2, 1]$ denoting the embedding parameter in (2.8). Combining (3.43), (3.44) and using the approximation property (2.17) for $\mathbf{\Pi}_N$ in Lemma 2.4.1 yield

$$\begin{aligned} \|\mathbf{u} - \mathbf{u}_h\|_0 &\leq Ch^{\min\{s+\sigma, \ell+1\}} \|\mathbf{u}\|_{s+\sigma} + Ch^{\min\{s, \ell\}+\sigma} [\|\mathbf{u}\|_s + \|\nabla \times \mathbf{u}\|_s] \\ &\quad + Ch^\sigma [\|\mathbf{u} - \mathbf{u}_h\|_{\mathbf{V}(h)} + \|p - p_h\|_{Q(h)}]. \end{aligned}$$

Since $\|\mathbf{u}\|_s \leq \|\mathbf{u}\|_{s+\sigma}$ and $\min\{s + \sigma, \ell + 1\} \geq \min\{s, \ell\} + \sigma$, the error estimate in Theorem 3.4.4 follows from Theorem 3.4.1. It remains to prove the bound in (3.44); this is undertaken in the following section.

3.6.2 Proof of the auxiliary bound in (3.44)

In order to prove (3.44), we invoke the Helmholtz decomposition in (3.23) and write

$$\mathbf{\Pi}_N\mathbf{u} - \mathbf{u}_h^c = \mathbf{w}_0^c + \nabla\varphi, \quad (3.45)$$

with $\mathbf{w}_0^c \in \mathbf{X}_h$ and $\varphi \in Q_h^c$.

We then let $\mathbf{w} = \mathbf{H}\mathbf{w}_0^c$ be the exactly divergence-free approximation of \mathbf{w}_0^c from Lemma 2.4.4. From (3.45) and the orthogonality property (ii) in Lemma 3.3.6, we obtain

$$(\mathbf{u} - \mathbf{u}_h, \mathbf{\Pi}_N \mathbf{u} - \mathbf{u}_h^c) = (\mathbf{u} - \mathbf{u}_h, \mathbf{w}_0^c) = (\mathbf{u} - \mathbf{u}_h, \mathbf{w}_0^c - \mathbf{w}) + (\mathbf{u} - \mathbf{u}_h, \mathbf{w}).$$

Hence,

$$\frac{|(\mathbf{u} - \mathbf{u}_h, \mathbf{\Pi}_N \mathbf{u} - \mathbf{u}_h^c)|}{\|\mathbf{u} - \mathbf{u}_h\|_0} \leq \|\mathbf{w}_0^c - \mathbf{w}\|_0 + \|\mathbf{w}\|_0. \quad (3.46)$$

Therefore, it is sufficient to estimate $\|\mathbf{w}_0^c - \mathbf{w}\|_0$ and $\|\mathbf{w}\|_0$.

Step 1: Estimate of $\|\mathbf{w}_0^c - \mathbf{w}\|_0$. We claim that

$$\|\mathbf{w}_0^c - \mathbf{w}\|_0 \leq Ch^\sigma [\|\mathbf{u} - \mathbf{\Pi}_N \mathbf{u}\|_{\text{curl}} + \|\mathbf{u} - \mathbf{u}_h\|_{\mathbf{V}(h)}], \quad (3.47)$$

with a constant $C > 0$ independent of the mesh size.

To see this, note that, in view of the definition of \mathbf{H} and (3.45), there holds

$$\nabla \times \mathbf{w} = \nabla \times \mathbf{w}_0^c = \nabla \times (\mathbf{\Pi}_N \mathbf{u} - \mathbf{u}_h^c). \quad (3.48)$$

Thus, the result in Lemma 2.4.4, the triangle inequality and Corollary 3.4.8 yield

$$\begin{aligned} \|\mathbf{w}_0^c - \mathbf{w}\|_0 &\leq Ch^\sigma \|\nabla \times (\mathbf{\Pi}_N \mathbf{u} - \mathbf{u}_h^c)\|_0 \\ &\leq Ch^\sigma [\|\nabla \times (\mathbf{\Pi}_N \mathbf{u} - \mathbf{u})\|_0 + \|\nabla_h \times (\mathbf{u} - \mathbf{u}_h)\|_0 + \|\nabla_h \times (\mathbf{u}_h - \mathbf{u}_h^c)\|_0] \\ &\leq Ch^\sigma [\|\mathbf{u} - \mathbf{\Pi}_N \mathbf{u}\|_{\text{curl}} + \|\mathbf{u} - \mathbf{u}_h\|_{\mathbf{V}(h)}], \end{aligned}$$

which proves (3.47).

Step 2: Estimate of $\|\mathbf{w}\|_0$. Next, we claim that, for a sufficiently small mesh size,

$$\|\mathbf{w}\|_0 \leq C \|\mathbf{u} - \mathbf{\Pi}_N \mathbf{u}\|_0 + Ch^\sigma [\|\mathbf{u} - \mathbf{\Pi}_N \mathbf{u}\|_{\text{curl}} + \|\mathbf{u} - \mathbf{u}_h\|_{\mathbf{V}(h)} + \|p - p_h\|_{Q(h)}], \quad (3.49)$$

with a constant $C > 0$ independent of the mesh size.

To prove (3.49) we employ a duality approach. To this end, let \mathbf{z} be the solution of the dual problem (3.39) with right-hand side $\mathbf{w} = \mathbf{H}\mathbf{w}_0^c$. Again, $\mathbf{w} \in H(\text{div}^0; \Omega)$ so that $\mathbf{z} \in H^\sigma(\Omega)^3$, $\nabla \times \mathbf{z} \in H^\sigma(\Omega)^3$, with $\sigma \in (1/2, 1]$ in (2.8), and the bound (3.40) holds. The dual problem (3.39) can be written in mixed formulation as

$$\nabla \times \nabla \times \mathbf{z} - k^2 \mathbf{z} + \nabla r = \mathbf{w} \quad \text{in } \Omega, \quad (3.50)$$

$$\nabla \cdot \mathbf{z} = 0 \quad \text{in } \Omega, \quad (3.51)$$

$$\mathbf{n} \times \mathbf{z} = \mathbf{0} \quad \text{on } \Gamma, \quad (3.52)$$

$$r = 0 \quad \text{on } \Gamma. \quad (3.53)$$

Since $\mathbf{w} \in H(\text{div}^0; \Omega)$, we actually have $r \equiv 0$.

Let us denote by $(\mathbf{z}_h, r_h) \in \mathbf{V}_h \times Q_h$ the discontinuous Galerkin approximation of (3.50)–(3.53) given by:

$$\begin{aligned} \tilde{\mathcal{A}}_h(\mathbf{z}_h, \mathbf{v}) - \tilde{b}_h(\mathbf{v}, r_h) &= (\mathbf{w}, \mathbf{v}), \\ \tilde{b}_h(\mathbf{z}_h, q) - c_h(r_h, q) &= 0 \end{aligned} \quad (3.54)$$

for all $(\mathbf{v}, q) \in \mathbf{V}_h \times Q_h$. Here and in the following, we use the notation

$$\tilde{\mathcal{A}}_h(\mathbf{z}, \mathbf{v}) = \tilde{a}_h(\mathbf{z}, \mathbf{v}) - k^2(\mathbf{z}, \mathbf{v}).$$

Up to a sign change, the formulation (3.54) is of the same form as the one in (3.15). It can be readily seen that Theorem 3.4.1 and Corollary 3.4.3 apply to (3.54). Hence, for a sufficiently small mesh size, the discrete solution (\mathbf{z}_h, r_h) exists and is unique. Moreover, the following a-priori error bound holds:

$$\|\mathbf{z} - \mathbf{z}_h\|_{\mathbf{V}(h)} + \|r_h\|_{Q(h)} \leq Ch^\sigma [\|\mathbf{z}\|_\sigma + \|\nabla \times \mathbf{z}\|_\sigma] \leq Ch^\sigma \|\mathbf{w}\|_0. \quad (3.55)$$

Here, we have taken into account that $r \equiv 0$ and have also used the stability bound in (3.40).

After these preliminary considerations, we multiply the equation in (3.39) by \mathbf{w} and integrate by parts. Recalling the equivalence of the forms a and \tilde{a}_h on $\mathbf{V} \times \mathbf{V}$, we obtain

$$\|\mathbf{w}\|_0^2 = \tilde{\mathcal{A}}_h(\mathbf{z}, \mathbf{w}) = \tilde{\mathcal{A}}_h(\mathbf{z} - \mathbf{\Pi}^c \mathbf{z}, \mathbf{w}) + \tilde{\mathcal{A}}_h(\mathbf{\Pi}^c \mathbf{z}, \mathbf{w}), \quad (3.56)$$

with $\mathbf{\Pi}^c$ denoting the Galerkin projection from (2.19).

By the definition of the projection $\mathbf{\Pi}^c$ and the property $\nabla \times \mathbf{w} = \nabla \times \mathbf{w}_0^c$, we conclude that

$$\begin{aligned} \tilde{\mathcal{A}}_h(\mathbf{z} - \mathbf{\Pi}^c \mathbf{z}, \mathbf{w}) &= -(\mathbf{z} - \mathbf{\Pi}^c \mathbf{z}, \mathbf{w}_0^c) - k^2(\mathbf{z} - \mathbf{\Pi}^c \mathbf{z}, \mathbf{w}) \\ &= -(\mathbf{z} - \mathbf{\Pi}^c \mathbf{z}, \mathbf{w}_0^c - \mathbf{w}) - (1 + k^2)(\mathbf{z} - \mathbf{\Pi}^c \mathbf{z}, \mathbf{w}). \end{aligned}$$

The approximation result for $\mathbf{\Pi}^c$ in Lemma 2.4.2 and the bound in (3.40) yield

$$\|\mathbf{z} - \mathbf{\Pi}^c \mathbf{z}\|_0 \leq \|\mathbf{z} - \mathbf{\Pi}^c \mathbf{z}\|_{\text{curl}} \leq Ch^\sigma \|\mathbf{w}\|_0. \quad (3.57)$$

For later use, we further point out that the stability of $\mathbf{\Pi}^c$ in the norm $\|\cdot\|_{\text{curl}}$ and the bound in (3.40) give

$$\|\mathbf{\Pi}^c \mathbf{z}\|_0 \leq C \|\mathbf{w}\|_0. \quad (3.58)$$

Hence, by using the Cauchy-Schwarz inequality and the estimates (3.47) and (3.57) we conclude that

$$\begin{aligned} |\tilde{\mathcal{A}}_h(\mathbf{z} - \mathbf{\Pi}^c \mathbf{z}, \mathbf{w})| &\leq \|\mathbf{z} - \mathbf{\Pi}^c \mathbf{z}\|_0 \|\mathbf{w} - \mathbf{w}_0^c\|_0 + C \|\mathbf{z} - \mathbf{\Pi}^c \mathbf{z}\|_0 \|\mathbf{w}\|_0 \\ &\leq Ch^{2\sigma} \|\mathbf{w}\|_0 [\|\mathbf{u} - \mathbf{\Pi}_N \mathbf{u}\|_{\text{curl}} + \|\mathbf{u} - \mathbf{u}_h\|_{\mathbf{V}(h)}] + Ch^\sigma \|\mathbf{w}\|_0^2. \end{aligned} \quad (3.59)$$

It remains to bound the term $\tilde{\mathcal{A}}_h(\mathbf{\Pi}^c \mathbf{z}, \mathbf{w})$ in (3.56). To this end, in view of (3.48) and (3.45), we first note that

$$\begin{aligned} \tilde{\mathcal{A}}_h(\mathbf{\Pi}^c \mathbf{z}, \mathbf{w}) &= (\nabla \times \mathbf{\Pi}^c \mathbf{z}, \nabla \times \mathbf{w}) - k^2(\mathbf{\Pi}^c \mathbf{z}, \mathbf{w}) \\ &= (\nabla \times \mathbf{\Pi}^c \mathbf{z}, \nabla \times (\mathbf{\Pi}_N \mathbf{u} - \mathbf{u}_h^c)) - k^2(\mathbf{\Pi}^c \mathbf{z}, \mathbf{w} - \mathbf{w}_0^c) - k^2(\mathbf{\Pi}^c \mathbf{z}, \mathbf{w}_0^c) \\ &= (\nabla \times \mathbf{\Pi}^c \mathbf{z}, \nabla \times (\mathbf{\Pi}_N \mathbf{u} - \mathbf{u}_h^c)) - k^2(\mathbf{\Pi}^c \mathbf{z}, \mathbf{w} - \mathbf{w}_0^c) - k^2(\mathbf{\Pi}^c \mathbf{z}, \mathbf{\Pi}_N \mathbf{u} - \mathbf{u}_h^c) \\ &= \tilde{\mathcal{A}}_h(\mathbf{\Pi}^c \mathbf{z}, \mathbf{\Pi}_N \mathbf{u} - \mathbf{u}_h^c) - k^2(\mathbf{\Pi}^c \mathbf{z}, \mathbf{w} - \mathbf{w}_0^c). \end{aligned}$$

Here, we have used that

$$(\mathbf{\Pi}^c \mathbf{z}, \nabla \varphi) = (\mathbf{z}, \nabla \varphi) = 0, \quad (3.60)$$

which follows readily from the definition of $\mathbf{\Pi}^c$ and the fact that $\mathbf{z} \in H(\operatorname{div}^0; \Omega)$. Employing (3.58) and (3.47) we get

$$\begin{aligned} |\tilde{\mathcal{A}}_h(\mathbf{\Pi}^c \mathbf{z}, \mathbf{w})| &\leq |\tilde{\mathcal{A}}_h(\mathbf{\Pi}^c \mathbf{z}, \mathbf{\Pi}_N \mathbf{u} - \mathbf{u}_h^c)| + C \|\mathbf{\Pi}^c \mathbf{z}\|_0 \|\mathbf{w} - \mathbf{w}_0^c\|_0 \\ &\leq |\tilde{\mathcal{A}}_h(\mathbf{\Pi}^c \mathbf{z}, \mathbf{\Pi}_N \mathbf{u} - \mathbf{u}_h^c)| \\ &\quad + Ch^\sigma \|\mathbf{w}\|_0 [\|\mathbf{u} - \mathbf{\Pi}_N \mathbf{u}\|_{\operatorname{curl}} + \|\mathbf{u} - \mathbf{u}_h\|_{\mathbf{V}(h)}]. \end{aligned} \quad (3.61)$$

In order to estimate $|\tilde{\mathcal{A}}_h(\mathbf{\Pi}^c \mathbf{z}, \mathbf{\Pi}_N \mathbf{u} - \mathbf{u}_h^c)|$, we consider the expansion

$$\begin{aligned} \tilde{\mathcal{A}}_h(\mathbf{\Pi}^c \mathbf{z}, \mathbf{\Pi}_N \mathbf{u} - \mathbf{u}_h^c) &= \tilde{\mathcal{A}}_h(\mathbf{\Pi}^c \mathbf{z}, \mathbf{\Pi}_N \mathbf{u} - \mathbf{u}) \\ &\quad + \tilde{\mathcal{A}}_h(\mathbf{\Pi}^c \mathbf{z}, \mathbf{u} - \mathbf{u}_h) + \tilde{\mathcal{A}}_h(\mathbf{\Pi}^c \mathbf{z}, \mathbf{u}_h - \mathbf{u}_h^c) \\ &\equiv T_1 + T_2 + T_3, \end{aligned}$$

and estimate the terms T_1 , T_2 , and T_3 individually.

By further expanding T_1 , we have

$$T_1 = \tilde{\mathcal{A}}_h(\mathbf{\Pi}^c \mathbf{z} - \mathbf{z}, \mathbf{\Pi}_N \mathbf{u} - \mathbf{u}) + \tilde{\mathcal{A}}_h(\mathbf{z}, \mathbf{\Pi}_N \mathbf{u} - \mathbf{u}).$$

Employing the variational formulation of the dual problem (3.39), we bound the second term as follows:

$$\tilde{\mathcal{A}}_h(\mathbf{z}, \mathbf{\Pi}_N \mathbf{u} - \mathbf{u}) = (\mathbf{w}, \mathbf{\Pi}_N \mathbf{u} - \mathbf{u}) \leq \|\mathbf{w}\|_0 \|\mathbf{\Pi}_N \mathbf{u} - \mathbf{u}\|_0.$$

Hence, by Lemma 2.4.2 and (3.40), T_1 can be estimated by

$$\begin{aligned} |T_1| &\leq C \|\mathbf{\Pi}_N \mathbf{u} - \mathbf{u}\|_{\operatorname{curl}} \|\mathbf{\Pi}^c \mathbf{z} - \mathbf{z}\|_{\operatorname{curl}} + \|\mathbf{w}\|_0 \|\mathbf{\Pi}_N \mathbf{u} - \mathbf{u}\|_0 \\ &\leq Ch^\sigma \|\mathbf{w}\|_0 \|\mathbf{\Pi}_N \mathbf{u} - \mathbf{u}\|_{\operatorname{curl}} + \|\mathbf{w}\|_0 \|\mathbf{\Pi}_N \mathbf{u} - \mathbf{u}\|_0. \end{aligned} \quad (3.62)$$

For T_2 , we claim that

$$|T_2| = |\tilde{b}_h(\mathbf{\Pi}^c \mathbf{z}, p - p_h)| \leq Ch^\sigma \|\mathbf{w}\|_0 \|p - p_h\|_{Q(h)}. \quad (3.63)$$

Indeed, using the symmetry of $\tilde{\mathcal{A}}_h$ and the error equation (3.17), together with the fact that by (3.16) the residual $R_1(\mathbf{u}, p; \mathbf{\Pi}^c \mathbf{z})$ vanishes, we have

$$\begin{aligned} |\tilde{\mathcal{A}}_h(\mathbf{\Pi}^c \mathbf{z}, \mathbf{u} - \mathbf{u}_h)| &= |\tilde{b}_h(\mathbf{\Pi}^c \mathbf{z}, p - p_h)| \\ &\leq |\tilde{b}_h(\mathbf{\Pi}^c \mathbf{z} - \mathbf{z}, p - p_h)| + |\tilde{b}_h(\mathbf{z}, p - p_h)|. \end{aligned}$$

The continuity of \tilde{b} from Proposition 3.3.3 and equation (3.57) then yield

$$|\tilde{b}_h(\mathbf{\Pi}^c \mathbf{z} - \mathbf{z}, p - p_h)| \leq C \|\mathbf{\Pi}^c \mathbf{z} - \mathbf{z}\|_{\operatorname{curl}} \|p - p_h\|_{Q(h)} \leq Ch^\sigma \|\mathbf{w}\|_0 \|p - p_h\|_{Q(h)}.$$

Estimating the residual $R_2(\mathbf{z}; q)$ of the dual problem as in Proposition 3.3.3 and (3.42) and using the bound in (3.40), results in

$$\begin{aligned} |\tilde{b}_h(\mathbf{z}, p - p_h)| &= |R_2(\mathbf{z}; p - p_h)| \leq C_R \mathcal{E}_{2,h}(\mathbf{z}) \|p - p_h\|_{Q(h)} \\ &\leq Ch^\sigma \|\mathbf{z}\|_\sigma \|p - p_h\|_{Q(h)} \leq Ch^\sigma \|\mathbf{w}\|_0 \|p - p_h\|_{Q(h)}, \end{aligned}$$

which completes the proof of the bound (3.63) for T_2 .

Finally, to bound T_3 , we use the continuity property in Proposition 3.3.3, the discrete formulation (3.54) and the Cauchy-Schwarz inequality:

$$\begin{aligned}
|T_3| &\leq |\tilde{\mathcal{A}}_h(\mathbf{\Pi}^c \mathbf{z} - \mathbf{z}, \mathbf{u}_h - \mathbf{u}_h^c)| + |\tilde{\mathcal{A}}_h(\mathbf{z} - \mathbf{z}_h, \mathbf{u}_h - \mathbf{u}_h^c)| + |\tilde{\mathcal{A}}_h(\mathbf{z}_h, \mathbf{u}_h - \mathbf{u}_h^c)| \\
&\leq C \|\mathbf{u}_h - \mathbf{u}_h^c\|_{\mathbf{V}(h)} [\|\mathbf{\Pi}^c \mathbf{z} - \mathbf{z}\|_{\text{curl}} + \|\mathbf{z} - \mathbf{z}_h\|_{\mathbf{V}(h)}] \\
&\quad + \|\mathbf{w}\|_0 \|\mathbf{u}_h - \mathbf{u}_h^c\|_0 + |\tilde{b}_h(\mathbf{u}_h - \mathbf{u}_h^c, r_h)|,
\end{aligned} \tag{3.64}$$

with \mathbf{z}_h denoting the first component of the approximation in (3.54). From Corollary 3.4.8 we have

$$\|\mathbf{u}_h - \mathbf{u}_h^c\|_{\mathbf{V}(h)} \leq C \|\mathbf{u} - \mathbf{u}_h\|_{\mathbf{V}(h)}, \quad \|\mathbf{u}_h - \mathbf{u}_h^c\|_0 \leq Ch \|\mathbf{u} - \mathbf{u}_h\|_{\mathbf{V}(h)}.$$

This, combined with the continuity of \tilde{b}_h from Proposition 3.3.3, the fact that $r \equiv 0$, the energy estimate from Theorem 3.4.1 applied to (3.54), and the stability bound in (3.40), yields the following estimate for the last term in (3.64):

$$\begin{aligned}
|\tilde{b}_h(\mathbf{u}_h - \mathbf{u}_h^c, r_h)| &\leq C \|\mathbf{u} - \mathbf{u}_h\|_{\mathbf{V}(h)} \|r - r_h\|_{Q(h)} \\
&\leq Ch^\sigma [\|\mathbf{z}\|_\sigma + \|\nabla \times \mathbf{z}\|_\sigma + \|r\|_{\sigma+1}] \|\mathbf{u} - \mathbf{u}_h\|_{\mathbf{V}(h)} \\
&\leq Ch^\sigma \|\mathbf{w}\|_0 \|\mathbf{u} - \mathbf{u}_h\|_{\mathbf{V}(h)}.
\end{aligned}$$

Therefore, again by applying Corollary 3.4.8 and Theorem 3.4.1 to (3.54), the stability estimate (3.40), and equation (3.57) we conclude that

$$|T_3| \leq h^\sigma \|\mathbf{w}\|_0 \|\mathbf{u} - \mathbf{u}_h\|_{\mathbf{V}(h)}. \tag{3.65}$$

Gathering the estimates (3.61), (3.62), (3.63), and (3.65) gives

$$\begin{aligned}
|\tilde{\mathcal{A}}(\mathbf{\Pi}^c \mathbf{z}, \mathbf{w})| &\leq Ch^\sigma \|\mathbf{w}\|_0 [\|\mathbf{u} - \mathbf{\Pi}_N \mathbf{u}\|_{\text{curl}} + \|\mathbf{u} - \mathbf{u}_h\|_{\mathbf{V}(h)} + \|p - p_h\|_{Q(h)}] \\
&\quad + \|\mathbf{w}\|_0 \|\mathbf{u} - \mathbf{\Pi}_N \mathbf{u}\|_0.
\end{aligned} \tag{3.66}$$

Inserting (3.59) and (3.66) into (3.56) then shows that

$$\begin{aligned}
\|\mathbf{w}\|_0 &\leq Ch^\sigma \|\mathbf{w}\|_0 + C \|\mathbf{u} - \mathbf{\Pi}_N \mathbf{u}\|_0 \\
&\quad + Ch^\sigma [\|\mathbf{u} - \mathbf{\Pi}_N \mathbf{u}\|_{\text{curl}} + \|\mathbf{u} - \mathbf{u}_h\|_{\mathbf{V}(h)} + \|p - p_h\|_{Q(h)}].
\end{aligned} \tag{3.67}$$

Hence, for a sufficiently small mesh size, we obtain the result in (3.49).

Step 3. Conclusion. The bound (3.44) now follows from (3.46), (3.47) and (3.49).

Elements	$\ell = 1$		$\ell = 2$		$\ell = 3$	
	$\ \mathbf{u} - \mathbf{u}_h\ _{\mathbf{V}(h)}$	r	$\ \mathbf{u} - \mathbf{u}_h\ _{\mathbf{V}(h)}$	r	$\ \mathbf{u} - \mathbf{u}_h\ _{\mathbf{V}(h)}$	r
26	1.876e-1	-	2.009e-2	-	5.045e-4	-
104	9.135e-2	1.04	5.004e-3	2.01	6.471e-5	2.96
416	4.456e-2	1.04	1.250e-3	2.00	8.131e-6	2.99
1664	2.194e-2	1.02	3.123e-4	2.00	1.017e-6	3.00

Table 3.1: Example 1. Convergence of $\|\mathbf{u} - \mathbf{u}_h\|_{\mathbf{V}(h)}$ with $k = 1$.

Elements	$\ell = 1$		$\ell = 2$		$\ell = 3$	
	$\ p - p_h\ _{Q(h)}$	r	$\ p - p_h\ _{Q(h)}$	r	$\ p - p_h\ _{Q(h)}$	r
26	9.226e-2	-	1.213e-2	-	2.728e-4	-
104	2.715e-2	1.76	1.332e-3	3.19	1.489e-5	4.19
416	6.774e-3	2.00	1.551e-4	3.10	8.132e-7	4.19
1664	1.609e-3	2.07	1.867e-5	3.05	4.638e-8	4.13

Table 3.2: Example 1. Convergence of $\|p - p_h\|_{Q(h)}$ with $k = 1$.

Elements	$\ell = 1$		$\ell = 2$		$\ell = 3$	
	$\ \mathbf{u} - \mathbf{u}_h\ _{\mathbf{V}(h)}$	r	$\ \mathbf{u} - \mathbf{u}_h\ _{\mathbf{V}(h)}$	r	$\ \mathbf{u} - \mathbf{u}_h\ _{\mathbf{V}(h)}$	r
26	1.131	-	1.265e-1	-	1.243e-2	-
104	5.405e-1	1.06	3.217e-2	1.98	1.582e-3	2.97
416	2.635e-1	1.04	8.078e-3	1.99	1.985e-4	2.99
1664	1.302e-1	1.02	2.022e-3	2.00	2.483e-5	3.00

Table 3.3: Example 1. Convergence of $\|\mathbf{u} - \mathbf{u}_h\|_{\mathbf{V}(h)}$ with $k = 2$.

3.7 Numerical experiments

In this section we present a series of numerical experiments to highlight the practical performance of the mixed DG method introduced and analyzed in this article for the numerical approximation of the indefinite time-harmonic Maxwell equations (3.6)–(3.9). For simplicity, we restrict ourselves to two-dimensional model problems; additionally, we note that throughout this section we select the constants appearing in the interior penalty stabilization functions defined in (3.14) as follows:

$$\alpha = 10\ell^2 \quad \text{and} \quad \gamma = 1.$$

The dependence of α on the polynomial degree ℓ has been chosen in order to guarantee the Gårding-type inequality stated in Proposition 3.3.4 holds independently of ℓ , cf. [43], for example.

Elements	$\ell = 1$		$\ell = 2$		$\ell = 3$	
	$\ p - p_h\ _{Q(h)}$	r	$\ p - p_h\ _{Q(h)}$	r	$\ p - p_h\ _{Q(h)}$	r
26	5.745e-1	-	7.298e-2	-	6.752e-3	-
104	1.700e-1	1.76	8.377e-3	3.12	3.652e-4	4.21
416	4.232e-2	2.01	9.933e-4	3.08	2.026e-5	4.17
1664	1.002e-2	2.08	1.209e-4	3.04	1.174e-6	4.11

Table 3.4: Example 1. Convergence of $\|p - p_h\|_{Q(h)}$ with $k = 2$.

Elements	$\ell = 1$		$\ell = 2$		$\ell = 3$	
	$\ \mathbf{u} - \mathbf{u}_h\ _{\mathbf{V}(h)}$	r	$\ \mathbf{u} - \mathbf{u}_h\ _{\mathbf{V}(h)}$	r	$\ \mathbf{u} - \mathbf{u}_h\ _{\mathbf{V}(h)}$	r
26	3.902	-	1.276	-	1.429e-1	-
104	2.017	0.95	2.971e-1	2.10	2.289e-2	2.64
416	9.871e-1	1.03	7.401e-2	2.01	2.952e-3	2.96
1664	4.864e-1	1.02	1.849e-2	2.00	3.715e-4	2.99

Table 3.5: Example 1. Convergence of $\|\mathbf{u} - \mathbf{u}_h\|_{\mathbf{V}(h)}$ with $k = 4$.

3.7.1 Example 1

In this first example we select $\Omega \subset \mathbb{R}^2$ to be the square domain $(-1, 1)^2$. Furthermore, we set $\mathbf{j} = \mathbf{0}$ and select suitable non-homogeneous boundary conditions for \mathbf{u} , i.e., $\mathbf{n} \times \mathbf{u} = \mathbf{g}$, where \mathbf{g} is a given tangential trace, so that the analytical solution to the two-dimensional analogue of (3.6)–(3.9) is given by the smooth field

$$\mathbf{u}(x, y) = (\sin(ky), \sin(kx))^T, \quad p = 0.$$

Here, the boundary conditions for \mathbf{u} are enforced in the usual DG manner by adding boundary terms into the formulation (3.13); more precisely, the right-hand side of the first equation in (3.13) is replaced by the term

$$f_h(\mathbf{v}) = (\mathbf{j}, \mathbf{v}) - \int_{\mathcal{F}_h^B} \mathbf{g} \cdot \nabla_h \times \mathbf{v} \, ds + \int_{\mathcal{F}_h^B} \mathbf{a} \mathbf{g} \cdot (\mathbf{n} \times \mathbf{v}) \, ds,$$

see [43, 45] for details.

We investigate the asymptotic convergence of the mixed DG method on a sequence of successively finer (quasi-uniform) unstructured triangular meshes for $\ell = 1, 2, 3$ as the wave number k increases. To this end, in Tables 3.1, 3.2, Tables 3.3, 3.4, and Tables 3.5, 3.6 we present numerical experiments for $k = 1, 2, 4$, respectively. For each wave number k we show the number of elements in the computational mesh, the corresponding DG-norms of the error in the numerical approximation to both \mathbf{u} and p , and the numerical rate of convergence r . Here, we observe that (asymptotically) $\|\mathbf{u} - \mathbf{u}_h\|_{\mathbf{V}(h)}$ converges to zero at the optimal rate $\mathcal{O}(h^\ell)$, for each fixed ℓ and each k , as h tends to zero, as predicted by Theorem 3.4.1. On the other hand, for this mixed-order method, $\|p - p_h\|_{Q(h)}$ converges to zero at the rate $\mathcal{O}(h^{\ell+1})$, for each ℓ and k , as h tends to zero; this rate is indeed optimal, though this is not reflected by Theorem 3.4.1, cf. [44]. In particular, we make two key observations: firstly, we note that for a given fixed

	$\ell = 1$		$\ell = 2$		$\ell = 3$	
Elements	$\ p - p_h\ _{Q(h)}$	r	$\ p - p_h\ _{Q(h)}$	r	$\ p - p_h\ _{Q(h)}$	r
26	2.077	-	6.953e-1	-	5.923e-2	-
104	5.961e-1	1.80	6.828e-2	3.35	4.982e-3	3.57
416	1.541e-1	1.95	7.722e-3	3.14	3.105e-4	4.00
1664	3.796e-2	2.02	9.207e-4	3.07	1.909e-5	4.02

Table 3.6: Example 1. Convergence of $\|p - p_h\|_{Q(h)}$ with $k = 4$.

mesh and fixed polynomial degree, an increase in the wave number k leads to an increase in the DG-norm of the error in the approximation to both \mathbf{u} and p . Indeed, as pointed out in [40] (see also Chapter 2) and [1], where interior penalty and curl-conforming finite element methods, respectively, were employed for the numerical approximation of (3.1)–(3.2), the pre-asymptotic region increases as k increases. Secondly, we observe that the DG-norm of the error decreases when either the mesh is refined, or the polynomial degree is increased as we would expect for this smooth problem.

Finally, in Figure 3.1 we present a comparison of the $L^2(\Omega)^2$ -norm of the error in the approximation to \mathbf{u} , with the square root of the number of degrees of freedom in the finite element space \mathbf{V}_h . Here, we observe that (asymptotically) $\|\mathbf{u} - \mathbf{u}_h\|_0$ converges to zero at the rate $\mathcal{O}(h^{\ell+1})$, for each fixed ℓ and each k , as h tends to zero. This is in full agreement with the optimal rate predicted by Corollary 3.4.5. Numerical experiments also indicate that the $L^2(\Omega)$ -norm of the error in the approximation to p converges to zero at the optimal rate $\mathcal{O}(h^{\ell+2})$, for each fixed ℓ and each k , as h tends to zero; for brevity, these results have been omitted.

3.7.2 Example 2

In this second example, we investigate the performance of the mixed DG method (3.13) for a problem with a non-smooth solution. To this end, let Ω be the L-shaped domain $(-1, 1)^2 \setminus [0, 1) \times (-1, 0]$ and select \mathbf{j} (and suitable non-homogeneous boundary conditions for \mathbf{u}) so that the analytical solution (\mathbf{u}, p) to the two-dimensional analogue of (3.6)–(3.9) is given, in terms of the polar coordinates (r, ϑ) , by

$$\mathbf{u}(x, y) = \nabla S(r, \vartheta), \quad p = 0, \quad (3.68)$$

where

$$S(r, \vartheta) = (kr)^{2/3} \sin(2\vartheta/3).$$

The analytical solution given by (3.68) then contains a singularity at the re-entrant corner located at the origin of Ω ; in particular, we note that \mathbf{u} lies in the Sobolev space $H^{2/3-\varepsilon}(\Omega)^2$, $\varepsilon > 0$.

In this example we again consider the convergence of the mixed DG method (3.13) on a sequence of successively finer (quasi-uniform) unstructured triangular meshes for $\ell = 1, 2, 3$ as the wave number k increases. To this end, in Tables 3.7, 3.8 and Tables 3.9, 3.10 we present numerical experiments for $k = 1, 4$, respectively. Here, we observe that for $k = 1$, the error $\|\mathbf{u} - \mathbf{u}_h\|_{\mathbf{V}(h)}$ converges to zero at a slightly superior rate than the optimal one of $\mathcal{O}(h^{2/3})$,

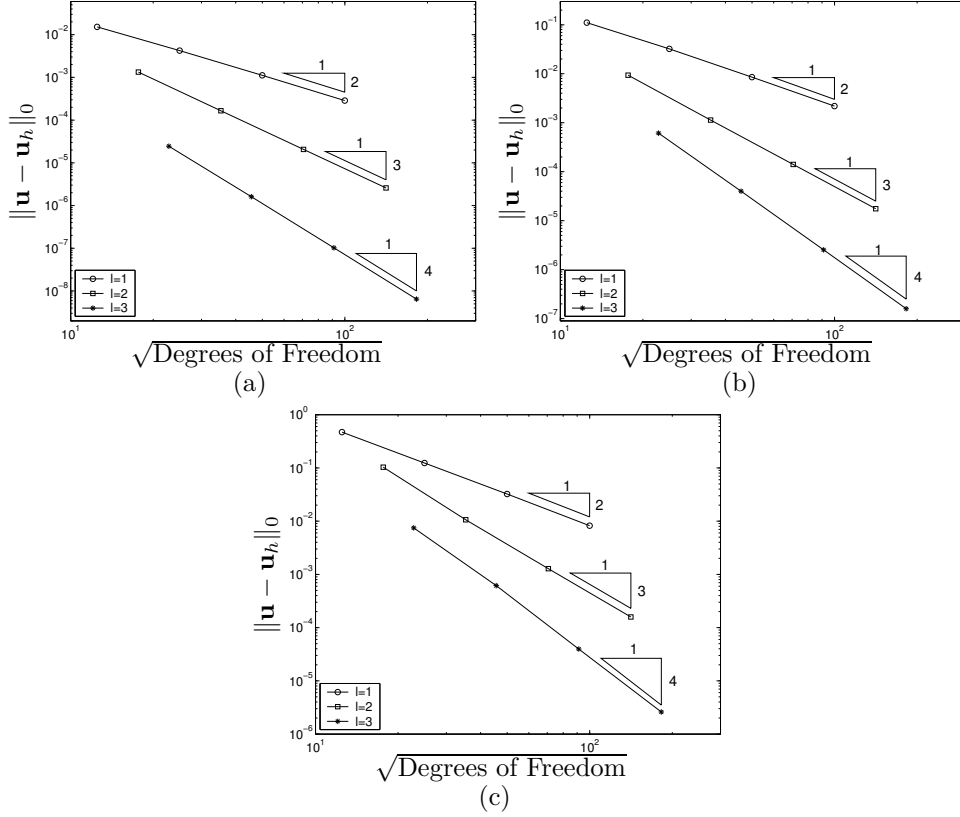


Figure 3.1: Example 1. Convergence of $\|\mathbf{u} - \mathbf{u}_h\|_0$ for: (a) $k = 1$; (b) $k = 2$; (c) $k = 4$.

for each ℓ , as h tends to zero, predicted by Theorem 3.4.1, cf. Table 3.7. We remark that analogous behavior is also observed when the interior penalty mixed DG method is applied to the low-frequency problem studied in [44]. However, for the higher wave number of $k = 4$, we now see that the rate of convergence of $\|\mathbf{u} - \mathbf{u}_h\|_{\mathbf{V}(h)}$ does seem to be slowly tending towards the optimal predicted one, cf. Table 3.9. On the other hand, from Tables 3.8 and 3.10 we see that $\|p - p_h\|_{Q(h)}$ converges to zero at the optimal rate of $\mathcal{O}(h^{2/3})$, for each ℓ and each k , as h tends to zero, predicted by Theorem 3.4.1, though now, the rate of convergence tends to the optimal one from below at the smaller wave number of $k = 1$. As in the previous example, we see that the DG-norm of the error in the approximation to both \mathbf{u} and p increases as the wave number k increases for a fixed mesh size and polynomial degree. However, for a fixed mesh and wave number, while an increase in the polynomial degree leads to a decrease in $\|\mathbf{u} - \mathbf{u}_h\|_{\mathbf{V}(h)}$, the opposite behavior is observed for the error in the approximation to p ; indeed, we observe that for both $k = 1, 4$, an increase in ℓ leads to an increase of $\|p - p_h\|_{Q(h)}$ on a given (fixed) mesh.

Finally, we end this section by considering the rate of convergence of the error in the approximation to \mathbf{u} measured in terms of the $L^2(\Omega)^2$ -norm. To this end, in Tables 3.11 and 3.12 we present numerical experiments for $k = 1, 4$, respectively.

Elements	$\ell = 1$		$\ell = 2$		$\ell = 3$	
	$\ \mathbf{u} - \mathbf{u}_h\ _{\mathbf{V}(h)}$	r	$\ \mathbf{u} - \mathbf{u}_h\ _{\mathbf{V}(h)}$	r	$\ \mathbf{u} - \mathbf{u}_h\ _{\mathbf{V}(h)}$	r
24	7.871e-1	-	7.339e-1	-	6.536e-1	-
96	5.073e-1	0.63	4.144e-1	0.83	3.504e-1	0.90
384	2.613e-1	0.96	1.980e-1	1.07	1.620e-1	1.11
1536	1.187e-1	1.14	8.652e-2	1.19	6.945e-2	1.22
6144	5.188e-2	1.19	3.504e-2	1.30	2.495e-2	1.48

Table 3.7: Example 2. Convergence of $\|\mathbf{u} - \mathbf{u}_h\|_{\mathbf{V}(h)}$ with $k = 1$.

Elements	$\ell = 1$		$\ell = 2$		$\ell = 3$	
	$\ p - p_h\ _{Q(h)}$	r	$\ p - p_h\ _{Q(h)}$	r	$\ p - p_h\ _{Q(h)}$	r
24	1.460	-	1.918	-	2.337	-
96	1.408	0.05	1.713	0.16	1.982	0.24
384	1.127	0.32	1.291	0.41	1.446	0.46
1536	7.938e-1	0.51	8.807e-1	0.55	9.718e-1	0.57
6144	5.241e-1	0.60	5.744e-1	0.62	6.305e-1	0.62

Table 3.8: Example 2. Convergence of $\|p - p_h\|_{Q(h)}$ with $k = 1$.

The regularity assumptions required in the statement of Theorem 3.4.4 do not hold; as a consequence, the only proven result is $\|\mathbf{u} - \mathbf{u}_h\|_0 \leq \|\mathbf{u} - \mathbf{u}_h\|_{\mathbf{V}(h)} = \mathcal{O}(h^{2/3})$, for each ℓ and k , as h tends to zero. The results obtained for the wave number $k = 4$ indicate that the convergence rate is asymptotically optimal in this case, whereas the results for $k = 1$ point to a convergence rate like $\mathcal{O}(h^{2 \times 2/3})$.

3.8 Concluding remarks

In this chapter, we have introduced and analyzed a new interior penalty method for the indefinite time-harmonic Maxwell equations written in mixed form. The proposed scheme can be viewed as a non-stabilized variant of the mixed DG method proposed in [63]; in particular, except for the standard interior penalty stabilization terms, here we exclude all the additional stabilization terms introduced in the DG formulation analyzed in [63]. Employing the techniques developed in Chapter 2, we have derived optimal a-priori estimates for the error measured in terms of both the energy-norm, as well as the L^2 -norm. The current analysis relies on exploiting duality techniques, and thereby only holds in the case of smooth material coefficients. The extension of this work to problems with non-smooth coefficients, by extending more general analysis approaches for conforming methods (such as the ones in [9] or [38]) to the discontinuous Galerkin context, is currently under investigation.

The DG method proposed in this chapter for the indefinite time-harmonic Maxwell's equations in mixed form could be employed in the context of incompressible magneto-hydrodynamics (MHD). The equations of MHD describe the flow of a viscous, incompressible and electrically conducting fluid. The govern-

Elements	$\ell = 1$		$\ell = 2$		$\ell = 3$	
	$\ \mathbf{u} - \mathbf{u}_h\ _{\mathbf{V}(h)}$	r	$\ \mathbf{u} - \mathbf{u}_h\ _{\mathbf{V}(h)}$	r	$\ \mathbf{u} - \mathbf{u}_h\ _{\mathbf{V}(h)}$	r
24	8.206e-1	-	7.812e-1	-	7.175e-1	-
96	3.611e-1	1.18	3.429e-1	1.19	3.011e-1	1.25
384	1.830e-1	0.98	1.525e-1	1.17	1.289e-1	1.22
1536	1.059e-1	0.79	7.225e-2	1.08	5.741e-2	1.17
6144	6.808e-2	0.64	5.129e-2	0.49	3.827e-2	0.59

Table 3.9: Example 2. Convergence of $\|\mathbf{u} - \mathbf{u}_h\|_{\mathbf{V}(h)}$ with $k = 4$.

Elements	$\ell = 1$		$\ell = 2$		$\ell = 3$	
	$\ p - p_h\ _{Q(h)}$	r	$\ p - p_h\ _{Q(h)}$	r	$\ p - p_h\ _{Q(h)}$	r
24	7.661	-	9.056	-	10.00	-
96	5.293	0.53	5.847	0.63	6.404	0.64
384	3.410	0.63	3.715	0.65	4.058	0.66
1536	2.156	0.66	2.336	0.67	2.559	0.67
6144	1.364	0.66	1.475	0.66	1.607	0.67

Table 3.10: Example 2. Convergence of $\|p - p_h\|_{Q(h)}$ with $k = 4$.

ing partial differential equations are obtained by coupling the incompressible Navier-Stokes equations with Maxwell's equations. A conforming discretization of the *mixed* formulation of the incompressible MHD equations has been proposed by Schötzau and Schneebeli in [70] and analyzed by Schötzau in [71].

Elements	$\ell = 1$		$\ell = 2$		$\ell = 3$	
	$\ \mathbf{u} - \mathbf{u}_h\ _0$	r	$\ \mathbf{u} - \mathbf{u}_h\ _0$	r	$\ \mathbf{u} - \mathbf{u}_h\ _0$	r
24	5.091e-1	-	4.651e-1	-	4.137e-1	-
96	3.248e-1	0.65	2.634e-1	0.82	2.223e-1	0.90
384	1.687e-1	0.95	1.270e-1	1.05	1.035e-1	1.10
1536	7.867e-2	1.10	5.667e-2	1.16	4.512e-2	1.20
6144	3.631e-2	1.12	2.421e-2	1.23	1.719e-2	1.39

Table 3.11: Example 2. Convergence of $\|\mathbf{u} - \mathbf{u}_h\|_0$ with $k = 1$.

Elements	$\ell = 1$		$\ell = 2$		$\ell = 3$	
	$\ \mathbf{u} - \mathbf{u}_h\ _0$	r	$\ \mathbf{u} - \mathbf{u}_h\ _0$	r	$\ \mathbf{u} - \mathbf{u}_h\ _0$	r
24	3.606e-1	-	2.725e-1	-	2.213e-1	-
96	2.180e-1	0.73	1.506e-1	0.86	1.144e-1	0.95
384	1.351e-1	0.69	8.801e-2	0.78	6.426e-2	0.83
1536	8.411e-2	0.68	5.294e-2	0.73	3.797e-2	0.76
6144	5.339e-2	0.66	3.423e-2	0.63	2.469e-2	0.62

Table 3.12: Example 2. Convergence of $\|\mathbf{u} - \mathbf{u}_h\|_0$ with $k = 4$.

Part II

Interior Penalty Method for Transient Wave Propagation

Chapter 4

Interior Penalty Method for the Acoustic Wave Equation

The content of this chapter has been accepted for publication in SIAM J. on Numerical Analysis; see [33] (in collaboration with Marcus J. Grote ¹ and Dominik Schötzau ²).

Abstract

The symmetric interior penalty discontinuous Galerkin finite element method is presented for the numerical discretization of the second-order scalar wave equation. The resulting stiffness matrix is symmetric positive definite and the mass matrix is essentially diagonal; hence, the method is inherently parallel and, leads to fully explicit time integration when coupled with an explicit time-stepping scheme. Optimal a priori error bounds are derived in the energy norm and the L^2 -norm for the semi-discrete formulation. In particular, the error in the energy norm is shown to converge with the optimal order $\mathcal{O}(h^{\min\{s,\ell\}})$ with respect to the mesh size h , the polynomial degree ℓ , and the regularity exponent s of the continuous solution. Under additional regularity assumptions, the L^2 -error is shown to converge with the optimal order $\mathcal{O}(h^{\ell+1})$. Numerical results confirm the expected convergence rates and illustrate the versatility of the method.

4.1 Introduction

The numerical solution of the wave equation is of fundamental importance to the simulation of time dependent acoustic, electromagnetic, or elastic waves.

¹Prof. Dr. Marcus J. Grote, Department of Mathematics, University of Basel, Rheinsprung 21, 4051 Basel, Switzerland, email: Marcus.Grote@unibas.ch.

²Prof. Dr. Dominik Schötzau, Mathematics Department, University of British Columbia, 121-1984 Mathematics Road, Vancouver V6T 1Z2, Canada, email: schoetzau@math.ubc.ca.

For such wave phenomena the scalar second-order wave equation often serves as a model problem. Finite element methods (FEMs) can easily handle inhomogeneous media or complex geometry. However, if explicit time-stepping is subsequently employed, the mass matrix arising from the spatial discretization by standard continuous finite elements must be inverted at each time step: a major drawback in terms of efficiency. For low order Lagrange (\mathcal{P}^1) elements, so-called mass lumping overcomes this problem [18, 46], but for higher order elements this procedure can lead to unstable schemes unless particular finite elements and quadrature rules are used [24]. In addition, continuous Galerkin methods impose significant restrictions on the underlying mesh and discretization; in particular, they do not easily accommodate hanging nodes.

To avoid these difficulties, we consider instead discontinuous Galerkin (DG) methods. Based on discontinuous finite element spaces, these methods easily handle elements of various types and shapes, irregular non-matching grids, and even locally varying polynomial order; thus, they are ideally suited for *hp*-adaptivity. Here continuity is weakly enforced across mesh interfaces by adding suitable bilinear forms, so-called numerical fluxes, to standard variational formulations. These fluxes are easily included within an existing conforming finite element code.

Because individual elements decouple, DG FEMs are also inherently parallel – see [20, 22, 23, 19] for further details and recent reviews. Moreover, the mass matrix arising from the spatial DG discretization is block-diagonal, with block size equal to the number of degrees of freedom per element; it can therefore be inverted at very low computational cost. In fact, for a judicious choice of (locally orthogonal) shape functions, the mass matrix is diagonal. Hence when combined with explicit time integration, the resulting time marching scheme will essentially be fully explicit.

The origins of DG methods can be traced back to the seventies, where they were proposed for the numerical solution of hyperbolic neutron transport equations, as well as for the weak enforcement of continuity in Galerkin methods for elliptic and parabolic problems – see Cockburn, Karniadakis, and Shu [20] for a review of the development of DG methods. When applied to second-order hyperbolic problems, most DG methods first require the problem to be reformulated as a first-order hyperbolic system, for which various DG methods are available. In [22], for instance, Cockburn and Shu use a DG FEM in space combined with a Runge-Kutta scheme in time to discretize hyperbolic conservation laws. Hesthaven and Warburton [36] used the same approach to implement high-order methods for Maxwell's equations in first-order hyperbolic form. Space-time DG methods for linear symmetric first-order hyperbolic systems are presented by Falk and Richter in [30], and later generalized by Monk and Richter in [57], and by Houston, Jensen and Süli in [39]. A first DG method for the acoustic wave equation in its original second-order formulation was recently proposed by Wheeler and Rivi ere [67]; it is based on a *non-symmetric* interior penalty formulation and requires additional stabilization terms for optimal convergence in the L^2 -norm [66].

Here we propose and analyze the *symmetric* interior penalty DG method for the spatial discretization of the (second-order, scalar) wave equation. In particular, we shall derive optimal a priori error bounds in the energy norm and the L^2 -norm for the semi-discrete formulation. Besides the common advantages of DG-methods mentioned above, a symmetric discretization of the wave equa-

tion in its second-order form offers an additional advantage, which also pertains to the classical continuous Galerkin formulation. When the finite element discretization of the spatial operator leads to a symmetric positive definite stiffness matrix, the semi-discrete, second-order in time system of differential equations will conserve (a discrete version of) the energy for all time; thus, it is free of any (unnecessary) damping. The dispersive properties of the symmetric interior penalty DG method were recently analyzed by Ainsworth, Monk and Muniz [2].

The outline of this chapter is as follows. In Section 4.2 we describe the setting of our model problem. Next, we present in Section 4.3 the symmetric interior penalty DG method for the wave equation. Our two main results, optimal error bounds in the energy norm and the L^2 -norm for the semi-discrete scheme, are stated at the beginning of Section 4.4 and proved subsequently. The analysis relies on an idea suggested by Arnold et al [5] together with the approach presented by Perugia and Schötzau in [61] to extend the DG bilinear forms by suitable lifting operators. In Section 4.5, we demonstrate the sharpness of our theoretical error estimates by a series of numerical experiments. By combining our DG method with the second order Newmark scheme we obtain a fully discrete method. To illustrate the versatility of our method, we also propagate a wave across an inhomogenous medium with discontinuity, where the underlying finite element mesh contains hanging nodes. Finally, we conclude with some remarks on possible extensions of our DG method to electromagnetic and elastic waves.

4.2 Model problem

We consider the (second-order) scalar wave equation

$$u_{tt} - \nabla \cdot (c \nabla u) = f \quad \text{in } J \times \Omega, \quad (4.1)$$

$$u = 0 \quad \text{on } J \times \partial\Omega, \quad (4.2)$$

$$u|_{t=0} = u_0 \quad \text{in } \Omega, \quad (4.3)$$

$$u_t|_{t=0} = v_0 \quad \text{in } \Omega, \quad (4.4)$$

where $J = (0, T)$ is a finite time interval and Ω is a bounded domain in \mathbb{R}^d , $d = 2, 3$. For simplicity, we assume that Ω is a polygon ($d = 2$) or a polyhedron ($d = 3$). The (known) source term f lies in $L^2(J; L^2(\Omega))$, while $u_0 \in H_0^1(\Omega)$ and $v_0 \in L^2(\Omega)$ are prescribed initial conditions. We assume that the speed of propagation, $\sqrt{c(x)}$, is piecewise smooth and satisfies the bounds

$$0 < c_* \leq c(x) \leq c^* < \infty, \quad x \in \overline{\Omega}. \quad (4.5)$$

The standard variational form of (4.1)–(4.4) is to find $u \in L^2(J; H_0^1(\Omega))$, with $u_t \in L^2(J; L^2(\Omega))$ and $u_{tt} \in L^2(J; H^{-1}(\Omega))$, such that $u|_{t=0} = u_0$, $u_t|_{t=0} = v_0$ and

$$\langle u_{tt}, v \rangle + a(u, v) = (f, v) \quad \forall v \in H_0^1(\Omega), \quad \text{a.e. in } J. \quad (4.6)$$

Here, the time derivatives are understood in a distributional sense, $\langle \cdot, \cdot \rangle$ denotes the duality pairing between $H^{-1}(\Omega)$ and $H_0^1(\Omega)$, (\cdot, \cdot) is the inner product in $L^2(\Omega)$, and $a(\cdot, \cdot)$ is the elliptic bilinear form given by

$$a(u, v) = (c \nabla u, \nabla v). \quad (4.7)$$

It is well-known that problem (4.6) is well-posed [52]. Moreover, the weak solution u can be shown to be continuous in time, that is

$$u \in C^0(\bar{J}; H_0^1(\Omega)), \quad u_t \in C^0(\bar{J}; L^2(\Omega)); \quad (4.8)$$

see [52, Theorems 8.1 and 8.2 in Chapter III] for details. In particular, this result implies that the initial conditions in (4.3) and (4.4) are well-defined.

4.3 Discontinuous Galerkin discretization

We shall now discretize the wave equation (4.1)–(4.4) by using the interior penalty discontinuous Galerkin finite element method in space, while leaving the time dependence continuous.

4.3.1 Preliminaries

We consider shape-regular meshes \mathcal{T}_h that partition the domain Ω into disjoint elements $\{K\}$, such that $\bar{\Omega} = \cup_{K \in \mathcal{T}_h} \bar{K}$. For simplicity, we assume that the elements are triangles or parallelograms in two space dimensions, and tetrahedra or parallelepipeds in three dimensions, respectively. The diameter of element K is denoted by h_K , and the mesh size h is given by $h = \max_{K \in \mathcal{T}_h} h_K$. We assume that the partition is aligned with the discontinuities of the wave speed \sqrt{c} . Generally, we allow for irregular meshes with hanging nodes. However, we assume that the local mesh sizes are of bounded variation, that is, there is a positive constant κ , depending only on the shape-regularity of the mesh, such that

$$\kappa h_K \leq h_{K'} \leq \kappa^{-1} h_K, \quad (4.9)$$

for all neighboring elements K and K' .

An interior face of \mathcal{T}_h is the (nonempty) interior of $\partial K^+ \cap \partial K^-$, where K^+ and K^- are two adjacent elements of \mathcal{T}_h . Similarly, a boundary face of \mathcal{T}_h is the (nonempty) interior of $\partial K \cap \partial \Omega$, which consists of entire faces of ∂K . We denote by \mathcal{F}_h^I the set of all interior faces of \mathcal{T}_h , by \mathcal{F}_h^B the set of all boundary faces, and set $\mathcal{F}_h = \mathcal{F}_h^I \cup \mathcal{F}_h^B$. Here we generically refer to any element of \mathcal{F}_h as a “face”, both in two and in three dimensions.

For any piecewise smooth function v we now introduce the following trace operators. Let $F \in \mathcal{F}_h^I$ be an interior face shared by two neighboring elements K^+ and K^- and let $x \in F$; we write \mathbf{n}^\pm to denote the unit outward normal vectors on the boundaries ∂K^\pm . Denoting by v^\pm the trace of v taken from within K^\pm , we define the jump and average of v at $x \in F$ by

$$[[v]] := v^+ \mathbf{n}^+ + v^- \mathbf{n}^-, \quad \{v\} := (v^+ + v^-)/2,$$

respectively. On every boundary face $F \in \mathcal{F}_h^B$, we set $[[v]] := v \mathbf{n}$ and $\{v\} := v$. Here, \mathbf{n} is the unit outward normal vector on $\partial \Omega$.

For a piecewise smooth vector-valued function \mathbf{q} , we analogously define the average across interior faces by $\{\{\mathbf{q}\}\} := (\mathbf{q}^+ + \mathbf{q}^-)/2$, and on boundary faces we set $\{\{\mathbf{q}\}\} := \mathbf{q}$. The jump of a vector-valued function will not be used.

We note for later use that for a vector-valued function \mathbf{q} with *continuous* normal components across a face f , the trace identity

$$v^+ (\mathbf{n}^+ \cdot \mathbf{q}^+) + v^- (\mathbf{n}^- \cdot \mathbf{q}^-) = [[v]] \cdot \{\{\mathbf{q}\}\} \quad \text{on } f,$$

immediately follows from the above definitions.

4.3.2 Discretization in space

For a given partition \mathcal{T}_h of Ω and an approximation order $\ell \geq 1$, we wish to approximate the solution $u(t, \cdot)$ of (4.1)–(4.4) in the finite element space

$$V^h := \{v \in L^2(\Omega) : v|_K \in \mathcal{S}^\ell(K) \quad \forall K \in \mathcal{T}_h\}, \quad (4.10)$$

where $\mathcal{S}^\ell(K)$ is the space $\mathcal{P}^\ell(K)$ of polynomials of total degree at most ℓ on K , if K is a triangle or a tetrahedra, or the space $\mathcal{Q}^\ell(K)$ of polynomials of degree at most ℓ in each variable on K , if K is a parallelogram or a parallelepiped.

Then, we consider the following (semi-discrete) discontinuous Galerkin approximation of (4.1)–(4.4): find $u^h : \bar{J} \times V^h \rightarrow \mathbb{R}$ such that

$$(u_{tt}^h, v) + a_h(u^h, v) = (f, v) \quad \forall v \in V^h, \quad t \in J, \quad (4.11)$$

$$u^h|_{t=0} = \Pi_h u_0, \quad (4.12)$$

$$u_t^h|_{t=0} = \Pi_h v_0. \quad (4.13)$$

Here, Π_h denotes the L^2 -projection onto V^h , and the discrete bilinear form a_h on $V^h \times V^h$ is given by

$$\begin{aligned} a_h(u, v) := & \sum_{K \in \mathcal{T}_h} \int_K c \nabla u \cdot \nabla v \, dx - \sum_{F \in \mathcal{F}_h} \int_F \llbracket u \rrbracket \cdot \{c \nabla v\} \, dA \\ & - \sum_{F \in \mathcal{F}_h} \int_F \llbracket v \rrbracket \cdot \{c \nabla u\} \, dA + \sum_{F \in \mathcal{F}_h} \int_F \mathbf{a} \llbracket u \rrbracket \cdot \llbracket v \rrbracket \, dA. \end{aligned} \quad (4.14)$$

The last three terms in (4.14) correspond to jump and flux terms at element boundaries; they vanish when $u, v \in H_0^1(\Omega) \cap H^{1+\sigma}(\Omega)$, for $\sigma > \frac{1}{2}$. Hence the above semi-discrete discontinuous Galerkin formulation (4.11) is consistent with the original continuous problem (4.6).

In (4.14) the function \mathbf{a} penalizes the jumps of u and v over the faces of \mathcal{T}_h . It is referred to as interior penalty stabilization function and is defined as follows. We first introduce the function \mathbf{h} by

$$\mathbf{h}|_F = \begin{cases} \min\{h_K, h_{K'}\}, & F \in \mathcal{F}_h^I, F = \partial K \cap \partial K', \\ h_K, & F \in \mathcal{F}_h^B, F = \partial K \cap \partial \Omega. \end{cases}$$

For $x \in F$, we further define \mathbf{c} by

$$\mathbf{c}|_F(x) = \begin{cases} \max\{c|_K(x), c|_{K'}(x)\}, & F \in \mathcal{F}_h^I, F = \partial K \cap \partial K', \\ c|_K(x), & F \in \mathcal{F}_h^B, F = \partial K \cap \partial \Omega. \end{cases}$$

Then, on each $F \in \mathcal{F}_h$, we set

$$\mathbf{a}|_F := \alpha \mathbf{c} \mathbf{h}^{-1}, \quad (4.15)$$

where α is a positive parameter independent of the local mesh sizes and the coefficient c .

To conclude this section we recall the following stability result for the discontinuous Galerkin form a_h .

LEMMA 4.3.1. *There exists a threshold value $\alpha_{\min} > 0$ which only depends on the shape-regularity of the mesh, the approximation order ℓ , the dimension d , and the bounds in (4.5), such that for $\alpha \geq \alpha_{\min}$*

$$a_h(v, v) \geq C_{\text{coer}} \left(\sum_{K \in \mathcal{T}_h} \|c^{\frac{1}{2}} \nabla v\|_{0,K}^2 + \sum_{F \in \mathcal{F}_h} \|\mathbf{a}^{\frac{1}{2}}[[v]]\|_{0,F}^2 \right), \quad v \in V^h,$$

where the constant C_{coer} is independent of c and h .

The proof of this lemma follows readily from the arguments in [5]. However, to make explicit the dependence of α_{\min} on the bounds in (4.5), we present the proof of a slightly more general stability result in Lemma 4.4.4 below. Throughout the rest of the paper we shall assume that $\alpha \geq \alpha_{\min}$, so that by Lemma 4.3.1 the semi-discrete problem (4.11)–(4.13) has a unique solution.

We remark that the condition $\alpha \geq \alpha_{\min}$ can be omitted by using other symmetric DG discretizations of the div-grad operator, such as the LDG method; see, e.g., [5] for details. It can also be avoided by using the non-symmetric interior penalty method proposed in [66]. However, since the symmetry of a_h is crucial in the analysis below, our error estimates (Section 4.4) do not hold for the nonsymmetric DG method in [66].

REMARK 4.3.2. *Because the bilinear form a_h is symmetric and coercive, for $\alpha \geq \alpha_{\min}$, the semi discrete DG formulation (4.11)–(4.13) with $f = 0$ conserves the (discrete) energy*

$$E_h(t) := \frac{1}{2} \|u_t^h(t)\|_0^2 + \frac{1}{2} a_h(u^h(t), u^h(t)).$$

4.4 A-priori error estimates

We shall now derive optimal a-priori error bounds for the DG method (4.11)–(4.13), first with respect to the DG energy norm and then with respect to the L^2 -norm. These two key results are stated immediately below, while their proofs are postponed to subsequent sections.

4.4.1 Main results

To state our a-priori error bounds, we define the space

$$V(h) = H_0^1(\Omega) + V^h.$$

On $V(h)$, we define the DG energy norm

$$\|v\|_h^2 := \sum_{K \in \mathcal{T}_h} \|c^{\frac{1}{2}} \nabla v\|_{0,K}^2 + \sum_{F \in \mathcal{F}_h} \|\mathbf{a}^{\frac{1}{2}}[[v]]\|_{0,F}^2.$$

Furthermore, for $1 \leq p \leq \infty$ we will make use of the Bochner space $L^p(J; V(h))$, endowed with the norm

$$\|v\|_{L^p(J; V(h))} = \begin{cases} \left(\int_J \|v\|_h^p dt \right)^{1/p}, & 1 \leq p < \infty, \\ \text{ess sup}_{t \in J} \|v\|_h, & p = \infty. \end{cases}$$

Our first main result establishes an optimal error estimate of the energy norm $\|\cdot\|_h$ of the error. It also gives a bound in the $L^2(\Omega)$ -norm on the error in the first time derivative.

THEOREM 4.4.1. *Let the analytical solution u of (4.1)–(4.4) satisfy*

$$u \in L^\infty(J; H^{1+\sigma}(\Omega)), \quad u_t \in L^\infty(J; H^{1+\sigma}(\Omega)), \quad u_{tt} \in L^1(J; H^\sigma(\Omega)),$$

for a regularity exponent $\sigma > \frac{1}{2}$, and let u^h be the semi-discrete discontinuous Galerkin approximation obtained by (4.11)–(4.13), with $\alpha \geq \alpha_{\min}$. Then, the error $e = u - u^h$, satisfies the estimate

$$\begin{aligned} \|e_t\|_{L^\infty(J; L^2(\Omega))} + \|e\|_{L^\infty(J; V(h))} &\leq C \left[\|e_t(0)\|_0 + \|e(0)\|_h \right] \\ &+ Ch^{\min\{\sigma, \ell\}} \left[\|u\|_{L^\infty(J; H^{1+\sigma}(\Omega))} + T\|u_t\|_{L^\infty(J; H^{1+\sigma}(\Omega))} + \|u_{tt}\|_{L^1(J; H^\sigma(\Omega))} \right], \end{aligned}$$

with a constant C that is independent of T and h .

We remark that the fact that $u_t \in L^\infty(J; H^{1+\sigma}(\Omega))$ implies that u is continuous in time on \overline{J} with values in $H^{1+\sigma}(\Omega)$. Similarly, $u_{tt} \in L^1(J; H^\sigma(\Omega))$ implies the continuity of u_t on \overline{J} with values in $H^\sigma(\Omega)$. In Theorem 4.4.1 we thus implicitly assume that the initial conditions satisfy $u_0 \in H^{1+\sigma}(\Omega)$ and $v_0 \in H^\sigma(\Omega)$. Hence, standard approximation properties imply that

$$\|e_t(0)\|_0 = \|v_0 - \Pi_h v_0\|_0 \leq Ch^{\min\{\sigma, \ell+1\}} \|v_0\|_\sigma,$$

$$\|e(0)\|_h = \|u_0 - \Pi_h u_0\|_h \leq Ch^{\min\{\sigma, \ell\}} \|u_0\|_{1+\sigma};$$

see also Lemma 4.4.6 below. As a consequence, Theorem 4.4.1 yields optimal convergence in the (DG) energy norm

$$\|e_t\|_{L^\infty(J; L^2(\Omega))} + \|e\|_{L^\infty(J; V(h))} \leq Ch^{\min\{\sigma, \ell\}},$$

with a constant $C = C(T)$ that is independent of h .

Next, we state an optimal error estimate with respect to the L^2 -norm (in space). To do so, we need to assume elliptic regularity, that is, we assume that there is a stability constant C_S , such that for any $\lambda \in L^2(\Omega)$ the solution of the problem

$$-\nabla \cdot (c\nabla z) = \lambda \quad \text{in } \Omega, \quad z = 0 \quad \text{on } \Gamma, \quad (4.16)$$

belongs to $H^2(\Omega)$ and satisfies the stability bound

$$\|z\|_2 \leq C_S \|\lambda\|_0. \quad (4.17)$$

This condition is certainly satisfied for convex domains and smooth coefficients. Then, the following L^2 -error bound holds.

THEOREM 4.4.2. *Assume elliptic regularity as in (4.16)–(4.17) and let the analytical solution u of (4.1)–(4.4) satisfy*

$$u \in L^\infty(J; H^{1+\sigma}(\Omega)), \quad u_t \in L^\infty(J; H^{1+\sigma}(\Omega)), \quad u_{tt} \in L^1(J; H^\sigma(\Omega)),$$

for a regularity exponent $\sigma > \frac{1}{2}$. Let u^h be the semi-discrete discontinuous Galerkin approximation obtained by (4.11)–(4.13) with $\alpha \geq \alpha_{\min}$. Then, the error $e = u - u^h$ satisfies the estimate

$$\|e\|_{L^\infty(J; L^2(\Omega))} \leq Ch^{\min\{\sigma, \ell\}+1} \left[\|u_0\|_{1+\sigma} + \|u\|_{L^\infty(J; H^{1+\sigma}(\Omega))} + T\|u_t\|_{L^\infty(J; H^{1+\sigma}(\Omega))} \right],$$

with a constant C that is independent of T and the mesh size.

For smooth solutions, Theorem 4.4.2 thus yields optimal convergence rates in the L^2 -norm:

$$\|e\|_{L^\infty(J;L^2(\Omega))} \leq Ch^{\ell+1},$$

with a constant C that is independent of h .

The rest of this section is devoted to the proofs of Theorem 4.4.1 and Theorem 4.4.2. We shall first collect preliminary results in Section 4.4.2. In Section 4.4.3, we present the proof of Theorem 4.4.1. Following an argument by Baker [6] for conforming finite element approximations, we shall then derive the estimate of Theorem 4.4.2 in Section 4.4.4.

4.4.2 Preliminaries

Extension of the DG form a_h

The DG form a_h in (4.14) does not extend in a standard way to a continuous form on the (larger) space $V(h) \times V(h)$. Indeed the average $\{c\nabla v\}$ on a face $F \in \mathcal{F}_h$ is not well-defined in general for $v \in H^1(\Omega)$. To circumvent this difficulty, we shall extend the form a_h in a non-standard and non-consistent way to the space $V(h) \times V(h)$, by using the lifting operators from [5] and the approach in [61]. Thus, for $v \in V(h)$ we define the lifted function, $\mathcal{L}_c(v) \in (V^h)^d$, $d = 2, 3$, by requiring that

$$\int_{\Omega} \mathcal{L}_c(v) \cdot \mathbf{w} \, dx = \sum_{F \in \mathcal{F}_h} \int_F \llbracket v \rrbracket \cdot \{c\mathbf{w}\} \, dA, \quad \mathbf{w} \in (V^h)^d, \quad (4.18)$$

where c is the material coefficient from (4.1). We shall now show that the lifting operator \mathcal{L}_c is stable in the DG norm; see [61] for a similar result for the LDG method.

LEMMA 4.4.3. *There exists a constant C_{inv} which only depends on the shape-regularity of the mesh, the approximation order ℓ , and the dimension d such that*

$$\|\mathcal{L}_c(v)\|_0^2 \leq \alpha^{-1} c^* C_{\text{inv}}^2 \sum_{F \in \mathcal{F}_h} \|\mathbf{a}^{\frac{1}{2}} \llbracket v \rrbracket\|_{0,F}^2,$$

for any $v \in V(h)$.

Moreover, if the speed of propagation $c^{\frac{1}{2}}$ is piecewise constant, with discontinuities aligned with the finite element mesh \mathcal{T}_h , then

$$\|c^{-\frac{1}{2}} \mathcal{L}_c(v)\|_0^2 \leq \alpha^{-1} C_{\text{inv}}^2 \sum_{F \in \mathcal{F}_h} \|\mathbf{a}^{\frac{1}{2}} \llbracket v \rrbracket\|_{0,F}^2.$$

Proof. We have

$$\begin{aligned}
\|\mathcal{L}_c(v)\|_0 &= \max_{\mathbf{w} \in (V^h)^d} \frac{\sum_{F \in \mathcal{F}_h} \int_F \llbracket v \rrbracket \cdot \{\{c\mathbf{w}\}\} dA}{\|\mathbf{w}\|_0} \\
&\leq \max_{\mathbf{w} \in (V^h)^d} \frac{(\sum_{F \in \mathcal{F}_h} \int_F \mathbf{a} \llbracket v \rrbracket^2 dA)^{\frac{1}{2}} (\sum_{F \in \mathcal{F}_h} \int_F \mathbf{a}^{-1} |\{\{c\mathbf{w}\}\}|^2 dA)^{\frac{1}{2}}}{\|\mathbf{w}\|_0} \\
&\leq \alpha^{-\frac{1}{2}} \max_{\mathbf{w} \in (V^h)^d} \frac{(\sum_{F \in \mathcal{F}_h} \int_F \mathbf{a} \llbracket v \rrbracket^2 dA)^{\frac{1}{2}} (\sum_{F \in \mathcal{F}_h} \int_F \mathbf{h} c^{-1} |\{\{c\mathbf{w}\}\}|^2 dA)^{\frac{1}{2}}}{\|\mathbf{w}\|_0} \\
&\leq \alpha^{-\frac{1}{2}} (c^*)^{\frac{1}{2}} \max_{\mathbf{w} \in (V^h)^d} \frac{(\sum_{F \in \mathcal{F}_h} \int_F \mathbf{a} \llbracket v \rrbracket^2 dA)^{\frac{1}{2}} (\sum_{K \in \mathcal{T}_h} h_K \int_{\partial K} |\mathbf{w}|^2 dA)^{\frac{1}{2}}}{\|\mathbf{w}\|_0}
\end{aligned}$$

Here, we have used the Cauchy-Schwarz inequality, the definition of \mathbf{a} in (4.15), and the upper bound for c in (4.5). We recall the inverse inequality

$$\|\mathbf{w}\|_{0,\partial K}^2 \leq C_{\text{inv}}^2 h_K^{-1} \|\mathbf{w}\|_{0,K}^2, \quad \mathbf{w} \in (\mathcal{S}^\ell(K))^d, \quad (4.19)$$

with a constant C_{inv} that only depends on the shape-regularity of the mesh, the approximation order ℓ and the dimension d . Using this bound, we obtain

$$\left(\sum_{K \in \mathcal{T}_h} h_K \int_{\partial K} |\mathbf{w}|^2 dA \right)^{\frac{1}{2}} \leq C_{\text{inv}} \|\mathbf{w}\|_0,$$

which shows the first statement.

With $c^{\frac{1}{2}}$ piecewise constant, we have $c^{-\frac{1}{2}}w \in (V^h)^d$ for all $w \in (V^h)^d$. Hence, we can replace w by $c^{-\frac{1}{2}}w$ in equation (4.18), and obtain as before

$$\begin{aligned}
\|c^{-\frac{1}{2}}\mathcal{L}_c(v)\|_0 &= \max_{\mathbf{w} \in (V^h)^d} \frac{\sum_{F \in \mathcal{F}_h} \int_F \llbracket v \rrbracket \cdot \{\{c^{\frac{1}{2}}\mathbf{w}\}\} dA}{\|\mathbf{w}\|_0} \\
&\leq \alpha^{-\frac{1}{2}} \max_{\mathbf{w} \in (V^h)^d} \frac{(\sum_{F \in \mathcal{F}_h} \int_F \mathbf{a} \llbracket v \rrbracket^2 dA)^{\frac{1}{2}} (\sum_{F \in \mathcal{F}_h} \int_F \mathbf{h} c^{-1} |\{\{c^{\frac{1}{2}}\mathbf{w}\}\}|^2 dA)^{\frac{1}{2}}}{\|\mathbf{w}\|_0} \\
&\leq \alpha^{-\frac{1}{2}} \max_{\mathbf{w} \in (V^h)^d} \frac{(\sum_{F \in \mathcal{F}_h} \int_F \mathbf{a} \llbracket v \rrbracket^2 dA)^{\frac{1}{2}} (\sum_{K \in \mathcal{T}_h} h_K \int_{\partial K} |\mathbf{w}|^2 dA)^{\frac{1}{2}}}{\|\mathbf{w}\|_0} \\
&\leq \alpha^{-\frac{1}{2}} C_{\text{inv}} \left(\sum_{F \in \mathcal{F}_h} \|\mathbf{a}^{\frac{1}{2}} \llbracket v \rrbracket\|_{0,F}^2 \right)^{\frac{1}{2}},
\end{aligned}$$

which completes the proof. \square

Next, we introduce the auxiliary bilinear form

$$\begin{aligned}
\tilde{a}_h(u, v) &:= \sum_{K \in \mathcal{T}_h} \int_K c \nabla u \cdot \nabla v dx - \sum_{K \in \mathcal{T}_h} \int_K \mathcal{L}_c(u) \cdot \nabla v dx \\
&\quad - \sum_{K \in \mathcal{T}_h} \int_K \mathcal{L}_c(v) \cdot \nabla u dx + \sum_{F \in \mathcal{F}_h} \int_F \mathbf{a} \llbracket u \rrbracket \cdot \llbracket v \rrbracket dA.
\end{aligned} \quad (4.20)$$

The following result establishes that \tilde{a}_h is continuous and coercive on the entire space $V(h) \times V(h)$; hence it is well-defined. Furthermore, since

$$\tilde{a}_h = a_h \quad \text{on } V^h \times V^h, \quad \tilde{a}_h = a \quad \text{on } H_0^1(\Omega) \times H_0^1(\Omega), \quad (4.21)$$

the form \tilde{a}_h can be viewed as an extension of the two forms a_h and a to the space $V(h) \times V(h)$.

LEMMA 4.4.4. *Let the interior penalty parameter \mathbf{a} be defined as in (4.15) and set*

$$\alpha_{\min} = 4 c_{\star}^{-1} c^{\star} C_{\text{inv}}^2,$$

for a general piecewise smooth c , and

$$\alpha_{\min} = 4 C_{\text{inv}}^2,$$

for a piecewise constant c , with discontinuities aligned with the finite element mesh \mathcal{T}_h . C_{inv} is the constant from Lemma 4.4.3.

Setting $C_{\text{cont}} = 2$ and $C_{\text{coer}} = 1/2$, we have for $\alpha \geq \alpha_{\min}$

$$\begin{aligned} |\tilde{a}_h(u, v)| &\leq C_{\text{cont}} \|u\|_h \|v\|_h, & u, v \in V(h), \\ \tilde{a}_h(u, u) &\geq C_{\text{coer}} \|u\|_h^2, & u \in V(h). \end{aligned}$$

In particular, the coercivity bound implies the result in Lemma 4.3.1.

Proof. By taking into account the bounds in (4.5) and Lemma 4.4.3, application of the Cauchy-Schwarz inequality readily gives in the general case

$$|\tilde{a}_h(u, v)| \leq \max\{2, \alpha^{-1} c_{\star}^{-1} c^{\star} C_{\text{inv}}^2 + 1\} \|u\|_h \|v\|_h.$$

For $\alpha \geq \alpha_{\min}$, the continuity of \tilde{a}_h immediately follows. The case of piecewise constant c follows analogously.

To show the coercivity of the form \tilde{a}_h , we note that

$$\tilde{a}_h(u, u) = \sum_{K \in \mathcal{T}_h} \|c^{\frac{1}{2}} \nabla u\|_{0,K}^2 - 2 \sum_{K \in \mathcal{T}_h} \int_K \mathcal{L}_c(u) \cdot \nabla u \, dx + \sum_{F \in \mathcal{F}_h} \|\mathbf{a}^{\frac{1}{2}} \llbracket u \rrbracket\|_{0,F}^2.$$

By using the weighted Cauchy-Schwarz inequality, the geometric-arithmetic inequality $ab \leq \frac{\varepsilon a^2}{2} + \frac{b^2}{2\varepsilon}$, valid for any $\varepsilon > 0$, the bounds in (4.5), and the stability bound for the lifting operator in Lemma 4.4.3, we obtain for general c

$$\begin{aligned} 2 \sum_{K \in \mathcal{T}_h} \int_K \mathcal{L}_c(u) \cdot \nabla u \, dx &= 2 \sum_{K \in \mathcal{T}_h} \int_K c^{-\frac{1}{2}} \mathcal{L}_c(u) \cdot c^{\frac{1}{2}} \nabla u \, dx \\ &\leq 2 \sum_{K \in \mathcal{T}_h} \|c^{-\frac{1}{2}} \mathcal{L}_c(u)\|_{0,K} \|c^{\frac{1}{2}} \nabla u\|_{0,K} \\ &\leq \varepsilon \sum_{K \in \mathcal{T}_h} \|c^{\frac{1}{2}} \nabla u\|_{0,K}^2 + \varepsilon^{-1} c_{\star}^{-1} \sum_{K \in \mathcal{T}_h} \|\mathcal{L}_c(u)\|_{0,K}^2 \\ &\leq \varepsilon \sum_{K \in \mathcal{T}_h} \|c^{\frac{1}{2}} \nabla u\|_{0,K}^2 + \varepsilon^{-1} \alpha^{-1} c_{\star}^{-1} c^{\star} C_{\text{inv}}^2 \sum_{F \in \mathcal{F}_h} \|\mathbf{a}^{\frac{1}{2}} \llbracket u \rrbracket\|_{0,F}^2, \end{aligned}$$

for a parameter $\varepsilon > 0$ still at our disposal. We conclude that

$$\tilde{a}_h(u, u) \geq (1 - \varepsilon) \sum_{K \in \mathcal{T}_h} \|c^{\frac{1}{2}} \nabla u\|_{0,K}^2 + (1 - \varepsilon^{-1} \alpha^{-1} c_{\star}^{-1} c^{\star} C_{\text{inv}}^2) \sum_{F \in \mathcal{F}_h} \|\mathbf{a}^{\frac{1}{2}} \llbracket u \rrbracket\|_{0,F}^2.$$

For $\varepsilon = \frac{1}{2}$ and $\alpha \geq \alpha_{\min}$, we obtain the desired coercivity bound.

For a piecewise constant c we use the bound for $\|c^{-\frac{1}{2}} \mathcal{L}_c(u)\|_0^2$ from Lemma 4.4.4 and proceed analogously. \square

Error equation

Because \tilde{a}_h coincides with a_h on $V^h \times V^h$, the semi-discrete scheme in (4.11)–(4.13) is equivalent to:

$$\begin{aligned} & \text{find } u^h : \bar{J} \times V^h \rightarrow \mathbb{R} \text{ such that } u^h|_{t=0} = \Pi_h u_0, u_t^h|_{t=0} = \Pi_h v_0 \text{ and} \\ & (u_{tt}^h, v) + \tilde{a}_h(u^h, v) = (f, v) \quad \forall v \in V^h. \end{aligned} \quad (4.22)$$

We shall use the formulation in (4.22) as the basis of our error analysis.

To derive an error equation, we first define for $u \in H^{1+\sigma}(\Omega)$ with $\sigma > 1/2$,

$$r_h(u; v) = \sum_{F \in \mathcal{F}_h} \int_F \llbracket v \rrbracket \cdot \{ \{ c \nabla u - c \mathbf{\Pi}_h(\nabla u) \} \} dA, \quad v \in V(h). \quad (4.23)$$

Here $\mathbf{\Pi}_h$ denotes the L^2 -projection onto $(V^h)^d$. The assumption $u \in H^{1+\sigma}(\Omega)$ ensures that $r_h(u; v)$ is well-defined. From the definition in (4.23) it is immediate that $r_h(u; v) = 0$ when $v \in H_0^1(\Omega)$.

LEMMA 4.4.5. *Let the analytical solution u of (4.1)–(4.4) satisfy*

$$u \in L^\infty(J; H^{1+\sigma}(\Omega)), \quad u_{tt} \in L^1(J; L^2(\Omega)).$$

Let u^h be the semi-discrete discontinuous Galerkin approximation obtained by (4.22). Then, the error $e = u - u^h$ satisfies

$$(e_{tt}, v) + \tilde{a}_h(e, v) = r_h(u; v), \quad \forall v \in V^h, \text{ a.e. in } J,$$

with $r_h(u; v)$ given in (4.23).

Proof. Let $v \in V^h$. Since $u_{tt} \in L^1(J; L^2(\Omega))$, we have $\langle u_{tt}, v \rangle = (u_{tt}, v)$ almost everywhere in J . Hence, using the discrete formulation in (4.11)–(4.13), we obtain that

$$(e_{tt}, v) + \tilde{a}_h(e, v) = (u_{tt}, v) + \tilde{a}_h(u, v) - (f, v), \quad \text{a.e. in } J.$$

Now, by definition of \tilde{a}_h , the fact that $\mathcal{L}_c(u) = 0$ and that $\llbracket u \rrbracket = 0$ on all faces, the defining properties of the L^2 -projection $\mathbf{\Pi}_h$, and the definition of the lifted element $\mathcal{L}_c(v)$, we obtain

$$\tilde{a}_h(u, v) = \sum_{K \in \mathcal{T}_h} \int_K c \nabla u \cdot \nabla v \, dx - \sum_{F \in \mathcal{F}_h} \int_F \llbracket v \rrbracket \cdot \{ \{ c \mathbf{\Pi}_h(\nabla u) \} \} dA.$$

Since $u_{tt} \in L^1(J; L^2(\Omega))$ and $f \in L^2(J; L^2(\Omega))$ we have that $\nabla \cdot (c \nabla u) \in L^2(\Omega)$ almost everywhere in J , which implies that $c \nabla u$ has continuous normal components across all interior faces. Therefore, elementwise integration by parts combined with the trace operators defined in Section 4.3.1 yields

$$\begin{aligned} \tilde{a}_h(u, v) &= - \sum_{K \in \mathcal{T}_h} \int_K \nabla \cdot (c \nabla u) v \, dx + \sum_{F \in \mathcal{F}_h} \int_F \llbracket v \rrbracket \cdot \{ \{ c \nabla u \} \} dA \\ &\quad - \sum_{F \in \mathcal{F}_h} \int_F \llbracket v \rrbracket \cdot \{ \{ c \mathbf{\Pi}_h(\nabla u) \} \} dA. \end{aligned}$$

From the definition of $r_h(u, v)$ in (4.23), we therefore conclude that

$$(u_{tt}, v) + \tilde{a}_h(u, v) = (u_{tt} - \nabla \cdot (c \nabla u), v) + r_h(u; v),$$

and obtain

$$(e_{tt}, v) + \tilde{a}_h(e, v) = (u_{tt} - \nabla \cdot (c \nabla u) - f, v) + r_h(u; v) = r_h(u; v),$$

where we have used the differential equation (4.1). \square

Approximation properties

Let Π_h and $\mathbf{\Pi}_h$ denote the L^2 -projections onto V^h and $(V^h)^d$, respectively. We recall the following approximation properties; see [18].

LEMMA 4.4.6. *Let $K \in \mathcal{T}_h$. Then:*

(i) *For $v \in H^t(K)$, $t \geq 0$, we have*

$$\|v - \Pi_h v\|_{0,K} \leq Ch_K^{\min\{t, \ell+1\}} \|v\|_{t,K},$$

with a constant C that is independent of the local mesh size h_K and only depends on the shape-regularity of the mesh, the approximation order ℓ , the dimension d , and the regularity exponent t .

(ii) *For $v \in H^{1+\sigma}(K)$, $\sigma > \frac{1}{2}$, we have*

$$\begin{aligned} \|\nabla v - \nabla(\Pi_h v)\|_{0,K} &\leq Ch_K^{\min\{\sigma, \ell\}} \|v\|_{1+\sigma, K}, \\ \|v - \Pi_h v\|_{0, \partial K} &\leq Ch_K^{\min\{\sigma, \ell\} + \frac{1}{2}} \|v\|_{1+\sigma, K}, \\ \|\nabla v - \mathbf{\Pi}_h(\nabla v)\|_{0, \partial K} &\leq Ch_K^{\min\{\sigma, \ell+1\} - \frac{1}{2}} \|v\|_{1+\sigma, K}, \end{aligned}$$

with a constant C that is independent of the local mesh size h_K and only depends on the shape-regularity of the mesh, the approximation order ℓ , the dimension d , and the regularity exponent σ .

As a consequence of the approximation properties in Lemma 4.4.6, we obtain the following results.

LEMMA 4.4.7. *Let $u \in H^{1+\sigma}(\Omega)$, $\sigma > \frac{1}{2}$. Then:*

(i) *We have*

$$\|u - \Pi_h u\|_h \leq C_A h^{\min\{\sigma, \ell\}} \|u\|_{1+\sigma},$$

with a constant C_A that is independent of the mesh size and only depends on α , the constant κ in (4.9), the bounds in (4.5), and the constants in Lemma 4.4.6.

(ii) *For $v \in V(h)$, the form $r_h(u; v)$ in (4.23) can be bounded by*

$$|r_h(u; v)| \leq C_R h^{\min\{\sigma, \ell\}} \left(\sum_{F \in \mathcal{F}_h} \|\mathbf{a}^{\frac{1}{2}} \llbracket v \rrbracket\|_{0,F}^2 \right)^{\frac{1}{2}} \|u\|_{1+\sigma},$$

with a constant C_R independent of h , which only depends on α , the bounds in (4.5), and the constants in Lemma 4.4.6.

Proof. The estimate in (i) is an immediate consequence of Lemma 4.4.6, the definition of \mathbf{a} and the bounded variation property (4.9). To show the bound in (ii), we apply the Cauchy-Schwarz inequality and obtain

$$\begin{aligned} |r_h(u; v)| &\leq \left(\sum_{F \in \mathcal{F}_h} \int_F \mathbf{a} \llbracket v \rrbracket^2 ds \right)^{\frac{1}{2}} \left(\sum_{F \in \mathcal{F}_h} \int_F \mathbf{a}^{-1} |\llbracket c \nabla u - c \mathbf{\Pi}_h(\nabla u) \rrbracket|^2 ds \right)^{\frac{1}{2}} \\ &\leq \alpha^{-\frac{1}{2}} c_\star^{-\frac{1}{2}} c^\star \left(\sum_{F \in \mathcal{F}_h} \|\mathbf{a}^{\frac{1}{2}} \llbracket v \rrbracket\|_{0,F}^2 \right)^{\frac{1}{2}} \left(\sum_{K \in \mathcal{T}_h} h_K \|\nabla u - \mathbf{\Pi}_h(\nabla u)\|_{0, \partial K}^2 \right)^{\frac{1}{2}}. \end{aligned}$$

Applying the approximation properties in Lemma 4.4.6 completes the proof. \square

4.4.3 Proof of Theorem 4.4.1

We are now ready to complete the proof of Theorem 4.4.1. We begin by proving the following auxiliary result.

LEMMA 4.4.8. *Let the analytical solution u of (4.1)–(4.4) satisfy*

$$u \in L^\infty(J; H^{1+\sigma}(\Omega)), \quad u_t \in L^\infty(J; H^{1+\sigma}(\Omega))$$

for $\sigma > \frac{1}{2}$. Let $v \in C^0(\bar{J}; V(h))$ and $v_t \in L^1(J; V(h))$. Then we have

$$\begin{aligned} \int_J |r_h(u; v_t)| dt &\leq C_R h^{\min\{\sigma, \ell\}} \|v\|_{L^\infty(J; V(h))} \\ &\quad \cdot \left[2 \|u\|_{L^\infty(J; H^{1+\sigma}(\Omega))} + T \|u_t\|_{L^\infty(J; H^{1+\sigma}(\Omega))} \right], \end{aligned}$$

where C_R is the constant from the bound (ii) in Lemma 4.4.7.

Proof. From the definition of r_h in (4.23) and integration by parts, we obtain

$$\begin{aligned} \int_J r_h(u; v_t) dt &= \int_J \sum_{F \in \mathcal{F}_h} \int_F \llbracket v_t \rrbracket \cdot \{c \nabla u - c \mathbf{\Pi}_h(\nabla u)\} dA dt \\ &= - \int_J \sum_{F \in \mathcal{F}_h} \int_F \llbracket v \rrbracket \cdot \{c \nabla u_t - c \mathbf{\Pi}_h(\nabla u_t)\} dA dt \\ &\quad + \left[\sum_{F \in \mathcal{F}_h} \int_F \llbracket v \rrbracket \cdot \{c \nabla u - c \mathbf{\Pi}_h(\nabla u)\} dA \right]_{t=0}^{t=T} \\ &= - \int_J r_h(u_t; v) dt + \left[r_h(u; v) \right]_{t=0}^{t=T}. \end{aligned}$$

Lemma 4.4.7 then implies the two estimates

$$\left| \int_J r_h(u_t; v) dt \right| \leq C_R h^{\min\{\sigma, \ell\}} T \|v\|_{L^\infty(J; V(h))} \|u_t\|_{L^\infty(J; H^{1+\sigma}(\Omega))}$$

and

$$\left| \left[r_h(u; v) \right]_{t=0}^{t=T} \right| \leq 2C_R h^{\min\{\sigma, \ell\}} \|v\|_{L^\infty(J; V(h))} \|u\|_{L^\infty(J; H^{1+\sigma}(\Omega))},$$

which concludes the proof of the lemma. \square

To complete the proof of Theorem 4.4.1, we now set $e = u - u^h$ and recall that Π_h is the L^2 -projection onto V^h . Because of (4.8), we have

$$e \in C^0(\bar{J}; V(h)) \cap C^1(\bar{J}; L^2(\Omega)).$$

Next, we use the symmetry of \tilde{a}_h and the error equation in Lemma 4.4.5 to obtain

$$\begin{aligned} \frac{1}{2} \frac{d}{dt} [\|e_t\|_0^2 + \tilde{a}_h(e, e)] &= (e_{tt}, e_t) + \tilde{a}_h(e, e_t) \\ &= (e_{tt}, (u - \Pi_h u)_t) + \tilde{a}_h(e, (u - \Pi_h u)_t) \\ &\quad + r_h(u; (\Pi_h u - u^h)_t). \end{aligned} \tag{4.24}$$

We fix $s \in J$ and integrate (4.24) over the time interval $(0, s)$. This yields

$$\begin{aligned} \frac{1}{2}\|e_t(s)\|_0^2 + \frac{1}{2}\tilde{a}_h(e(s), e(s)) &= \frac{1}{2}\|e_t(0)\|_0^2 + \frac{1}{2}\tilde{a}_h(e(0), e(0)) \\ &\quad + \int_0^s (e_{tt}, (u - \Pi_h u)_t) dt + \int_0^s \tilde{a}_h(e, (u - \Pi_h u)_t) dt \\ &\quad + \int_0^s r_h(u; (\Pi_h u - u^h)_t) dt. \end{aligned}$$

Integration by parts of the third term on the right-hand side yields

$$\int_0^s (e_{tt}, (u - \Pi_h u)_t) dt = - \int_0^s (e_t, (u - \Pi_h u)_{tt}) dt + \left[(e_t, (u - \Pi_h u)_t) \right]_{t=0}^{t=s}.$$

From the stability properties of \tilde{a}_h in Lemma 4.4.4 and standard Hölder's inequalities, we conclude that

$$\begin{aligned} \frac{1}{2}\|e_t(s)\|_0^2 + \frac{1}{2}C_{\text{coer}}\|e(s)\|_h^2 &\leq \frac{1}{2}\|e_t(0)\|_0^2 + \frac{1}{2}C_{\text{cont}}\|e(0)\|_h^2 \\ &\quad + \|e_t\|_{L^\infty(J; L^2(\Omega))} \left(\|(u - \Pi_h u)_{tt}\|_{L^1(J; L^2(\Omega))} + 2\|(u - \Pi_h u)_t\|_{L^\infty(J; L^2(\Omega))} \right) \\ &\quad + C_{\text{cont}}T\|e\|_{L^\infty(J; V(h))} \|(u - \Pi_h u)_t\|_{L^\infty(J; V(h))} \\ &\quad + \left| \int_J r_h(u; (\Pi_h u - u^h)_t) dt \right|. \end{aligned}$$

Since this inequality holds for any $s \in J$, it also holds for the maximum over J , that is

$$\|e_t\|_{L^\infty(J; L^2(\Omega))}^2 + C_{\text{coer}}\|e\|_{L^\infty(J; V(h))}^2 \leq \|e_t(0)\|_0^2 + C_{\text{cont}}\|e(0)\|_h^2 + T_1 + T_2 + T_3,$$

with

$$\begin{aligned} T_1 &= 2\|e_t\|_{L^\infty(J; L^2(\Omega))} \left(\|(u - \Pi_h u)_{tt}\|_{L^1(J; L^2(\Omega))} + 2\|(u - \Pi_h u)_t\|_{L^\infty(J; L^2(\Omega))} \right), \\ T_2 &= 2C_{\text{cont}}T\|e\|_{L^\infty(J; V(h))} \|(u - \Pi_h u)_t\|_{L^\infty(J; V(h))}, \\ T_3 &= 2 \left| \int_J r_h(u; (\Pi_h u - u^h)_t) dt \right|. \end{aligned}$$

Using the geometric-arithmetic mean inequality $|ab| \leq \frac{1}{2\varepsilon}a^2 + \frac{\varepsilon}{2}b^2$, valid for any $\varepsilon > 0$, and the approximation results in Lemma 4.4.6, we conclude that

$$\begin{aligned} T_1 &\leq \frac{1}{2}\|e_t\|_{L^\infty(J; L^2(\Omega))}^2 + 2 \left(\|(u - \Pi_h u)_{tt}\|_{L^1(J; L^2(\Omega))} + 2\|(u - \Pi_h u)_t\|_{L^\infty(J; L^2(\Omega))} \right)^2 \\ &\leq \frac{1}{2}\|e_t\|_{L^\infty(J; L^2(\Omega))}^2 + 4\|(u - \Pi_h u)_{tt}\|_{L^1(J; L^2(\Omega))}^2 + 16\|(u - \Pi_h u)_t\|_{L^\infty(J; L^2(\Omega))}^2, \\ &\leq \frac{1}{2}\|e_t\|_{L^\infty(J; L^2(\Omega))}^2 + Ch^{2\min\{\sigma, \ell\}} \left(\|u_{tt}\|_{L^1(J; H^\sigma(\Omega))}^2 + h^2\|u_t\|_{L^\infty(J; H^{1+\sigma}(\Omega))}^2 \right), \end{aligned}$$

with a constant C that only depends on the constants in Lemma 4.4.6. Similarly,

$$\begin{aligned} T_2 &\leq \frac{1}{4}C_{\text{coer}}\|e\|_{L^\infty(J; V(h))}^2 + 4\frac{C_{\text{cont}}^2}{C_{\text{coer}}}T^2\|(u - \Pi_h u)_t\|_{L^\infty(J; V(h))}^2 \\ &\leq \frac{1}{4}C_{\text{coer}}\|e\|_{L^\infty(J; V(h))}^2 + T^2Ch^{2\min\{\sigma, \ell\}}\|u_t\|_{L^\infty(J; H^{1+\sigma}(\Omega))}^2, \end{aligned}$$

where the constant C depends on C_{coer} , C_{cont} and the constant C_A in Lemma 4.4.7.

It remains to bound the term T_3 . To do so, we use Lemma 4.4.8 to obtain

$$T_3 \leq 2C_R \mathcal{R} h^{\min\{\sigma, \ell\}} \|\Pi_h u - u^h\|_{L^\infty(J; V(h))},$$

with

$$\mathcal{R} := \left[2\|u\|_{L^\infty(J; H^{1+\sigma}(\Omega))} + T\|u_t\|_{L^\infty(J; H^{1+\sigma}(\Omega))} \right].$$

The triangle inequality, the geometric-arithmetic mean, and the approximation properties of Π_h in Lemma 4.4.7 then yield

$$\begin{aligned} T_3 &\leq 2C_R \mathcal{R} h^{\min\{\sigma, \ell\}} \left[\|e\|_{L^\infty(J; V(h))} + \|u - \Pi_h u\|_{L^\infty(J; V(h))} \right] \\ &\leq \frac{1}{4} C_{\text{coer}} \|e\|_{L^\infty(J; V(h))}^2 + Ch^{2\min\{\sigma, \ell\}} \left[\|u\|_{L^\infty(J; H^{1+\sigma}(\Omega))}^2 + \mathcal{R}^2 \right], \end{aligned}$$

with a constant C that only depends on C_{coer} , C_R , and C_A . Combining the above estimates for T_1 , T_2 and T_3 then shows that

$$\begin{aligned} \frac{1}{2} \|e_t\|_{L^\infty(J; L^2(\Omega))}^2 + \frac{1}{2} C_{\text{coer}} \|e\|_{L^\infty(J; V(h))}^2 &\leq \|e_t(0)\|_0^2 + C_{\text{cont}} \|e(0)\|_h^2 \\ &\quad + Ch^{2\min\{\sigma, \ell\}} \left[\|u_{tt}\|_{L^1(J; H^\sigma(\Omega))}^2 + T^2 \|u_t\|_{L^\infty(J; H^{1+\sigma}(\Omega))}^2 + \|u\|_{L^\infty(J; H^{1+\sigma}(\Omega))}^2 \right], \end{aligned}$$

with a constant that is independent of T and the mesh size. This concludes the proof of Theorem 4.4.1.

4.4.4 Proof of Theorem 4.4.2

To prove the error estimate in Theorem 4.4.2, we first establish the following variant of [6, Lemma 2.1].

LEMMA 4.4.9. *For $u \in H^{1+\sigma}(\Omega)$ with $\sigma > \frac{1}{2}$, let $w^h \in V^h$ be the solution of*

$$\tilde{a}_h(w^h, v) = \tilde{a}_h(u, v) - r_h(u; v) \quad \forall v \in V^h.$$

Then, we have

$$\|u - w^h\|_h \leq C_E h^{\min\{\sigma, \ell\}} \|u\|_{1+\sigma},$$

with a constant C_E that is independent of h and only depends on C_{coer} , C_{cont} in Lemma 4.4.4 and C_A , C_R in Lemma 4.4.7.

Moreover, if the elliptic regularity defined in (4.16) and (4.17) holds, we have the L^2 -bound

$$\|u - w^h\|_0 \leq C_L h^{\min\{\sigma, \ell\}+1} \|u\|_{1+\sigma}.$$

with a constant C_L that is independent of h and only depends on the stability constant C_S in (4.17), C_{coer} , C_{cont} in Lemma 4.4.4 and C_A , C_R in Lemma 4.4.7.

Proof. We first remark that the approximation w^h is well-defined, because of the stability properties in Lemma 4.4.4 and the estimates in Lemma 4.4.7. To prove the estimate for $\|u - w^h\|_h$, we first use the triangle inequality,

$$\|u - w^h\|_h \leq \|u - \Pi_h u\|_h + \|\Pi_h u - w^h\|_h. \quad (4.25)$$

From the approximation properties of Π_h in Lemma 4.4.7, we immediately infer that

$$\|u - \Pi_h u\|_h \leq C_A h^{\min\{\sigma, \ell\}} \|u\|_{1+\sigma}.$$

It remains to bound $\|\Pi_h u - w^h\|_h$. From the coercivity and continuity of \tilde{a}_h in Lemma 4.4.4, the definition of w^h , and the bound in Lemma 4.4.7, we conclude that

$$\begin{aligned} C_{\text{coer}} \|\Pi_h u - w^h\|_h^2 &\leq \tilde{a}_h(\Pi_h u - w^h, \Pi_h u - w^h) \\ &= \tilde{a}_h(\Pi_h u - u, \Pi_h u - w^h) + \tilde{a}_h(u - w^h, \Pi_h u - w^h) \\ &= \tilde{a}_h(\Pi_h u - u, \Pi_h u - w^h) + r_h(u; \Pi_h u - w^h) \\ &\leq C_{\text{cont}} \|\Pi_h u - u\|_h \|\Pi_h u - w^h\|_h + C_R h^{\min\{\sigma, \ell\}} \|u\|_{1+\sigma} \|\Pi_h u - w^h\|_h. \end{aligned}$$

Thus,

$$\|\Pi_h u - w^h\|_h \leq \left(\frac{C_{\text{cont}} C_A + C_R}{C_{\text{coer}}} \right) h^{\min\{\sigma, \ell\}} \|u\|_{1+\sigma},$$

which proves the bound for $\|u - w^h\|_h$.

We shall now prove the L^2 -bound. To do so, let $z \in H_0^1(\Omega)$ be the solution of

$$-\nabla \cdot (c \nabla z) = u - w^h \quad \text{in } \Omega, \quad z = 0 \quad \text{on } \Gamma. \quad (4.26)$$

Then, the elliptic regularity assumption in (4.16) and (4.17) implies that

$$z \in H^2(\Omega), \quad \|z\|_2 \leq C_S \|u - w^h\|_0. \quad (4.27)$$

Next, we multiply (4.26) by $u - w^h$ and integrate the resulting expression by parts. Since $c \nabla z$ has continuous normal components across all interior faces, we have

$$\begin{aligned} \|u - w^h\|_0^2 &= \sum_{K \in \mathcal{T}_h} \left[\int_K c \nabla z \cdot \nabla (u - w^h) dx - \int_{\partial K} c \nabla z \cdot \mathbf{n}_K (u - w^h) dA \right] \\ &= \sum_{K \in \mathcal{T}_h} \int_K c \nabla z \cdot \nabla (u - w^h) dx - \sum_{F \in \mathcal{F}_h} \int_F \{ \{ c \nabla z \} \} \cdot [[u - w^h]] dA, \end{aligned}$$

with \mathbf{n}_K denoting the unit outward normal on ∂K . By definition of \tilde{a}_h and r_h , we immediately find that

$$\|u - w^h\|_0^2 = \tilde{a}_h(z, u - w^h) - r_h(z; u - w^h).$$

From the symmetry of \tilde{a}_h , the definition of w^h , and the fact that $[[z]] = 0$ on all faces, we conclude that

$$\begin{aligned} \|u - w^h\|_0^2 &= \tilde{a}_h(u - w^h, z - \Pi_h z) - r_h(u; z - \Pi_h z) - r_h(z; u - w^h) \\ &=: T_1 + T_2 + T_3. \end{aligned} \quad (4.28)$$

We shall now derive upper bounds for each individual term T_1 , T_2 , and T_3 in (4.28).

To estimate the term T_1 , we use the continuity of \tilde{a}_h , the approximation result in Lemma 4.4.7 with $\sigma = 1$, and the bound in (4.27). Thus,

$$\begin{aligned} T_1 &\leq C_{\text{cont}} \|u - w^h\|_h \|z - \Pi_h z\|_h \\ &\leq C_{\text{cont}} C_A h \|u - w^h\|_h \|z\|_2 \\ &\leq C_{\text{cont}} C_A C_S h \|u - w^h\|_h \|u - w^h\|_0. \end{aligned}$$

By using Lemma 4.4.7 and the stability bound in (4.27), we can estimate T_2 by

$$\begin{aligned} T_2 &\leq C_R h^{\min\{\sigma, \ell\}} \|z - \Pi_h z\|_h \|u\|_{1+\sigma} \\ &\leq C_R C_A h^{\min\{\sigma, \ell\}+1} \|z\|_2 \|u\|_{1+\sigma} \\ &\leq C_R C_A C_S h^{\min\{\sigma, \ell\}+1} \|u - w^h\|_0 \|u\|_{1+\sigma}. \end{aligned}$$

Similarly,

$$T_3 \leq C_R h \|z\|_2 \|u - w^h\|_h \leq C_R C_S h \|u - w^h\|_0 \|u - w^h\|_h.$$

The use of these bounds for T_1 , T_2 and T_3 in (4.28) then leads to

$$\|u - w^h\|_0 \leq Ch \|u - w^h\|_h + Ch^{\min\{\sigma, \ell\}+1} \|u\|_{1+\sigma}.$$

which completes the proof of the lemma, since $\|u - w^h\|_h \leq Ch^{\min\{\sigma, \ell\}} \|u\|_{1+\sigma}$. \square

Now, let u be defined by the exact solution of (4.1)–(4.4). We may define $w^h(t, \cdot) \in V^h$ almost everywhere in J by

$$\tilde{a}_h(w^h(t, \cdot), v) = \tilde{a}_h(u(t, \cdot), v) - r_h(u(t, \cdot); v) \quad \forall v \in V^h. \quad (4.29)$$

If $u \in L^\infty(J; H^{1+\sigma}(\Omega))$, it can be readily seen that $w^h \in L^\infty(J; V(h))$. Moreover, if we also have $u_t \in L^\infty(J; H^{1+\sigma}(\Omega))$, then $w_t^h \in L^\infty(J; V(h))$ and

$$\tilde{a}_h(w_t^h, v) = \tilde{a}_h(u_t, v) - r_h(u_t; v), \quad v \in V^h, \text{ a.e. in } J,$$

as well as

$$\tilde{a}_h(w^h(0), v) = \tilde{a}_h(u_0, v) - r_h(u_0; v), \quad v \in V^h.$$

Therefore Lemma 4.4.9 immediately implies the following estimates.

LEMMA 4.4.10. *Let w^h be defined by (4.29). Under the regularity assumptions of Theorem 4.4.2, we have*

$$\begin{aligned} \|(u - w^h)_t\|_{L^\infty(J; V(h))} &\leq C_E h^{\min\{\sigma, \ell\}} \|u_t\|_{L^\infty(J; H^{1+\sigma}(\Omega))}, \\ \|(u - w^h)(0)\|_h &\leq C_E h^{\min\{\sigma, \ell\}} \|u_0\|_{1+\sigma}. \end{aligned}$$

Moreover, if elliptic regularity as defined in (4.16) and (4.17) holds, we have the L^2 -bounds

$$\begin{aligned} \|(u - w^h)_t\|_{L^\infty(J; L^2(\Omega))} &\leq C_L h^{\min\{\sigma, \ell\}+1} \|u_t\|_{L^\infty(J; H^{1+\sigma}(\Omega))}, \\ \|(u - w^h)(0)\|_0 &\leq C_L h^{\min\{\sigma, \ell\}+1} \|u_0\|_{1+\sigma}. \end{aligned}$$

The constants C_E and C_L are as in Lemma 4.4.9.

To complete the proof of Theorem 4.4.2, let $w^h \in L^\infty(J; V(h))$ be defined by (4.29) and consider

$$\|e\|_{L^\infty(J; L^2(\Omega))}^2 \leq 2\|u - w^h\|_{L^\infty(J; L^2(\Omega))}^2 + 2\|w^h - u^h\|_{L^\infty(J; L^2(\Omega))}^2. \quad (4.30)$$

The first term can be estimated from the L^2 -bounds in Lemma 4.4.9. We shall now derive an estimate for the second term. First, we fix $v \in L^\infty(J; V^h)$ and

assume that $v_t \in L^\infty(J; V^h)$. From the definition of w^h in (4.29) and the error equation in Lemma 4.4.5, we have

$$\begin{aligned} ((u^h - w^h)_{tt}, v) + \tilde{a}_h(u^h - w^h, v) &= (u_{tt}^h, v) + \tilde{a}_h(u^h, v) - \tilde{a}_h(w^h, v) - (w_{tt}^h, v) \\ &= (u_{tt}^h, v) + \tilde{a}_h(u^h - u, v) + r_h(u; v) - (w_{tt}^h, v) \\ &= (u_{tt}, v) - (w_{tt}^h, v). \end{aligned}$$

We rewrite this identity as

$$\frac{d}{dt}((u^h - w^h)_t, v) - ((u^h - w^h)_t, v_t) + \tilde{a}_h(u^h - w^h, v) = \frac{d}{dt}((u - w^h)_t, v) - ((u - w^h)_t, v_t),$$

which yields

$$-((u^h - w^h)_t, v_t) + \tilde{a}_h(u^h - w^h, v) = \frac{d}{dt}((u - w^h)_t, v) - ((u - w^h)_t, v_t). \quad (4.31)$$

Let $\tau \in (0, T]$ be fixed, and consider the function

$$\hat{v}(t, \cdot) = \int_t^\tau (u^h - w^h)(s, \cdot) ds, \quad t \in \bar{J}.$$

Note that

$$\hat{v}(\tau, \cdot) = 0, \quad \hat{v}_t(t, \cdot) = -(u^h - w^h)(t, \cdot), \quad \text{a.e. } t \in \bar{J}.$$

Next, choose $v = \hat{v}$ in (4.31) which yields

$$((u^h - w^h)_t, u^h - w^h) - \tilde{a}_h(\hat{v}_t, \hat{v}) = \frac{d}{dt}((u - u^h)_t, \hat{v}) + ((u - w^h)_t, u^h - w^h).$$

Since the DG form $\tilde{a}_h(\cdot, \cdot)$ is symmetric, we obtain

$$\frac{1}{2} \frac{d}{dt} \|u^h - w^h\|_0^2 - \frac{1}{2} \frac{d}{dt} \tilde{a}_h(\hat{v}, \hat{v}) = \frac{d}{dt}((u - u^h)_t, \hat{v}) + ((u - w^h)_t, u^h - w^h).$$

Integration over $(0, \tau)$ and using that $\hat{v}(\tau, \cdot) = 0$ then yields

$$\begin{aligned} \|(u^h - w^h)(\tau)\|_0^2 - \|(u^h - w^h)(0)\|_0^2 + \tilde{a}_h(\hat{v}(0), \hat{v}(0)) &= \\ -2((u - u^h)_t(0), \hat{v}(0)) + 2 \int_0^\tau ((u - w^h)_t, u^h - w^h) dt. \end{aligned} \quad (4.32)$$

Since $u_t(0) = v_0$, $u_t^h(0) = \Pi_h v_0$, and $\hat{v}(0)$ belongs to V^h , we conclude that

$$((u - u^h)_t(0), \hat{v}(0)) = (v_0 - \Pi_h v_0, \hat{v}(0)) = 0.$$

Hence, the first term on the right-hand side of (4.32) vanishes. Moreover, the coercivity of the form \tilde{a}_h in Lemma 4.4.4 ensures that $\tilde{a}_h(\hat{v}(0), \hat{v}(0)) \geq 0$. This leads to the inequality

$$\|(u^h - w^h)(\tau)\|_0^2 \leq \|(u^h - w^h)(0)\|_0^2 + 2 \int_0^\tau \|(u - w^h)_t\|_0 \|u^h - w^h\|_0 dt. \quad (4.33)$$

By using the Cauchy-Schwarz inequality and the geometric-arithmetic mean inequality, we obtain

$$\begin{aligned} 2 \int_0^\tau \|(u - w^h)_t\|_0 \|u^h - w^h\|_0 dt &\leq 2T \|(u - w^h)_t\|_{L^\infty(J; L^2(\Omega))} \|u^h - w^h\|_{L^\infty(J; L^2(\Omega))} \\ &\leq \frac{1}{2} \|u^h - w^h\|_{L^\infty(J; L^2(\Omega))}^2 + 2T^2 \|(u - w^h)_t\|_{L^\infty(J; L^2(\Omega))}^2. \end{aligned}$$

Because this upper bound is independent of τ , it also holds for the supremum over $\tau \in J$, which yields the estimate

$$\begin{aligned} \frac{1}{2} \|u^h - w^h\|_{L^\infty(J; L^2(\Omega))}^2 &\leq \|(u^h - w^h)(0)\|_0^2 + 2T^2 \|(u - w^h)_t\|_{L^\infty(J; L^2(\Omega))}^2 \\ &\leq 2 \|(u^h - u)(0)\|_0^2 + 2 \|(u - w^h)(0)\|_0^2 + 2T^2 \|(u - w^h)_t\|_{L^\infty(J; L^2(\Omega))}^2. \end{aligned}$$

Next, we use this estimate in (4.30) to obtain

$$\begin{aligned} \|e\|_{L^\infty(J; L^2(\Omega))}^2 &\leq 2 \|u - w^h\|_{L^\infty(J; L^2(\Omega))}^2 \\ &\quad + 8 \|u_0 - \Pi_h u_0\|_0^2 + 8 \|u_0 - w^h(0)\|_0^2 + 8T^2 \|(u - w^h)_t\|_{L^\infty(J; L^2(\Omega))}^2. \end{aligned}$$

From the L^2 -approximation properties in Lemma 4.4.6, Lemma 4.4.9, and Lemma 4.4.10 we finally conclude that

$$\begin{aligned} \|e\|_{L^\infty(J; L^2(\Omega))}^2 &\leq h^{2 \min\{\sigma, \ell\} + 2} \left[\max\{8C, 8C_L^2\} \|u_0\|_{1+\sigma}^2 \right. \\ &\quad \left. + 2C_L^2 \|u\|_{L^\infty(J; H^{1+\sigma}(\Omega))}^2 + 8C_L T^2 \|u_t\|_{L^\infty(J; H^{1+\sigma}(\Omega))}^2 \right]. \end{aligned}$$

Here, C is the constant from Lemma 4.4.6. This completes the proof of Theorem 4.4.2.

4.5 Numerical results

We shall now present a series of numerical experiments which verify the sharpness of the theoretical error bounds stated in Theorem 4.4.1 and Theorem 4.4.2. Furthermore, we shall demonstrate the robustness and flexibility of our DG method by propagating a pulse through an inhomogeneous medium with discontinuity on a finite element mesh with hanging nodes.

To obtain a fully discrete discretization of the wave equation, we choose to augment our DG spatial discretization with the second-order Newmark scheme in time; see, e.g. [65, Sections 8.5–8.7]. The resulting scheme has been implemented using the general purpose finite element library `deal.II`³, which provides powerful $C++$ classes for the handling of the meshes, the degrees of freedom, and the solution of linear systems of equations; see [8, 7]. In all our examples, the DG stabilization parameter is set to $\alpha = 20$.

4.5.1 Time discretization

The discretization of (4.1)–(4.4) in space by the DG method (4.11)–(4.13) leads to the linear second-order system of ordinary differential equations

$$\mathbf{M}\ddot{\mathbf{u}}^h(t) + \mathbf{A}\mathbf{u}^h(t) = \mathbf{f}^h(t), \quad t \in J, \quad (4.34)$$

³URL: www.dealii.org.

with initial conditions

$$\mathbf{M}\mathbf{u}^h(0) = \mathbf{u}_0^h, \quad \mathbf{M}\dot{\mathbf{u}}^h(0) = \mathbf{v}_0^h. \quad (4.35)$$

Here, \mathbf{M} denotes the mass matrix and \mathbf{A} the stiffness matrix. To discretize (4.34) in time, we employ the Newmark time stepping scheme; see, e. g., [65]. We let k denote the time step and set $t_n = n \cdot k$. Then the Newmark method consists in finding approximations $\{\mathbf{u}_n^h\}_n$ to $\mathbf{u}^h(t_n)$ such that

$$(\mathbf{M} + k^2\beta\mathbf{A})\mathbf{u}_1^h = [\mathbf{M} - k^2(\frac{1}{2} - \beta)\mathbf{A}]\mathbf{u}_0^h + k\mathbf{M}\mathbf{v}_0^h + k^2[\beta\mathbf{f}_1^h + (\frac{1}{2} - \beta)\mathbf{f}_0^h], \quad (4.36)$$

and

$$\begin{aligned} (\mathbf{M} + k^2\beta\mathbf{A})\mathbf{u}_{n+1}^h &= [2\mathbf{M} - k^2(\frac{1}{2} - 2\beta + \gamma)\mathbf{A}]\mathbf{u}_n^h - [\mathbf{M} + k^2(\frac{1}{2} + \beta - \gamma)\mathbf{A}]\mathbf{u}_{n-1}^h \\ &\quad + k^2[\beta\mathbf{f}_{n+1}^h + (\frac{1}{2} - 2\beta + \gamma)\mathbf{f}_n + (\frac{1}{2} + \beta - \gamma)\mathbf{f}_{n-1}], \end{aligned} \quad (4.37)$$

for $n = 1, \dots, N - 1$. Here, $\mathbf{f}_n := \mathbf{f}(t_n)$ while $\beta \geq 0$ and $\gamma \geq 1/2$ are free parameters that still can be chosen. We recall that for $\gamma = 1/2$ the Newmark scheme is second-order accurate in time, whereas it is only first order accurate for $\gamma > 1/2$. For $\beta = 0$, the Newmark scheme (4.36)–(4.37) requires at each time step the solution of a linear system with the mass matrix \mathbf{M} . However, because individual elements decouple, \mathbf{M} is block-diagonal with a block size equal to the number of degrees of freedom per element. It can be inverted at very low computational cost and the scheme is essentially fully explicit. In fact, if the basis functions are chosen mutually orthogonal, \mathbf{M} reduces to the identity; see [20] and the references therein. Then, with $\gamma = 1/2$, the explicit Newmark method corresponds to the standard leap-frog scheme.

For $\beta > 0$, the resulting scheme is implicit and involves the solution of a linear system with the symmetric positive definite stiffness matrix \mathbf{A} at each time step. We finally note that the second-order Newmark scheme with $\gamma = 1/2$ is unconditionally stable for $\beta \geq 1/4$, whereas for $1/4 > \beta \geq 0$ the time step k has to be restricted by a CFL condition. In the case $\beta = 0$, the condition is $k^2\lambda_{\max}(\mathbf{A}) \leq 4(1 - \varepsilon)$, $\varepsilon \in (0, 1)$, where $\lambda_{\max}(\mathbf{A})$ is the maximal eigenvalue of the DG stiffness matrix \mathbf{A} (which is of the order $\mathcal{O}(h^{-2})$, and also depends on α).

In all our tests, we will employ the explicit second-order Newmark scheme, setting $\gamma = 1/2$ and $\beta = 0$ in (4.36)–(4.37).

4.5.2 Example 1: smooth solution

First, we consider the two-dimensional wave equation (4.1)–(4.4) in $J \times \Omega = (0, 1) \times (0, 1)^2$, with $c \equiv 1$ and data f, u_0 and v_0 chosen such that the analytical solution is given by

$$u(x_1, x_2, t) = t^2 \sin(\pi x_1) \sin(\pi x_2). \quad (4.38)$$

This solution is arbitrarily smooth so that all our theoretical regularity assumptions are satisfied. We discretize this problem using the polynomial spaces $\mathcal{Q}^\ell(K)$, $\ell = 1, 2, 3$, on a sequence $\{\mathcal{T}_h\}_{i \geq 1}$ of square meshes of size $h_i = 2^{-i}$. With increasing polynomial degree ℓ and decreasing mesh size h_i , smaller time

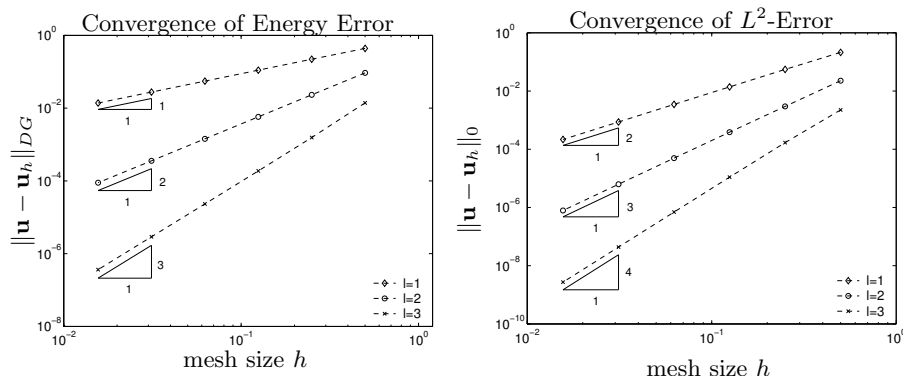


Figure 4.1: Example 1.1: Convergence of the error at time $T = 1$ in the energy norm and the L^2 -norm for $\ell = 1, 2, 3$.

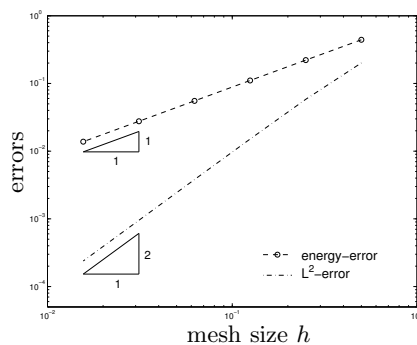


Figure 4.2: Example 1.2: Convergence of the error at time $T = 1$ in the energy norm and the L^2 -norm for $\ell = 1$.

steps k_i are necessary to ensure stability. We found that the choice $k_i = h_i/20$ provides a stable time discretization on every mesh. Because our numerical scheme is second-order accurate in time, the time integration of (4.38) is exact so that the spatial error is the only error component in the discrete solution.

In Figure 4.1 we show the relative errors at time $T = 1$ in the energy norm and in the L^2 -norm, as we decrease the mesh size h_i . The numerical results corroborate with the expected theoretical rates of $\mathcal{O}(h^\ell)$ for the energy norm and of $\mathcal{O}(h^{\ell+1})$ for the L^2 -norm – see Theorem 4.4.1 and Theorem 4.4.2.

Next, we modify the data so that the analytical solution u is given by

$$u(x_1, x_2, t) = \sin(t^2) \sin(\pi x_1) \sin(\pi x_2). \quad (4.39)$$

Although u remains arbitrarily smooth, it is no longer integrated exactly in time by (4.36)–(4.37). Since the Newmark scheme is only second-order accurate, we repeat the above experiment only for the lowest order spatial discretization, $\ell = 1$. Again, we set $k_i = h_i/20$. In Figure 4.2, the relative errors for the fully discrete approximation of (4.39) show convergence rates of order h in the energy

norm and order h^2 in the L^2 -norm, thereby confirming the theoretical estimates of Theorems 4.4.1 and 4.4.2.

4.5.3 Example 2: singular solution

Here, we consider the two-dimensional wave equation (4.1)–(4.4) on the L-shaped domain $\Omega = (-1, 1)^2 \setminus [0, 1)^2$. We set $c = 1$ everywhere and choose the data f, u_0 and v_0 such that the analytical solution u is given in polar coordinates (r, ϕ) by

$$u(r, \phi, t) = t^2 r^{2/3} \sin(2/3 \phi). \quad (4.40)$$

Although u is smooth in time (and can even be integrated exactly in time), it has a spatial singularity at the origin, such that $u \in C^\infty(\bar{J}; H^{5/3}(\Omega))$. Hence, this example is well-suited to establish the sharpness of the regularity assumptions in our theoretical results. Since u is inhomogeneous at the boundary of Ω , we need to impose inhomogeneous Dirichlet conditions within our DG discretization. We do so in straightforward fashion by modifying the semi-discrete formulation as follows: find $u^h(t, \cdot) : J \rightarrow V^h$ such that

$$(u_{tt}^h, v) + a_h(u^h, v) = (f, v) + \sum_{F \in \mathcal{F}_h^B} \int_F g(\mathbf{a}v - c\nabla v \cdot \mathbf{n}) dA. \quad (4.41)$$

Here, g is the boundary data and \mathbf{n} is the outward unit normal vector on $\partial\Omega$.

We discretize (4.41) by using bilinear polynomials ($\ell = 1$) on the same sequence of meshes as before. Again, we set $k_i = h_i/20$ and integrate the problem up to $T = 1$. For the analytical solution u in (4.40), the regularity assumptions in Theorem 4.4.1 hold with $\sigma = 2/3$. Thus, Theorem 4.4.1 predicts numerical convergence rates of $2/3$ in the energy norm, as confirmed by our numerical results in Table 4.5.3.

As the elliptic regularity assumptions (4.16)–(4.17) from Theorem 4.4.2 is violated, we do not expect L^2 -error rates of the order $1 + \sigma$ for this problem. Indeed, in Table 4.5.3 we observe convergence rates close to $4/3$. To explain this behavior, let us consider the following weaker elliptic regularity assumption: for any $\lambda \in L^2(\Omega)$ we assume that the solution of the problem

$$-\nabla \cdot (c\nabla z) = \lambda \quad \text{in } \Omega, \quad z = 0 \quad \text{on } \partial\Omega, \quad (4.42)$$

belongs to $H^{1+s}(\Omega)$ for a parameter $s \in (1/2, 1]$ and satisfies the stability bound

$$\|z\|_{1+s} \leq C_S \|\lambda\|_0, \quad (4.43)$$

for a stability constant C_S . The results from Lemma 4.4.9 and Lemma 4.4.10 can be easily adapted to this case. As a consequence, the L^2 -bound for $e = u - u^h$ from Theorem 4.4.2 can then be generalized to this weaker setting as

$$\begin{aligned} \|e\|_{L^\infty(J; L^2(\Omega))} &\leq Ch^{\min\{\sigma, \ell\}+s} [\|u_0\|_{1+\sigma} \\ &\quad + \|u\|_{L^\infty(J; H^{1+\sigma}(\Omega))} + T\|u_t\|_{L^\infty(J; H^{1+\sigma}(\Omega))}]. \end{aligned}$$

For the L-shaped domain Ω and $c \equiv 1$, the (weaker) regularity assumption in (4.42)–(4.43) holds with $s = 2/3$, which underpins the rate $\sigma + s = 4/3$ observed in Table 4.5.3.

i	cells	energy-error		L^2 -error	
1	12	1.11e-01	-	1.61e-02	-
2	48	7.18e-02	0.62	5.96e-03	1.43
3	192	4.61e-02	0.64	2.27e-03	1.40
4	768	2.94e-02	0.65	8.72e-04	1.38
5	3072	1.87e-02	0.66	3.38e-04	1.37
6	12288	1.18e-02	0.66	1.32e-04	1.36

Table 4.1: Example 2: Relative errors at time $T = 1$ in the energy norm and L^2 -norm, and corresponding numerical convergence rates.

4.5.4 Example 3: inhomogeneous medium

Finally, we consider (4.1)–(4.4) on the rectangular domain $\Omega = (-1, 2) \times (-1, 1)$, with homogeneous initial and boundary conditions and the piecewise constant material coefficient

$$c(x_1, x_2) = \begin{cases} 0.1, & x_1 \leq 0, \\ 1, & \text{else} \end{cases}$$

The wave is locally excited until $t = 0.2$ by the source term

$$f(x_1, x_2, t) = \begin{cases} 1, & 0.2 < x_1 < 0.4 \text{ and } t < 0.2, \\ 0, & \text{else.} \end{cases}$$

We discretize the problem by the DG method (4.11)–(4.13) on a fixed mesh \mathcal{T}_h that consists of *non-matching components*, which are adapted to the discontinuity c ; see Figure 4.5.4. The mesh \mathcal{T}_h is composed of 9312 non-uniform squares, where the smallest local mesh size is given by $h_{\min} \approx 0.016$. The hanging nodes are naturally incorporated in the DG-method without any difficulty. Here, the time step $k = 0.002$, that is $k \approx h_{\min}/8$ proved to be sufficiently small to ensure the stability of the explicit Newmark method ($\beta = 0$).

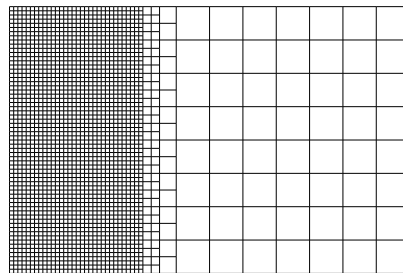


Figure 4.3: Example 3: Domain Ω with a finite element mesh \mathcal{T}_h that is adapted to the values of the piecewise constant wave speed \sqrt{c} .

In Figure 4.4, the numerical solution is shown after $n = 100, 300, 900$ and 2000 time steps, respectively. The initial pulse splits in two planar wave fronts, propagating to either side of the domain. After $n = 300$ time steps, the left moving wave reaches the much slower medium 1, resulting in a much steeper and narrower wave front. Meanwhile, the right moving wave rapidly arrives at

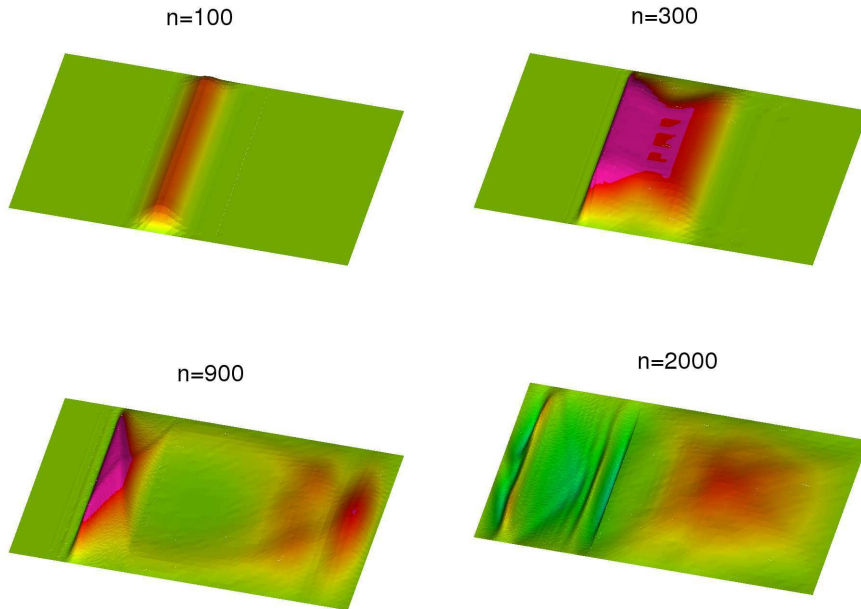


Figure 4.4: Example 3: Wave with fixed boundaries propagating in an inhomogeneous medium. The approximate DG solutions u_n^h reported at times $t_n = 0.2, 0.6, 1.8, 4$ reflect the qualitative behavior of a wave with data from Example 3.

the boundary at $x_1 = 2$, where it is reflected and eventually reaches the slow region too. The discontinuous interface at $x_1 = 0$ generates multiple reflections, which interact with each other at later times.

4.6 Concluding remarks

We have presented and analyzed the symmetric interior penalty discontinuous Galerkin finite element method (DG FEM) for the numerical solution of the (second-order) scalar wave equation. Taking advantage of the symmetry of the method, we have carried out an a priori error analysis of the semi-discrete method and derived optimal error bounds in the energy norm and, under additional regularity assumptions, optimal error bounds in the L^2 -norm. Our numerical results confirm the expected convergence rates and demonstrate the versatility of the method. The error analysis of the fully discrete scheme is the subject of ongoing work.

Based on discontinuous finite element spaces, the proposed DG method easily handles elements of various types and shapes, irregular non-matching grids, and even locally varying polynomial order. As continuity is only weakly enforced across mesh interfaces, domain decomposition techniques immediately apply. Since the resulting mass matrix is essentially diagonal, the method is inherently parallel and leads to fully explicit time integration schemes. Moreover,

as the stiffness matrix is symmetric positive definite, the DG method shares the following two important properties with the classical continuous Galerkin approach. First, the semi-discrete formulation conserves (a discrete version of) the energy for all time, and therefore it is non-dissipative. Second, if implicit time integration is used to overcome CFL constraints, the resulting linear system to be solved at each time step will also be symmetric positive definite.

The symmetric interior penalty DG FEM, applied here to the scalar wave equation, can also be utilized for other second-order hyperbolic equations, such as in electromagnetics (see Chapter 5) or elasticity. In fact, our error analysis for the semi-discrete (scalar) case readily extends to the second-order (vector) wave equation for time dependent elastic waves.

Moreover, our analysis in Sections 4.4.3 and 4.4.3 for the proof of the error estimates can be applied to other *symmetric* discontinuous Galerkin schemes, such as, e. g., the LDG method [5].

In further studies, an analysis of full discretizations of (4.11)–(4.13) should be provided, in particular a more detailed dependence of CFL conditions on the wave speed c and on the interior penalty stabilization parameter α . This analysis should be feasible by a straightforward extension of techniques for conforming FEM, and relies on the estimation of eigenvalues of the DG form a_h .

In Lemma 4.4.4, we stated the independence of the minimal interior penalty stabilization parameter α_{\min} on wave speed c , in the case where c is piecewise constant. For general coefficients c , our analysis led to an α_{\min} that depends on the ratio of the upper and lower bounds for c in the computational domain. Numerical experiments suggest however, that this dependence is not sharp, and that indeed α_{\min} seems to be independent of c also for more general wave speed coefficients. An analytical verification of this fact would be interesting.

Chapter 5

Interior Penalty Method for Maxwell's Equations in Time Domain

The content of the first part of this chapter (energy error estimates) has been accepted for publication in a special volume of *Journal of Computational and Applied Mathematics (JCAM)* reflecting some of the talks presented at the 7th International Conference Mathematical and Numerical Aspects of Waves (WAVES'05); [34] (in collaboration with Marcus J. Grote ¹ and Dominik Schötzau ²).

Abstract

We develop the symmetric interior penalty discontinuous Galerkin (DG) method for the spatial discretization in the method of lines approach of the time-dependent Maxwell equations in second-order form. We derive optimal a-priori estimates for the semi-discrete error in the energy norm. For smooth solutions, these estimates hold for DG discretizations on general finite element meshes. For low-regularity solutions that have singularities in space, the theoretical estimates hold on conforming, affine meshes. Moreover, on conforming triangular meshes, we derive optimal error estimates in the L^2 -norm. Finally, we evaluate our theoretical results by a series of numerical experiments.

5.1 Introduction

The development of new more sophisticated algorithms for the numerical solution of Maxwell's equations is dictated by increasingly complex applications

¹Prof. Dr. Marcus J. Grote, Department of Mathematics, University of Basel, Rheinsprung 21, 4051 Basel, Switzerland, email: Marcus.Grote@unibas.ch.

²Prof. Dr. Dominik Schötzau, Mathematics Department, University of British Columbia, 121-1984 Mathematics Road, Vancouver V6T 1Z2, Canada, email: schoetzau@math.ubc.ca.

in electromagnetics. In 1966 Yee [76] introduced the first and probably most popular method, the Finite Difference Time Domain (FDTD) scheme, which is simple and efficient. However, the FDTD scheme can only be applied on structured (Cartesian) grids and suffers from the inaccurate representation of the solution on curved boundaries (staircase approximation) [14, 72]. Moreover, higher order FDTD methods are generally difficult to implement near interfaces and boundaries.

In contrast, Finite Element Methods (FEMs) easily handle complex boundaries and unstructured grids, even when higher order discretizations are used. They also provide rigorous a posteriori error estimates which are useful for local adaptivity and error control. Different FE discretizations of Maxwell's equations are available, such as the edge elements of Nédélec [59], the node-based first order formulation of Lee and Madsen [51], the node-based curl-curl formulation of Paulsen and Lynch [60], or the node-based least-squares FEM by Jiang, Wu, and Povinelli [47] – see also Monk [53].

Edge elements are probably the most satisfactory from a theoretical point of view [55], in particular because they correctly represent singular behavior at reentrant corners. However, they are less attractive for time-dependent computations, because the solution of a linear system is required at every time iteration. Indeed, in the case of triangular or tetrahedral edge elements, the entries of the diagonal matrix resulting from mass-lumping are not necessarily strictly positive [29]; therefore, explicit time stepping cannot be used in general. In contrast, nodal elements naturally lead to a fully explicit scheme when mass-lumping is applied both in space and time [29], but cannot correctly represent corner singularities in general.

Discontinuous Galerkin (DG) finite element methods offer an attractive alternative to edge elements for the numerical solution of Maxwell's equations, in particular for time-dependent problems. Not only do they accommodate elements of various types and shapes, irregular non-matching grids, and even locally varying polynomial order, and hence offer great flexibility in the mesh design, but they also lead to (block-) diagonal mass matrices and therefore yield fully explicit, inherently parallel methods when coupled with explicit time stepping. Indeed, the mass matrix arising from a DG discretization is always block-diagonal, with block size equal to the number of degrees of freedom per element; hence, it can be inverted at very low computational cost. In fact, for constant material coefficients, the mass matrix is truly diagonal for a judicious choice of (locally orthogonal) shape functions. Because continuity across element interfaces is weakly enforced merely by adding suitable bilinear forms (so-called numerical fluxes) to the standard variational formulation, the implementation of DG-FE methods is straightforward within existing FE software libraries.

For first-order hyperbolic systems, various DG finite element methods are available. In [22], for instance, Cockburn and Shu use a DG FEM in space combined with a Runge-Kutta scheme in time to discretize hyperbolic conservation laws. In [50], Kopriva, Woodruff and Hussaini developed discontinuous Galerkin methods, which combine high-order spectral elements with a fourth order low-storage Runge-Kutta scheme. Warburton [74], and Hesthaven and Warburton [36] used a similar approach for their Runge-Kutta discontinuous Galerkin (RKDG) method, which combines high-order spatial accuracy with a fourth order low-storage Runge-Kutta scheme. While successful, their

scheme does not conserve energy due to upwinding. Fezoui, Lanteri, Lohrengel and Piperno [32] used central fluxes instead, yet the convergence rate of their scheme remains sub-optimal. Recently, Chen, Cockburn, and Reitich developed a high-order RKDG method for Maxwell's equations in first-order hyperbolic form, which achieves high-order convergence both in space and time by using a strong stability preserving (low storage) SSP-RK scheme [15]. By using locally divergence-free polynomials Cockburn, Li, and Shu developed a locally divergence-free DG method for the first-order Maxwell system [21].

For the second order (scalar) wave equation Rivière and Wheeler proposed a nonsymmetric formulation, which required additional stabilization for optimal convergence [66, 67]. A symmetric interior penalty DG FEM is presented in Chapter 4 of this thesis. Recently, Chung and Engquist [17] proposed a hybrid DG/continuous FE approach for the acoustic wave equation.

Here, we propose and analyze the symmetric interior penalty DG method for the spatial discretization of Maxwell's equations in *second order* form. After stating the model problem in Section 5.2, we describe the interior penalty DG variational formulation in Section 5.3. In Section 5.4, we state optimal a-priori error bounds in the energy norm and in the L^2 -norm. In the case of solutions with smoothness beyond H^1 , the error bound (Theorem 5.4.1) holds for arbitrary DG-FE discretizations, whereas in the case of lower regularity, the error bound (Theorem 5.4.2) only holds for conforming meshes. The optimal L^2 -error bound (Theorem (5.4.3)) is valid for DG discretizations on conforming, triangular or tetrahedral meshes. The proofs of Theorems 5.4.1 and 5.4.2 and technical approximation results are provided in Section 5.5. The proof of Theorem 5.4.3 is more involved and is presented in Section 5.6. Numerical experiments to validate our DG method and the theoretical error bounds and concluding remarks are presented in Section 5.7.

5.2 Model problem

The evolution of a time-dependent electromagnetic field $\mathbf{E}(\mathbf{x}, t)$, $\mathbf{H}(\mathbf{x}, t)$ propagating through a linear isotropic medium is determined by Maxwell's equations:

$$\begin{aligned}\varepsilon \mathbf{E}_t &= \nabla \times \mathbf{H} - \sigma \mathbf{E} + \mathbf{j}, \\ \mu \mathbf{H}_t &= -\nabla \times \mathbf{E}.\end{aligned}$$

Here, the coefficients μ , ε , and σ denote the relative magnetic permeability, the relative electric permittivity, and the conductivity of the medium, respectively. The source term \mathbf{j} corresponds to the applied current density. By eliminating the magnetic field \mathbf{H} , Maxwell's equations reduce to a second-order vector wave equation for the electric field \mathbf{E} :

$$\varepsilon \mathbf{E}_{tt} + \sigma \mathbf{E}_t + \nabla \times (\mu^{-1} \nabla \times \mathbf{E}) = \mathbf{j}_t.$$

If the electric field is eliminated instead, one easily finds that the magnetic field \mathbf{H} satisfies a similar vector wave equation.

Thus, we shall consider the following model problem: find the (electric or

magnetic) field $\mathbf{u}(\mathbf{x}, t)$, which satisfies

$$\begin{aligned} \varepsilon \mathbf{u}_{tt} + \sigma \mathbf{u}_t + \nabla \times (\mu^{-1} \nabla \times \mathbf{u}) &= \mathbf{f} && \text{in } \Omega \times J, \\ \mathbf{n} \times \mathbf{u} &= \mathbf{0} && \text{in } \Gamma \times J, \\ \mathbf{u}|_{t=0} &= \mathbf{u}_0 && \text{on } \Omega, \\ \mathbf{u}_t|_{t=0} &= \mathbf{v}_0 && \text{on } \Omega. \end{aligned} \quad (5.1)$$

Here, $J = (0, T)$ is a finite time interval and Ω is a bounded Lipschitz polyhedron in \mathbb{R}^3 with boundary $\Gamma = \partial\Omega$ and outward unit normal \mathbf{n} . For simplicity, we assume Ω to be simply-connected and Γ to be connected. The right-hand side \mathbf{f} is a given source term in $L^2(J; L^2(\Omega)^3)$, where $L^p(J; H^s(\Omega))$ denotes the standard Bochner space of (time-dependent) functions whose $\|\cdot\|_{s, \Omega}$ Sobolev-norm is p -integrable in time. The standard inner product in $L^2(\Omega)^3$ is denoted by $(\mathbf{u}, \mathbf{v}) := \int_{\Omega} \mathbf{u} \cdot \mathbf{v} \, d\mathbf{x}$.

The functions \mathbf{u}_0 and \mathbf{v}_0 are prescribed initial data with $\mathbf{u}_0 \in H_0(\text{curl}; \Omega)$ and $\mathbf{v}_0 \in L^2(\Omega)^3$, where $H_0(\text{curl}; \Omega)$ denotes the subspace of functions in

$$H(\text{curl}; \Omega) = \{ \mathbf{v} \in L^2(\Omega)^3 : \nabla \times \mathbf{v} \in L^2(\Omega)^3 \},$$

which have zero tangential component on $\partial\Omega$, the boundary of Ω . Furthermore, we assume that μ , ε and σ are scalar positive functions that satisfy

$$0 < \mu_* \leq \mu(\mathbf{x}) \leq \mu^* < \infty, \quad 0 < \varepsilon_* \leq \varepsilon(\mathbf{x}) \leq \varepsilon^* < \infty, \quad \mathbf{x} \in \Omega, \quad (5.2)$$

and

$$0 \leq \sigma(\mathbf{x}) \leq \sigma^* < \infty, \quad \mathbf{x} \in \Omega,$$

respectively. For simplicity, we also assume that μ is piecewise constant.

5.3 Discontinuous Galerkin discretization

We shall now discretize Maxwell's equations in space using the interior penalty discontinuous Galerkin method. First, we consider shape-regular meshes \mathcal{T}_h that partition the domain Ω into disjoint tetrahedral or affine hexahedral elements $\{K\}$, such that $\bar{\Omega} = \cup_{K \in \mathcal{T}_h} \bar{K}$. The diameter of element K is denoted by h_K , and the mesh size h is given by $h = \max_{K \in \mathcal{T}_h} h_K$. We assume that the partition is aligned with the discontinuities of the coefficient μ and that the local mesh sizes are of bounded variation, that is, there exists a positive constant κ , which depends only on the shape-regularity of the mesh, such that $\kappa h_K \leq h_{K'} \leq \kappa^{-1} h_K$, for all neighboring elements K and K' . We denote by \mathcal{F}_h^I the set of all interior faces, by \mathcal{F}_h^B the set of all boundary faces, and set $\mathcal{F}_h = \mathcal{F}_h^I \cup \mathcal{F}_h^B$.

For a given partition \mathcal{T}_h of Ω and an approximation order $\ell \geq 1$, we wish to approximate $\mathbf{u}(\cdot, t)$ in the finite element space

$$\mathbf{V}^h := \{ \mathbf{v} \in L^2(\Omega)^3 : \mathbf{v}|_K \in \mathcal{S}^\ell(K)^3, K \in \mathcal{T}_h \},$$

where $\mathcal{S}^\ell(K)$ is the space $\mathcal{P}^\ell(K)$ of polynomials of total degree at most ℓ on K , if K is a tetrahedron, and the space $\mathcal{Q}^\ell(K)$ of polynomials of degree at most ℓ in each variable on K , if K is a parallelepiped.

We consider the following (semi-discrete) discontinuous Galerkin formulation of (5.1): find $u^h : \bar{J} \times V^h \rightarrow \mathbb{R}$ such that

$$\begin{aligned} (\varepsilon \mathbf{u}_{tt}^h, \mathbf{v}) + (\sigma \mathbf{u}_t^h, \mathbf{v}) + a_h(\mathbf{u}^h, \mathbf{v}) &= (\mathbf{f}, \mathbf{v}), \quad \mathbf{v} \in \mathbf{V}^h, \quad t \in J, \\ \mathbf{u}^h|_{t=0} &= \mathbf{\Pi}_h \mathbf{u}_0, \\ \mathbf{u}_t^h|_{t=0} &= \mathbf{\Pi}_h \mathbf{v}_0. \end{aligned} \quad (5.3)$$

Here, $\mathbf{\Pi}_h$ denotes the L^2 -projection onto \mathbf{V}^h , while the discrete bilinear form a_h , defined on $\mathbf{V}^h \times \mathbf{V}^h$, is given by

$$\begin{aligned} a_h(\mathbf{u}, \mathbf{v}) &:= \sum_{K \in \mathcal{T}_h} \int_K \mu^{-1} (\nabla \times \mathbf{u}) \cdot (\nabla \times \mathbf{v}) \, dx - \sum_{f \in \mathcal{F}_h} \int_f \llbracket \mathbf{u} \rrbracket_T \cdot \{\!\!\{ \mu^{-1} \nabla \times \mathbf{v} \}\!\!\} \, dA \\ &\quad - \sum_{f \in \mathcal{F}_h} \int_f \llbracket \mathbf{v} \rrbracket_T \cdot \{\!\!\{ \mu^{-1} \nabla \times \mathbf{u} \}\!\!\} \, dA + \sum_{f \in \mathcal{F}_h} \int_f \mathbf{a} \llbracket \mathbf{u} \rrbracket_T \cdot \llbracket \mathbf{v} \rrbracket_T \, dA. \end{aligned}$$

We denote by $\llbracket \mathbf{v} \rrbracket_T$ and $\{\!\!\{ \mathbf{v} \}\!\!\}$, respectively, the tangential jumps and averages of a DG function \mathbf{v} across interior faces; see Section 2.2. On boundary faces we set $\llbracket \mathbf{v} \rrbracket_T := \mathbf{n} \times \mathbf{v}$ and $\{\!\!\{ \mathbf{v} \}\!\!\} := \mathbf{v}$.

The function \mathbf{a} penalizes the jumps of \mathbf{u} and \mathbf{v} over the faces of the triangulation. To define it, we first introduce the function \mathbf{h} and \mathbf{m} by

$$\begin{aligned} \mathbf{h}|_f &= \begin{cases} \min\{h_K, h_{K'}\}, & f \in \mathcal{F}_h^I, F = \partial K \cap \partial K', \\ h_K, & f \in \mathcal{F}_h^B, f = \partial K \cap \partial \Omega, \end{cases} \\ \mathbf{m}|_f &= \begin{cases} \min\{\mu_K, \mu_{K'}\}, & f \in \mathcal{F}_h^I, f = \partial K \cap \partial K', \\ \mu_K, & f \in \mathcal{F}_h^B, f = \partial K \cap \partial \Omega. \end{cases} \end{aligned}$$

Here, we denote by μ_K the restriction of the piecewise coefficient μ to element K . On each $f \in \mathcal{F}_h$, we then set

$$\mathbf{a}|_f := \alpha \mathbf{m}^{-1} \mathbf{h}^{-1}.$$

In Lemma 5.5.2 we shall show that there is a positive constant α_{\min} , independent of the local mesh sizes and the coefficient μ , such that for $\alpha \geq \alpha_{\min}$ the bilinear form a_h is coercive. Hence the DG approximation of (5.1) is well-defined. We note that larger values of α result in a more restrictive CFL condition in (explicit) time discretizations of (5.3).

REMARK 5.3.1. *When the interior penalty DG method is used for time-dependent computations, the FE solution consists of a superposition of discrete eigenmodes. Because of symmetry, the energy of the semi-discrete formulation (5.3) is conserved, so that all the modes neither grow nor decay. For eigenvalue computations, Buffa and Perugia [13] recently proved that the interior penalty DG discretization of the Maxwell operator is free of spurious modes: the discrete spectrum will eventually converge to the continuous spectrum, as $h \rightarrow 0$. Nonetheless, on any fixed mesh some of the discrete eigenmodes will not correspond to physical modes. Hesthaven and Warburton [36], and Warburton and Embree [75] showed that larger values of the penalty parameter in central flux or local discontinuous Galerkin (LDG) discretizations increase the separation between spurious and physical eigenmodes. Alternatively, if upwinding is used*

some of the spurious modes will be damped as well.

Clearly, as the mesh is refined, the energy present in the spurious modes will decrease and eventually vanish, as the numerical solution obtained with the interior penalty DG method converges to the exact solution; see Section 5.4.

5.4 A-priori error bounds

In this section we state optimal a-priori error bounds with respect to the DG energy norm. To that end, we set $\mathbf{V}(h) := H_0(\text{curl}; \Omega) + \mathbf{V}^h$ and introduce the semi-norm

$$|\mathbf{v}|_h^2 := \sum_{K \in \mathcal{T}_h} \|\mu^{-\frac{1}{2}}(\nabla \times \mathbf{v})\|_{0,K}^2 + \sum_{f \in \mathcal{F}_h} \|\mathbf{a}^{\frac{1}{2}}[\![\mathbf{v}]\!]_T\|_{0,f}^2.$$

The DG energy norm is then defined by

$$\|\mathbf{v}\|_h^2 := \|\varepsilon^{\frac{1}{2}}\mathbf{v}\|_{0,\Omega}^2 + |\mathbf{v}|_h^2.$$

For functions $\mathbf{v} \in H(\text{curl}; \Omega)$ it coincides with the standard energy norm. We further define the norms

$$\|\mathbf{v}\|_{L^p(J; \mathbf{V}(h))} = \begin{cases} \left(\int_J \|\mathbf{v}\|_h^p dt \right)^{1/p}, & 1 \leq p < \infty, \\ \text{ess sup}_{t \in J} \|\mathbf{v}\|_h, & p = \infty, \end{cases}$$

and set

$$|\mathbf{v}|_{L^p(J; \mathbf{V}(h))} = \begin{cases} \left(\int_J |\mathbf{v}|_h^p dt \right)^{1/p}, & 1 \leq p < \infty, \\ \text{ess sup}_{t \in J} |\mathbf{v}|_h, & p = \infty. \end{cases}$$

Then, we have the following error estimate.

THEOREM 5.4.1. *Let the analytical solution \mathbf{u} of (5.1) satisfy*

$$\mathbf{u} \in L^\infty(J; H^{1+s}(\Omega)^3), \quad \mathbf{u}_t \in L^\infty(J; H^{1+s}(\Omega)^3), \quad \mathbf{u}_{tt} \in L^1(J; H^s(\Omega)^3),$$

for $s > \frac{1}{2}$, and \mathbf{u}^h be the semi-discrete discontinuous Galerkin approximation with $\alpha \geq \alpha_{\min}$. Then, the error $\mathbf{e} = \mathbf{u} - \mathbf{u}^h$ satisfies

$$\begin{aligned} \|\varepsilon^{\frac{1}{2}}\mathbf{e}_t\|_{L^\infty(J; L^2(\Omega)^3)} + \|\mathbf{e}\|_{L^\infty(J; \mathbf{V}(h))} &\leq C \left(\|\varepsilon^{\frac{1}{2}}\mathbf{e}_t(0)\|_{0,\Omega} + |\mathbf{e}(0)|_h \right) \\ &+ C h^{\min\{s,\ell\}} \left(\|\mathbf{u}\|_{L^\infty(J; H^{1+s}(\Omega)^3)} + \|\mathbf{u}_t\|_{L^\infty(J; H^{1+s}(\Omega)^3)} + \|\mathbf{u}_{tt}\|_{L^1(J; H^s(\Omega)^3)} \right), \end{aligned}$$

with a constant $C > 0$ that is independent of the mesh size.

In Theorem 5.4.1 we implicitly assume that $\mathbf{u}_0 \in H^{1+s}(\Omega)^3$ and $\mathbf{v}_0 \in H^s(\Omega)^3$. Hence, the approximation properties of the L^2 -projection in Lemma 5.5.4 and Lemma 5.5.5 imply that

$$\|\varepsilon^{\frac{1}{2}}\mathbf{e}_t(0)\|_{0,\Omega} \leq C h^{\min\{s,\ell+1\}} \|\mathbf{v}_0\|_{s,\Omega}, \quad |\mathbf{e}(0)|_h \leq C h^{\min\{s,\ell\}} \|\mathbf{u}_0\|_{1+s,\Omega}.$$

As a consequence, Theorem 5.4.1 yields optimal convergence of order $\mathcal{O}(h^{\min\{s,\ell\}})$ in the DG energy norm.

In many instances, solutions to the Maxwell equations have singularities that do not satisfy the regularity assumptions in Theorem 5.4.1. Indeed, it is well-known that the strongest singularities have smoothness below $H^1(\Omega)^3$. We

shall now show that the DG method still converges under weaker yet realistic regularity assumptions provided that the meshes are conforming.

THEOREM 5.4.2. *Let the analytical solution \mathbf{u} of (5.1) satisfy*

$$\mathbf{u}, \mathbf{u}_t, \nabla \times \mathbf{u}, \nabla \times \mathbf{u}_t \in L^\infty(J; H^s(\Omega)^3) \quad \text{and} \quad \mathbf{u}_{tt}, \nabla \times \mathbf{u}_{tt} \in L^1(J; H^s(\Omega)^3),$$

for $s > \frac{1}{2}$. Next, let \mathcal{T}_h be a conforming triangulation of Ω into tetrahedra or hexahedra with edges parallel to the coordinate axes, and \mathbf{u}^h be the semi-discrete discontinuous Galerkin approximation obtained with $\alpha \geq \alpha_{\min}$. Then the error $\mathbf{e} = \mathbf{u} - \mathbf{u}^h$ satisfies

$$\begin{aligned} \|\varepsilon^{\frac{1}{2}} \mathbf{e}_t\|_{L^\infty(J; L^2(\Omega)^3)} + \|\mathbf{e}\|_{L^\infty(J; \mathbf{V}(h))} &\leq C \left(\|\varepsilon^{\frac{1}{2}} \mathbf{e}_t(0)\|_{0, \Omega} + |\mathbf{e}(0)|_h \right) \\ &+ C h^{\min\{s, \ell\}} \left(\|\mathbf{u}\|_{L^\infty(J; H^s(\Omega)^3)} + \|\nabla \times \mathbf{u}\|_{L^\infty(J; H^s(\Omega)^3)} \right. \\ &\quad + \|\mathbf{u}_t\|_{L^\infty(J; H^s(\Omega)^3)} + \|\nabla \times \mathbf{u}_t\|_{L^\infty(J; H^s(\Omega)^3)} \\ &\quad \left. + \|\mathbf{u}_{tt}\|_{L^1(J; H^s(\Omega)^3)} + \|\nabla \times \mathbf{u}_{tt}\|_{L^1(J; H^s(\Omega)^3)} \right), \end{aligned}$$

with a constant $C > 0$ that is independent of the mesh size.

If we additionally assume that $\mathbf{u}_0 \in H^{1+s}(\Omega)^3$ for $t > 0$, the bound in Theorem 5.4.2 yields again optimal convergence of the order $\mathcal{O}(h^{\min\{s, \ell\}})$ for the error in the energy norm.

Next, note that Theorem 5.4.1 and Theorem 5.4.2 immediately imply a (sub-optimal) bound for the error in the L^2 -norm $\|\mathbf{u} - \mathbf{u}^h\|_{L^\infty(J; L^2(\Omega)^3)}$. With the restriction to conforming tetrahedral meshes however, we will show that this estimate can be improved and that optimal order $\mathcal{O}(h^{\ell+1})$ can be obtained for smooth solutions and convex domains.

To this end, we recall the embedding stated in (2.8): under the foregoing assumptions on the domain Ω , there exists a regularity exponent $\sigma_E \in (1/2, 1]$, depending only on Ω , such that

$$\begin{aligned} H_0(\text{curl}; \Omega) \cap H(\text{div}; \Omega) &\hookrightarrow H^{\sigma_E}(\Omega)^3, \\ H(\text{curl}; \Omega) \cap H_0(\text{div}; \Omega) &\hookrightarrow H^{\sigma_E}(\Omega)^3. \end{aligned} \tag{5.4}$$

The maximal value of σ_E for which the above embedding holds is closely related to the regularity properties of the Laplacian in polyhedra and only depends on the opening angles at the corners and edges of the domain, cf. [4]. In particular, for a convex domain, (5.4) holds with $\sigma_E = 1$.

We now state our second main result, an estimate for the error of the semi-discrete solution \mathbf{u}^h in the L^2 -norm.

THEOREM 5.4.3. *Assume $\mu = 1$ and $\sigma = \text{constant}$ in (5.1).*

Let the analytical solution \mathbf{u} of (5.1) satisfy

$$\begin{aligned} \mathbf{u} &\in L^\infty(J, H^{s+\sigma_E}(\Omega)^3), & \nabla \times \mathbf{u} &\in L^\infty(J, H^s(\Omega)^3), \\ \mathbf{u}_t &\in L^\infty(J, H^{s+\sigma_E}(\Omega)^3), & \nabla \times \mathbf{u}_t &\in L^\infty(J, H^s(\Omega)^3), \end{aligned} \tag{5.5}$$

for an $s > \frac{1}{2}$ and the regularity exponent $\sigma_E \in (\frac{1}{2}, 1]$ from (5.4).

Let \mathcal{T}_h be a conforming triangulation of the domain Ω into tetrahedra and let \mathbf{u}^h be the semi-discrete approximation obtained on \mathcal{T}_h by (5.3) with $\alpha \geq \alpha_{\min}$.

Then, the error $\mathbf{e} = \mathbf{u} - \mathbf{u}^h$ satisfies

$$\begin{aligned} \|\mathbf{e}\|_{L^\infty(J;L^2(\Omega)^3)} &\leq Ch^{\min\{s,\ell\}+\sigma_E} \left[\|\mathbf{u}_0\|_{s+\sigma_E} + \|\nabla \times \mathbf{u}_0\|_s \right. \\ &\quad \left. + (1 + \sigma T + T^2) [\|\mathbf{u}\|_{L^\infty(J;H^{s+\sigma_E}(\Omega)^3)} + \|\nabla \times \mathbf{u}\|_{L^\infty(J;H^s(\Omega)^3)}] \right. \\ &\quad \left. + T [\|\mathbf{u}_t\|_{L^\infty(J;H^{s+\sigma_E}(\Omega)^3)} + \|\nabla \times \mathbf{u}_t\|_{L^\infty(J;H^s(\Omega)^3)}] \right], \end{aligned}$$

with a constant $C > 0$ independent of h and T .

A variant of Theorem 5.4.3 for non-constant conductivity σ will be commented on in Remark 5.6.6 in Section 5.6.

For smooth solutions on convex domains ($\sigma_E = 1$), Theorem 5.4.3 thus yields optimal convergence rates in the L^2 -norm:

$$\|\mathbf{e}\|_{L^\infty(J;L^2(\Omega)^3)} \leq Ch^{\ell+1}.$$

The bounds in Theorem 5.4.1 and Theorem 5.4.2 are proven in the next section. The proof of Theorem 5.4.3 is given in Section 5.6.

5.5 Proofs of Theorems 5.4.1 and 5.4.2

5.5.1 Extension of the DG form and stability properties

The bilinear DG form a_h , while well-defined on \mathbf{V}^h , is not well-defined on the larger space $\mathbf{V}(h)$. To extend the DG form to $\mathbf{V}(h)$, we follow an approach similar to [61] and introduce the auxiliary form

$$\begin{aligned} \tilde{a}_h(\mathbf{u}, \mathbf{v}) &= \sum_{K \in \mathcal{T}_h} \int_K \mu^{-1} (\nabla \times \mathbf{u}) \cdot (\nabla \times \mathbf{v}) dx - \sum_{f \in \mathcal{F}_h} \int_f [\![\mathbf{u}]\!]_T \cdot \{\!\{ \mu^{-1} \mathbf{\Pi}_h(\nabla \times \mathbf{v}) \}\!\} dA \\ &\quad - \sum_{f \in \mathcal{F}_h} \int_f [\![\mathbf{v}]\!]_T \cdot \{\!\{ \mu^{-1} \mathbf{\Pi}_h(\nabla \times \mathbf{u}) \}\!\} dA + \sum_{f \in \mathcal{F}_h} \int_f \mathbf{a} [\![\mathbf{u}]\!]_T \cdot [\![\mathbf{v}]\!]_T dA, \end{aligned}$$

where we recall that $\mathbf{\Pi}_h$ is the L^2 -projection onto \mathbf{V}^h . Note that \tilde{a}_h coincides with a_h on $\mathbf{V}^h \times \mathbf{V}^h$ and is well-defined on $H_0(\text{curl}; \Omega) \times H_0(\text{curl}; \Omega)$. This follows from the following result.

LEMMA 5.5.1. *For $\mathbf{v} \in \mathbf{V}(h)$ and $\mathbf{z} \in L^2(\Omega)^3$ there holds*

$$\sum_{f \in \mathcal{F}_h} \int_f [\![\mathbf{v}]\!]_T \cdot \{\!\{ \mu^{-1} \mathbf{\Pi}_h \mathbf{z} \}\!\} dA \leq C_{\text{inv}} \alpha^{-\frac{1}{2}} \left(\sum_{f \in \mathcal{F}_h} \|\mathbf{a}^{\frac{1}{2}} [\![\mathbf{v}]\!]_T\|_{0,f}^2 \right)^{\frac{1}{2}} \|\mu^{-\frac{1}{2}} \mathbf{z}\|_{0,\Omega},$$

with a constant C_{inv} that only depends on the shape-regularity of the mesh and the approximation order ℓ .

Proof. By the Cauchy-Schwarz inequality and the definition of the stabilization function \mathbf{a} we have

$$\begin{aligned} \sum_{f \in \mathcal{F}_h} \int_f [\![\mathbf{v}]\!]_T \cdot \{\!\{ \mu^{-1} \mathbf{\Pi}_h \mathbf{z} \}\!\} dA &\leq \alpha^{-\frac{1}{2}} \left(\sum_{f \in \mathcal{F}_h} \|\mathbf{a}^{\frac{1}{2}} [\![\mathbf{v}]\!]_T\|_{0,f}^2 \right)^{\frac{1}{2}} \\ &\quad \cdot \left(\sum_{f \in \mathcal{F}_h} \|\mathbf{m}^{\frac{1}{2}} \mathbf{h}^{\frac{1}{2}} \{\!\{ \mu^{-1} \mathbf{\Pi}_h \mathbf{z} \}\!\}\|_{0,f}^2 \right)^{\frac{1}{2}}. \end{aligned}$$

Using the definition of \mathbf{m} and \mathbf{h} and the assumption that μ is piecewise constant, we can bound the last term above by

$$\begin{aligned} \sum_{f \in \mathcal{T}_h} \|\mathbf{m}^{\frac{1}{2}} \mathbf{h}^{\frac{1}{2}} \{\{\mu^{-1} \mathbf{\Pi}_h \mathbf{z}\}\}\|_{0,f}^2 &\leq \sum_{K \in \mathcal{T}_h} h_K \mu_K \|\mu_K^{-1} \mathbf{\Pi}_h \mathbf{z}\|_{0,\partial K}^2 \\ &= \sum_{K \in \mathcal{T}_h} h_K \|\mathbf{\Pi}_h(\mu_K^{-\frac{1}{2}} \mathbf{z})\|_{0,\partial K}^2. \end{aligned}$$

Recalling the inverse inequality

$$\|\mathbf{w}\|_{0,\partial K}^2 \leq C_{\text{inv}}^2 h_K^{-1} \|\mathbf{w}\|_{0,K}^2, \quad \mathbf{w} \in (\mathcal{S}^\ell(K))^3,$$

with a constant C_{inv} that only depends on the shape-regularity of the mesh and the approximation order ℓ , and using the stability of the L^2 -projection, we obtain $\sum_{K \in \mathcal{T}_h} h_K \|\mathbf{\Pi}_h(\mu_K^{-\frac{1}{2}} \mathbf{z})\|_{0,\partial K}^2 \leq C_{\text{inv}}^2 \|\mu^{-\frac{1}{2}} \mathbf{z}\|_{0,\Omega}^2$. This completes the proof. \square

We are now ready to show the continuity and coercivity of \tilde{a}_h on $\mathbf{V}(h)$.

LEMMA 5.5.2. *Set $\alpha_{\min} = 4C_{\text{inv}}^2$, with C_{inv} denoting the constant from Lemma 5.5.1. For $\alpha \geq \alpha_{\min}$ we have*

$$|\tilde{a}_h(\mathbf{u}, \mathbf{v})| \leq C_{\text{cont}} |\mathbf{u}|_h |\mathbf{v}|_h, \quad a_h(\mathbf{v}, \mathbf{v}) \geq C_{\text{coer}} |\mathbf{v}|_h^2, \quad \mathbf{u}, \mathbf{v} \in \mathbf{V}(h),$$

with $C_{\text{cont}} = \sqrt{2}$ and $C_{\text{coer}} = \frac{1}{2}$.

Proof. The continuity of \tilde{a}_h is a straightforward application of the result in Lemma 5.5.1 and the Cauchy-Schwarz inequality. The coercivity property of \tilde{a}_h follows similarly by employing Lemma 5.5.1 and the geometric-arithmetic mean inequality:

$$\tilde{a}_h(\mathbf{u}, \mathbf{u}) \geq (1 - \alpha^{-\frac{1}{2}} C_{\text{inv}}) \left(\sum_{K \in \mathcal{T}_h} \|\mu^{-\frac{1}{2}} (\nabla \times \mathbf{u})\|_{0,K}^2 + \sum_{f \in \mathcal{F}_h} \|\mathbf{a}^{\frac{1}{2}} [\mathbf{u}]_T\|_{0,f}^2 \right),$$

which proves the coercivity of \tilde{a}_h with $C_{\text{coer}} = \frac{1}{2}$ provided that $\alpha \geq \alpha_{\min}$. \square

5.5.2 Error equation

We shall use the form \tilde{a}_h as the basis of our error analysis, similarly to the approach in Chapters 2 and 3. To do so, we define for $\mathbf{v} \in \mathbf{V}(h)$

$$r_h(\mathbf{u}; \mathbf{v}) = \sum_{f \in \mathcal{F}_h} \int_f [\mathbf{v}]_T \cdot \{\{\mu^{-1} (\nabla \times \mathbf{u}) - \mu^{-1} \mathbf{\Pi}_h (\nabla \times \mathbf{u})\}\} dA. \quad (5.6)$$

In order for $r_h(\mathbf{u}; \mathbf{v})$ to be well-defined, we also need to assume that $\nabla \times \mathbf{u} \in H^s(\Omega)^3$ for $s > 1/2$.

We note that from the definition in (5.6) immediately follows

$$r_h(\mathbf{u}; \mathbf{v}) = 0 \quad \text{when } \mathbf{v} \in H_0(\text{curl}; \Omega). \quad (5.7)$$

LEMMA 5.5.3. *Let the analytical solution \mathbf{u} of (5.1) satisfy*

$$\nabla \times \mathbf{u} \in L^\infty(J; H^s(\Omega)^3), \quad \mathbf{u}_t, \mathbf{u}_{tt} \in L^1(J; L^2(\Omega)^3),$$

for $s > \frac{1}{2}$. Let \mathbf{u}^h be the semi-discrete discontinuous Galerkin approximation obtained with $\alpha \geq \alpha_{\min}$. Then the error $\mathbf{e} = \mathbf{u} - \mathbf{u}^h$ satisfies

$$(\varepsilon \mathbf{e}_{tt}, \mathbf{v}) + (\sigma \mathbf{e}_t, \mathbf{v}) + \tilde{a}_h(\mathbf{e}, \mathbf{v}) = r_h(\mathbf{u}; \mathbf{v}), \quad \mathbf{v} \in \mathbf{V}^h, \text{ a.e. in } J.$$

Proof. Since $[[\mathbf{u}]]_T = \mathbf{0}$ across all faces, we have

$$\tilde{a}_h(\mathbf{u}, \mathbf{v}) = \sum_{K \in \mathcal{T}_h} \int_K \mu^{-1} (\nabla \times \mathbf{u}) \cdot (\nabla \times \mathbf{v}) \, d\mathbf{x} - \sum_{f \in \mathcal{F}_h} \int_f [[\mathbf{v}]]_T \cdot \{\mu^{-1} \mathbf{\Pi}_h(\nabla \times \mathbf{u})\} \, dA.$$

Integration by parts then leads to

$$\begin{aligned} \tilde{a}_h(\mathbf{u}, \mathbf{v}) &= \sum_{K \in \mathcal{T}_h} \int_K (\nabla \times (\mu^{-1} (\nabla \times \mathbf{u}))) \cdot \mathbf{v} \, d\mathbf{x} \\ &\quad + \sum_{f \in \mathcal{F}_h} \int_f [[\mathbf{v}]]_T \cdot \{\mu^{-1} (\nabla \times \mathbf{u})\} \, dA \\ &\quad - \sum_{f \in \mathcal{F}_h} \int_f [[\mathbf{v}]]_T \cdot \{\mu^{-1} \mathbf{\Pi}_h(\nabla \times \mathbf{u})\} \, dA. \end{aligned}$$

Therefore, we conclude that

$$\begin{aligned} (\varepsilon \mathbf{u}_{tt}, \mathbf{v}) + (\sigma \mathbf{u}_t, \mathbf{v}) + \tilde{a}_h(\mathbf{u}, \mathbf{v}) \\ &= (\varepsilon \mathbf{u}_{tt} + \sigma \mathbf{u}_t + \nabla \times (\mu^{-1} \nabla \times \mathbf{u}), \mathbf{v}) + r_h(\mathbf{u}; \mathbf{v}) \quad (5.8) \\ &= (\mathbf{f}, \mathbf{v}) + r_h(\mathbf{u}; \mathbf{v}), \end{aligned}$$

where in the last step we have used the fact that \mathbf{u} solves (5.1). This immediately yields the desired error equation. \square

5.5.3 Approximation results

In this section, we provide the approximation results that we need to prove Theorem 5.4.1 and Theorem 5.4.2.

To begin we recall the approximation properties of the L^2 -projection; see [18]. Here, we denote by $|\cdot|_{1,D}$ the standard semi-norm on the Sobolev space $H^1(D)^3$.

LEMMA 5.5.4. *Let $K \in \mathcal{T}_h$. Then:*

(i) For $\mathbf{v} \in H^s(K)^3$, $s \geq 0$, we have

$$\|\mathbf{v} - \mathbf{\Pi}_h \mathbf{v}\|_{0,K} \leq Ch_K^{\min\{s, \ell+1\}} \|\mathbf{v}\|_{s,K}.$$

(ii) For $\mathbf{v} \in H^{1+s}(K)^3$, $s > 0$, we have

$$\|\mathbf{v} - \mathbf{\Pi}_h \mathbf{v}\|_{1,K} \leq Ch_K^{\min\{s, \ell\}} \|\mathbf{v}\|_{1+s,K}.$$

(iii) For $\mathbf{v} \in H^s(K)^3$, $s > \frac{1}{2}$, we have

$$\|\mathbf{v} - \mathbf{\Pi}_h \mathbf{v}\|_{0,\partial K} \leq Ch_K^{\min\{s-\frac{1}{2}, \ell+\frac{1}{2}\}} \|\mathbf{v}\|_{s,K}.$$

The constants C are independent of the local mesh sizes and only depend on the shape-regularity of the mesh, the approximation order ℓ , and the regularity exponent s .

The approximation properties in Lemma 5.5.4 imply the following result.

LEMMA 5.5.5. *Let $\mathbf{u} \in H^{1+s}(\Omega)^3$, for $s > \frac{1}{2}$. Then we have*

$$\|\mathbf{u} - \mathbf{\Pi}_h \mathbf{u}\|_h \leq C_A h^{\min\{s, \ell\}} \|\mathbf{u}\|_{1+s, \Omega},$$

with a constant C_A that is independent of the mesh size and only depends on α , the bounds for the coefficients μ and ε , the shape-regularity of the mesh, the constant κ of the mesh variation, and the approximation order ℓ .

Similarly, the approximation properties for the L^2 -projection and the Cauchy-Schwarz inequality imply that $r_h(\mathbf{u}; \mathbf{v})$ in (5.6) can be bounded as follows; cf. [45, Proposition 6.2] or in Lemma 2.4.9 of Chapter 2.

LEMMA 5.5.6. *Let \mathbf{u} be such that $\nabla \times \mathbf{u} \in H^s(\Omega)^3$, for $s > \frac{1}{2}$. Then, $r_h(\mathbf{u}; \mathbf{v})$, defined in (5.6), satisfies*

$$|r_h(\mathbf{u}; \mathbf{v})| \leq C_R h^{\min\{s, \ell+1\}} |\mathbf{v}|_h \|\nabla \times \mathbf{u}\|_{s, \Omega}, \quad \mathbf{v} \in \mathbf{V}(h),$$

with a constant C_R that is independent of the mesh size and only depends on α , the bounds for the coefficient μ , the shape-regularity of the mesh, the constant κ of the mesh variation, and the approximation order ℓ .

Consequently, we also obtain the following result.

LEMMA 5.5.7. *Let \mathbf{u} satisfy*

$$\nabla \times \mathbf{u} \in L^\infty(J; H^s(\Omega)^3), \quad \nabla \times \mathbf{u}_t \in L^\infty(J; H^s(\Omega)^3),$$

for $s > \frac{1}{2}$. Let $\mathbf{v} \in C^0(\bar{J}; \mathbf{V}^h)$ and $\mathbf{v}_t \in L^\infty(\bar{J}; \mathbf{V}^h)$. Then there holds

$$\begin{aligned} \int_J |r_h(\mathbf{u}; \mathbf{v}_t)| dt &\leq C_R h^{\min\{s, \ell+1\}} |\mathbf{v}|_{L^\infty(J; \mathbf{V}(h))} \\ &\quad \cdot \left(2 \|\nabla \times \mathbf{u}\|_{L^\infty(J; H^s(\Omega)^3)} + T \|\nabla \times \mathbf{u}_t\|_{L^\infty(J; H^s(\Omega)^3)} \right), \end{aligned}$$

with C_R denoting the constant from Lemma 5.5.6.

Proof. Using integration by parts, we have

$$\begin{aligned} &\int_J r_h(\mathbf{u}; \mathbf{v}_t) dt \\ &= \int_J \sum_{f \in \mathcal{F}_h} \int_f [\mathbf{v}_t]_T \cdot \{ \mu^{-1} (\nabla \times \mathbf{u}) - \mu^{-1} \mathbf{\Pi}_h (\nabla \times \mathbf{u}) \} dA dt \\ &= - \int_J \sum_{f \in \mathcal{F}_h} \int_f [\mathbf{v}]_T \cdot \{ \mu^{-1} (\nabla \times \mathbf{u}_t) - \mu^{-1} \mathbf{\Pi}_h (\nabla \times \mathbf{u}_t) \} dA dt \\ &\quad + \left[\sum_{f \in \mathcal{F}_h} \int_f [\mathbf{v}]_T \cdot \{ \mu^{-1} (\nabla \times \mathbf{u}) - \mu^{-1} \mathbf{\Pi}_h (\nabla \times \mathbf{u}) \} dA \right]_{t=0}^{t=T} \\ &= - \int_J r_h(\mathbf{u}_t; \mathbf{v}) dt + \left[r_h(\mathbf{u}; \mathbf{v}) \right]_{t=0}^{t=T}. \end{aligned}$$

Lemma 5.5.6 then implies

$$\left| \left[r_h(\mathbf{u}; \mathbf{v}) \right]_{t=0}^{t=T} \right| \leq 2C_R h^{\min\{s, \ell\}} |\mathbf{v}|_{L^\infty(J; \mathbf{V}(h))} \|\nabla \times \mathbf{u}\|_{L^\infty(J; H^s(\Omega)^3)}.$$

Similarly, using Hölder's inequality,

$$\left| \int_J r_h(\mathbf{u}_t; \mathbf{v}) dt \right| \leq C_R h^{\min\{s, \ell\}} T |\mathbf{v}|_{L^\infty(J; \mathbf{V}(h))} \|\nabla \times \mathbf{u}_t\|_{L^\infty(J; H^s(\Omega)^3)}.$$

This concludes the proof. \square

Finally, we recall an approximation result for the Nédélec interpolant $\mathbf{\Pi}_N$ of the first kind that; see [58] or [55]. This result is restricted to conforming meshes \mathcal{T}_h ; cf. Theorem 5.4.2.

LEMMA 5.5.8. *Let \mathcal{T}_h be a conforming triangulation of the domain Ω into tetrahedra or hexahedra, with edges parallel to the coordinate axes, and assume that $\mathbf{u} \in H^s(\Omega)^3$, $\nabla \times \mathbf{u} \in H^s(\Omega)^3$, for $s > \frac{1}{2}$. Then, we have*

$$\|\mathbf{u} - \mathbf{\Pi}_N \mathbf{u}\|_{0, \Omega} + \|\nabla \times (\mathbf{u} - \mathbf{\Pi}_N \mathbf{u})\|_{0, \Omega} \leq C h^{\min\{s, \ell\}} \left(\|\mathbf{u}\|_{s, \Omega} + \|\nabla \times \mathbf{u}\|_{s, \Omega} \right),$$

with a constant $C > 0$ that is independent of the mesh size and only depends on the shape-regularity of the mesh and the approximation order ℓ .

Since for $\mathbf{u} \in H_0(\text{curl}; \Omega)$ the jumps $[\![\mathbf{u} - \mathbf{\Pi}_N \mathbf{u}]\!]_T$ vanish, Lemma 5.5.8 implies the following approximation result.

LEMMA 5.5.9. *Let \mathcal{T}_h be a conforming triangulation of the domain Ω into tetrahedra or hexahedra, with edges parallel to the coordinate axes, and assume that $\mathbf{u} \in H^s(\Omega)^3$, $\nabla \times \mathbf{u} \in H^s(\Omega)^3$, for $s > \frac{1}{2}$. Then, we have*

$$\|\mathbf{u} - \mathbf{\Pi}_N \mathbf{u}\|_h \leq C_N h^{\min\{s, \ell\}} \left(\|\mathbf{u}\|_{s, \Omega} + \|\nabla \times \mathbf{u}\|_{s, \Omega} \right),$$

with a constant $C_N > 0$ that is independent of the mesh size and only depends the bounds for the coefficients μ and ε , the shape-regularity of the mesh and the approximation order ℓ .

5.5.4 Proof of Theorem 5.4.1

Set $\mathbf{e} = \mathbf{u} - \mathbf{u}^h = \eta + \theta$ with $\eta = \mathbf{u} - \mathbf{\Pi}_h \mathbf{u}$ and $\theta = \mathbf{\Pi}_h \mathbf{u} - \mathbf{u}^h$. Using the symmetry of the form \tilde{a}_h and the error equation in Lemma 5.5.3, we obtain for any $t \in J$

$$\begin{aligned} \frac{1}{2} \frac{d}{dt} \left(\|\varepsilon^{\frac{1}{2}} \mathbf{e}_t\|_{0, \Omega}^2 + \tilde{a}_h(\mathbf{e}, \mathbf{e}) \right) + \|\sigma^{\frac{1}{2}} \mathbf{e}_t\|_{0, \Omega}^2 &= (\varepsilon \mathbf{e}_{tt}, \mathbf{e}_t) + \tilde{a}_h(\mathbf{e}, \mathbf{e}_t) + (\sigma \mathbf{e}_t, \mathbf{e}_t) \\ &= (\varepsilon \mathbf{e}_{tt}, \eta_t) + \tilde{a}_h(\mathbf{e}, \eta_t) + (\sigma \mathbf{e}_t, \eta_t) + r_h(\mathbf{u}; \theta_t). \end{aligned}$$

Integrating this identity over $(0, s)$, $s \in J$, and using the fact that $0 \leq \|\sigma^{\frac{1}{2}} \mathbf{e}_t\|_{0, \Omega}^2$ yields

$$\begin{aligned} \frac{1}{2} \|\varepsilon^{\frac{1}{2}} \mathbf{e}_t(s)\|_{0, \Omega}^2 + \frac{1}{2} \tilde{a}_h(\mathbf{e}(s), \mathbf{e}(s)) &\leq \frac{1}{2} \|\varepsilon^{\frac{1}{2}} \mathbf{e}_t(0)\|_{0, \Omega}^2 + \frac{1}{2} \tilde{a}_h(\mathbf{e}(0), \mathbf{e}(0)) \\ &+ \int_0^s (\varepsilon \mathbf{e}_{tt}, \eta_t) dt + \int_0^s \tilde{a}_h(\mathbf{e}, \eta_t) dt + \int_0^s (\sigma \mathbf{e}_t, \eta_t) dt + \int_0^s r_h(\mathbf{u}; \theta_t) dt. \end{aligned}$$

By integration by parts, we rewrite the third term on the right-hand side above as follows:

$$\int_0^s (\varepsilon \mathbf{e}_{tt}, \eta_t) dt = - \int_0^s (\varepsilon \mathbf{e}_t, \eta_{tt}) dt + \left[(\varepsilon \mathbf{e}_t, \eta_t) \right]_{t=0}^{t=s}.$$

Taking into account the continuity and coercivity properties of \tilde{a}_h in Lemma 5.5.2, and using standard Hölder inequalities, we conclude that

$$\begin{aligned} \frac{1}{2} \|\varepsilon^{\frac{1}{2}} \mathbf{e}_t(s)\|_{0,\Omega}^2 + \frac{1}{2} C_{\text{coer}} |\mathbf{e}(s)|_h^2 &\leq \frac{1}{2} \|\varepsilon^{\frac{1}{2}} \mathbf{e}_t(0)\|_{0,\Omega}^2 + \frac{1}{2} C_{\text{cont}} |\mathbf{e}(0)|_h^2 \\ &+ \|\varepsilon^{\frac{1}{2}} \mathbf{e}_t\|_{L^\infty(J;L^2(\Omega)^3)} \left(\|\varepsilon^{\frac{1}{2}} \eta_{tt}\|_{L^1(J;L^2(\Omega)^3)} + 2\|\varepsilon^{\frac{1}{2}} \eta_t\|_{L^\infty(J;L^2(\Omega)^3)} \right) \\ &+ C_{\text{cont}} T \|\mathbf{e}\|_{L^\infty(J;\mathbf{V}(h))} \|\eta_t\|_{L^\infty(J;\mathbf{V}(h))} \\ &+ \left| \int_J (\sigma \mathbf{e}_t, \eta_t) dt \right| + \left| \int_J r_h(\mathbf{u}; \theta_t) dt \right|. \end{aligned}$$

Since this inequality holds for any $s \in J$, we obtain

$$\begin{aligned} \|\varepsilon^{\frac{1}{2}} \mathbf{e}_t\|_{L^\infty(J;L^2(\Omega)^3)}^2 + C_{\text{coer}} |\mathbf{e}|_{L^\infty(J;\mathbf{V}(h))}^2 &\leq \|\varepsilon^{\frac{1}{2}} \mathbf{e}_t(0)\|_{0,\Omega}^2 + C_{\text{cont}} |\mathbf{e}(0)|_h^2 \\ &+ T_1 + T_2 + T_3 + T_4, \end{aligned}$$

with

$$\begin{aligned} T_1 &= 2\|\varepsilon^{\frac{1}{2}} \mathbf{e}_t\|_{L^\infty(J;L^2(\Omega)^3)} \left(\|\varepsilon^{\frac{1}{2}} \eta_{tt}\|_{L^1(J;L^2(\Omega)^3)} + 2\|\varepsilon^{\frac{1}{2}} \eta_t\|_{L^\infty(J;L^2(\Omega)^3)} \right), \\ T_2 &= 2C_{\text{cont}} T \|\mathbf{e}\|_{L^\infty(J;\mathbf{V}(h))} \|\eta_t\|_{L^\infty(J;\mathbf{V}(h))}, \\ T_3 &= 2 \int_J |(\sigma \mathbf{e}_t, \eta_t)| dt, \\ T_4 &= 2 \int_J |r_h(\mathbf{u}; \theta_t)| dt. \end{aligned}$$

Using the geometric-arithmetic mean inequality, the bounds for ε and the approximation results for the L^2 -projection in Lemma 5.5.4 gives

$$\begin{aligned} T_1 &\leq \frac{1}{4} \|\varepsilon^{\frac{1}{2}} \mathbf{e}_t\|_{L^\infty(J;L^2(\Omega)^3)}^2 \\ &+ Ch^{2\min\{s,\ell\}} \left(\|\mathbf{u}_{tt}\|_{L^1(J;H^s(\Omega)^3)}^2 + h^2 \|\mathbf{u}_t\|_{L^\infty(J;H^{1+s}(\Omega)^3)}^2 \right). \end{aligned}$$

Similarly, using the approximation result in Lemma 5.5.5,

$$T_2 \leq \frac{1}{4} C_{\text{coer}} |\mathbf{e}|_{L^\infty(J;\mathbf{V}(h))}^2 + CT^2 h^{2\min\{s,\ell\}} \|\mathbf{u}_t\|_{L^\infty(J;H^{1+s}(\Omega)^3)}^2.$$

Due to the bounds for σ and ε we obtain

$$\begin{aligned} T_3 &\leq 2T \|\sigma^{\frac{1}{2}} \mathbf{e}_t\|_{L^\infty(J;L^2(\Omega)^3)} \|\sigma^{\frac{1}{2}} \eta_t\|_{L^\infty(J;L^2(\Omega)^3)} \\ &\leq \frac{1}{4} \|\varepsilon^{\frac{1}{2}} \mathbf{e}_t\|_{L^\infty(J;L^2(\Omega)^3)}^2 + CT^2 h^{2\min\{s,\ell\}+2} \|\mathbf{u}_t\|_{L^\infty(J;H^{1+s}(\Omega)^3)}^2. \end{aligned}$$

It remains to bound the term T_4 . To do so, we use Lemma 5.5.7 and obtain

$$T_4 \leq 2C_R h^{\min\{s,\ell\}} \|\theta\|_{L^\infty(J;\mathbf{V}(h))} \mathcal{R},$$

with

$$\mathcal{R} := \left(2\|\nabla \times \mathbf{u}\|_{L^\infty(J;H^s(\Omega)^3)} + T\|\nabla \times \mathbf{u}_t\|_{L^\infty(J;H^s(\Omega)^3)} \right).$$

The triangle inequality, the geometric-arithmetic mean inequality, and the approximation properties in Lemma 5.5.5 then yield

$$\begin{aligned} T_4 &\leq \frac{1}{4} C_{\text{coer}} |\mathbf{e}|_{L^\infty(J; \mathbf{V}(h))}^2 \\ &\quad + Ch^{2 \min\{s, \ell\}} \left(\|\mathbf{u}\|_{L^\infty(J; H^{1+s}(\Omega)^3)}^2 + T^2 \|\mathbf{u}_t\|_{L^\infty(J; H^{1+s}(\Omega)^3)}^2 \right). \end{aligned}$$

Combining the above estimates for T_1 , T_2 , T_3 and T_4 shows that

$$\begin{aligned} \frac{1}{2} \|\varepsilon^{\frac{1}{2}} \mathbf{e}_t\|_{L^\infty(J; L^2(\Omega)^3)}^2 + \frac{1}{2} C_{\text{coer}} |\mathbf{e}|_{L^\infty(J; \mathbf{V}(h))}^2 &\leq \|\varepsilon^{\frac{1}{2}} \mathbf{e}_t(0)\|_{0, \Omega}^2 + C_{\text{cont}} |\mathbf{e}(0)|_h^2 \\ + Ch^{2 \min\{s, \ell\}} \left(\|\mathbf{u}_{tt}\|_{L^1(J; H^s(\Omega)^3)}^2 + \|\mathbf{u}_t\|_{L^\infty(J; H^{1+s}(\Omega)^3)}^2 + \|\mathbf{u}\|_{L^\infty(J; H^{1+s}(\Omega)^3)}^2 \right), \end{aligned}$$

with a constant C that is independent of the mesh size. This proves the desired estimate with respect to the semi-norm $|\cdot|_{L^\infty(J; \mathbf{V}(h))}$. The result for the full $L^\infty(J; \mathbf{V}(h))$ -norm is readily obtained by noting that

$$\begin{aligned} \|\varepsilon^{\frac{1}{2}} \mathbf{e}(s)\|_{0, \Omega} &\leq \left\| \int_0^s \varepsilon^{\frac{1}{2}} \mathbf{e}_t(t) dt \right\|_{0, \Omega} + \|\varepsilon^{\frac{1}{2}} \mathbf{e}(0)\|_{0, \Omega} \\ &\leq T \|\varepsilon^{\frac{1}{2}} \mathbf{e}_t\|_{L^\infty(J; L^2(\Omega)^3)} + \|\varepsilon^{\frac{1}{2}} \mathbf{e}(0)\|_{0, \Omega}. \end{aligned}$$

This concludes the proof of Theorem 5.4.1.

5.5.5 Proof of Theorem 5.4.2

The proof of the energy estimate in Theorem 5.4.2 follows the lines of the proof of Theorem 5.4.1. However, due to the lower spatial regularity of the analytical solution \mathbf{u} , we replace the L^2 -projection $\mathbf{\Pi}_h$ by the Nédélec interpolant of the first kind $\mathbf{\Pi}_N$ from Lemma 5.5.8. Analogously, we use Lemma 5.5.8 and Lemma 5.5.9 to estimate $\mathbf{u} - \mathbf{\Pi}_N \mathbf{u}$, or time derivatives thereof. With these modifications, the proof of Theorem 5.4.2 proceeds exactly as in Theorem 5.4.1.

5.6 Proof of the L^2 -error bound

In this section, we present the proof of our third main result in Theorem 5.4.3. The analysis follows the ideas of the proof for the L^2 -estimate of the error of the IP DG FEM for the scalar second-order wave equation, as we have presented in Chapter 4. However, in the Maxwell case the analysis is more involved. We employ techniques developed for the analysis of the IP DG FEM for Maxwell's equations in frequency domain in Chapter 2 to tackle the additional difficulties imposed by the Maxwell operator.

Throughout this section, we assume conforming tetrahedral meshes \mathcal{T}_h and the coefficient μ to be constant $\mu = 1$.

5.6.1 Auxiliary results

Since the finite element spaces of degree ℓ formed by the first kind of Nédélec's curl-conforming edge elements do not exhibit optimal approximation properties in the L^2 -norm (see, e. g., [58], [55, Theorem 5.41]), we will use the curl-conforming Nédélec interpolant $\mathbf{\Pi}_N$ of the second kind in the analysis of the

L^2 -error of our DG method. This is however to the expense of the restriction of our analysis to tetrahedral meshes.

For our analysis, we refer to the properties of the Nédélec interpolant of second kind $\mathbf{\Pi}_N$ stated in Sections 2.4.1, 2.4.2 and 2.4.3 of Chapter 2.

We begin by establishing the following result, a variant of [6, Lemma 2.1].

LEMMA 5.6.1. *On $\mathbf{V}(h) \times \mathbf{V}(h)$, define the bilinear form*

$$\tilde{\mathcal{A}}_h(\mathbf{u}, \mathbf{v}) := \tilde{a}_h(\mathbf{u}, \mathbf{v}) + (\mathbf{u}, \mathbf{v}). \quad (5.9)$$

For $\mathbf{u} \in H^s(\Omega)$, $\nabla \times \mathbf{u} \in H^s(\Omega)$ with $s > \frac{1}{2}$, let $\mathbf{w}^h \in \mathbf{V}^h$ be the solution of

$$\tilde{\mathcal{A}}_h(\mathbf{w}^h, \mathbf{v}) = \tilde{\mathcal{A}}_h(\mathbf{u}, \mathbf{v}) - r_h(\mathbf{u}; \mathbf{v}) \quad \forall \mathbf{v} \in \mathbf{V}^h.$$

Then, we have

$$\|\mathbf{u} - \mathbf{w}^h\|_h \leq C_E h^{\min\{s, \ell\}} \left[\|\mathbf{u}\|_s + \|\nabla \times \mathbf{u}\|_s \right],$$

with a constant C_E that is independent of h and only depends on C_{coer} , C_{cont} in Lemma 5.5.2 C_R in Lemma 5.5.6 and C_N in Lemma 2.4.1.

Proof. We first remark that because of definition 5.9 and the stability properties in Lemma the form $\tilde{\mathcal{A}}_h$ is continuous and coercive in the full DG norm $\|\cdot\|_h$ on $\mathbf{V}(h) \times \mathbf{V}(h)$:

$$\begin{aligned} \tilde{\mathcal{A}}_h(\mathbf{u}, \mathbf{v}) &\leq C_{\text{cont}} \|\mathbf{u}\|_h \|\mathbf{v}\|_h & \mathbf{u}, \mathbf{v} \in \mathbf{V}(h), \\ \tilde{\mathcal{A}}_h(\mathbf{v}, \mathbf{v}) &\geq C_{\text{coer}} \|\mathbf{v}\|_h^2 & \mathbf{v} \in \mathbf{V}(h), \end{aligned} \quad (5.10)$$

with the constants C_{cont} , C_{coer} from Lemma 5.5.2. Hence, together with the estimates in Lemma 5.5.6, the Lax-Milgram Lemma implies that the approximation \mathbf{w}^h is well-defined.

To prove the estimate for $\|\mathbf{u} - \mathbf{w}^h\|_h$, we first use the triangle inequality,

$$\|\mathbf{u} - \mathbf{w}^h\|_h \leq \|\mathbf{u} - \mathbf{\Pi}_N \mathbf{u}\|_h + \|\mathbf{\Pi}_N \mathbf{u} - \mathbf{w}^h\|_h.$$

From the approximation properties of $\mathbf{\Pi}_N$ in Lemma 2.4.1, we immediately infer that

$$\|\mathbf{u} - \mathbf{\Pi}_N \mathbf{u}\|_h \leq C_N h^{\min\{s, \ell\}} \left[\|\mathbf{u}\|_s + \|\nabla \times \mathbf{u}\|_s \right].$$

It remains to bound $\|\mathbf{\Pi}_N \mathbf{u} - \mathbf{w}^h\|_h$. From (5.10), the definition of \mathbf{w}^h , and the bounds in Lemma 2.4.1 and Lemma 5.5.6, we conclude that

$$\begin{aligned} C_{\text{coer}} \|\mathbf{\Pi}_N \mathbf{u} - \mathbf{w}^h\|_h^2 &\leq \tilde{\mathcal{A}}_h(\mathbf{\Pi}_N \mathbf{u} - \mathbf{w}^h, \mathbf{\Pi}_N \mathbf{u} - \mathbf{w}^h) \\ &= \tilde{\mathcal{A}}_h(\mathbf{\Pi}_N \mathbf{u} - \mathbf{u}, \mathbf{\Pi}_N \mathbf{u} - \mathbf{w}^h) + \tilde{\mathcal{A}}_h(\mathbf{u} - \mathbf{w}^h, \mathbf{\Pi}_N \mathbf{u} - \mathbf{w}^h) \\ &= \tilde{\mathcal{A}}_h(\mathbf{\Pi}_N \mathbf{u} - \mathbf{u}, \mathbf{\Pi}_N \mathbf{u} - \mathbf{w}^h) + r_h(\mathbf{u}; \mathbf{\Pi}_N \mathbf{u} - \mathbf{w}^h) \\ &\leq (C_{\text{cont}} C_N + C_R) h^{\min\{s, \ell\}} \left[\|\mathbf{u}\|_s + \|\nabla \times \mathbf{u}\|_s \right] \|\mathbf{\Pi}_N \mathbf{u} - \mathbf{w}^h\|_h. \end{aligned}$$

Thus

$$\|\mathbf{\Pi}_N \mathbf{u} - \mathbf{w}^h\|_h \leq \left(\frac{C_{\text{cont}} C_N + C_R}{C_{\text{coer}}} \right) h^{\min\{s, \ell\}} \left[\|\mathbf{u}\|_s + \|\nabla \times \mathbf{u}\|_s \right],$$

which proves the bound for $\|\mathbf{u} - \mathbf{w}^h\|_h$. \square

With \mathbf{w}^h from Lemma 5.6.1, we have the following orthogonality property, a key ingredient for our further analysis.

LEMMA 5.6.2. *Let the analytical solution of (5.1) satisfy $\mathbf{u} \in H^s\Omega$, $\nabla \times \mathbf{u} \in H^s(\Omega)$ and let \mathbf{w}^h be the projection from Lemma 5.6.1. Then the expression $\mathbf{u} - \mathbf{w}^h$ is discretely divergence free in the following sense*

$$(\mathbf{u} - \mathbf{w}^h, \nabla \varphi^h) = 0 \quad \forall \varphi^h \in S^h,$$

with $S^h \subset H_0^1(\Omega)$ from (2.13).

Proof. We recall that $\nabla S^h \subset H_0(\text{curl}; \Omega)$. Hence, from the definition of \mathcal{A}_h and \mathbf{w}^h , and the residual property (5.7) we have

$$\tilde{a}_h(\mathbf{u} - \mathbf{w}^h, \nabla \varphi^h) + (\mathbf{u} - \mathbf{w}^h, \nabla \varphi^h) = r_h(\mathbf{u}; \nabla \varphi^h) = 0.$$

Moreover, $\nabla \times \nabla \varphi^h = 0$ and $\llbracket \nabla \varphi^h \rrbracket_T = 0$, thus

$$\tilde{a}_h(\mathbf{u} - \mathbf{w}^h, \nabla \varphi^h) = 0.$$

The statement of the Lemma now follows directly. \square

In the next Lemma, we state the approximation result for the projection \mathbf{w}^h , which will be a central element of the proof of Theorem 5.4.3.

LEMMA 5.6.3. *Let $\mathbf{u} \in H^{s+\sigma_E}(\Omega)$, $\nabla \times \mathbf{u} \in H^s(\Omega)$ with $s > \frac{1}{2}$ and $\sigma_E \in (\frac{1}{2}, 1]$ the embedding parameter from (5.4), and let \mathbf{w}^h be defined as in Lemma 5.6.1. We have the L^2 -bound*

$$\|\mathbf{u} - \mathbf{w}^h\|_0 \leq C_L h^{\min\{s, \ell\} + \sigma_E} \left[\|\mathbf{u}\|_{s+\sigma_E} + \|\nabla \times \mathbf{u}\|_s \right].$$

with a constant C_L that is independent of h and only depends on C_E in Lemma 5.6.1, C_R in Lemma 5.5.6, C_N in Lemma 2.4.1, C_P in Lemma 2.4.2, C_c in Proposition 2.4.5, C_h in Lemma 2.4.4 and a stability constant C_S to be specified in the proof of this Lemma.

Proof. For the proof of the bound for $\|\mathbf{u} - \mathbf{w}^h\|_0$, we proceed along the lines of Section 2.6 in Chapter 2.

To this end, let $\mathbf{w}^c \in \mathbf{V}^c$ be the conforming approximation of \mathbf{w}^h from Proposition 2.4.5. We can write

$$\|\mathbf{u} - \mathbf{w}^h\|_0^2 = (\mathbf{u} - \mathbf{w}^h, \mathbf{u} - \mathbf{\Pi}_N \mathbf{u}) + (\mathbf{u} - \mathbf{w}^h, \mathbf{\Pi}_N \mathbf{u} - \mathbf{w}^c) + (\mathbf{u} - \mathbf{w}^h, \mathbf{w}^c - \mathbf{w}^h).$$

By using the Cauchy-Schwarz inequality and Proposition 2.4.7, we have

$$\|\mathbf{u} - \mathbf{w}^h\|_0 \leq \|\mathbf{u} - \mathbf{\Pi}_N \mathbf{u}\|_0 + C_c h \|\mathbf{u} - \mathbf{w}^h\|_h + \frac{|(\mathbf{u} - \mathbf{w}^h, \mathbf{\Pi}_N \mathbf{u} - \mathbf{w}^c)|}{\|\mathbf{u} - \mathbf{w}^h\|_0}. \quad (5.11)$$

For the last term on the right-hand side of (5.11), we claim that there holds:

$$\frac{|(\mathbf{u} - \mathbf{w}^h, \mathbf{\Pi}_N \mathbf{u} - \mathbf{w}^c)|}{\|\mathbf{u} - \mathbf{w}^h\|_0} \leq C \|\mathbf{u} - \mathbf{\Pi}_N \mathbf{u}\|_0 + C h^{\sigma_E} [\|\mathbf{u} - \mathbf{\Pi}_N \mathbf{u}\|_h + \|\mathbf{u} - \mathbf{w}^h\|_h], \quad (5.12)$$

with $C > 0$ independent of the mesh size and depending only on C_c , C_R , C_H , C_P , C_S , and with σ_E denoting the parameter in (5.4).

In order to prove (5.12), we proceed in several steps.

Step 1. Preliminaries: we start by invoking the Helmholtz decomposition in (2.12) and write

$$\mathbf{\Pi}_N \mathbf{u} - \mathbf{w}^c =: \mathbf{w}^0 \oplus \nabla r, \quad (5.13)$$

with $\mathbf{w}^0 \in \mathbf{X}^h$ and $r \in S^h$, \mathbf{X}^h and S^h being the spaces in (2.13) and (2.14). By using (5.13) and the orthogonality property $\mathbf{u} - \mathbf{w}^h$ in Lemma 5.6.2, we have

$$(\mathbf{u} - \mathbf{w}^h, \mathbf{\Pi}_N \mathbf{u} - \mathbf{w}^c) = (\mathbf{u} - \mathbf{w}^h, \mathbf{w}^0) = (\mathbf{u} - \mathbf{w}^h, \mathbf{w}^0 - \mathbf{w}) + (\mathbf{u} - \mathbf{w}^h, \mathbf{w}),$$

where we have defined $\mathbf{w} := \mathbf{H}\mathbf{w}^0$, the exactly divergence-free approximation of \mathbf{w}^0 from Lemma 2.4.4. Therefore,

$$\frac{|(\mathbf{u} - \mathbf{w}^h, \mathbf{\Pi}_N \mathbf{u} - \mathbf{w}^c)|}{\|\mathbf{u} - \mathbf{w}^h\|_0} \leq \|\mathbf{w}^0 - \mathbf{w}\|_0 + \|\mathbf{w}\|_0, \quad (5.14)$$

so that it remains to estimate $\|\mathbf{w}^0 - \mathbf{w}\|_0$ and $\|\mathbf{w}\|_0$.

Step 2: Estimate of $\|\mathbf{w}^0 - \mathbf{w}\|_0$: we claim that

$$\|\mathbf{w}^0 - \mathbf{w}\|_0 \leq C_H C_c h^{\sigma_E} [\|\mathbf{u} - \mathbf{\Pi}_N \mathbf{u}\|_h + \|\mathbf{u} - \mathbf{w}^h\|_h], \quad (5.15)$$

with constants C_H from Lemma 2.4.4 and C_c from Proposition 2.4.5.

To prove (5.15), note that, in view of the definition of \mathbf{H} and (5.13), there holds

$$\nabla \times \mathbf{w} = \nabla \times \mathbf{w}^0 = \nabla \times (\mathbf{\Pi}_N \mathbf{u} - \mathbf{w}^c). \quad (5.16)$$

Thus, the result in Lemma 2.4.4, the triangle inequality and Proposition 2.4.7 yield

$$\begin{aligned} \|\mathbf{w}^0 - \mathbf{w}\|_0 &\leq C_H h^{\sigma_E} \|\nabla \times (\mathbf{\Pi}_N \mathbf{u} - \mathbf{w}^c)\|_0 \\ &\leq C_H h^{\sigma_E} [\|\nabla \times (\mathbf{\Pi}_N \mathbf{u} - \mathbf{u})\|_0 + \|\nabla_h \times (\mathbf{u} - \mathbf{w}^h)\|_0 + \|\nabla_h \times (\mathbf{w}^h - \mathbf{w}^c)\|_0] \\ &\leq C_H C_c h^{\sigma_E} [\|\mathbf{u} - \mathbf{\Pi}_N \mathbf{u}\|_h + \|\mathbf{u} - \mathbf{w}^h\|_h]. \end{aligned}$$

This completes the proof of (5.15).

Step 3: Estimate of $\|\mathbf{w}\|_0$: We claim that there holds

$$\|\mathbf{w}\|_0 \leq C \|\mathbf{u} - \mathbf{\Pi}_N \mathbf{u}\|_0 + C h^{\sigma_E} [\|\mathbf{u} - \mathbf{\Pi}_N \mathbf{u}\|_h + \|\mathbf{u} - \mathbf{w}^h\|_h], \quad (5.17)$$

with constant $C > 0$ depending only on the constants C_P , C_S , C_c , C_R and C_H .

We will prove this bound for $\|\mathbf{w}\|_0$ by employing techniques of the duality approach presented in Section 2.6 in Chapter 2.

To this end, let \mathbf{z} be the solution of the problem

$$\begin{aligned} \nabla \times (\nabla \times \mathbf{z}) + \mathbf{z} &= \mathbf{w} && \text{in } \Omega, \\ \mathbf{n} \times \mathbf{z} &= 0 && \text{on } \Gamma. \end{aligned} \quad (5.18)$$

Since the right hand side of (5.18) $\mathbf{w} = \mathbf{H}\mathbf{w}^0$ is in $H(\text{div}^0; \Omega)$, we obtain as in [55, Lemma 7.7] that $\mathbf{z}, \nabla \times \mathbf{z} \in H_E^\sigma(\Omega)$ and

$$\|\mathbf{z}\|_{\sigma_E} + \|\nabla \times \mathbf{z}\|_{\sigma_E} \leq C_S \|\mathbf{w}\|_0, \quad (5.19)$$

with a stability constant C_S and the regularity parameter $\sigma_E \in (\frac{1}{2}, 1]$ from the embedding (5.4). With $\tilde{\mathcal{A}}_h$ from Lemma 5.6.1 and r_h from (5.6) holds

$$\tilde{\mathcal{A}}_h(\mathbf{z}, \mathbf{v}) - (\mathbf{w}, \mathbf{v}) = r_h(\mathbf{z}; \mathbf{w}) \quad \mathbf{v} \in \mathbf{V}^h. \quad (5.20)$$

This identity is derived analogously to (5.8) in the proof of Lemma 5.5.3. For the procession of our analysis, we further introduce the bilinear form

$$\mathcal{A}(\mathbf{u}, \mathbf{v}) := (\nabla \times \mathbf{u}, \nabla \times \mathbf{v}) + (\mathbf{u}, \mathbf{v}) \quad \mathbf{u}, \mathbf{v} \in H_0(\text{curl}; \Omega).$$

Note that with this definition, the projection defined in (2.19) is the $\mathcal{A}(\cdot, \cdot)$ -projection of $H_0(\text{curl}; \Omega)$ -functions onto the space \mathbf{V}^c . Moreover, since $[\mathbf{v}]_T = 0$ for all $\mathbf{v} \in H_0(\text{curl}; \Omega)$, the identity

$$\mathcal{A}(\mathbf{u}, \mathbf{v}) = \tilde{\mathcal{A}}_h(\mathbf{u}, \mathbf{v}) \quad \mathbf{u}, \mathbf{v} \in H_0(\text{curl}; \Omega) \quad (5.21)$$

holds with the form $\tilde{\mathcal{A}}_h$ from Lemma 5.6.1.

After these preliminary considerations, we multiply equation (5.18) by \mathbf{w} and integrate by parts to obtain

$$\|\mathbf{w}\|_0^2 = \mathcal{A}(\mathbf{z}, \mathbf{w}) = \mathcal{A}(\mathbf{z} - \mathbf{\Pi}^c \mathbf{z}, \mathbf{w}) + \mathcal{A}(\mathbf{\Pi}^c \mathbf{z}, \mathbf{w}), \quad (5.22)$$

with the projection $\mathbf{\Pi}^c$ from (2.19). Since $\nabla \times \mathbf{w} = \nabla \times \mathbf{w}^0$ and by the definition of the projection $\mathbf{\Pi}^c$, we conclude that

$$\begin{aligned} \mathcal{A}(\mathbf{z} - \mathbf{\Pi}^c \mathbf{z}, \mathbf{w}) &= -(\mathbf{z} - \mathbf{\Pi}^c \mathbf{z}, \mathbf{w}^0) + (\mathbf{z} - \mathbf{\Pi}^c \mathbf{z}, \mathbf{w}) \\ &= (\mathbf{z} - \mathbf{\Pi}^c \mathbf{z}, \mathbf{w} - \mathbf{w}^0). \end{aligned}$$

The approximation result for $\mathbf{\Pi}^c$ in Lemma 2.4.2 and the bound in (5.19) yield

$$\|\mathbf{z} - \mathbf{\Pi}^c \mathbf{z}\|_0 \leq \|\mathbf{z} - \mathbf{\Pi}^c \mathbf{z}\|_h \leq C_P C_S h^{\sigma_E} \|\mathbf{w}\|_0. \quad (5.23)$$

For later use, we also point out that the stability of $\mathbf{\Pi}^c$ and (5.19) give

$$\|\mathbf{\Pi}^c \mathbf{z}\|_0 \leq C_P C_S \|\mathbf{w}\|_0. \quad (5.24)$$

Hence, the Cauchy-Schwarz inequality and the estimates (5.15) and (5.23) yield

$$\begin{aligned} |\mathcal{A}(\mathbf{z} - \mathbf{\Pi}^c \mathbf{z}, \mathbf{w})| &\leq \|\mathbf{z} - \mathbf{\Pi}^c \mathbf{z}\|_0 \|\mathbf{w} - \mathbf{w}^0\|_0 \\ &\leq C h^{2\sigma_E} \|\mathbf{w}\|_0 [\|\mathbf{u} - \mathbf{\Pi}_N \mathbf{u}\|_h + \|\mathbf{u} - \mathbf{w}^h\|_h], \end{aligned} \quad (5.25)$$

with constant $C = C_P C_S C_H C_c$.

It remains to bound the term $\mathcal{A}(\mathbf{\Pi}^c \mathbf{z}, \mathbf{w})$ in (5.22). To this end, in view of (5.16), (5.13) and (2.19), we first note that

$$\begin{aligned} \mathcal{A}(\mathbf{\Pi}^c \mathbf{z}, \mathbf{w}) &= (\nabla \times \mathbf{\Pi}^c \mathbf{z}, \nabla \times \mathbf{w}) + (\mathbf{\Pi}^c \mathbf{z}, \mathbf{w}) \\ &= (\nabla \times \mathbf{\Pi}^c \mathbf{z}, \nabla \times (\mathbf{\Pi}_N \mathbf{u} - \mathbf{w}^c)) + (\mathbf{\Pi}^c \mathbf{z}, \mathbf{w} - \mathbf{w}^0) + (\mathbf{\Pi}^c \mathbf{z}, \mathbf{w}^0) \\ &= (\nabla \times \mathbf{\Pi}^c \mathbf{z}, \nabla \times (\mathbf{\Pi}_N \mathbf{u} - \mathbf{w}^c)) + (\mathbf{\Pi}^c \mathbf{z}, \mathbf{w} - \mathbf{w}^0) + (\mathbf{\Pi}^c \mathbf{z}, \mathbf{\Pi}_N \mathbf{u} - \mathbf{w}^c) \\ &= \mathcal{A}(\mathbf{\Pi}^c \mathbf{z}, \mathbf{\Pi}_N \mathbf{u} - \mathbf{w}^c) + (\mathbf{\Pi}^c \mathbf{z}, \mathbf{w} - \mathbf{w}^0) \\ &= \mathcal{A}(\mathbf{z}, \mathbf{\Pi}_N \mathbf{u} - \mathbf{w}^c) + (\mathbf{\Pi}^c \mathbf{z}, \mathbf{w} - \mathbf{w}^0). \end{aligned} \quad (5.26)$$

Here, we have used that

$$(\mathbf{\Pi}^c \mathbf{z}, \nabla r) = (\mathbf{z}, \nabla r) = 0,$$

which follows readily from the definition of $\mathbf{\Pi}^c$ and the fact that \mathbf{z} is divergence-free. From the identity (5.21) we further have

$$\mathcal{A}(\mathbf{z}, \mathbf{\Pi}_N \mathbf{u} - \mathbf{w}^c) = \mathcal{A}(\mathbf{z}, \mathbf{\Pi}_N \mathbf{u} - \mathbf{u}) + \tilde{\mathcal{A}}_h(\mathbf{z}, \mathbf{u} - \mathbf{w}^h) + \tilde{\mathcal{A}}_h(\mathbf{z}, \mathbf{w}^h - \mathbf{w}^c).$$

Using the symmetry of $\tilde{\mathcal{A}}_h(\cdot, \cdot)$, the definition of \mathbf{w}^h in Lemma 5.6.1 and identity (5.7), we note that $\tilde{\mathcal{A}}_h(\mathbf{z}, \mathbf{u} - \mathbf{w}^h) = r_h(\mathbf{u}; \mathbf{z}) = 0$. Thus, using the variational formulation of problem (5.18) and the identity (5.20) we obtain

$$\mathcal{A}(\mathbf{z}, \mathbf{\Pi}_N \mathbf{u} - \mathbf{w}^c) = (\mathbf{w}, \mathbf{\Pi}_N \mathbf{u} - \mathbf{u}) + (\mathbf{w}, \mathbf{w}^h - \mathbf{w}^c) + r_h(\mathbf{z}, \mathbf{w}^h - \mathbf{w}^c).$$

Using the Cauchy-Schwarz identity, Lemma 5.5.6, (5.19) and Proposition 2.4.7 yields

$$\begin{aligned} \mathcal{A}(\mathbf{z}, \mathbf{\Pi}_N \mathbf{u} - \mathbf{w}^c) &\leq \|\mathbf{w}\|_0 \left[\|\mathbf{\Pi}_N \mathbf{u} - \mathbf{u}\|_0 + \|\mathbf{w}^h - \mathbf{w}^c\|_0 \right] + C_R h^{\sigma_E} \|\nabla \times \mathbf{z}\|_{\sigma_E} \|\mathbf{w}^h - \mathbf{w}^c\|_h \\ &\leq C_c \|\mathbf{w}\|_0 \left[\|\mathbf{\Pi}_N \mathbf{u} - \mathbf{u}\|_0 + h \|\mathbf{w}^h - \mathbf{u}\|_0 + C_S C_R h^{\sigma_E} \|\mathbf{w}^h - \mathbf{u}\|_h \right] \\ &\leq C \|\mathbf{w}\|_0 \left[\|\mathbf{\Pi}_N \mathbf{u} - \mathbf{u}\|_0 + h^{\sigma_E} \|\mathbf{w}^h - \mathbf{u}\|_h \right], \end{aligned}$$

with $C > 0$ depending only on the constants C_c, C_R, C_S . Thus, after using the Cauchy-Schwarz inequality, (5.24) and (5.15) in (5.26), we conclude

$$\mathcal{A}(\mathbf{\Pi}^c \mathbf{z}, \mathbf{w}) \leq C \|\mathbf{w}\|_0 \|\mathbf{u} - \mathbf{\Pi}_N \mathbf{u}\|_0 + C h^{\sigma_E} \|\mathbf{w}\|_0 \left[\|\mathbf{u} - \mathbf{\Pi}_N \mathbf{u}\|_h + \|\mathbf{u} - \mathbf{w}^h\|_h \right], \quad (5.27)$$

with a constant $C >$ that depends only on the constants C_c, C_R, C_S, C_P and C_H .

Combining now (5.22), (5.25) and (5.27) proves claim (5.17).

Step 4. Conclusion: the proof of the bound (5.12) follows now from (5.14), (5.15) and (5.17).

To conclude the proof of the bound for $\|\mathbf{u} - \mathbf{w}^h\|_0$ we insert (5.12) into (5.11) and use the approximation results for $\mathbf{\Pi}_N$ in Lemma 2.4.1 and the bound for $\|\mathbf{u} - \mathbf{w}^h\|_h$ in Lemma 5.6.1 to obtain

$$\|\mathbf{u} - \mathbf{w}^h\|_0 \leq C h^{\min\{s+\sigma_E, \ell+1\}} \|\mathbf{u}\|_{s+\sigma_E} + C h^{\min\{s, \ell\} + \sigma_E} \left[\|\mathbf{u}\|_s + \|\nabla \times \mathbf{u}\|_s \right],$$

with $C > 0$ independent of the meshsize and depending only on the constants C_c, C_R, C_H, C_P, C_S and C_E from Lemma 5.6.1. We also used that $h^{\sigma_E} \leq h$ for the embedding parameter σ_E from (5.4). Finally, since $\|\mathbf{u}\|_s \leq \|\mathbf{u}\|_{s+\sigma_E}$ and $\min\{s + \sigma_E, \ell + 1\} \geq \min\{s, \ell\} + \sigma_E$, the bound in Lemma (5.6.3) follows. \square

Now, let u be defined by the exact solution of (5.1), and assume $\mathbf{u}, \mathbf{u}_t \in L^\infty(J; H^s(\Omega)^3)$, $\nabla \times \mathbf{u}, \nabla \times \mathbf{u}_t \in L^\infty(J; H^s(\Omega)^3)$, with $s > \frac{1}{2}$. With $\hat{\mathcal{A}}_h$ from Lemma 5.6.1, we may define $\mathbf{w}^h(t, \cdot) \in \mathbf{V}^h$ almost everywhere in J by

$$\tilde{\mathcal{A}}_h(\mathbf{w}^h(t, \cdot), \mathbf{v}) = \tilde{\mathcal{A}}_h(\mathbf{u}(t, \cdot), \mathbf{v}) - r_h(\mathbf{u}(t, \cdot); \mathbf{v}) \quad \forall \mathbf{v} \in \mathbf{V}^h. \quad (5.28)$$

It can be readily seen that $\mathbf{w}^h \in L^\infty(J; \mathbf{V}^h)$. Moreover, $\mathbf{w}_t^h \in L^\infty(J; \mathbf{V}^h)$ and

$$\tilde{\mathcal{A}}_h(\mathbf{w}_t^h, \mathbf{v}) = \tilde{\mathcal{A}}_h(\mathbf{u}_t, \mathbf{v}) - r_h(\mathbf{u}_t; \mathbf{v}), \quad \mathbf{v} \in \mathbf{V}^h, \text{ a.e. in } J,$$

as well as

$$\tilde{\mathcal{A}}_h(\mathbf{w}^h(0), \mathbf{v}) = \tilde{\mathcal{A}}_h(\mathbf{u}_0, \mathbf{v}) - r_h(\mathbf{u}_0; \mathbf{v}), \quad \mathbf{v} \in \mathbf{V}^h.$$

Therefore, Lemma 5.6.3 immediately implies the following estimates.

LEMMA 5.6.4. *Let \mathbf{w}^h be defined by (5.28). Under the regularity assumptions of Theorem 5.4.3, we have*

$$\begin{aligned} \|\mathbf{u} - \mathbf{w}^h\|_{L^\infty(J; L^2(\Omega)^3)} &\leq C_L h^{\min\{s, \ell\} + \sigma_E} \left[\|\mathbf{u}\|_{L^\infty(J; H^{s+\sigma_E}(\Omega)^3)} + \|\nabla \times \mathbf{u}\|_{L^\infty(J; H^s(\Omega)^3)} \right], \\ \|(\mathbf{u} - \mathbf{w}^h)_t\|_{L^\infty(J; L^2(\Omega)^3)} &\leq C_L h^{\min\{s, \ell\} + \sigma_E} \left[\|\mathbf{u}_t\|_{L^\infty(J; H^{s+\sigma_E}(\Omega)^3)} + \|\nabla \times \mathbf{u}_t\|_{L^\infty(J; H^s(\Omega)^3)} \right], \\ \|(\mathbf{u} - \mathbf{w}^h)(0)\|_0 &\leq C_L h^{\min\{s, \ell\} + \sigma_E} \left[\|\mathbf{u}_0\|_{s+\sigma_E} + \|\nabla \times \mathbf{u}_0\|_s \right]. \end{aligned}$$

The constant C_L is as in Lemma 5.6.3, and σ_E is the embedding parameter from (5.4).

5.6.2 Proof of Theorem 5.4.3

To complete the proof of Theorem 5.4.3, let $\mathbf{w}^h \in L^\infty(J; \mathbf{V}^h)$ be defined by (5.28) and consider

$$\|\mathbf{e}\|_{L^\infty(J; L^2(\Omega)^3)}^2 \leq 2\|\mathbf{u} - \mathbf{w}^h\|_{L^\infty(J; L^2(\Omega)^3)}^2 + 2\|\mathbf{w}^h - \mathbf{u}^h\|_{L^\infty(J; L^2(\Omega)^3)}^2. \quad (5.29)$$

The first term can be estimated from the L^2 -bounds in Lemma 5.6.1. We shall now derive an estimate for the second term. First, we fix $\mathbf{v} \in L^\infty(J; \mathbf{V}^h)$ and assume that $\mathbf{v}_t \in L^\infty(J; \mathbf{V}^h)$. From the definition of the form $\tilde{\mathcal{A}}_h$ in Lemma 5.6.1 and \mathbf{w}^h in (5.28), and the error equation in Lemma 5.5.3, we have

$$\begin{aligned} ((\mathbf{u}^h - \mathbf{w}^h)_{tt}, \mathbf{v}) + \tilde{a}_h(\mathbf{u}^h - \mathbf{w}^h, \mathbf{v}) &= (\mathbf{u}_{tt}^h, \mathbf{v}) + \tilde{a}_h(\mathbf{u}^h, \mathbf{v}) - \tilde{a}_h(\mathbf{w}^h, \mathbf{v}) - (\mathbf{w}_{tt}^h, \mathbf{v}) \\ &= (\mathbf{u}_{tt}^h, \mathbf{v}) + \tilde{a}_h(\mathbf{u}^h - \mathbf{u}, \mathbf{v}) + r_h(\mathbf{u}; \mathbf{v}) - (\mathbf{u} - \mathbf{w}^h, \mathbf{v}) - (\mathbf{w}_{tt}^h, \mathbf{v}) \\ &= (\mathbf{u}_{tt}, \mathbf{v}) + \sigma(\mathbf{e}_t, \mathbf{v}) - (\mathbf{u} - \mathbf{w}^h, \mathbf{v}) - (\mathbf{w}_{tt}^h, \mathbf{v}). \end{aligned}$$

We rewrite this identity as

$$\begin{aligned} \frac{d}{dt}((\mathbf{u}^h - \mathbf{w}^h)_t, \mathbf{v}) - ((\mathbf{u}^h - \mathbf{w}^h)_t, \mathbf{v}_t) + \tilde{a}_h(\mathbf{u}^h - \mathbf{w}^h, \mathbf{v}) \\ = \frac{d}{dt}((\mathbf{u} - \mathbf{w}^h)_t, \mathbf{v}) - ((\mathbf{u} - \mathbf{w}^h)_t, \mathbf{v}_t) + \sigma \frac{d}{dt}(\mathbf{e}, \mathbf{v}) - \sigma(\mathbf{e}, \mathbf{v}_t) - (\mathbf{u} - \mathbf{w}^h, \mathbf{v}), \end{aligned}$$

which yields

$$\begin{aligned} -((\mathbf{u}^h - \mathbf{w}^h)_t, \mathbf{v}_t) + \tilde{a}_h(\mathbf{u}^h - \mathbf{w}^h, \mathbf{v}) &= \frac{d}{dt}(\mathbf{e}_t, \mathbf{v}) - ((\mathbf{u} - \mathbf{w}^h)_t, \mathbf{v}_t) - ((\mathbf{u} - \mathbf{w}^h)_t, \mathbf{v}_t) \\ &\quad + \sigma \frac{d}{dt}(\mathbf{e}, \mathbf{v}) - \sigma(\mathbf{e}, \mathbf{v}_t) - (\mathbf{u} - \mathbf{w}^h, \mathbf{v}). \end{aligned} \quad (5.30)$$

Let $\tau \in (0, T]$ be fixed, and consider the function

$$\hat{\mathbf{v}}(t, \cdot) = \int_t^\tau (\mathbf{u}^h - \mathbf{w}^h)(s, \cdot) ds, \quad t \in \bar{J}.$$

It follows by this definition that

$$\hat{\mathbf{v}}(\tau, \cdot) = 0, \quad \hat{\mathbf{v}}_t(t, \cdot) = -(\mathbf{u}^h - \mathbf{w}^h)(t, \cdot), \quad \text{a.e. } t \in \bar{J}.$$

For later use, we note that for any $t \in \overline{J}$

$$\begin{aligned} \|\widehat{\mathbf{v}}(t)\|_0 &= \left\| \int_t^\tau (\mathbf{u}^h - \mathbf{w}^h)(s) ds \right\|_0 \leq \int_0^T \|(\mathbf{u}^h - \mathbf{w}^h)(s)\|_0 ds \\ &\leq T \|\mathbf{u}^h - \mathbf{w}^h\|_{L^\infty(J; L^2(\Omega)^3)}. \end{aligned} \quad (5.31)$$

and because this bound is independent of t , it also holds for the supremum over $t \in J$. Now, choose $\mathbf{v} = \widehat{\mathbf{v}}$ in (5.30) which yields

$$\begin{aligned} ((\mathbf{u}^h - \mathbf{w}^h)_t, \mathbf{u}^h - \mathbf{w}^h) - \widetilde{a}_h(\widehat{\mathbf{v}}_t, \widehat{\mathbf{v}}) &= \frac{d}{dt}(\mathbf{e}_t, \widehat{\mathbf{v}}) + ((\mathbf{u} - \mathbf{w}^h)_t, \mathbf{u}^h - \mathbf{w}^h) \\ &\quad + \sigma \frac{d}{dt}(\mathbf{e}, \widehat{\mathbf{v}}) + \sigma(\mathbf{e}, \mathbf{u}^h - \mathbf{w}^h) - (\mathbf{u} - \mathbf{w}^h, \widehat{\mathbf{v}}). \end{aligned}$$

Since the DG form $\widetilde{a}_h(\cdot, \cdot)$ is symmetric, we obtain

$$\begin{aligned} \frac{1}{2} \frac{d}{dt} \|\mathbf{u}^h - \mathbf{w}^h\|_0^2 - \frac{1}{2} \frac{d}{dt} \widetilde{a}_h(\widehat{\mathbf{v}}, \widehat{\mathbf{v}}) &= \frac{d}{dt}(\mathbf{e}_t, \widehat{\mathbf{v}}) + ((\mathbf{u} - \mathbf{w}^h)_t, \mathbf{u}^h - \mathbf{w}^h) \\ &\quad + \sigma \frac{d}{dt}(\mathbf{e}, \widehat{\mathbf{v}}) + \sigma(\mathbf{e}, \mathbf{u}^h - \mathbf{w}^h) - (\mathbf{u} - \mathbf{w}^h, \widehat{\mathbf{v}}). \end{aligned}$$

Integration over $(0, \tau)$ and using that $\widehat{\mathbf{v}}(\tau, \cdot) = 0$ then yields

$$\begin{aligned} &\|(\mathbf{u}^h - \mathbf{w}^h)(\tau)\|_0^2 - \|(\mathbf{u}^h - \mathbf{w}^h)(0)\|_0^2 + \widetilde{a}_h(\widehat{\mathbf{v}}(0), \widehat{\mathbf{v}}(0)) \\ &= -2(\mathbf{e}_t(0), \widehat{\mathbf{v}}(0)) + 2 \int_0^\tau ((\mathbf{u} - \mathbf{w}^h)_t, \mathbf{u}^h - \mathbf{w}^h) dt \\ &\quad - 2\sigma(\mathbf{e}(0), \widehat{\mathbf{v}}(0)) + 2\sigma \int_0^\tau (\mathbf{e}, \mathbf{u}^h - \mathbf{w}^h) dt - 2 \int_0^\tau (\mathbf{u} - \mathbf{w}^h, \widehat{\mathbf{v}}) dt \\ &=: T_1 + T_2 + T_3 + T_4 + T_5. \end{aligned} \quad (5.32)$$

Since $\mathbf{e}(0) = \mathbf{u}_0 - \mathbf{\Pi}_h \mathbf{u}_0$, $\mathbf{e}_t(0) = \mathbf{v}_0 - \mathbf{\Pi}_h \mathbf{v}_0$ and $\widehat{\mathbf{v}}(0)$ belongs to \mathbf{V}^h , we conclude that

$$T_1 = -(\mathbf{e}_t(0), \widehat{\mathbf{v}}(0)) = 0, \quad T_3 = -(\mathbf{e}(0), \widehat{\mathbf{v}}(0)) = 0,$$

Moreover, the positive semi-definiteness of the form \widetilde{a}_h in Lemma 5.5.2 ensures that $\widetilde{a}_h(\widehat{\mathbf{v}}(0), \widehat{\mathbf{v}}(0)) \geq 0$. This leads to the inequality

$$\|(\mathbf{u}^h - \mathbf{w}^h)(\tau)\|_0^2 \leq \|(\mathbf{u}^h - \mathbf{w}^h)(0)\|_0^2 + T_2 + T_4 + T_5. \quad (5.33)$$

By using the Cauchy-Schwarz inequality, a standard Hölder inequality and the geometric-arithmetic mean inequality, we obtain

$$\begin{aligned} T_2 &\leq 2T \|(\mathbf{u} - \mathbf{w}^h)_t\|_{L^\infty(J; L^2(\Omega)^3)} \|\mathbf{u}^h - \mathbf{w}^h\|_{L^\infty(J; L^2(\Omega)^3)} \\ &\leq \frac{1}{4} \|\mathbf{u}^h - \mathbf{w}^h\|_{L^\infty(J; L^2(\Omega)^3)}^2 + 4T^2 \|(\mathbf{u} - \mathbf{w}^h)_t\|_{L^\infty(J; L^2(\Omega)^3)}^2, \\ T_4 &= 2\sigma \int_0^\tau (\mathbf{u} - \mathbf{w}^h, \mathbf{u}^h - \mathbf{w}^h) dt - 2\sigma \int_0^\tau (\mathbf{u}^h - \mathbf{w}^h, \mathbf{u}^h - \mathbf{w}^h) dt \\ &\leq 2\sigma T \|\mathbf{u} - \mathbf{w}^h\|_0 \|\mathbf{u}^h - \mathbf{w}^h\|_0 \\ &\leq \frac{1}{4} \|\mathbf{u}^h - \mathbf{w}^h\|_{L^\infty(J; L^2(\Omega)^3)}^2 + 4\sigma^2 T^2 \|\mathbf{u} - \mathbf{w}^h\|_{L^\infty(J; L^2(\Omega)^3)}^2, \end{aligned}$$

where we have also used that $-\sigma\|\mathbf{u}^h - \mathbf{w}^h\|_0^2 \leq 0$, and, employing the bound (5.31),

$$\begin{aligned} T_5 &\leq 2T \|\mathbf{u} - \mathbf{w}^h\|_{L^\infty(J;L^2(\Omega)^3)} \|\widehat{\mathbf{v}}\|_{L^\infty(J;L^2(\Omega)^3)} \\ &\leq 2T^2 \|\mathbf{u} - \mathbf{w}^h\|_{L^\infty(J;L^2(\Omega)^3)} \|\mathbf{u}^h - \mathbf{w}^h\|_{L^\infty(J;L^2(\Omega)^3)} \\ &\leq \frac{1}{4} \|\mathbf{u}^h - \mathbf{w}^h\|_{L^\infty(J;L^2(\Omega)^3)}^2 + 4T^4 \|\mathbf{u} - \mathbf{w}^h\|_{L^\infty(J;L^2(\Omega)^3)}^2. \end{aligned}$$

The upper bounds for T_2, T_4, T_5 are independent of τ , and hold therefore also for the supremum over $\tau \in J$. Thus, (5.32) yields the estimate

$$\begin{aligned} \|\mathbf{u}^h - \mathbf{w}^h\|_{L^\infty(J;L^2(\Omega)^3)}^2 &\leq \frac{3}{4} \|\mathbf{u}^h - \mathbf{w}^h\|_{L^\infty(J;L^2(\Omega)^3)}^2 + \|(\mathbf{u}^h - \mathbf{w}^h)(0)\|_0^2 \\ &\quad + 4T^2 \|(\mathbf{u} - \mathbf{w}^h)_t\|_{L^\infty(J;L^2(\Omega)^3)}^2 + 4(\sigma^2 T^2 + T^4) \|\mathbf{u} - \mathbf{w}^h\|_{L^\infty(J;L^2(\Omega)^3)}^2 \end{aligned}$$

which leads to

$$\begin{aligned} \frac{1}{4} \|\mathbf{u}^h - \mathbf{w}^h\|_{L^\infty(J;L^2(\Omega)^3)}^2 &\leq 2\|(\mathbf{u}^h - \mathbf{u})(0)\|_0^2 + 2\|(\mathbf{u} - \mathbf{w}^h)(0)\|_0^2 \\ &\quad + 4T^2 \|(\mathbf{u} - \mathbf{w}^h)_t\|_{L^\infty(J;L^2(\Omega)^3)}^2 + 4(\sigma^2 T^2 + T^4) \|\mathbf{u} - \mathbf{w}^h\|_{L^\infty(J;L^2(\Omega)^3)}^2. \end{aligned}$$

Next, we use this estimate in (5.29) to obtain

$$\begin{aligned} \|\mathbf{e}\|_{L^\infty(J;L^2(\Omega)^3)}^2 &\leq 16 \|\mathbf{u}_0 - \mathbf{\Pi}_h \mathbf{u}_0\|_0^2 + 16 \|(\mathbf{u} - \mathbf{w}^h)(0)\|_0^2 \\ &\quad + 32T^2 \|(\mathbf{u} - \mathbf{w}^h)_t\|_{L^\infty(J;L^2(\Omega)^3)}^2 + (2 + 32\sigma^2 T^2 + 32T^4) \|\mathbf{u} - \mathbf{w}^h\|_{L^\infty(J;L^2(\Omega)^3)}^2. \end{aligned}$$

From the approximation properties in Lemma 5.5.4 and Lemma 5.6.4, we conclude that

$$\begin{aligned} \|\mathbf{e}\|_{L^\infty(J;L^2(\Omega)^3)}^2 &\leq 16C^2 h^{2\min\{s+\sigma_E, \ell+1\}} \|\mathbf{u}_0\|_{s+\sigma_E} \\ &\quad + 16C_L^2 h^{2(\min\{s, \ell\} + \sigma_E)} \left[(\|\mathbf{u}_0\|_{s+\sigma_E} + \|\nabla \times \mathbf{u}_0\|_s)^2 \right. \\ &\quad + 2T^2 (\|\mathbf{u}_t\|_{L^\infty(J;H^{s+\sigma_E}(\Omega)^3)} + \|\nabla \times (\mathbf{u}_t)\|_{L^\infty(J;H^s(\Omega)^3)})^2 \\ &\quad \left. + 2(1 + \sigma^2 T^2 + T^4) (\|\mathbf{u}\|_{L^\infty(J;H^{s+\sigma_E}(\Omega)^3)} + \|\nabla \times (\mathbf{u})\|_{L^\infty(J;H^s(\Omega)^3)})^2 \right]. \end{aligned}$$

Here, C is the constant from Lemma 5.5.4 and C_L is the constant from Lemma 5.6.1. Finally, since $\|\mathbf{u}\|_s \leq \|\mathbf{u}\|_{s+\sigma_E}$ and $\min\{s + \sigma_E, \ell + 1\} \geq \min\{s, \ell\} + \sigma_E$, the proof of Theorem 5.4.3 follows.

REMARK 5.6.5. *From the proof of Theorem 5.4.3 we see that the $\mathcal{O}(T^2)$ -term in the bound for the L^2 -error arises from the fact that we used the augmented variant $\tilde{\mathcal{A}}_h$ of the form \tilde{a}_h in the definition of the auxiliary function \mathbf{w}_h . This modification of the form \tilde{a}_h was essential to obtain the orthogonality property of $\mathbf{u} - \mathbf{w}^h$ in Lemma 5.6.2. It can however be renounced in the case of divergence-free data and initial conditions. Then $\mathbf{u}, \mathbf{u}_t, \mathbf{u}_{tt}$ can shown to be divergence-free, and the DG approximations $\mathbf{u}^h, \mathbf{u}_t^h, \mathbf{u}_{tt}^h$ are in the space \mathbf{X}^h from (2.14). In this case, the entire analysis in Section 5.6 can be performed with \mathbf{V}^h replaced by \mathbf{X}^h and $\tilde{\mathcal{A}}_h$ replaced by \tilde{a}_h . In particular, from the definition of $\mathbf{w}^h \in \mathbf{X}^h$ by*

$$\tilde{a}_h(\mathbf{w}^h, \mathbf{v}) = \tilde{a}_h(\mathbf{u}, \mathbf{v}) - r_h(\mathbf{u}; \mathbf{v}) \quad \forall \mathbf{v} \in \mathbf{X}^h,$$

the orthogonality property in Lemma 5.6.2 follows immediately and the bound in Theorem 5.4.3 holds without the $\mathcal{O}(T^2)$ -term.

REMARK 5.6.6. *If the coefficient $\sigma \in L^\infty(\Omega)$ is not constant, an additional term $CT h^{\min\{s+\sigma_E, \ell+1\}} \|\mathbf{u}_0\|_{s+\sigma_E}$ has to be added in the bound for the L^2 -error in Theorem 5.4.3. This term stems from the expression T_3 in the proof of the bound for $\|\mathbf{u}^h - \mathbf{w}^h\|_{L^\infty(J; L^2(\Omega)^3)}^2$, which in this case does not vanish, but can be bounded by*

$$\begin{aligned} 2(\sigma \mathbf{e}(0), \widehat{\mathbf{v}}(0)) &\leq 2\|\sigma\|_\infty T \|\mathbf{e}(0)\|_0 \|\mathbf{u}^h - \mathbf{w}^h\|_{L^\infty(J; \Omega)^3} \\ &\leq \frac{1}{8} \|\mathbf{u}^h - \mathbf{w}^h\|_{L^\infty(J; \Omega)^3}^2 + 8\|\sigma\|_\infty^2 T^2 \|\mathbf{e}(0)\|_0^2, \end{aligned}$$

using the Cauchy-Schwarz inequality, the bound (5.31) and the geometric-arithmetic mean inequality.

5.7 Numerical results

In this section, we validate the theoretical error bounds derived in the previous sections, as well as the feasibility of our method for the approximation of travelling electromagnetic waves in general media and geometries.

Applying DG method (5.3) to the model problem (5.1) results in a symmetric system of linear second-order ODE's

$$\mathbf{M}(\varepsilon) \ddot{\mathbf{u}}^h(t) + \mathbf{M}(\sigma) \dot{\mathbf{u}}^h(t) + \mathbf{A} \mathbf{u}^h(t) = \mathbf{f}^h(t), \quad t \in J, \quad (5.34)$$

with initial conditions

$$\mathbf{M} \mathbf{u}^h(0) = \mathbf{u}_0^h, \quad \mathbf{M} \dot{\mathbf{u}}^h(0) = \mathbf{v}_0^h. \quad (5.35)$$

Here, \mathbf{M} denotes the mass matrix, \mathbf{A} the DG stiffness matrix, and $\mathbf{M}(\varepsilon)$, $\mathbf{M}(\sigma)$ denote the mass matrices with weights ε, σ , respectively. To obtain a full discretization of (5.3), we approximately solve (5.35) by a time stepping scheme.

We implement the fully discrete scheme using the C^{++} classes of `deal.II`³; see [8, 7]. We note here that `deal.II` only supports quadrilateral and hexahedral finite element meshes. As a consequence, the requirements on the grid \mathcal{T}_h in Theorem 5.4.3 for optimal L^2 -convergence are not met, and numerical experiments based on the `deal.II` library cannot validate the theoretical L^2 -bound from Theorem 5.4.3.

All numerical examples are based on the two-dimensional version of the model problem (5.1).

5.7.1 Time discretization

We let k denote the time step and set $t_n = n \cdot k$. For the choice of the time stepping method for finding approximations $\{\mathbf{u}_n^h\}_n$ to $\mathbf{u}^h(t_n)$ we differentiate between two cases. If the medium Ω is non-conducting, i. e., $\sigma \equiv 0$, $\mathbf{M}(\sigma) = \mathbf{0}$, we choose the second-order explicit Newmark scheme (see Chapter 4, Section 4.5.1). This corresponds to the leap-frog scheme

$$\mathbf{M} \mathbf{u}_1^h = \left[\mathbf{M} - \frac{k^2}{2} \mathbf{A} \right] \mathbf{u}_0^h + k \mathbf{M} \mathbf{v}_0^h + \frac{k^2}{2} \mathbf{f}_0^h, \quad (5.36)$$

³URL: www.dealii.org.

and

$$\mathbf{M}\mathbf{u}_{n+1}^h = [2\mathbf{M} - k^2\mathbf{A}]\mathbf{u}_n^h - \mathbf{M}\mathbf{u}_{n-1}^h + k^2\mathbf{f}_n,$$

for $n = 1, \dots, N-1$ and $\mathbf{f}_n := \mathbf{f}(t_n)$.

For materials with conducting regions where $\sigma > 0$, $\mathbf{M}(\sigma) \neq \mathbf{0}$, the Newmark scheme is always implicit; see, e.g. [65, Sections 8.5–8.7]. Therefore, we employ the classical explicit fourth-order Runge-Kutta scheme in this case.

The DG mass matrix $\mathbf{M}(\varepsilon)$ is block-diagonal, with block size equal to the number of degrees of freedom per element. We invert $\mathbf{M}(\varepsilon)$ blockwise in the assembling process. As a result, we do not need to solve any linear systems in the time integration procedure and obtain a fully explicit scheme.

REMARK 5.7.1. *Higher order explicit and centered schemes for (5.34) with $\mathbf{M}(\sigma) = \mathbf{0}$ can be derived using the so-called modified equation approach; see, e. g. [48, pp. 216]. The idea is here, to employ equation (5.34) to represent higher order time derivatives in the Taylor expansion of $\mathbf{y}(t) := \mathbf{M}(\varepsilon)\mathbf{u}^h(t)$. For example, a centered fourth order scheme is derived by replacing*

$$\ddot{\mathbf{y}}(t) = \mathbf{f}^h(t) - \mathbf{A}\mathbf{u}^h(t), \quad \mathbf{y}^{(3)}(t) = \dot{\mathbf{f}}^h(t) - \mathbf{A}\dot{\mathbf{u}}^h(t)$$

and

$$\mathbf{y}^{(4)}(t) = \ddot{\mathbf{f}}^h(t) - \mathbf{A}\ddot{\mathbf{u}}^h(t) = \ddot{\mathbf{f}}^h(t) - \mathbf{A}[\mathbf{M}^{-1}(\varepsilon)\mathbf{f}^h(t) - \mathbf{M}^{-1}(\varepsilon)\mathbf{A}\mathbf{u}^h(t)]$$

in the Taylor expansions

$$\begin{aligned} \mathbf{y}(t_1) &= \mathbf{y}(t_0) + k\dot{\mathbf{y}}(t_0) + \frac{k^2}{2}\ddot{\mathbf{y}}(t_0) + \frac{k^3}{3!}\mathbf{y}^{(3)}(t_0) + \frac{k^4}{4!}\mathbf{y}^{(4)}(t_0) + \mathcal{O}(k^5) \\ \mathbf{y}(t_{n+1}) &= 2\mathbf{y}(t_n) - \mathbf{y}(t_{n-1}) + k^2\ddot{\mathbf{y}}(t_n) + \frac{k^4}{4!}\mathbf{y}^{(4)}(t_n) + \mathcal{O}(k^6). \end{aligned}$$

Since the DG mass matrix $\mathbf{M}(\varepsilon)$ is essentially diagonal, the resulting scheme is fully explicit.

5.7.2 Example 1: smooth solution

In a first set of examples, we consider (5.1) on the two-dimensional domain $\Omega = (0, 1)$ and for times $J = [0, T]$ with $T = 0.5$. In this section, we assume homogeneous material parameters $\varepsilon = \mu = 1$.

We first study the approximation of a wave evolving through an isolating medium Ω , that is we set $\sigma = 0$ (Example 1.1).

We choose the initial and source data such, that the solution is given by the smooth vector field

$$\mathbf{u}(x_1, x_2, t) = \frac{t^2}{2} \begin{pmatrix} \cos(\pi x_1) \sin(\pi x_2) \\ -\sin(\pi x_1) \cos(\pi x_2) \end{pmatrix}. \quad (5.37)$$

We discretize (5.1) on a sequence $\{\mathcal{T}_h\}_{i \geq 1}$ of square meshes of size $h_i = 2^{-i}$ using the polynomial spaces $\mathcal{Q}^\ell(K)$, $\ell = 1, 2, 3$. We choose the stabilization parameter $\alpha = 30$. We note that α_{\min} depends on the polynomial degree of the discretization, and for $\ell = 1, 2$, $\alpha = 20$ would have sufficed for stability of the DG method.

We approximate the semi-discrete solution at time $T = 0.5$ by employing the leap-frog scheme (5.36)–(5.37) with time step $k_i = h_i/20$ on mesh \mathcal{T}_{h_i} . We

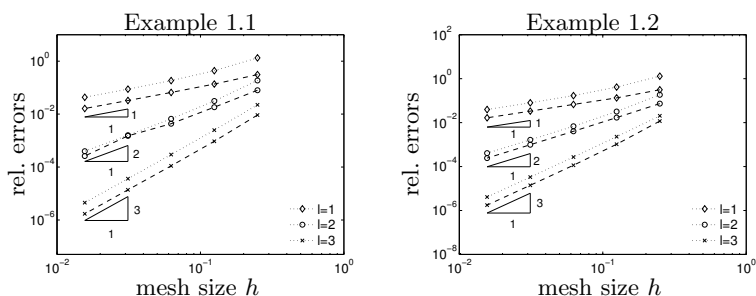


Figure 5.1: Examples 1.1 and 1.2: Convergence of the relative errors at time $T = 0.5$ in the energy norm (–) and the L^2 -norm (·) for $\ell = 1, 2, 3$.

found that this choice of k_i provides a stable time discretization on every mesh and for every polynomial degree. Because the leap-frog scheme is second-order accurate in time, the time integration of (5.37) is exact. The spatial error is the only error component in the discrete solution.

Next, we modify the source data from Example 1.1 such, that the smooth field (5.37) solves our model problem in a conductor Ω with $\sigma = 1$ (Example 1.2). For an explicit time integration, we employ the classical fourth order Runge-Kutta scheme. Again, setting the time step $k_i = h_i/20$ on mesh \mathcal{T}_{h_i} showed to be sufficient for stability, and the time integration is exact.

In Figure 5.1, we report the relative errors in the energy- and the L^2 -norm for the fully discrete approximation of (5.37), in an insulator (Example 1.1, left plot) and in a conductor (Example 1.2, right plot) respectively. The analytical solution (5.37) is arbitrarily smooth, so that the assumptions of Theorem 5.4.1 are met. Indeed, for the error in the DG energy norm, we observe optimal order convergence $\mathcal{O}^\ell(h)$ in the mesh size h (dash-dotted lines).

In order to predict the convergence of the discrete solution in the L^2 -norm, we can however not refer to Theorem 5.4.3, which states optimal L^2 -rates. By discretizing in space on *quadrilateral* meshes, we have violated one assumption of this Theorem. Therefore, we have to fall back on the estimate in Theorem 5.4.1 for a theoretical bound of the L^2 -error. Indeed, in Figure 5.1 we observe only sub-optimal convergence rates of order $\mathcal{O}^\ell(h)$ for the error in the L^2 -norm (dotted lines). This proves that the restriction of the error bound in Theorem 5.4.3 to *triangular* meshes cannot be released.

We note here, that sub-optimal L^2 -convergence is also observed for the underlying *conforming* FE discretizations, using full polynomial spaces $\mathcal{Q}^\ell(K)$ on quadrilateral or hexahedral meshes. To illustrate this, we report in Table 5.1 the convergence rates obtained by approximating (5.37) in the setting of Example 1.1 with Nédélec's lowest order $H(\text{curl}; \Omega)$ -conforming edge elements of second kind. As with the DG discretization, the convergence order in the energy norm (the $H(\text{curl}; \Omega)$ -norm) is optimal, whereas it is one order sub-optimal for the convergence in the L^2 -norm. This deficiency stems from the fact that the approximation with full polynomial spaces $\mathcal{Q}^\ell(K)$ insufficiently separates the discrete gradients from discretely divergence free functions; a discrete Helmholtz decomposition in the sense of (2.12) does not exist for Nédélec's second family of edge elements on quadrilaterals or hexahedrals; see, e. g., [55, Section 8.2.3].

# elements	Energy error		L^2 -error	
	4	1.232e+01	-	5.152e+00
16	1.389e+00	3.15	4.900e-01	3.39
64	3.793e-01	1.87	2.755e-01	0.83
256	1.044e-01	1.86	1.435e-01	0.94
1024	3.298e-02	1.66	7.252e-02	0.98
4096	1.299e-02	1.34	3.636e-02	1.00
16384	5.975e-03	1.12	1.819e-02	1.00

Table 5.1: Example 1.1, *conforming*: Discretization on a sequence of square meshes using Nédélec’s second family of edge elements of polynomial order $\ell = 1$. On quadrilateral and hexahedral meshes, these elements yield only sub-optimal convergence rates of the error in the L^2 -norm.

5.7.3 Example 2: singular solution

In order to validate the error bound for an analytical solution with low spatial regularity in Theorem 5.4.2, we consider the two-dimensional Maxwell’s equation (5.1) on the L-shaped domain $\Omega = (-1, 1)^2 \setminus [0, 1]^2$. We set $\mu = \varepsilon = 1$ and $\sigma = 0$ everywhere and choose the source and initial data such, that the analytical solution is given in polar coordinates (r, ϕ) by

$$\mathbf{u}(r, \phi, t) = \frac{t^2}{2} \nabla(r^{2/3} \sin(2/3 \phi)). \quad (5.38)$$

Since the tangential part of \mathbf{u} is inhomogeneous at the boundary of Ω , we need to impose inhomogeneous Dirichlet conditions $\mathbf{n} \times \mathbf{u} = g$ on $\partial\Omega$ within our DG discretization. We do so in straightforward fashion by modifying the semi-discrete formulation as follows: find $\mathbf{u}^h(t, \cdot) : J \rightarrow \mathbf{V}^h$ such that

$$(\mathbf{u}_{tt}^h, \mathbf{v}) + a_h(\mathbf{u}^h, \mathbf{v}) = (\mathbf{f}, \mathbf{v}) + \sum_{F \in \mathcal{F}_h^B} \int_F g(\mathbf{a}(\mathbf{n} \times \mathbf{v}) - \mu^{-1} \nabla \times \mathbf{v}) dA. \quad (5.39)$$

Here g is the boundary data (which is scalar in $2d$) and \mathbf{n} is the outward unit normal vector on $\partial\Omega$.

We discretize (5.39) by using bilinear polynomials ($\ell = 1$) on the same sequence of meshes as before. We set the stabilization parameter $\alpha = 20$ and integrate the problem up to $T = 1$ employing the leap-frog scheme with time step $k_i = h_i/20$ on mesh \mathcal{T}_{h_i} .

\mathbf{u} is smooth in time (and is integrated exactly in time by the leap-frog scheme). The spatial part of \mathbf{u} is the gradient of the strongest corner singularity of the Dirichlet-Laplacian on Ω , the $H^{\frac{2}{3}}(\Omega)$ -function $r^{2/3} \sin(2/3 \phi)$. Hence, $\mathbf{u} \in C^\infty(\bar{J}; H^{2/3}(\Omega)^2)$ and $\nabla \times \mathbf{u} = 0$, and the regularity assumptions in Theorem 5.4.2 are satisfied by the field (5.38) with regularity exponent $\sigma_E = 2/3$.

Thus, Theorem 5.4.2 predicts numerical convergence rates of $2/3$ in the energy norm (and in the L^2 -norm), as confirmed by our numerical results in Table 5.7.3.

i	# elements	energy-error		L^2 -error	
1	48	2.132e-01	-	1.719e-01	-
2	192	1.322e-01	0.69	1.162e-01	0.57
3	768	8.247e-02	0.68	7.628e-02	0.61
4	3072	5.166e-02	0.67	4.926e-02	0.63
5	12288	3.243e-02	0.67	3.150e-02	0.65

Table 5.2: Example 2: Numerical convergence rates for the approximation of the low regularity solution (5.39) on L-shaped domain.

5.7.4 Example 3: inhomogeneous medium

As a third numerical experiment, we approximate an electromagnetic wave evolving through the domain Ω in Figure 5.2. Ω is composed of materials with different electric permeability ε and conductivity σ :

$$\varepsilon = \begin{cases} 1, & \text{white region} \\ 10, & \text{grey region} \\ 100, & \text{dark region} \end{cases}, \quad \sigma = \begin{cases} 0, & \text{white and grey region} \\ 0.3, & \text{dark region} \end{cases}.$$

The magnetic permeability μ is constant equal to 1 everywhere in Ω . We im-

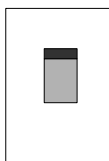


Figure 5.2: Example 3: Domain Ω composed of different materials.

pose homogeneous initial and source data. The wave is excited through the inhomogeneous boundary data at the top edge of the domain Ω

$$g(x, t) = \cos(2\pi t) \frac{1}{\sqrt{2\pi b}} e^{-\frac{x^2}{2b^2}}, \quad b = 0.2. \quad (5.40)$$

On the rest of the boundary $\partial\Omega$ is perfectly conducting, that is, \mathbf{u} satisfies homogeneous Dirichlet conditions.

We discretize the model problem (5.1) by the DG method (5.3) using polynomial of degree $\ell = 2$ on a fixed mesh \mathcal{T}_h that consists of *non-matching components* (generating at most one hanging node per edge), which are adapted to the discontinuities of ε (recall that the wave speed in the medium is given by $(\mu\varepsilon)^{-\frac{1}{2}}$); see Figure 5.7.4. The mesh \mathcal{T}_h is composed of 4608 non-uniform rectangles, where the smallest local mesh size is given by $h_{min} \approx 0.01$. The hanging nodes are naturally incorporated in the DG-method without any difficulty. Compared to the square meshes used in Sections 5.7.2 and 5.7.3, the aspect ratio of the elements in \mathcal{T}_h has deteriorated. We have to account for this in the choice of the IP stabilization parameter α , which is set to 50 in this computation. For the time integration, we have employed the implicit Euler method with time step $k = 0.01$ to approximate the solution \mathbf{u} up to time

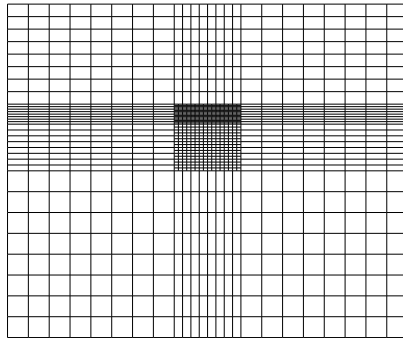


Figure 5.3: Example 3: Domain Ω with a finite element mesh \mathcal{T}_h that is adapted to the values of the piecewise constant wave speed \sqrt{c} .

$T = 10$. (When using the explicit fourth-order Runge-Kutta scheme, a time step $k = 0.15 \cdot h_{min}$ was necessary to ensure a stable integration for longer times.)

In Figure 5.4, the intensity $|\mathbf{u}| = \sqrt{(u_1^2 + u_2^2)}$ is shown for times $t_n = 2, 3.5, 5, 7$. At time $t_n = 2$ the wave excited at the top edge of the computational domain Ω has already hit the slowest medium (the dark region in Figure 5.2). At the corners of the interface of the two media, strong field intensities appear. At time $t_n = 3.5$, the wave enters the region with medium wave speed (the grey region in Figure 5.2) from the side. At time $t_n = 5$, the wave front travelling through the slow (dark) region reaches the grey region as well. Finally, at time $t_n = 5$, the wave has traveled through the entire domain and reflections at the perfectly conducting boundaries give rise to interference patterns. Moreover, we can observe a superposition of the two wave fronts that have entered the grey region from the sides and from the dark region above respectively.

In summary, although one cannot exclude the presence of spurious modes in the DG solution computed on a *quadrilateral* mesh, the discrete solution can adequately reflect the qualitative behavior of the electromagnetic wave.

5.8 Concluding remarks

We have presented and analyzed the symmetric interior penalty discontinuous Galerkin (DG) method for the time-dependent Maxwell equations in second-order form. For smooth solutions, we derive optimal a-priori error estimates in the energy norm on general finite element meshes (Theorem 5.4.1). On conforming meshes, we derive optimal a-priori error estimates in the energy norm for low-regularity solutions that have singularities in space (Theorem 5.4.2). Moreover, on conforming triangular or tetrahedral meshes, we derive optimal a-priori estimates in the L^2 -norm.

The 2d numerical experiments in Section 5.7 validate the theoretical estimates for the energy error in Theorems 5.4.1 and 5.4.2. However, the use of C^{++} classes of the employed FE library `deal.II` is restricted to quadrilateral and hexahedral meshes. Therefore, we could not validate the theoretical L^2 -error bound from Theorem 5.4.3. In fact, we observe only sub-optimal L^2 -rates on quadrilateral meshes. This deficiency is not inherent to our DG method; the

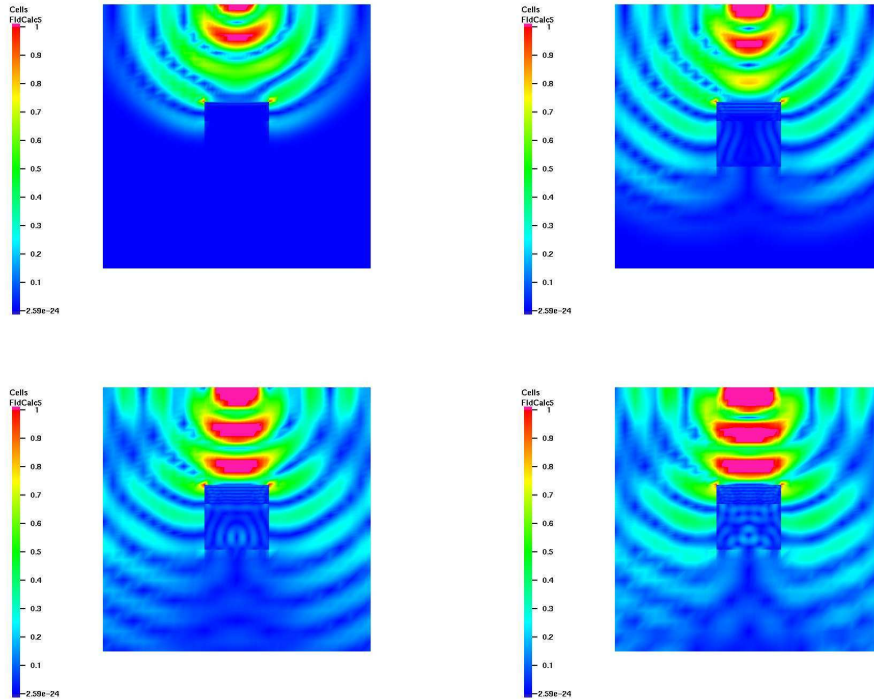


Figure 5.4: Example 3: Electromagnetic wave propagating through an inhomogeneous medium. The intensity of the approximate DG solutions u_n^h is reported at times $t_n = 2, 3.5, 5, 7$. It reflects the qualitative behavior of the electric field component of an electromagnetic wave excited at the top edge of the computational domain by the data in (5.40), and meeting perfectly conducting boundaries at the remaining three edges.

same sub-optimal rate is obtained with the conforming FE discretization when using Nédélec's curl-conforming elements of second type.

Based on discontinuous finite element spaces, the proposed DG method easily handles elements of various types and shapes, irregular non-matching grids, and even locally varying polynomial order. As continuity is only weakly enforced across mesh interfaces, domain decomposition techniques immediately apply. Since the resulting mass matrix is essentially diagonal, the method is inherently parallel and leads to fully explicit methods when coupled with explicit time integration. Moreover, as the stiffness matrix is symmetric positive definite, the interior penalty DG method shares the following important property with the standard continuous Galerkin approach: the semi-discrete formulation conserves (a discrete version of) the energy for all time; therefore, it is non-dissipative.

For future work it would be nice to be able to do computations with our proposed DG method on *triangular* FE meshes. Moreover, in view of fully explicit time stepping methods, it would be interesting to study the topic of *local time stepping*, where the time step is adapted to the *local* spatial mesh size. We note that in the recent research paper [64], Piperno proposed such

a time stepping method, coupled with a DG discretization of the *first-order* Maxwell's equations (1.9)–(1.10).

Finally, the topics for future research raised in Section 4.6 of Chapter 4 for the IP DG FEM of the acoustic wave equation carry over to the Maxwell case.

Appendix: A norm-equivalence property

We report the proof of the key approximation result that is stated in Proposition 2.4.5. The proof is due to Houston ⁴, Perugia ⁵ and Schötzau ⁶ and has been presented in [40]. The techniques in [45, 44] for the analysis of mixed DG methods and in [49] for the study of a-posteriori error estimation for DG discretizations of diffusion problems are employed.

Step 1 (Preliminaries). We begin by introducing the following notation. Recall that each element $K \in \mathcal{T}_h$ is the image of the reference element \widehat{K} under an affine mapping F_K ; that is, $K = F_K(\widehat{K})$ for all $K \in \mathcal{T}_h$, where $F_K(\widehat{\mathbf{x}}) = B_K \widehat{\mathbf{x}} + \mathbf{b}_K$ and $B_K \in \mathbb{R}^{3 \times 3}$, $\mathbf{b}_K \in \mathbb{R}^3$. Without loss of generality, we assume that $\det B_K > 0$. We define

$$\mathbb{D}^\ell(K) = \left\{ \mathbf{q} : \mathbf{q} \circ F_K = \frac{1}{\det B_K} B_K \widehat{\mathbf{q}}, \widehat{\mathbf{q}} \in \mathbb{P}^{\ell-1}(\widehat{K})^3 \oplus \widetilde{\mathbb{P}}^{\ell-1}(\widehat{K}) \widehat{\mathbf{x}} \right\},$$

where $\widetilde{\mathbb{P}}^{\ell-1}(\widehat{K})$ denotes the space of homogeneous polynomials of total degree exactly $\ell - 1$ in $\widehat{\mathbf{x}} = (\widehat{x}_1, \widehat{x}_2, \widehat{x}_3)$ on \widehat{K} . A polynomial $\mathbf{q} \in \mathbb{D}^\ell(K)$ can be represented as $\mathbf{q}(\mathbf{x}) = \mathbf{r}(\mathbf{x}) + \widetilde{s}(\mathbf{x}) \mathbf{x}$, with $\mathbf{r} \in \mathbb{P}^{\ell-1}(K)^3$ and $\widetilde{s} \in \widetilde{\mathbb{P}}^{\ell-1}(K)$.

Next, we assign to each face $f \in \mathcal{F}_h$ a unit normal vector \mathbf{n}_f . Then there is a unique element $K \in \mathcal{T}_h$ such that $f \subset \partial K$ and f is the image of the corresponding reference face \widehat{f} on \widehat{K} under the elemental mapping F_K , and such that $\mathbf{n}_f = B_K^{-T} \widehat{\mathbf{n}}_{\widehat{f}} / |B_K^{-T} \widehat{\mathbf{n}}_{\widehat{f}}|$, where $\widehat{\mathbf{n}}_{\widehat{f}}$ is the outward unit normal vector to \widehat{f} ; cf. [55, Equation (5.21)]. We set

$$\mathbb{D}^\ell(f) = \left\{ \mathbf{q}|_f : \mathbf{q} \circ F_K = B_K \widehat{\mathbf{q}}, \mathbf{q} \in \mathbb{D}^\ell(\widehat{K}), \widehat{\mathbf{q}} \cdot \widehat{\mathbf{n}}_{\widehat{f}} = 0 \right\}.$$

In local coordinates \mathbf{x} on the face f , a function $\mathbf{q}|_f \in \mathbb{D}^\ell(f)$ is given by $\mathbf{q}|_f(\mathbf{x}) = \mathbf{r}(\mathbf{x}) + \widetilde{s}(\mathbf{x}) \mathbf{x}$, where $\mathbf{r} \in \mathbb{P}^{\ell-1}(f)^2$ and $\widetilde{s} \in \widetilde{\mathbb{P}}^{\ell-1}(f)$. Notice that $\mathbf{q}|_f$ is tangential to f .

Finally, we assign to each edge e a unit vector \mathbf{t}_e in the direction of e , and denote by $\mathbb{P}^\ell(e)$ the space of polynomials of degree at most ℓ on e .

Step 2 (Moments for Nédélec's elements of the second type). We introduce a basis for $\mathbb{P}^\ell(K)^3$ based on the moments employed in the definition of Nédélec's second family of elements introduced in [59]. Following [55], we use the following moments that are identical on K and \widehat{K} , up to sign changes, under the transformation $\mathbf{v} \circ F_K = B_K^{-T} \widehat{\mathbf{v}}$ (this can be easily seen as in [55, Lemma 5.34 and Section 8]).

For an edge e , let $\{q_e^i\}_{i=1}^{N_e}$ denote a basis of $\mathbb{P}^\ell(e)$. Similarly, let $\{\mathbf{q}_f^i\}_{i=1}^{N_f}$ be a basis of $\mathbb{D}^{\ell-1}(f)$ for a face f , and $\{\mathbf{q}_K^i\}_{i=1}^{N_b}$ a basis of $\mathbb{D}^{\ell-2}(K)$ for element K .

⁴Prof. P. Houston, Department of Mathematics, University of Leicester, Leicester LE1 7RH, England, email: Paul.Houston@mcs.le.ac.uk

⁵Prof. I. Perugia, Dipartimento di Matematica, Università di Pavia, Via Ferrata 1, 27100 Pavia, Italy, email: perugia@dimat.unipv.it

⁶Prof. D. Schötzau, Mathematics Department, University of British Columbia, 121-1984 Mathematics Road, Vancouver V6T 1Z2, Canada, email: schoetzau@math.ubc.ca

Fix $K \in \mathcal{T}_h$ and let $\mathbf{v} \in \mathbb{P}^\ell(K)^3$. We introduce the following moments:

$$\begin{aligned} M_K^e(\mathbf{v}) &= \left\{ \int_e (\mathbf{v} \cdot \mathbf{t}_e) q_e^i ds : i = 1, \dots, N_e \right\}, & \text{for any edge } e \text{ of } K, \\ M_K^f(\mathbf{v}) &= \left\{ \frac{1}{\text{area}(f)} \int_f \mathbf{v} \cdot \mathbf{q}_f^i ds : i = 1, \dots, N_f \right\}, & \text{for any face } f \text{ of } K, \\ M_K^b(\mathbf{v}) &= \left\{ \int_K \mathbf{v} \cdot \mathbf{q}_K^i d\mathbf{x} : i = 1, \dots, N_b \right\}. \end{aligned}$$

It is well-known that the above moments uniquely define the polynomial $\mathbf{v} \in \mathbb{P}^\ell(K)^3$; see [59, 55]. For a face f of K , the tangential trace $\mathbf{n}_f \times \mathbf{v}$ is uniquely determined by the moments M_K^f and the moments $\{M_K^e\}_{e \in \mathcal{E}(f)}$, where $\mathcal{E}(f)$ is the set of the edges of f ; see [59, Section 3.1] or [55, Lemma 8.11]. Hence, any $\mathbf{v} \in \mathbb{P}^\ell(K)^3$ can be written in the form

$$\mathbf{v} = \sum_{e \in \mathcal{E}(K)} \sum_{i=1}^{N_e} v_{K,e}^i \boldsymbol{\varphi}_{K,e}^i + \sum_{f \in \mathcal{F}(K)} \sum_{i=1}^{N_f} v_{K,f}^i \boldsymbol{\varphi}_{K,f}^i + \sum_{i=1}^{N_b} v_{K,b}^i \boldsymbol{\varphi}_{K,b}^i. \quad (41)$$

Here, we use $\mathcal{E}(K)$ and $\mathcal{F}(K)$ to denote the sets of edges and faces of K , respectively. The functions $\{\boldsymbol{\varphi}_{K,e}^i\}$, $\{\boldsymbol{\varphi}_{K,f}^i\}$, and $\{\boldsymbol{\varphi}_{K,b}^i\}$ are Lagrange basis functions on $\mathbb{P}^\ell(K)^3$ with respect to the moments given above.

Step 3 (Bound on the elemental $H(\text{curl})$ -norm). Let $\mathbf{v} \in \mathbb{P}^\ell(K)^3$ be represented as in (41). We prove the following elemental bound on the $H(\text{curl})$ -norm in terms of the moments in Step 2: there exists a positive constant C , independent of the mesh size, such that

$$\begin{aligned} & h_K^{-2} \|\mathbf{v}\|_{0,K}^2 + \|\nabla \times \mathbf{v}\|_{0,K}^2 \\ & \leq Ch_K^{-1} \left[\sum_{e \in \mathcal{E}(K)} \sum_{i=1}^{N_e} (v_{K,e}^i)^2 + \sum_{f \in \mathcal{F}(K)} \sum_{i=1}^{N_f} (v_{K,f}^i)^2 + \sum_{i=1}^{N_b} (v_{K,b}^i)^2 \right]. \end{aligned} \quad (42)$$

On the reference element, this follows from the representation (41) and the Cauchy-Schwarz inequality. On a general element K , we note that since the transformation $\mathbf{v} \circ F_K = B_K^{-T} \widehat{\mathbf{v}}$ preserves the moments in Step 2, and that

$$\|\mathbf{v}\|_{0,K}^2 \leq Ch_K \|\widehat{\mathbf{v}}\|_{0,\widehat{K}}^2, \quad \|\nabla \times \mathbf{v}\|_{0,K}^2 \leq Ch_K^{-1} \|\widehat{\nabla} \times \widehat{\mathbf{v}}\|_{0,\widehat{K}}^2,$$

with a constant independent of the mesh size (see, e.g., [3, Lemma 5.2]), the bound in (42) is obtained.

Step 4 (Bound on the tangential jumps). Given an interior face f , shared by two elements K_1 and K_2 , we write $\mathcal{E}(f)$ to denote the set of edges of f . Given $\mathbf{v}_1 \in \mathbb{P}^\ell(K_1)^3$ and $\mathbf{v}_2 \in \mathbb{P}^\ell(K_2)^3$, we prove that, using the representation in (41), there exist positive constants C_1 and C_2 , independent of the mesh size, such that

$$\int_f |\mathbf{n}_f \times (\mathbf{v}_1 - \mathbf{v}_2)|^2 ds \leq C_1 \left[\sum_{i=1}^{N_f} (v_{K_1,f}^i - v_{K_2,f}^i)^2 + \sum_{e \in \mathcal{E}(f)} \sum_{i=1}^{N_e} (v_{K_1,e}^i - v_{K_2,e}^i)^2 \right],$$

and

$$\left[\sum_{i=1}^{N_f} (v_{K_1,f}^i - v_{K_2,f}^i)^2 + \sum_{e \in \mathcal{E}(f)} \sum_{i=1}^{N_e} (v_{K_1,e}^i - v_{K_2,e}^i)^2 \right] \leq C_2 \int_f |\mathbf{n}_f \times (\mathbf{v}_1 - \mathbf{v}_2)|^2 ds. \quad (43)$$

To see this, we first consider the case where K_1 and K_2 are of reference size. Since the moments on f and on the edges $e \in \mathcal{E}(f)$ uniquely determine the jump $\mathbf{n}_f \times (\mathbf{v}_1 - \mathbf{v}_2)$, the claim follows from the equivalence of norms in finite dimensional spaces. For general elements K_1 and K_2 , the claim is obtained from a scaling argument taking into account that the transformation $\mathbf{v} \circ F_K = B_K^{-T} \widehat{\mathbf{v}}$ preserves tangential components and the moments in Step 2, modulo sign changes.

The analogous bound holds on the boundary. Let K be the element containing the boundary face f and $\mathbf{v} \in \mathbb{P}^\ell(K)^3$. Using the representation in (41), there exist positive constants C_1 and C_2 , independent of the mesh size, such that

$$\int_f |\mathbf{n}_f \times \mathbf{v}|^2 ds \leq C_1 \left[\sum_{i=1}^{N_f} (v_{K,f}^i)^2 + \sum_{e \in \mathcal{E}(f)} \sum_{i=1}^{N_e} (v_{K,e}^i)^2 \right],$$

and

$$\left[\sum_{i=1}^{N_f} (v_{K,f}^i)^2 + \sum_{e \in \mathcal{E}(f)} \sum_{i=1}^{N_e} (v_{K,e}^i)^2 \right] \leq C_2 \int_f |\mathbf{n}_f \times \mathbf{v}|^2 ds.$$

Step 5 (Approximation property). Let us now prove the result in Proposition 2.4.5. To this end, it is sufficient to show the following result: for all $\mathbf{v} \in \mathbf{V}_h$, there exists $\bar{\mathbf{v}} \in \mathbf{V}_h^c$ such that

$$\|\mathbf{v} - \bar{\mathbf{v}}\|_0^2 \leq C \|\mathbf{h}^{\frac{1}{2}} \llbracket \mathbf{v} \rrbracket_T\|_{\mathcal{F}_h}^2, \quad (44)$$

$$\|\mathbf{v} - \bar{\mathbf{v}}\|_0^2 + \|\nabla \times (\mathbf{v} - \bar{\mathbf{v}})\|_0^2 \leq C \|\mathbf{h}^{-\frac{1}{2}} \llbracket \mathbf{v} \rrbracket_T\|_{\mathcal{F}_h}^2, \quad (45)$$

with a positive constant C , independent of the mesh size.

To prove the claims above, let $\{v_{K,e}^i\}$, $\{v_{K,f}^i\}$ and $\{v_{K,b}^i\}$ denote the moments of \mathbf{v} , according to (41). Further, we write $N(e)$ to denote the set of all elements that share the edge e , and by $N(f)$ the set of all elements that share the face f . The cardinality of these sets are denoted by $|N(e)|$ and $|N(f)|$, respectively. Due to the shape-regularity of the meshes \mathcal{T}_h , we have that $1 \leq |N(e)| \leq N$, uniformly in the mesh size; additionally, $1 \leq |N(f)| \leq 2$. Let $\bar{\mathbf{v}} \in \mathbf{V}_h^c$ be the unique function whose edge moments are

$$\bar{v}_{K,e}^i = \begin{cases} \frac{1}{|N(e)|} \sum_{K' \in N(e)} v_{K',e}^i & \text{if } e \in \mathcal{E}_h^{\mathcal{I}}, \\ 0 & \text{if } e \in \mathcal{E}_h^{\mathcal{B}}, \end{cases}$$

$i = 1, \dots, N_e$, whose face moments are

$$\bar{v}_{K,f}^i = \begin{cases} \frac{1}{|N(f)|} \sum_{K' \in N(f)} v_{K',f}^i & \text{if } f \in \mathcal{F}_h^{\mathcal{I}}, \\ 0 & \text{if } f \in \mathcal{F}_h^{\mathcal{B}}, \end{cases}$$

$i = 1, \dots, N_f$, and whose remaining moments are

$$\bar{v}_{K,b}^i = v_{K,b}^i, \quad i = 1, \dots, N_b.$$

Obviously, the function $\bar{\mathbf{v}}$ defined by the above moments belongs to \mathbf{V}_h^c .

From the bound in (42) in Step 3, we have

$$\begin{aligned} & h_K^{-2} \|\mathbf{v} - \bar{\mathbf{v}}\|_{0,K}^2 + \|\nabla \times (\mathbf{v} - \bar{\mathbf{v}})\|_{0,K}^2 \\ & \leq Ch_K^{-1} \left[\sum_{e \in \mathcal{E}(K)} \sum_{i=1}^{N_e} (v_{K,e}^i - \bar{v}_{K,e}^i)^2 + \sum_{f \in \mathcal{F}(K)} \sum_{i=1}^{N_f} (v_{K,f}^i - \bar{v}_{K,f}^i)^2 \right]. \end{aligned}$$

Let e first be an interior edge in $\mathcal{E}(K)$ and denote by $\mathcal{F}(e)$ the faces sharing the edge e . For $f \in \mathcal{F}(e)$, we denote by K_f and K'_f the elements that share f . Employing the definition of $\bar{v}_{K,e}^i$, the Cauchy-Schwarz inequality, bound (43) from Step 4, and the shape-regularity assumption gives

$$\begin{aligned} \sum_{i=1}^{N_e} (v_{K,e}^i - \bar{v}_{K,e}^i)^2 & \leq C \sum_{K' \in N(e)} \sum_{i=1}^{N_e} (v_{K,e}^i - v_{K',e}^i)^2 \\ & \leq C \sum_{f \in \mathcal{F}(e)} \sum_{i=1}^{N_e} (v_{K_f,e}^i - v_{K'_f,e}^i)^2 \\ & \leq C \sum_{f \in \mathcal{F}(e)} \int_f |[\![\mathbf{v}]\!]_T|^2 ds. \end{aligned}$$

An analogous result holds for a boundary edge e .

Similarly, for an interior face $f \in \mathcal{F}(K)$, we have

$$\sum_{i=1}^{N_f} (v_{K,f}^i - \bar{v}_{K,f}^i)^2 \leq C \sum_{K' \in N(f)} \sum_{i=1}^{N_f} (v_{K,f}^i - v_{K',f}^i)^2 \leq C \int_f |[\![\mathbf{v}]\!]_T|^2 ds,$$

where we have again used the bound (43) from Step 4. An analogous results holds for boundary faces.

Combining the above estimates yields

$$\begin{aligned} & h_K^{-2} \|\mathbf{v} - \bar{\mathbf{v}}\|_{0,K}^2 + \|\nabla \times (\mathbf{v} - \bar{\mathbf{v}})\|_{0,K}^2 \\ & \leq Ch_K^{-1} \left[\sum_{e \in \mathcal{E}(K)} \sum_{f \in \mathcal{F}(e)} \int_f |[\![\mathbf{v}]\!]_T|^2 ds + \sum_{f \in \mathcal{F}(K)} \int_f |[\![\mathbf{v}]\!]_T|^2 ds \right]. \end{aligned}$$

Summing over all elements, taking into account the shape-regularity of the mesh, we deduce (44) and (45).

Bibliography

- [1] M. Ainsworth and J. Coyle. Hierarchic *hp*-edge element families for Maxwell's equations on hybrid quadrilateral/triangular meshes. *Comput. Methods Appl. Mech. Engrg.* , 190:6709–6733, 2001.
- [2] M. Ainsworth, P. Monk, and W. Muniz. Dispersive and dissipative properties of discontinuous Galerkin finite element methods for the second order wave equation. Technical Report 21, Strathclyde University, Glasgow, Mathematics Department, 2004. to appear in *J. Sci. Comput.* .
- [3] A. Alonso and A. Valli. An optimal domain decomposition preconditioner for low-frequency time-harmonic Maxwell equations. *Math. Comp.* , 68:607–631, 1999.
- [4] C. Amrouche, C. Bernardi, M. Dauge, and V. Girault. Vector potentials in three-dimensional non-smooth domains. *Math. Models Appl. Sci.* , 21:823–864, 1998.
- [5] D. N. Arnold, F. Brezzi, B. Cockburn, and L. D. Marini. Unified analysis of discontinuous Galerkin methods for elliptic problems. *SIAM J. Numer. Anal.* , 39:1749–1779, 2001.
- [6] G. A. Baker. Error estimates for finite element methods for second order hyperbolic equations. *SIAM J. Numer. Anal.* , 13(4):564–576, 1976.
- [7] W. Bangerth, R. Hartmann, and G. Kanschat. `deal`. II *Differential Equations Analysis Library, Technical Reference*. IWR, Universität Heidelberg. <http://www.dealii.org>.
- [8] W. Bangerth and G. Kanschat. Concepts for object-oriented finite element software – the `deal`. II library. Report 99-43, Sonderforschungsbereich 3-59, IWR, Universität Heidelberg, 1999.
- [9] D. Boffi and L. Gastaldi. Edge finite elements for the approximation of Maxwell resolvent operator. *Modél. Math. Anal. Numér.* , 36:293–305, 2002.
- [10] F. Brezzi, J. Rappaz, and P. A. Raviart. Finite dimensional approximation of nonlinear problems. Part I: Branches of nonsingular solutions. *Numer. Math.* , 36:1–25, 1980.
- [11] A. Buffa. Remarks on the discretization of some non-coercive operator with applications to Maxwell equations with jumping coefficients. Technical report, IMATI-CNR, Pavia, 2003.

- [12] A. Buffa, R. Hiptmair, T. von Petersdorff, and C. Schwab. Boundary element methods for Maxwell transmission problems in Lipschitz domains. *Numer. Math.* , 95:459–485, 2003.
- [13] A. Buffa and I. Perugia. Discontinuous Galerkin approximation of the Maxwell eigenproblem. Technical Report PV–24, IMATI-CNR Pavia, 2005. technical report.
- [14] A. C. Cangellaris and D. B. Wright. Analysis of the numerical error caused by the stair-stepped approximation of a conducting boundary in FDTD simulations of electromagnetic phenomena. *IEEE Trans. Antennas Propag.* , 39:1518–1525, 1991.
- [15] M. H. Chen, B. Cockburn, and F. Reitich. High-order RKDG methods for computational electromagnetics. *J. Sci. Comput.* , 22:205–226, 2005.
- [16] Z. Chen, Q. Du, and J. Zou. Finite element methods with matching and nonmatching meshes for Maxwell equations with discontinuous coefficients. *SIAM J. Numer. Anal.* , 37:1542–1570, 2000.
- [17] E. T. Chung and B. Engquist. Optimal discontinuous Galerkin methods for wave propagation. preprint.
- [18] P. G. Ciarlet. *The finite element method for elliptic problems*. North-Holland, Amsterdam, 1978.
- [19] B. Cockburn. Discontinuous Galerkin methods for convection-dominated problems. In T. Barth and H. Deconink, editors, *High-Order Methods for Computational Physics*, volume 9 of *Lect. Notes Comput. Sci. Engrg.* , pages 69–224. Springer-Verlag, 1999.
- [20] B. Cockburn, G. E. Karniadakis, and C. W. Shu. The development of discontinuous Galerkin methods. In B. Cockburn, G. E. Karniadakis, and C. W. Shu, editors, *Discontinuous Galerkin Methods: Theory, Computation and Applications*, volume 11 of *Lect. Notes Comput. Sci. Engrg.* , pages 3–50. Springer-Verlag, 2000.
- [21] B. Cockburn, F. Li, and C. W. Shu. Locally divergence-free discontinuous Galerkin methods for the Maxwell equations. *J. Comput. Phys.* , 194:588–610, 2004.
- [22] B. Cockburn and C. W. Shu. TVB Runge–Kutta local projection discontinuous Galerkin method for conservation laws II: General framework. *Math. Comp.* , 52(186):411–435, 1989.
- [23] B. Cockburn and C. W. Shu. Runge–Kutta discontinuous Galerkin methods for convection–dominated problems. *J. Sci. Comput.* , 16:173–261, 2001.
- [24] G. Cohen, P. Joly, J. E. Roberts, and N. Tordjman. Higher order triangular finite elements with mass lumping for the wave equation. *SIAM J. Numer. Anal.* , 38:2047–2078, 2001.
- [25] M. Costabel and M. Dauge. Singularities of electromagnetic fields in polyhedral domains. *Arch. Ration. Mech. Anal.* , 151:221–276, 2000.

- [26] M. Costabel and M. Dauge. Weighted regularization of Maxwell equations in polyhedral domains. *Numer. Math.* , 93:239–277, 2002.
- [27] L. Demkowicz and I. Babuska. p -interpolation error estimates for edge finite elements of variable order in two dimensions. *SIAM J. Numer. Anal.* , 41(4):1195–1208, 2004.
- [28] L. Demkowicz and L. Vardapetyan. Modeling of electromagnetic absorption/scattering problems using hp -adaptive finite elements. *Comput. Methods Appl. Mech. Engrg.* , 152:103–124, 1998.
- [29] A. Elmkies and P. Joly. Finite elements and mass lumping for Maxwell’s equations: the 2d case. *Numerical Analysis, C. R. Acad. Sci. Paris*, 324:1287–1293, 1997.
- [30] R. S. Falk and G. R. Richter. Explicit finite element methods for symmetric hyperbolic equations. *SIAM J. Numer. Anal.* , 36(3):935–952, 1999.
- [31] P. Fernandes and G. Gilardi. Magnetostatic and electrostatic problems in inhomogeneous anisotropic media with irregular boundary and mixed boundary conditions. *Math. Models Methods Appl. Sci.* , 7:957–991, 1997.
- [32] L. Fezoui, S. Lanteri, S. Lohrengel, and S. Piperno. Convergence and stability of a discontinuous Galerkin time-domain methods for the 3D heterogeneous Maxwell equations on unstructured meshes. *Modél. Math. Anal. Numér.* , 39(6):1149–1176, 2005.
- [33] M. J. Grote, A. Schneebeli, and D. Schötzau. Discontinuous Galerkin finite element method for the wave equation. Technical Report 3, Mathematisches Institut, Universität Basel, 2005. To appear in SIAM J. on Numerical Analysis.
- [34] M. J. Grote, A. Schneebeli, and D. Schötzau. Interior penalty discontinuous galerkin method for Maxwell’s equations: Energy norm error estimates. Technical Report 3, Mathematisches Institut, Universität Basel, 2006. To appear in Journal of Computational an Applied Mathematics (JCAM), special volume (WAVES 2005).
- [35] U. Hasler, A. Schneebeli, and D. Schötzau. Mixed finite element approximation of incompressible MHD problems based on weighted regularization. *Appl. Numer. Math.* , 51:19–45, 2004.
- [36] J. S. Hesthaven and T. Warburton. Nodal high-order methods on unstructured grids. I. Time-domain solution of Maxwell’s equations. *J. Comput. Phys.* , 181:186–221, 2002.
- [37] J. S. Hesthaven and T. Warburton. High order nodal discontinuous Galerkin methods for the Maxwell eigenvalue problem. *Royal Soc. London Ser A 362*, pages 493–524, 2004.
- [38] R. Hiptmair. Finite elements in computational electromagnetism. *Acta Numerica*, pages 237–339, 2003.

- [39] P. Houston, M. Jensen, and E. Süli. *hp*-discontinuous Galerkin finite element methods with least-squares stabilization. *J. Sci. Comput.* , 17:3–25, 2002.
- [40] P. Houston, I. Perugia, A. Schneebeli, and D. Schötzau. Interior penalty method for the indefinite time-harmonic Maxwell equations. *Numer. Math.* , 100(3):485–518, 2005.
- [41] P. Houston, I. Perugia, A. Schneebeli, and D. Schötzau. Mixed discontinuous Galerkin approximation of the Maxwell operator: The indefinite case. *Modél. Math. Anal. Numér.* , 39(4):727–753, 2005.
- [42] P. Houston, I. Perugia, and D. Schötzau. Energy norm a posteriori error estimation for mixed discontinuous Galerkin approximations of the Maxwell operator. Technical report, University of Leicester, Department of Mathematics, 2003.
- [43] P. Houston, I. Perugia, and D. Schötzau. *hp*-DGFEM for Maxwell’s equations. In F. Brezzi, A. Buffa, S. Corsaro, and A. Murli, editors, *Numerical Mathematics and Advanced Applications ENUMATH 2001*, pages 785–794. Springer-Verlag, 2003.
- [44] P. Houston, I. Perugia, and D. Schötzau. Mixed discontinuous Galerkin approximation of the Maxwell operator: Non-stabilized formulation. Technical report, University of Leicester, Department of Mathematics, 2003.
- [45] P. Houston, I. Perugia, and D. Schötzau. Mixed discontinuous Galerkin approximation of the Maxwell operator. *SIAM J. Numer. Anal.* , 42:434–459, 2004.
- [46] T. Hughes. *The Finite Element Method: Linear Static and Dynamic Finite Element Analysis*. Prentice Hall, 1987.
- [47] B. Jiang, J. Wu, and L. A. Povinelli. The origin of spurious solutions in computational electromagnetics. *J. Comput. Phys.* , 125:104, 1996.
- [48] P. Joly. Variational methods for time-dependent wave propagation problems. In M. Ainsworth, P. Davies, D. Duncan, P. Martin, and B. Rynne, editors, *Topics in Computational Wave Propagation: Direct and Inverse Problems*, pages 201–264. Springer, 2003.
- [49] O. A. Karakashian and F. Pascal. A posteriori error estimation for a discontinuous Galerkin approximation of second order elliptic problems. Technical report, University of Tennessee, Department of Mathematics, 2003. Report can be retrieved from: <http://www.math.utk.edu/~ohannes/papers.html>. To appear in *SIAM J. Numer. Anal.* .
- [50] D. Kopriva, S. L. Woodruff, and M. Y. Hussaini. *Discontinuous spectral element approximation of Maxwell’s equations*. In B. Cockburn, G. E. Karniadakis, and C. W. Shu, editors, *Discontinuous Galerkin Methods: Theory, Computation and Applications*, volume 11 of *Lect. Notes Comput. Sci. Engng.* , pages 355–362. Springer-Verlag, 2000.

- [51] R. L. Lee and N. K. Madsen. A mixed finite element formulation for Maxwell's equations in the time domain. *J. Comput. Phys.* , 88:284–304, 1990.
- [52] J. L. Lions and E. Magenes. *Non-homogeneous Boundary Value Problems and Applications, Volume I*. Springer–Verlag, New York, 1972.
- [53] P. Monk. A comparison of three mixed methods for the time-dependent Maxwell's equations. *SIAM J. Sci. Statist. Comput.* , 13:1097–1122, 1992.
- [54] P. Monk. A finite element method for approximating the time-harmonic Maxwell equations. *Numer. Math.* , 63:243–261, 1992.
- [55] P. Monk. *Finite element methods for Maxwell's equations*. Oxford University Press, New York, 2003.
- [56] P. Monk. A simple proof of convergence for an edge element discretization of Maxwell's equations. In C. Carstensen, S. Funken, W. Hackbusch, R. Hoppe, and P. Monk, editors, *Computational electromagnetics*, volume 28 of *Lect. Notes Comput. Sci. Engrg.* , pages 127–141. Springer–Verlag, 2003.
- [57] P. Monk and G. R. Richter. A discontinuous Galerkin method for linear symmetric hyperbolic systems in inhomogeneous media. *J. Sci. Comput.* , 22–23(1–3):443–477, 2005.
- [58] J. C. Nédélec. Mixed finite elements in \mathbb{R}^3 . *Numer. Math.* , 35:315–341, 1980.
- [59] J. C. Nédélec. A new family of mixed finite elements in \mathbb{R}^3 . *Numer. Math.* , 50:57–81, 1986.
- [60] K. D. Paulsen and D. R. Lynch. Elimination of vector parasities in finite element Maxwell solutions. *IEEE Trans. Microwave Theory Tech.* , 39:395–404, 1991.
- [61] I. Perugia and D. Schötzau. An *hp*-analysis of the local discontinuous Galerkin method for diffusion problems. *J. Sci. Comput.* , 17:561–571, 2002.
- [62] I. Perugia and D. Schötzau. The *hp*-local discontinuous Galerkin method for low-frequency time-harmonic Maxwell equations. *Math. Comp.* , 72:1179–1214, 2003.
- [63] I. Perugia, D. Schötzau, and P. Monk. Stabilized interior penalty methods for the time-harmonic Maxwell equations. *Comput. Methods Appl. Mech. Engrg.* , 191:4675–4697, 2002.
- [64] S. Piperno. Symplectic local time-stepping in non-dissipative DGTD methods applied to wave propagation problems. Technical Report 282, CER-MICS, INRIA, 2005.
- [65] P. A. Raviart and J. M. Thomas. *Introduction à l'Analyse Numérique des Équations aux Dérivées Partielles*. Masson, Paris, 1983.

- [66] B. Rivière and M. F. Wheeler. Discontinuous finite element methods for acoustic and elastic wave problems, I: Semidiscrete error estimates. Technical Report 01-02, TICAM, UT Austin, 2001.
- [67] B. Rivière and M. F. Wheeler. Discontinuous finite element methods for acoustic and elastic wave problems. In *ICM2002-Beijing satellite conference on scientific computing*, volume 329 of *Contemporary Mathematics*, pages 271–282. AMS, 2003.
- [68] A. Schatz. An observation concerning Ritz-Galerkin methods with indefinite bilinear forms. *Math. Comp.* , 28:959–962, 1974.
- [69] A. Schneebeli. An H(curl)-conforming FEM: Nédélec’s elements of first type. 2002.
<http://www.dealii.org/4.0.0/reports/nedelec/main.html>.
- [70] A. Schneebeli and D. Schötzau. Mixed finite elements for incompressible magneto-hydrodynamics. *C. R. Acad. Sci. Paris, Série I*, 337:71–74, 2003.
- [71] D. Schötzau. Mixed finite element methods for incompressible magneto-hydrodynamics. *Numer. Math.* , 96:771–800, 2004.
- [72] A. Taflove. *Computational Electrodynamics: The finite-difference time-domain method*. Artech House, Boston, 1995.
- [73] L. Vardapetyan and L. Demkowicz. *hp*-adaptive finite elements in electromagnetics. *Comput. Methods Appl. Mech. Engrg.* , 169:331–344, 1999.
- [74] T. Warburton. *Application of the Discontinuous Galerkin Method to Maxwell’s Equations Using Unstructured Polymorphic hp-Finite Elements*. In B. Cockburn, G. E. Karniadakis, and C. W. Shu, editors, *Discontinuous Galerkin Methods: Theory, Computation and Applications*, volume 11 of *Lect. Notes Comput. Sci. Engrg.* , pages 451–458. Springer-Verlag, 2000.
- [75] T. Warburton and M. Embree. The role of the penalty in the local discontinuous Galerkin method for Maxwell’s eigenvalue problem. *Comput. Methods Appl. Mech. Engrg.* , 2005. in press.
- [76] K. S. Yee. Numerical solution of initial boundary value problems involving Maxwell’s equations in isotropic media. *IEEE Trans. Antennas Propag.* , 14:302–307, 1966.

curriculum vitae

Anna Schneebeili

Personal Data

Date of birth: August 9, 1976

Place of birth: Zurich, CH

Nationality: Swiss

Education

2002 – 2006: Doctoral studies at the Mathematical Institute, University of Basel

PhD in Mathematics: July 6, 2006

Advisor: Prof. Dr. Marcus J. Grote, Basel

Co-advisor: Prof. Dr. Ilaria Perugia, University of Pavia, Italy

1996 – 2001: Studies of mathematics at the Federal Institute of Technology (ETH) Zurich, with specialization in applied mathematics and numerics

Diplom in Mathematik (equivalent to a MSc in mathematics) with distinction received in April 2001

Advisor of diploma thesis: Prof. Dr. Christoph Schwab, ETH Zurich

1992 – 1996: Kantonsschule Baden, Aargau, (gymnasium), scientific-technical branch

Matura received in June 1996

1988 – 1992: Bezirksschule Wettingen, Aargau (secondary school)

1983 – 1988: Primarschule Wettingen, Aargau (primary school)

Internships and Further Education

September 2001 – December 2001: Language studies in London, GB

Cambridge Certificate of Proficiency in English received in December 2001

April 2001 – August 2001: Internship in the group of theoretical physics at the research centre of ABB Corporate Ltd in Dättwil, Switzerland

The following professors were the main contributors to my academic education:

P. Arbenz, F. Delbaen, M. Grote, M. Gutknecht, R. Hiptmair, R. Jeltsch, H. Knörrer, J. Marti, A. Prohl, M. Salmhofer, D. Schötzau, C. Schwab, R. Sperb, M. Struwe, E. Trubowitz, G. Wüstholtz, E. Zehnder